VOL. 20 NO. 2 FEBRUARY 1969
PUBLISHED MONTHLY

JOURNAL OF

ELECTROANALYTICAL CHEMISTRY

AND INTERFACIAL ELECTROCHEMISTRY

International Journal devoted to all Aspects of Electroanalytical Chemistry, Double Layer Studies, Electrokinetics, Colloid Stability, and Electrode Kinetics.

ELSEVIER

GENERAL INFORMATION

Types of contributions

(a) Original research work not previously published in other periodicals.
(b) Reviews on recent developments in various fields.
(c) Short communications.
(d) Bibliographical notes and book reviews.

Languages

Papers will be published in English, French or German.

Submission of papers

Papers should be sent to one of the following Editors:
Professor J. O'M. Bockris, John Harrison Laboratory of Chemistry, University of Pennsylvania, Philadelphia 4, Pa. 19104, U.S.A.
Dr. R. H. Ottewill, Department of Chemistry, The University, Bristol 8, England.
Dr. R. Parsons, Department of Chemistry, The University, Bristol 8, England.
Professor C. N. Reilley, Department of Chemistry, University of North Carolina, Chapel Hill, N.C. 27515, U.S.A.

Authors should preferably submit two copies in double-spaced typing on pages of uniform size. Legends for figures should be typed on a separate page. The figures should be in a form suitable for reproduction, drawn in Indian ink on drawing paper or tracing paper, with lettering etc. in thin pencil. The sheets of drawing or tracing paper should preferably be of the same dimensions as those on which the article is typed. Photographs should be submitted as clear black and white prints on glossy paper. Standard symbols should be used in line drawings, the following are available to the printers:

▼ ▽ ■ ⌑ ● ◎ ▪ ◘ ⌖ ⧈ ▪ + ×

All references should be given at the end of the paper. They should be numbered and the numbers should appear in the text at the appropriate places.
A summary of 50 to 200 words should be included.

Reprints

Fifty reprints will be supplied free of charge. Additional reprints (minimum 100) can be ordered at quoted prices. They must be ordered on order forms which are sent together with the proofs.

Publication

The *Journal of Electroanalytical Chemistry and Interfacial Electrochemistry* appears monthly. For 1969, each volume has 3 issues and 4 volumes will appear.
Subscription price: $ 70.00 or Sfr. 304.00 per year; $ 17.50 or Sfr. 76.00 per volume; plus postage. Additional cost for copies by air mail available on request. For subscribers in the U.S.A. and Canada, 2nd class postage paid at Jamaica, N.Y. For advertising rates apply to the publishers.

Subscriptions

Subscriptions should be sent to:

ELSEVIER SEQUOIA S.A., P.O. Box 851, 1001 Lausanne 1, Switzerland

ELECTROANALYTICAL CHEMISTRY AND INTERFACIAL ELECTROCHEMISTRY
Elsevier Sequoia S.A., Lausanne – Printed in The Netherlands

THE THERMODYNAMIC TREATMENT OF MONOLAYER PHASE FORMATION

R. D. ARMSTRONG AND ELIZABETH BARR
Department of Physical Chemistry, University of Newcastle upon Tyne, Newcastle upon Tyne, NE1 7RU (England)
(Received July 18th 1968)

INTRODUCTION

The Gibbs treatment of the electrical double layer can be extended to include situations where charge crosses the interphase, *e.g.*, the Pt–H electrode[1]. In this paper we shall deal with the thermodynamic situation that arises when a monolayer of an anodic film may be formed, and use the relationships derived for the particular case where the film is the mercury salt of butobarbitone (5-*n*-butyl-5-ethylbarbituric acid).

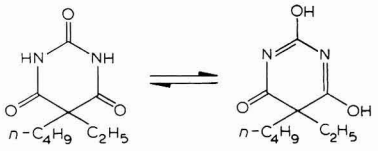

THERMODYNAMIC ANALYSIS

Consider an amalgam M(Hg) which in contact with a solution, CX, forms a monolayer phase, MX, over a certain range of potential. By "monolayer phase" we imply that for $E < E_r, \Gamma_{MX} = 0$, whilst for $E > E_r, \Gamma_{MX}$ is finite and approximately constant. Taking the Gibbs surfaces to be defined by the relations, $\Gamma_{H_2O} = 0$ and $\Gamma_{Hg^+} = 0$ at constant T,P, the Gibbs equation is

$$d\gamma + \Gamma_e d\bar{\mu}_e + \Gamma_{M^+} d\bar{\mu}_{M^+} + \Gamma_{C^+} d\bar{\mu}_{C^+} + \Gamma_{X^-} d\bar{\mu}_{X^-} + \Gamma_{MX} d\bar{\mu}_{MX} = 0 \quad (1)$$

If the monolayer is in equilibrium with M^+ ions in the metal and X^- ions in the solution then

$$\bar{\mu}_{MX(monolayer)} = \bar{\mu}_{M^+} + \bar{\mu}_{X^-}$$

Thus for a thin layer, the electrochemical potential of the phase is a function of the interfacial potential whereas for a thick layer there is only one interfacial potential (E_{rb}) at which equilibrium is possible. If we suppose that the layer is stoichiometric and write the electroneutrality condition:

$$q_M/F = \Gamma_{M^+} - \Gamma_e = \Gamma_{X^-} - \Gamma_{C^+}$$

equation (1) reduces to

$$d\gamma + (q_M + F\Gamma_{MX})dE + (\Gamma_{M^+} + \Gamma_{MX})d\mu_M + (\Gamma_{MX} + \Gamma_{X^-})d\mu_{CX} = 0 \quad (2)$$

where the potential is measured by an electrode which is reversible to C^+.

The analogue of the Lippmann equation is

$$-\left(\frac{\partial\gamma}{\partial E}\right)_{P,T,\mu_i} = q_M + F\Gamma_{MX} \quad (3)$$

and the (thermodynamic) double-layer capacity is given as:

$$-\left(\frac{\partial^2\gamma}{\partial E^2}\right)_{P,T,\mu_i} = C_{dl} = \left(\frac{\partial q_M}{\partial E}\right)_{P,T,\mu_i} + F\left(\frac{\partial\Gamma_{MX}}{\partial E}\right)_{P,T,\mu_i} \quad (4)$$

For a non-stoichiometric layer, q_M in eqns. (2), (3) and (4) must be understood to present the excess charge in the layer (with due regard for sign) as well as that on the metal.

The form of the γ–E, $(q_M + F\Gamma_{MX})$–E and C_{dl}–E curves can be obtained from the above relationships provided that the significance of γ as a surface free energy is realised. Thus, at any potential the stable condition of the surface is that which gives rise to a minimum for γ. At $E > E_r$ this means a film-covered surface (γ_F), at $E < E_r$ this isa film-free surface (γ_0), whilst at $E = E_r$ the two conditions are equally probable. Since we have postulated a discontinuous change in Γ_{MX} at E_r we will in

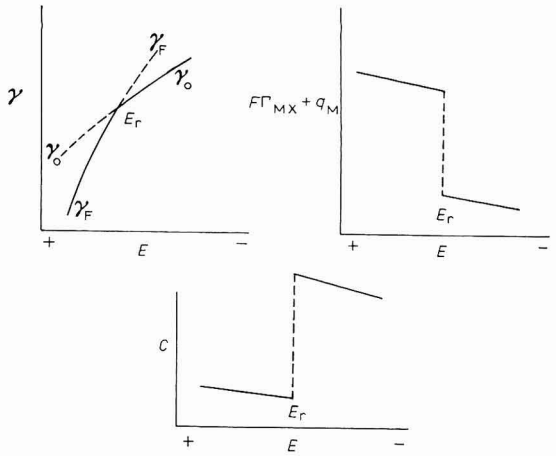

Fig. 1. Schematic γ–E, $(F\Gamma_{MX} + q_M)$–E and C–E curves for a system where monolayer phase formation occurs. E_r is the monolayer reversible potential.

general find discontinuities in the $(F\Gamma_{MX} - q_M)$–E and C_{dl}–E curves, whereas the tangent to the γ–E curve is double-valued at E_r (Fig. 1). Similar behaviour would be found for the adsorption of an organic substance at an electrode provided that the adsorption isotherm shows a discontinuity, *e.g.*, a Frumkin isotherm with an appropriate interaction coefficient.

The fact that E_r and E_{rb} may differ has been noted many times previously, *e.g.*, ref. 2. There is, however, no simple relationship between E_r and E_{rb} when potential-

dependent surface free energies are used. All that can be said is that the free energy change per unit area on film formation is $\gamma_0 - \gamma_F$ and if this is negative at $E = E_{rb}$ then the monolayer is more stable than the bulk phase. The term γ_F may be written $\gamma_F = \gamma_{32} + \gamma_{21}$ where γ_{32} is the film–solution surface free energy and γ_{21} is the film–metal surface free energy. It is, however, important to recognize that γ_{32} and γ_{21} cannot be separately measured and that γ_{32} cannot be equated[2] with the solution–bulk phase surface free energy.

EXPERIMENTAL

The solutions investigated were: (a) 1 *M* KNO_3 + 0.05 *M* borax (base solution), (b) 1 *M* KNO_3 + 0.05 *M* borax + 0.01 *M* butobarbitone. Some additional measurements were made using (c) 1 *M* KNO_3 + 0.05*M* borax + 0.01 *M* veronal (diethylbarbituric acid). Solutions were made up in triply-distilled water with AR-grade reagents where possible. The mercury was cleaned chemically and then distilled twice *in vacuo*. Saturated calomel reference electrodes were used throughout. Measurements were made at 25 ± 1°. Where necessary, control to ± 0.1° was achieved by means of an air thermostat.

The surface tension of the Hg–solution interface was evaluated by measuring the maximum diameter (± 10μ) and the height above the maximum diameter (± 10μ) of a sessile mercury drop (diameter ~ 1 cm). The value of γ (± 1%) was obtained from these measurements by use of the formula given by PORTER[3]. A more refined treatment of the results[4] was not justified because of the limited accuracy of the location of the maximum diameter.

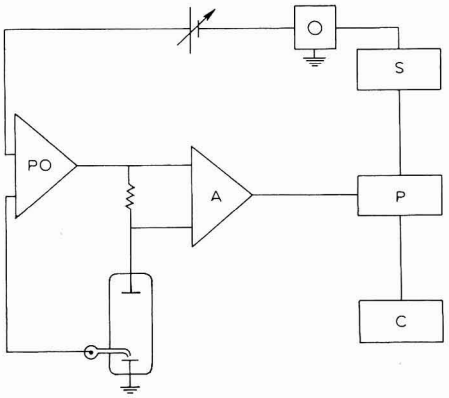

Fig. 2. Apparatus for time-dependent impedance measurements: (O), oscillator; (S), phase shifter; (P), phase sensitive detector; (C), chart recorder; (A), amplifier; (PO), potentiostat.

Drop-time measurements on individual drops were made using an interval timer (Advance TC7). With conventional polarographic capillaries, the reproducibility was ± 1 msec for a 5-sec drop.

Impedance measurements were made on a sitting mercury drop electrode using a potentiostat through which a sinusoidal waveform was injected. By the incorporation of a phase sensitive detector into the apparatus (Fig. 2) it was possible to make

time-dependent impedance measurements to an accuracy of $\sim 1\%$ with a resolution of ~ 5 sec. Some further measurements were made using a conventional Wien bridge[5] and a HMDE.

RESULTS

For the base solution, γ_z was found as 424 ± 4 dyn cm^{-1} at $E_z = -0.535$ V (SCE) by the sessile drop method. This value, which was used to obtain γ-values from the drop-time measurements and as an integration constant for the impedance measurements, compares well with the value quoted by PAYNE[6] for 1 M KNO_3 (420.9 dyn cm^{-1}). The drop-time measurements are shown in Fig. 3. For the butobarbitone solution the curve obtained varied with the drop-time used (up to 10 sec), indicating that adsorption equilibrium had not been achieved in the drop-life time. The results

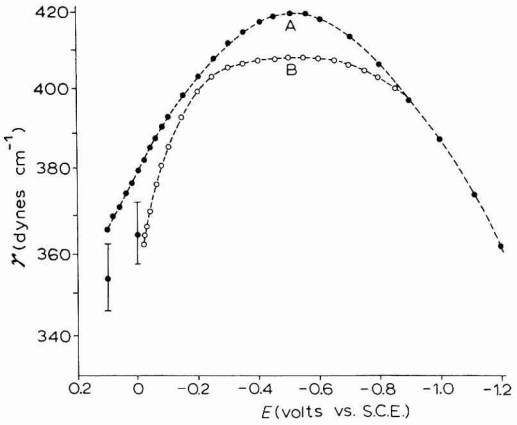

Fig. 3. Apparent surface tension from drop-time measurements: (A), 1 M KNO_3 + 0.05 M borax; (B), 1 M KNO_3 + 0.05 M borax + 0.01 M butobarbitone.

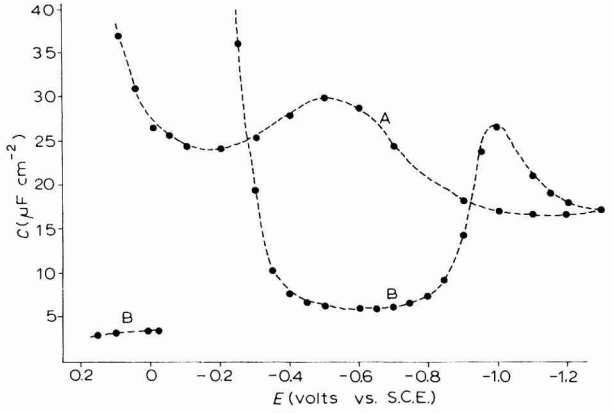

Fig. 4. Double-layer capacity measurements (400 Hz): (A) 1 M KNO_3 + 0.05 M borax; (B), 1 M KNO_3 + 0.05 M borax + 0.01 M butobarbitone.

also showed a marked irreproducibility at $E > -0.022$ V which is the monolayer reversible potential in this system[7] (E_r).

Impedance measurements for the base solution showed that the interfacial impedance was purely capacitative (Fig. 4) for potentials as anodic as ~ 0.150 V where a pseudocapacity due to mercury dissolution was found. Butobarbitone also exhibited a purely capacitative impedance provided that sufficiently low measurement frequencies were used. There was a discontinuity at -0.022 V (E_r) and at more positive potentials the capacity was found to be time-dependent (Fig. 5a), but frequency-independent.

For the veronal solution, the impedance (Fig. 5b) in the monolayer region ($E_r = -0.059$ V) showed a simpler time-dependence.

By double integration of the C–E curves and the use of γ-values obtained from

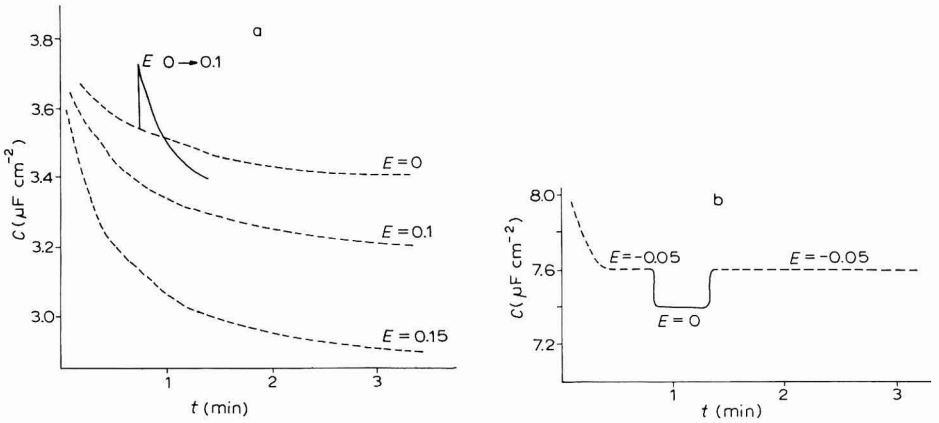

Fig. 5. Time-dependence of double-layer capacity (4 kHz) for potentials (SCE) in the monolayer region: (a), 1 M KNO_3 + 0.05 M borax + 0.01 M butobarbitone; (b), 1 M KNO_3 + 0.05 M borax + 0.01 M veronal.

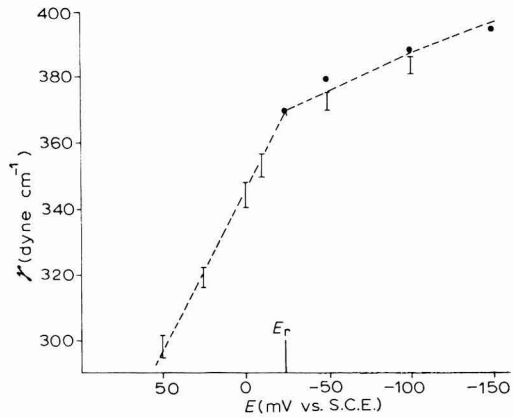

Fig. 6. Surface tension measurements around the monolayer reversible potential for 1 M KNO_3 + 0.05 M borax + 0.01 M butobarbitone. (I), sessile drop; (•), capacity.

the sessile drop measurements, a composite γ–E curve was constructed for the butobarbitone solution at potentials about E_r (Fig. 6). The γ-values at $E > E_r$ were reproducible to 1% and did not show hysteresis effects. The capacity measurements around (E_r) are shown in more detail in Fig. 7.

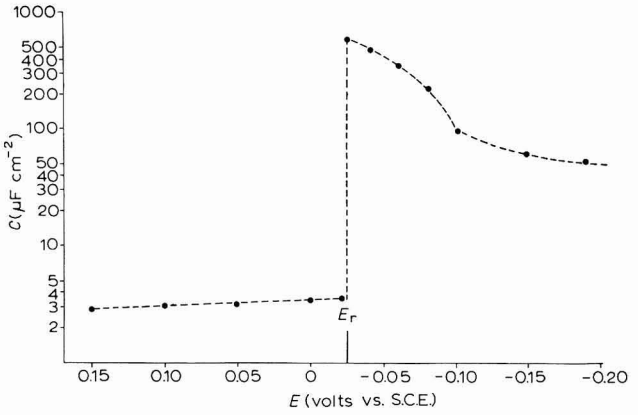

Fig. 7. Double-layer capacity measurements about E_r for 1 M KNO_3 + 0.05 M borax + 0.01 M butobarbitone.

DISCUSSION

(i) Interfacial tension

It is important to recognize that reliable γ-values can be obtained at all potentials only from the sessile drop measurements. The attempt by VORONOVA AND STROMBERG[8] to arrive at conclusions on the basis of drop-time measurements is clearly suspect because of the lack of reproducibility found in the present experiments. It is probable that a capillary electrometer would also give erroneous γ-values because of variation in the contact angle.

It is apparent from Figs. 6 and 7 that the γ–E and C–E behaviour predicted for monolayer phase formation (Fig. 1) is indeed found. The monolayer phase is probably a linear polymer[7,9,10]

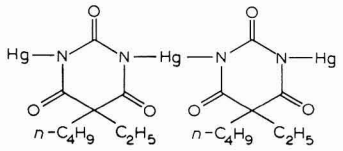

The slope of the γ–E curve at E_r has the two values:

$$\left(\frac{\partial\gamma}{\partial E}\right)_{E^+ \to E_r} = q_M{}^2 + q_{MON} = 90 \pm 13 \mu C\ cm^{-2}$$

$$\left(\frac{\partial\gamma}{\partial E}\right)_{E^- \to E_r} = q_M{}^1 = 43 \pm 2\ \mu C\ cm^{-2}$$

where $q_M{}^1$ is the charge on the metal before monolayer formation, $q_M{}^2$ that after, and

q_{MON} is used instead of $F\Gamma_{MX}$ used previously. An independent estimate of $q_{MON}+q_M{}^2-q_M{}^1$ is avaible from the integration of the i–t transient due to film formation when a small potentiostatic perturbation is applied to the system. This gives a value[7] of $75\pm15\,\mu C\,cm^{-2}$, which agrees within experimental error with the value obtained above ($90-43\pm15\,\mu C$).

Previous work from these laboratories has always tacitly assumed that $q_M{}^1=q_M{}^2$ when comparing the charge obtained by integration of i–t transients with molecular models. We see that an alternative procedure would be to use a molecular model to evaluate $q_M{}^2$. In the present case, q_{MON} is estimated as $72\pm2\,\mu C\,cm^{-2}$ which leads to a value for $q_M{}^2$ of $18\pm15\,\mu C\,cm^{-2}$.

Thus, it is seen that physically as anodic potentials are reached, q_M increases rapidly resulting in a high field across the interphase. At E_r, discharge across the interphase occurs resulting in the formation of a phase monolayer and a discontinuous decrease in q_M with a corresponding decrease in the field ($=4\pi q_M/\varepsilon$). In such a system it is conceivable that two potentials exist for which $q_M=0$, *i.e.*, at the e.c.m. and also at some potential in the monolayer region.

(ii) Impedance measurements

Before the measured capacity in the monolayer region can be equated with the thermodynamic double-layer capacity, it is necessary to be certain that equilibrium is achieved at the measurement frequency (>300 Hz). This seems unlikely, since the response to an abrupt change of potential indicates there are processes occurring that are characterised by time constants of the order of minutes. Thus, it is probable that the measured (steady-state) capacities represent:

$$\left(\frac{\partial q_M}{\partial E}\right)_{P,T,\mu_i,q_{MON}}$$

rather than

$$\left(\frac{\partial(q_M+q_{MON})}{\partial E}\right)_{P,T,\mu_i}$$

The magnitude of this capacity is consistent with the view that the film is stoichiometric and behaving as an insulator with an effective dielectric constant of ~2.

The observation that the steady-state capacity decreases with increasing anodic potential in the monolayer region (Fig. 7) is difficult to understand when the effects of electrostatic compression are considered. However, for mercury butobarbitone the instantaneous change in capacity due to an anodic perturbation is in the correct sense for an explanation in terms of electrostatic compression, *i.e.*, it increases, though to explain the magnitude of the change a compressibility an order of magnitude greater that of water would need to be invoked. The time-dependence which is observed suggests that following a step function change in potential, q_M instantaneously changes, whilst Γ_{MX} slowly reaches its equilibrium value.

Finally, it should be observed that the present analysis is only applicable to systems where there is reason to believe that equilibrium is achieved. One would therefore not expect it to be applicable to the Pt–O system because of the considerable hysteresis effects which are observed there.

SUMMARY

The thermodynamic situation arising when an anodic phase monolayer may be present on an electrode, is treated. The relations derived are used to discuss the significance of surface tension and impedance measurements in the potential region where the mercury salts of the barbituric acids are "adsorbed" on a mercury electrode.

REFERENCES

1 A. FRUMKIN, O. PETRY, A. KOSSAYA, V. ENTINA AND V. TOPOLEV, *J. Electroanal. Chem.*, 16 (1968) 175.
2 D. A. VERMILYEA, *Advan. Electrochem. Eng.*, 3, (1963) 211.
3 A. W. PORTER, *Phil. Mag.*, 25 (1938) 752.
4 O. L. WHEELER, H. V. TARTAR AND E. C. LINGAFELTER, *J. Am. Chem. Soc.*, 67 (1945) 2115.
5 R. D. ARMSTRONG, W. P. RACE AND H. R. THIRSK, *Electrochim. Acta*, 13 (1968) 215.
6 R. PAYNE. *J. Electrochem. Soc.*, 113 (1966) 999.
7 J. W. OLDFIELD, Ph. D. Thesis, University of Newcastle upon Tyne, 1967.
8 K. R. VORONOVA AND A. G. STROMBERG, *Zh. Obshch. Khim.*, 31 (1961) 2786.
9 C. O. BJORLING, A. BERGGREN AND B. NUGGARD, *Acta. Chem. Scand.*, 16 (1962) 1451.
10 E. M. COHEN, *Dissertation Abstr.*, 26 (1965) 108.

ELECTROANALYTICAL CHEMISTRY AND INTERFACIAL ELECTROCHEMISTRY
Elsevier Sequoia S.A., Lausanne – Printed in The Netherlands

INSTRUMENT FOR THE AUTOMATIC MEASUREMENT OF THE ELECTRODE ADMITTANCE*

R. DE LEVIE AND A. A. HUSOVSKY
Department of Chemistry, Georgetown University, Washington, D. C. 20007 (U.S.A.)
(Received August 8th, 1968)

INTRODUCTION

The measurement of the electrode admittance is fundamental to modern electrochemistry. On the basis of the Lippmann equation[1], GOUY[2] accurately predicted the double-layer capacitance of aqueous solutions like 0.5 *M* Na_2SO_4 and 0.5 *M* H_2SO_4 from surface tension measurements of unparalleled precision. The direct measurement of the electrode admittance became possible only after PROSKURNIN AND FRUMKIN[3] had demonstrated the effect of organic impurities on the capacitance of stationary electrodes, and after GRAHAME[4] had developed instrumentation to circumvent this problem by using a dropping mercury electrode. Since then, bridge measurements of the electrode admittance have been used extensively, and have contributed significantly to our understanding of the double-layer structure[5], the kinetics of electrode reactions[6] and adsorption processes[7], and, recently, of the interplay between adsorption and electrode kinetics[8]. All these developments were based on bridge measurements like those of GRAHAME[4], which are precise but time-consuming.

Many attempts have been made to obtain the same information more rapidly. So-called a.c. polarography was developed by MACALEAVY[9] and BREYER AND GUTMANN[10], but it neglected the effects of resistance in series with the electrode and the phase relationship between voltage and current. Modern instrumentation goes back to two patents of JESSOP, who introduced phase-sensitive detection[11] and automatic compensation for series resistance *via* positive feedback[12]. An instrument incorporating these innovations[13] has found a rather limited acceptance for general electrochemical work as it was designed primarily for analytical use. Only recently have JESSOP's ideas been incorporated in other instruments. DEFORD *et al.*[14] described an instrument which monitors the absolute magnitude and the in-phase component of the electrode admittance, using both positive feedback and phase-sensitive rectification. A different approach is that of HAYES AND REILLEY[15], who described an instrument which elegantly avoids the difficulties of positive feedback and uses a multiplier for phase-selective detector. In the present communication, we will describe an instrument similar to that of DEFORD *et al.*[14] with the incorporation of modern lock-in techniques. This instrument has been in continuous use for well over a year without major

* This manuscript is submitted for publication with the understanding that the United States Government is authorized to reproduce and distribute reprints for governmental purposes.

breakdown, and has been applied to a number of problems ranging from measurements of double-layer capacitance and faradaic impedance to those of photo-emission of electrons. It is specifically designed for use with a dropping mercury electrode.

CIRCUIT DESCRIPTION

An alternating voltage is derived *via* follower 1 and a divider network from an external oscillator, and is fed to the summing point (negative input) of a potentiostat–booster combination, 3+4, see Fig. 1. Also fed to that summing point are an initial potential derived from the power supply *via* a potentiometer, a voltage ramp from integrator 2, the output of follower 5 sensing the potential of a reference electrode (the usual negative feedback loop) and a fraction of the output of current amplifier, 6. The latter signal provides the positive feedback[12,14,16] correcting for resistance between the reference electrode and the negative input of amplifier 6.

The output of amplifier 6 is passed through a second order high-pass filter 7, further amplified (8) and inverted (9). The outputs of 8 and 9 are chopped by FET series switches, summed by amplifier 10 and finally averaged by a third-order low-pass Butterworth filter 11. The signal driving the FET choppers is derived from the a.c. input after phase-shifting (12), squaring, proportioning (13) and inverting (14). Thus,

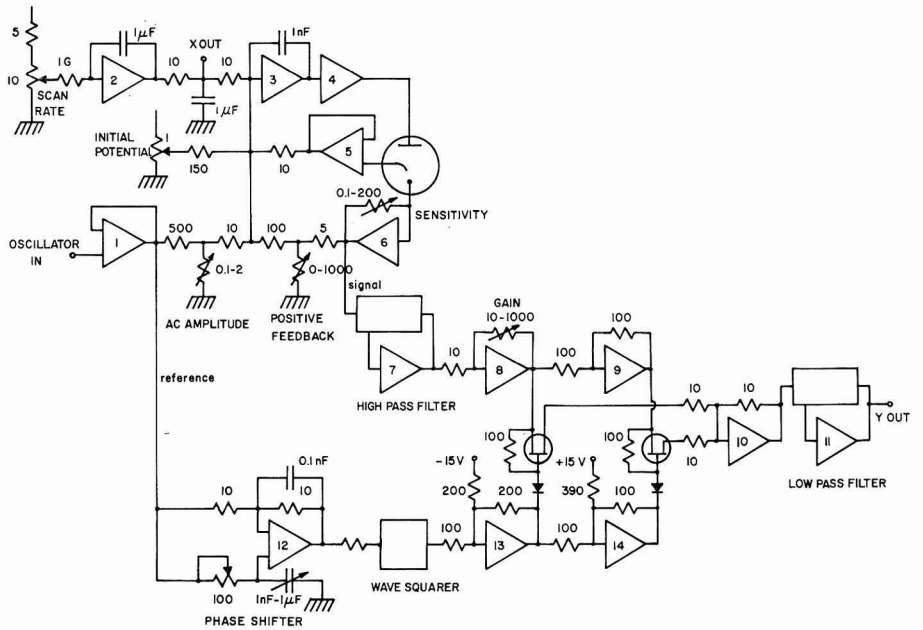

Fig. 1. The electronic circuit used. Amplifiers 1–6 control the voltage, and amp. 7–14 measure the current *via* synchronous rectification. Amp. 2: Philbrick SP 2 AU; amp. 4: Burr Brown 3016/25; amp. 6: Philbrick P 45 AU; all other amp.: Philbrick P 65 AHU. Resistors: Sprague metal film type 420 EBC 3, values in kΩ (except for 1 GΩ in ramp generator circuit); transistors: MPF 105. Resistor box in positive feedback loop: General Radio 1434 G. The compensated resistance is given by $RR'/10(R+5)$ for $R \ll 100$, where R' is the value of the feedback resistor across amp. 6 (sensitivity) and R the value dialed on the positive feedback resistor box, all values taken in kΩ. Only one of two identical phase-shifting RC networks is shown on the positive input of amp.12.

amplifiers 7–14 comprise a simple lock-in amplifier[11,17] and may be replaced by a commercial unit.

The following switches were omitted from Fig. 1 for greater clarity: a reset-hold-scan switch on the ramp generator 2, a switch connecting the positive input of follower 5 directly to the output of booster 4 (for use with 2 electrodes and dummy cells), a switch replacing the cell by a dummy consisting of a resistor in series with either

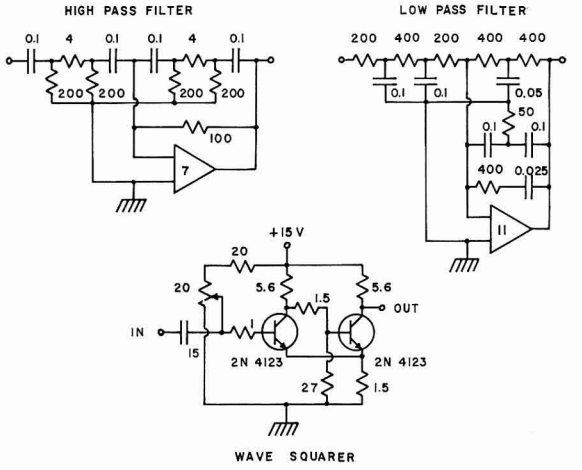

Fig. 2. The (second-order) high-pass filter, (third-order) low-pass filter and wave-squarer of Fig. 1. Amplifiers: Philbrick P 65 AHU. Resistance in kΩ, capacitance in μF.

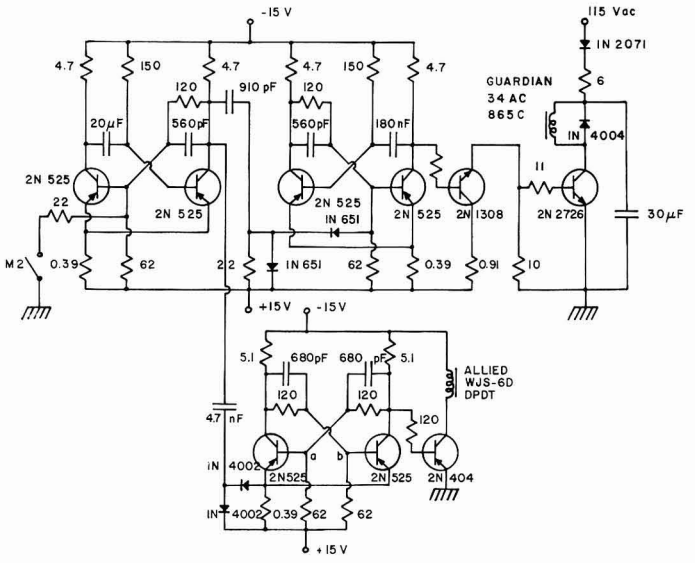

Fig. 3. Circuit driving the hammer coil (Guardian) and a double-pole double-throw relay (Allied) which switches one phase-shifting RC combination on amp. 12 for another, thus yielding alternately in-phase and quadrature readings. Connecting point a or b to ground *via* 22 kΩ will fix the position of the relay so that only one vector component is registered, as in Fig. 4. Resistance in kΩ.

another resistor or a capacitor (for phase adjustment and calibration), and finally a relay-driven switch replacing one adjustable resistor–capacitor combination by another, similar one in the phase-shifting network of amplifier 12. Details of the filters and of the wave squarer (a simple Schmidt trigger) are given in Fig. 2. The potentiometers for initial potential and ramp speed can be connected to +15V, ground, or −15V on the Philbrick PR300 power supply used. Separate +15V and −15V wires lead from the power supply to each amplifier. Right at the amplifier sockets, 15-μF electrolytic capacitors are connected between ground and the power supply terminals in order to prevent high-frequency signal transmission *via* the power supply. The ground bus is made out of 1/8 in. o.d. copper tubing, with connections kept as short as possible. Oscillator used: General Radio 1310A; XY recorder: Hewlett Packard 7035 BM.

Figure 3 illustrates the switching mechanism which regulates the drop-time. A synchronous motor drives a cam which actuates two microswitches, M1 and M2. Closing of M1 deactivates the electrical pen lift on the recorder, so that a data point is plotted. Closing of M2 drives a hammer which dislodges a mercury droplet f om the electrode, and also replaces one phase-shifting network (Fig. 1, amplifier 12) by the other. Thus, alternate readings can yield the in-phase and quadrature components of the electrode admittance. A manual switch-setting overrides the alternation of phase-shifting networks in case only one component is wanted.

INSTRUMENT PERFORMANCE

Measurements on a dummy cell (0.1–1 μF in series with 0.1–100 kΩ) indicated that adequate correction for uncompensated resistance up to about 10 kΩ can be achieved at frequencies up to about 1 kHz. At higher frequencies, phase shifts in the feedback loop prevent proper compensation. Reduction of the feedback capacitor across the potentiostat amplifier (3 in Fig. 1) raises the frequency limit, but invariably leads to uncontrollable oscillations when the dummy is replaced by an actual electrochemical cell. Other feedback configurations[16] and other amplifiers have been tried, but the performance seems to be roughly the same. Apparently, stray capacitance and inductance in the instrument, the cell and the cell leads, limits the frequency response.

The lower frequency limit of the instrument is determined by the Butterworth filters used. The filters of Fig. 2 have 3 db. points of about 16 Hz. Operation at somewhat lower frequencies using other filters, is quite feasible as long as the frequency used significantly exceeds those associated with drop growth[18] and as long as the low-pass output filter does not introduce a measurable time-lag which would lead to a response which is too low, especially when the instrument is calibrated with a dummy cell. This latter point is not always appreciated[19].

A fair idea of the performance of the instrument can be obtained from the following examples. Figure 4 shows actual measurements (every single mercury droplet yields one single point) of the double-layer capacitance of 0.1 *M* KCl at 200 Hz. Comparison with data obtained by GRAHAME[20], Fig. 5, shows agreement to within the readability of the recorder data. Figure 6 shows the in-phase and quadrature components of the electrode impedance of a solution of hexamethylphosphoramide. Note that the desad* peaks exhibit both in-phase and quadrature components at this

* desorption–adsorption

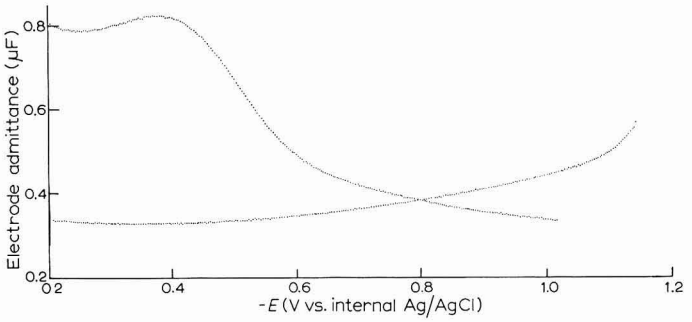

Fig. 4. Quadrature component of the electrode admittance for 0.1 *M* KCl at 25°. Alternating voltage: 200 Hz, amplitude 10 mV (20 mV top-to-top). Compensated resistance: 322Ω. Every single point corresponds to one mercury droplet. Drop-time regulated at 6.00 sec. Bottom curve shifted by 0.8 V, covering range, −1.0 to −1.8 V. An independent, duplicate run does not differ by more than 0.5 mm in admittance over the whole range of potentials; 0.5 mm corresponds to 0.15 μF cm^{-2}. This suggests that the main source of error is the readability of the recorder trace. A digital voltmeter, gated by the pen-lowering signal, might be used to circumvent this difficulty if higher readability is required. Instrument sensitivity was calibrated with capacitors of accurately known capacitance, hence the admittance axis is indicated in terms of microfarads. The proper unit of admittance, Ω^{-1}, is obtained by multiplication of the capacitance, in farads, by the angular frequency ω of the sine wave used. This explains the use of, *e.g.*, 318 Hz (ω = 2000 rad sec^{-1}) in Fig. 6.

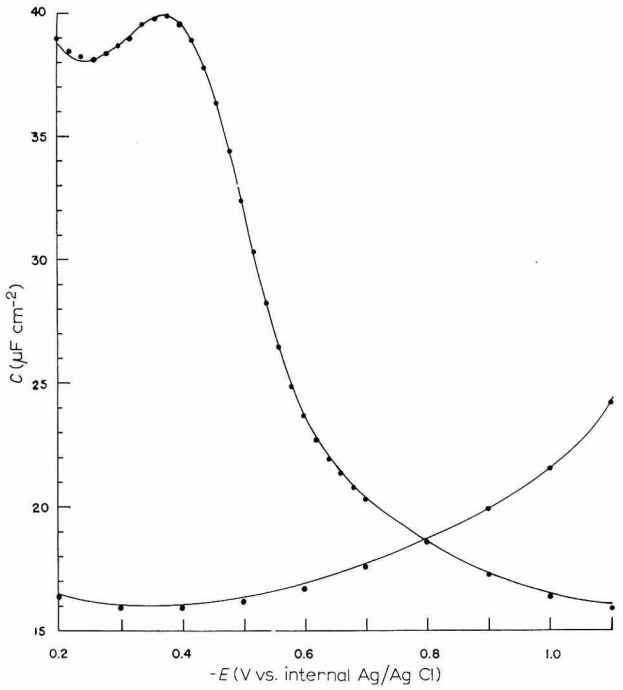

Fig. 5. Comparison of double-layer capacitance data calcd. from Fig. 4 (points) and bridge measurements of GRAHAME[20] (line). Note the expanded capacitance scale. For the calculation, the following measured data were used: mercury mass flow rate 0.635±0.007 mg sec^{-1}, drop age 5.867±0.010 sec, corresponding to a spherical drop of 2.045±0.015 mm^2 surface area. The potential scale used is 37 mV negative with respect to 0.1 NCE, 16 mV more positive than NCE.

frequency, in agreement with theory[21]. Figure 7 illustrates the redox* peak of indium(III) in thiocyanate, and the negative Faradaic admittance[22,23] in the region of the polarographic minimum, Fig. 8. Bridge measurements in the latter region are often hampered by oscillations[24] resulting from the interplay of the negative admittance and the inductance of bridge transformers. Figure 9 shows the highly irreversible reduction of hex*aquo*nickel(II) and the more reversible reduction of a basic nickel polymer. The latter is not obvious from the d.c. polarogram (Fig. 10) in view of its

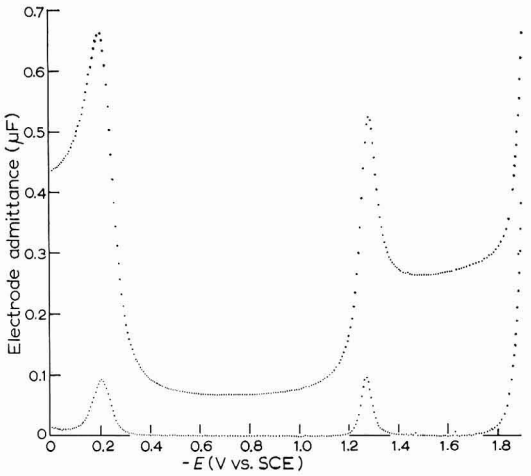

Fig. 6. Quadrature (top) and in-phase (bottom) components of the electrode admittance of 0.1 *M* NaF satd. with N_2O and containing 0.1% (v/v) of hexamethylphosphoramide, $OP(N(CH_3)_2)_3$. Alternating voltage: 318 Hz, amplitude 10 mV. Compensated resistance: 616 Ω. Note the in-phase components of the desad peaks.

low concentration (about 0.1% of the total nickel concentration). Finally, Fig. 11 shows how this type of instrumentation can be used to measure electrochemical photocurrents. In this case, the wave generator is omitted, and the mercury drop illuminated with monochromatic light, obtained in our set-up from a 100-W mercury lamp (PEK 110) with quartz collimator lense, interference filter, two choppers and focusing lenses. One chopper interrupts the light beam at a frequency in the range, 15–1000 Hz, with a separate photo-detector providing the reference signal for the synchronous rectification. The second chopper rotates at 0.1 Hz, alternately passing and interrupting the light beam for periods of 5 sec. It also actuates the microswitches regulating the pen lift and drop hammer. Consequently, alternate points indicate photo-current and dark current, see Fig. 12. The above data are presented for the purpose of illustration only. We will elaborate on the electrochemical aspects of some of the above systems in another publication.

DISCUSSION

A.c. polarography without correction for uncompensated resistance is restricted to low frequencies, low solution resistivity and low concentrations of electroreducible substances, for the effects of uncompensated (solution and capillary) resistance to be

* reduction–oxidation

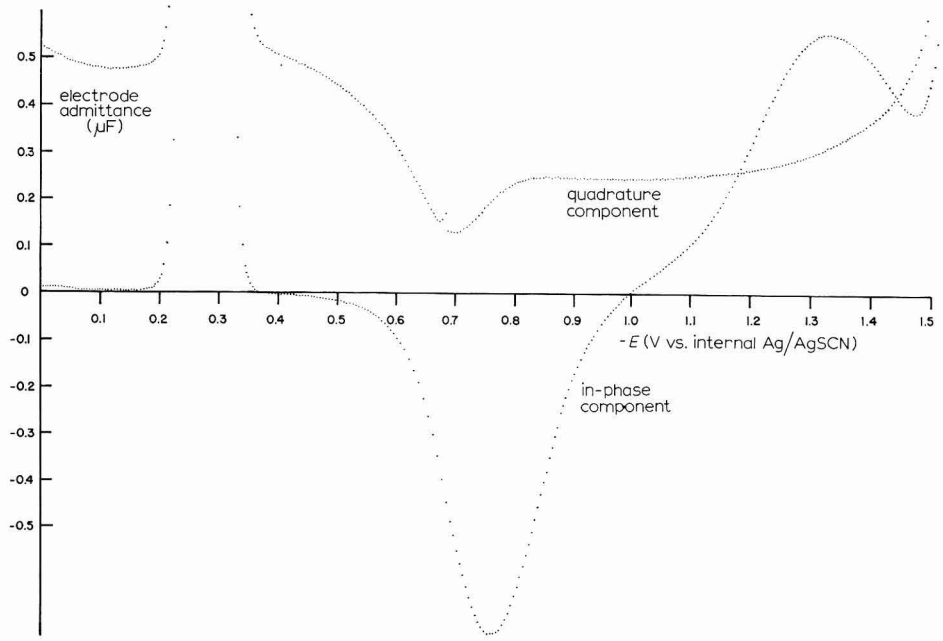

Fig. 7. In-phase and quadrature components of the electrode admittance of 2 mM $In(SCN)_3$ in 1.0 M NaSCN acidified with HSCN to pH 3.24 at 25°. Alternating voltage: 31.8 Hz, amplitude 10 mV. Compensated resistance: 206 Ω. The redox peak is seen in both in-phase and quadrature components around −0.28 V, and the negative faradaic admittance is clearly visible, especially on the in-phase component (the few high points near −0.67 V on the quadrature component are due to a momentary oscillatory behavior of the instrument, which will occur when a mercury droplet does not dislodge properly from the capillary).

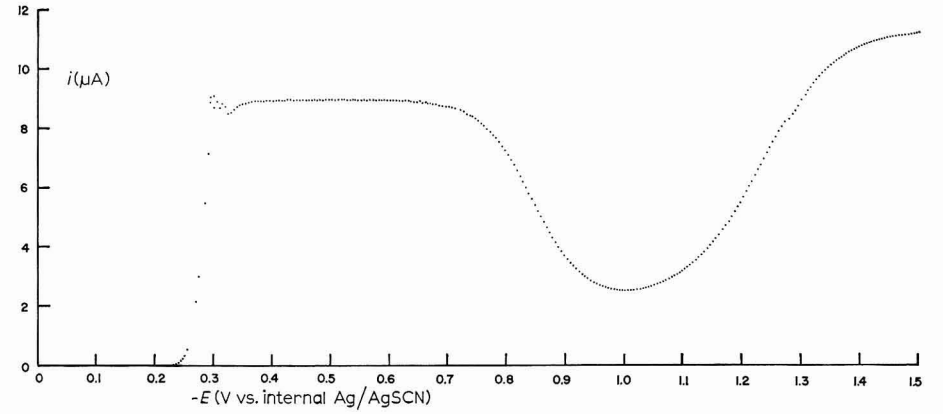

Fig. 8. Polarogram of the solution of Fig. 7, obtained by applying zero alternating voltage and connecting the recorder Y input directly to the output of amp. 6 (Fig. 1). Curve given here for reference, showing the position of the wave (with maximum) near −0.3 V, and of the polarographic minimum.

negligible. One would think that positive feedback might eliminate this restriction completely, but this is not yet quite the case. Positive feedback forces the circuit to live continuously in the shadow of oscillations, resulting from phase shifts at high frequencies in small stray capacitances (Such oscillations may not always be apparent from the recorder output, since the synchronous rectifier rejects them quite efficiently; we have found it very useful to monitor more or less continuously the output of the summing amplifier (# 10 in Fig. 1) on a scope (Hewlett Packard 130 C) which is also used for occasional checks of square wave symmetry and of other signals in the instrument). In order to restrain the oscillations, we must restrict either the upper frequency limit of the instrument or

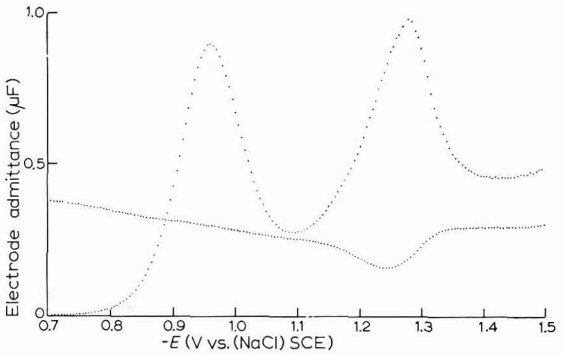

Fig. 9. In-phase and quadrature components of the electrode admittance of 0.1 M $Ni(ClO_4)_2$ in 2.8 M $LiClO_4$ at pH 6.88; $Ni(OH)_2$ removed by centrifuge. Alternating voltage: 318 Hz; 10 mV amplitude. Compensated resistance: 193 Ω. The slow reduction of Ni^{2+} near −0.9 V and the much faster reduction of a small amount (about 0.1 mM) of polymeric nickel around −1.28 V are most easily seen on the in-phase component. Note the negative faradaic capacitance around −1.24 V.

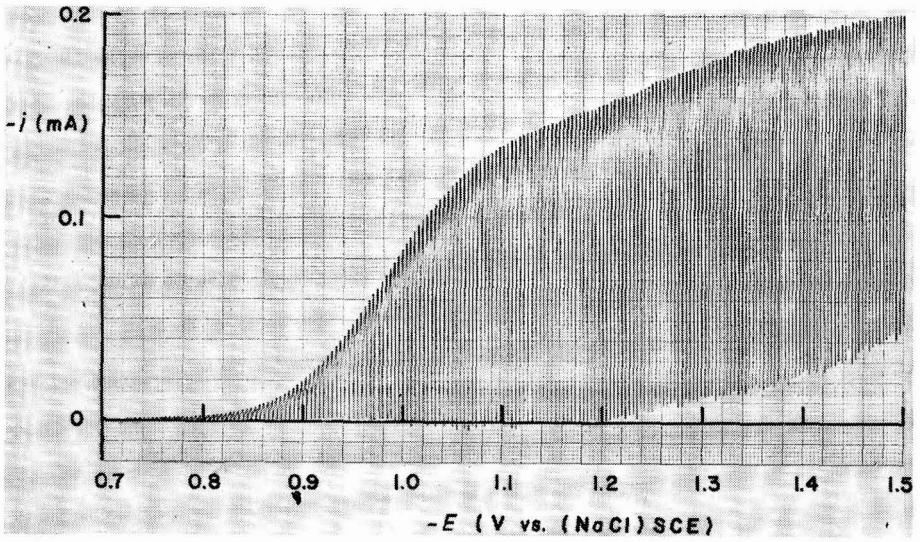

Fig. 10. Polarogram of the solution of Fig. 9, showing the absence of a distinguishable wave near −1.28 V. Figs. 9 and 10 also illustrate that a "totally irreversible" polarographic wave still gives rise to a small faradaic admittance, in accordance with MATSUDA's calculations[6].

the maximum resistance which the instrument can correct for. The present instrument yields results within the limits of recorder precision and readability (about $\pm 0.5\%$ of full scale) in solutions of 0.1 *M* ionic strength up to at least 500 Hz, and still performs quite reasonably in solutions of 0.01 *M* ionic strength. In 0.001 *M* solutions, useful data have been obtained only with a larger feedback capacitor (10 nF) across the potentiostat amplifier (#3 in Fig. 1) with a consequent diminution of usable frequency range. This makes the instrument still practicable for measurements of double-layer capacitance or photo-current in such dilute solutions, but severely limits its usefulness for the study of electrode kinetics at low ionic strength.

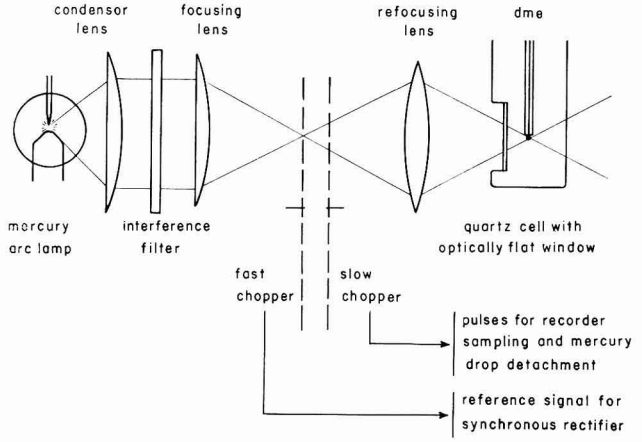

Fig. 11. The optical set-up used for the measurement of photo-effects. All optical elements are quartz. The fast (15–1000 Hz) chopper provides a reference signal for the synchronous rectifier, the slow (0.1 Hz) chopper regulates recorder sampling and drop-time *via* two microswitches.

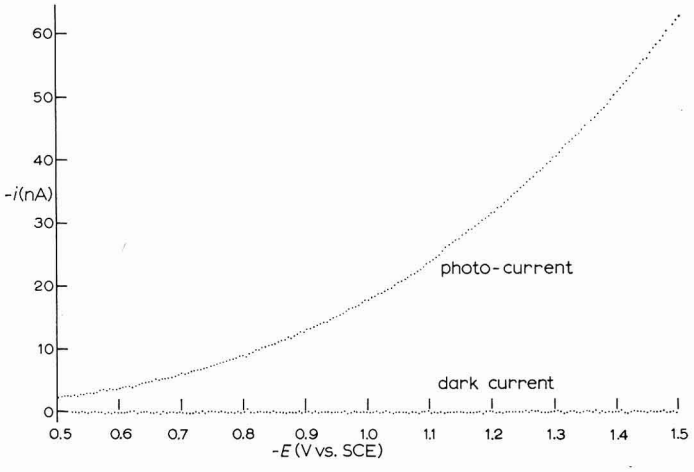

Fig. 12. Photo-current of 0.5 *M* NaF satd. with N_2O, measured with the set-up of Fig. 11. Wavelength: 366 nm, half-width 10 nm. Frequency of fast chopper: 15.9 Hz; compensated resistance 140 Ω. The above data fit a linear plot[30] of $(-i)^{0.4}$ *vs.* $-E$.

The frequency limitation is not a fundamental one but rather is inherent to the present design. Nevertheless it appears that an approach like that of HAYES AND REILLEY[15], which corrects *a posteriori* for the iR drop, is more readily extended to significantly higher frequencies. On the other hand, such an approach is not feasible when the electrochemical signal is generated in the electrode rather than in the external circuit, as is the case with photo-emission of electrons.

The proper amount of positive feedback is found[14] by monitoring the in-phase component of the admittance in a region of potentials where no in-phase component should be present. Such a region can almost always be found. First, the required instrument sensitivity is selected and the instrument is phased (Fig. 1, amplifier 12) using a series resistor–capacitor combination as dummy cell and the appropriate, calculated compensation for the series resistance. Proper phasing is achieved when the in-phase component vanishes from the output. The same procedure is then repeated with the cell, this time adjusting only the amount of positive feedback while leaving the sensitivity and phase controls untouched. In order to set the second pair of phase controls orthogonal to the first, the dummy cell capacitor is replaced by a resistor, and the phase control potentiometer adjusted until the quadrature component in the output vanishes (on many commercial lock-in amplifiers which might be substituted for amplifiers 7–14, a 90°-phase shift can easily be obtained by turning a switch).

Since the uncompensated solution resistance depends on the size of the mercury drop, proper correction can only be achieved at one moment in drop life. The solution resistance decreases with time, so that overcompensation will occur after the selected balancing time, making the circuit more prone to oscillations. Therefore, the balancing point must be taken just before the drop falls, *i.e.*, when the solution resistance is smallest and varies least. Only the reading taken at that moment is properly corrected for uncompensated resistance, and this is why the present instrument presents one data point per drop. Averaging of the signal over drop life[19] amounts to only partial correction of uncompensated resistance.

The uncompensated resistance is treated here as a function of drop size only, although, strictly speaking, it also depends on the electrode admittance. This is a consequence of the shielding effect of the bottom end of the capillary, which results in an uneven current distribution. As long as Y_{el} is small, one has the secondary current distribution around the drop. The dimensionless parameter involved appears to be $\varrho r Y_{el}$ where ϱ is the solution resistivity (in Ω cm), r the drop radius (in cm) and Y_{el} the specific electrode admittance (in Ω^{-1} cm^{-2}). A secondary current distribution around the mercury drop can be anticipated* whenever $\varrho r Y_{el} \ll 1$. Since ϱ is of the order of $10/m$ Ω cm where m is the ionic strength in moles/l, and r is of the order of 0.1 cm near the end of the drop life, Y_{el} should be much smaller than m Ω^{-1} cm^{-2} in order that the solution resistance be constant, and this is usually the case. For low-frequency double-layer capacitance measurements this condition is certainly satisfied, but at high frequencies it may not be, as the following estimate shows: $C = 20 \mu$F cm^{-2} and $\omega = 500$ sec^{-1} (about 80 Hz), or 500000 sec^{-1} (about 80 kHz) yields $Y_{el} = 10^{-2}$ Ω^{-1} cm^{-2} or 1 Ω^{-1} cm^{-2}, respectively.

* See also the model experiments by GARDNER[31]. Apparently, the values of the dimensionless parameter, ϕ, given there are too large by a factor of 10^6. In these experiments, the current density at the bottom of the model electrode exceeds that calculated by MATYÁŠ[26], presumably as a result of the close proximity of the auxiliary electrode.

In the complete absence of shielding, the solution resistance around a mercury drop[25] is $\varrho/4\pi r$ Ω cm^2, whereas the maximum effect of shielding (*viz.*, the case of a primary current distribution, $\varrho r Y_{el} \gg 1$) corresponds [26,27] to an increase in resistance by a factor of 1.455.

Consequently, the dependence of solution resistance on electrode admittance is small anyway, and has never been observed directly with capacitance measurements. The effect might become important whenever the faradaic admittance exceeds the double-layer capacitance by many orders of magnitude. The same holds for the similar effect resulting from uneven mass transport[28,29].

Negative feedback enhances noise quite significantly, so that frequency-selective detectors are called for if low signal levels are required. Fortunately, phase-selective detectors are automatically frequency-selective. In a synchronous rectifier like the one used here, even harmonics do not contribute to the output, and $(2n+1)$th harmonics are attenuated by a factor $(2n+1)$ when both switches are conducting for exactly half of the period of the fundamental frequency. If the square wave driving the FET switches is asymmetrical, then harmonics are attenuated by a factor $[1-(-1)^n \cos n\delta]/n$ where δ is the asymmetry of the square wave in radians (*i.e.*, periods of $\pi+\delta$ and $\pi-\delta$ rather than two equal half-periods of π radians).

Using scale expansion to avoid the first part of the sweep which is often not quite linear, asymmetry of 0.04 radians in the square wave driving the FETs is readily detected on a monitoring scope. Such asymmetry would correspond to an error of 0.4% in the signal at the fundamental frequency, whereas any second harmonic is still attenuated more than 60 times. Hence, no significant amount of second harmonic ends up in the output, and the response at the fundamental frequency is not measurably affected, when the square wave is adjusted visually for correct symmetry with the potentiometer in the wave-squaring circuit, Fig. 2. As the amounts of nth harmonics resulting from non-linearities in the admittance–voltage relation are proportional to the nth power of the amplitude, the contributions of third, fifth etc., harmonics are usually negligible at excitation levels of 10-mV amplitude or less.

In most commercial lock-in amplifiers, the signal first passes a narrow band pass filter in order to reject odd harmonics and to decrease the possibility of amplifier overload. However, very good frequency stability is required of both the oscillator and the filter lest phase shifts are introduced. Moreover, some sharply tuned filters tend to generate slowly decaying oscillations at their resonant frequency upon sudden variations in signal level as occur at drop fall, and these may still contribute measurably to the output at the end of the next drop life. The present instrument does not have, nor require, any such tuned filtering, and a change in operating frequency is achieved simply by changing the oscillator frequency.

Complete correction for uncompensated resistance may not always be feasible, as it may lead to oscillations. The error resulting from incomplete correction can readily be estimated from the recorded data. For a purely capacitive electrode admittance, the relative error in the measured capacitance is simply $(Y'/Y'')^2$ where Y' and Y'' are the measured in-phase and quadrature components. Thus, if $Y'/Y''=0.05$, the relative error in the measured capacitance is only 0.003, and even when Y' is 10% of Y'', the resulting error in Y'' is only 1%. Thus, the error in Y'' is almost always negligible, and moreover there is a clear warning whenever the instrumental compensation is inadequate, by the appearance of a non-zero in-phase

component in a region of potentials where it should not be present. If necessary, the resulting error in Y'' can be corrected by calculation *via*

$$Y_{\text{corr}}'' = Y''\{1 + (Y'/Y'')^2\}$$

The remaining, still uncompensated part of the resistance can be estimated from $Y'/\{(Y')^2 + (Y'')^2\}$ and might be used to check the reliability of data in the region where the electrode admittance is not purely capacitive. In general, *a posteriori* correction of data has not been found necessary unless the solutions are very dilute (less than 0.01 *M* ionic strength).

Strictly speaking, the present instrument records components of current rather than an admittance, *i.e.*, the recorder response is directly proportional to the amplitude of the alternating voltage. Division by the latter amplitude no doubt could have been accomplished by slightly modifying the recorder[15] but this does not seem to serve much purpose since the amplitude of the oscillator output is as stable as the amplifiers used in signal handling in the instrument.

The present instrument provides data automatically, with the accuracy, speed, and convenience of a polarogram. The usefulness of the obtainable information can be judged from the illustrations given. The available frequency range is almost three orders of magnitude smaller than that of the best bridges, so that the instrument has only limited applicability to investigations of very fast electrode kinetics. However, for many measurements the instrument is quite adequate, and there its speed and reliability are very helpful features.

ACKNOWLEDGEMENTS

Dr. L. P. MORGENTHALER and Mr. W. H. CRAIG gave valuable assistance in the design and construction of electronic circuits. The application to photo-emission of electrons was worked out in cooperation with Miss J. C. KREUSER and Mr. P. A. FENTON. Figures 9 and 10 were taken from the yet unpublished work of B. KENNEDY AND L. P. MORGENTHALER on the hydrolysis products of nickel. The present research was supported in part by the National Science Foundation under Grant GP 5432 and by the Air Force Office of Scientific Research, Office of Airospace Research, United States Air Force, under AFOSR grant 68-1344.

SUMMARY

An instrument is described which will automatically plot the in-phase and quadrature components of the electrode admittance in the fashion of a polarogram. Correction for uncompensated series resistance is achieved by positive feedback, and synchronous rectification is used for signal detection. The limitations of the instrument are discussed, and illustrations of its applicability are given.

REFERENCES

1 G. LIPPMANN, *Compt. Rend.*, 76 (1873) 1407; *Pogg. Ann.*, 149 (1873) 561; *J. Phys.*, 3 (1874) 41.
2 G. GOUY, *Ann. Chim. Phys.*, 29 (1903) 145.
3 M. PROSKURNIN AND A. N. FRUMKIN, *Trans. Faraday Soc.*, 31 (1935) 110.
4 D. C. GRAHAME, *J. Am. Chem. Soc.*, 63 (1941) 1207.

5 D. C. GRAHAME, *Chem. Rev.*, 41 (1947) 441.
6 J. E. B. RANDLES, *Discussions Faraday Soc.*, 1 (1947) 11,47; H. MATSUDA, *Z. Elektrochem.*, 62 (1958) 977.
7 V. I. MELIK GAIKAZYAN, *Zh. Fiz. Khim.*, 26 (1952) 560.
8 P. DELAHAY, *J. Phys. Chem.*, 70 (1966) 2069, 2373.
9 C. MACALEAVY, *Belgian patent 443,003* (1941); *French patent 886,848* (1942).
10 B. BREYER AND F. GUTMANN, *Trans. Faraday Soc.*, 42 (1946) 645,650; 43 (1947) 785, *Discussions Faraday Soc.*, 1 (1947) 19.
11 G. JESSOP, *British patent 640,768* (1950).
12 G. JESSOP, *British patent 776,543* (1957).
13 Univector Polarograph Unit, Cambridge Instrument Company, Ltd., London.
14 E. R. BROWN, T. G. MCCORD, D. E. SMITH AND D. D. DEFORD, *Anal. Chem.*, 38 (1966) 1119.
15 S. W. HAYES AND C. N. REILLEY, *Anal. Chem.*, 37 (1965) 1322.
16 W. JACKSON AND P. J. ELVING, *Anal. Chem.*, 28 (1956) 378; C. F. MORRISON, *Generalized Instrumentation for Research and Teaching*, Washington State University Press, Pullman (Wash.), 1964, p. 96; D. POULI, J. R. HUFF AND J. C. PEARSON, *Anal. Chem.*, 38 (1966) 382; G. LAUER AND R. A. OSTERYOUNG, *Anal. Chem.*, 38 (1966) 1106.
17 J. SCHÖN, W. MEHL AND H. GERISCHER, *Z. Elektrochem.*, 59 (1955) 144; Z. KOWALSKI AND J. SRZEDNICKI, *J. Electroanal. Chem.*, 8 (1964) 399.
18 M. T. KELLEY AND D. J. FISHER, *Anal. Chem.*, 28 (1956) 1130.
19 R. F. EVILIA AND A. J. DIEFENDERFER, *Anal. Chem.*, 39 (1967) 1885.
20 D. C. GRAHAME, *Techn. Rept. to U.S.Office of Naval Research*, 1 (March 9, 1950); 7 (Dec. 13, 1951).
21 A. N. FRUMKIN AND V. I. MELIK GAIKAZYAN, *Dokl. Akad. Nauk SSSR*, 77 (1951) 855.
22 H. SHIRAI, *J. Chem. Soc. Japan, Pure Chem. Sect.*, 81 (1960) 1248.
23 N. TANAKA, T. TAKEUCHI AND R. TAMAMUSHI, *Bull. Chem. Soc. Japan*, 37 (1964) 1435.
24 M. SLUYTERS-REHBACH, B. TIMMER AND J. H. SLUYTERS, *Z. Physik. Chem. Frankfurt*, 52 (1967) 1.
25 D. ILKOVIČ, *Collection Czech. Chem. Commun.*, 4 (1932) 480.
26 Z. MATYÁŠ, *Věstn. Kralov. Ceske Spolecnosti Nauk, Třída Mat. Přírod.*, 30 (1944) 1.
27 I. M. KOLTHOFF, J. C. MARSHALL AND S. L. GUPTA, *J. Electroanal. Chem.*, 3 (1962) 209.
28 H. MATSUDA, *Bull. Chem. Soc. Japan*, 26 (1953) 342.
29 R. DE LEVIE, *J. Electroanal. Chem.*, 9 (1965) 311.
30 YU.YA.GUREVICH, A. M. BRODSKII AND V. G. LEVICH, *Elektrokhim.*, 3 (1967) 1302.
31 A. W. GARDNER, *Polarography 1964*, edited by G. J. HILLS, MacMillan, London, 1966, p. 187.

ELECTROANALYTICAL CHEMISTRY AND INTERFACIAL ELECTROCHEMISTRY
Elsevier Sequoia S.A., Lausanne – Printed in The Netherlands

GLASS REFERENCE ELECTRODES IN MOLTEN (Li,K)NO_3

G. GIORGIO BOMBI, GIAN-ANTONIO MAZZOCCHIN AND MARIO FIORANI*
Istituto di Chimica Analitica dell'Università, Padova (Italy)
(Received July 13th, 1968)

INTRODUCTION

Electrochemical cells in which the two half-cells are separated by a glass diaphragm have been widely employed in the study of molten salt systems[1,2]. Particularly, a half-cell of the type:

$$\mathrm{Ag}\,\left|\begin{array}{l}\mathrm{Ag^+\ diluted\ in\ a}\\ \\ \text{molten salt solvent}\end{array}\right|\,\text{glass}\,\Big|$$

has been proposed for use as a reference half-cell in molten alkali halides[3] and nitrates[4]. A half-cell of this kind, including the glass partition, will, in the following, be referred to as "glass reference electrode" or GRE.

An obvious advantage of the use of a solid partition instead of a liquid junction obtained *via* a porous partition, an asbestos fibre, or simply a hole, lies in the fact that the former completely prevents any cross-contamination of the contents of the two half-cells. Another, more fundamental, advantage is often claimed, *i.e.*, that (owing to the fact that glasses are essentially cationic conductors) the junction potential of a glass diaphragm should be easier to calculate than the potential of a liquid junction.

In the particular case of a cell in which the salt phases and the glass contain a single cation it is, in fact, easy to show that the junction potential vanishes. However, when more than one cation is present, not only will all the cations be able, as a general rule, to migrate in the glass but, in addition, ion exchange reactions between glass and salt phases will occur.

It has been shown[5] that, under rather general assumptions, the junction potential at the interface between a cation exchanger and a solution containing several univalent cations depends on the activities, a_i, of the cations in the solution through the equation

$$E_j = \text{const.} + (RT/F)\ \ln\ (\Sigma_i k_i a_i) \qquad (1)$$

The "selectivity ratios", k_i, are given by $k_i = (u_i/u_1)K_{1i}$ where u_i is the mobility of i-th cation in the exchanger and K_{1i} is the equilibrium constant for the ion-exchange reaction involving the first and i-th cation (obviously $k_1 = K_{11} = 1$).

This equation accounts for the behaviour of pH- and cation-sensitive glass

* Present address: *Istituto di Chimica Generale dell'Università, Cattedra di Chimica Analitica, Camerino (Italy).*

electrodes in water[6]; its validity in a molten salt system was recently demonstrated by NOTZ AND KEENAN[7], who studied the behaviour of a Pyrex glass membrane electrode in molten NH_4NO_3 containing various solute cations. An important consequence of eqn. (1) is that a cation having a low mobility in the glass can affect the glass–melt potential, since the selectivity ratio, k, depends also on the equilibrium constant, K.

Pyrex and soft-glass GRE's have been extensively used in this laboratory as reference electrodes in molten $(Li,K)NO_3$[8–12] and $(Na,K)NO_3$[13,14]: in the present paper the results of an investigation on the behaviour of these electrodes in $(Li,K)NO_3$ are reported.

EXPERIMENTAL

The GRE's (Fig. 1) were prepared from 9-mm o.d. and 6-mm i.d. Pyrex or ordinary soft-glass (about 71% SiO_2, 4% Al_2O_3, 1% B_2O_3, 15% Na_2O, 2% K_2O, 7% CaO) by blowing a bulb having a diameter of 9–10 mm and a minimum wall thickness (at the bottom) of about 0.1–0.2 mm. The standard tapered cone, A, served to insert

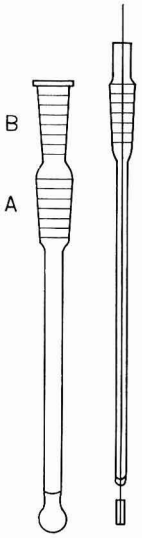

Fig. 1. Glass reference electrode.

the electrodes in the experimental cell; the standard tapered stopper, B, bore a Pt wire sealed in a glass tube ending with a Pt foil (4 × 10 mm). The foil was silver-plated in a cyanide bath according to the procedure described by IVES AND JANZ[15]. The electrodes were filled to a 2-cm height with an approximately 10^{-2} m solution of $AgNO_3$ in $(Li,K)NO_3$ (43 mole% $LiNO_3$) and kept in an oven at about 160°.

The cell and thermostat, as well as the method of preparation of the solvent and the operating procedure, are essentially as previously described[11]; chemicals other than $LiNO_3$ and KNO_3 were all reagent-grade and were used without further purification. Temperature was controlled within ±0.2°; the e.m.f.-values were measured with a Solartron type LM 1420 integrating digital voltmeter.

RESULTS

Asymmetry potential

The asymmetry potential of the GRE's was measured at 10-degree intervals between 150° and 200° by means of the cell

$$\mathrm{Pt}\,\left|\,\mathrm{Ag}\,\right|\,\begin{matrix}(\mathrm{Li,K})\mathrm{NO_3}\\ \mathrm{AgNO_3}(m_1)\end{matrix}\,\Big|\,\mathrm{glass}\,\Big|\,\begin{matrix}(\mathrm{Li,K})\mathrm{NO_3}\\ \mathrm{AgNO_3}(m_2)\end{matrix}\,\Big|\,\mathrm{Ag}\,\Big|\,\mathrm{Pt} \qquad (2)$$

for $m_1 = m_2$, *i.e.*, by immersing the GRE's in a solution having the same silver nitrate content as inside the bulb.

The potential of the inner electrode was always more negative than that of the outer electrode; for different GRE's (both of Pyrex and of soft-glass) the difference ranged between 30 and 40 mV and was practically independent of the temperature (within ±1 mV) and of aging (as was found also by INMAN[4]). This value of the asymmetry potential is higher than that found by other authors[4,7]; however, the asymmetry potential is probably strongly affected by the details (*e.g.*, temperature) of the blowing procedure.

Electrical resistance

The electrical resistance of the GRE's was measured with an a.c. impedance bridge or with an electronic ohmmeter (in the latter case, silver electrodes and identical silver nitrate solutions inside and outside the GRE's were used).

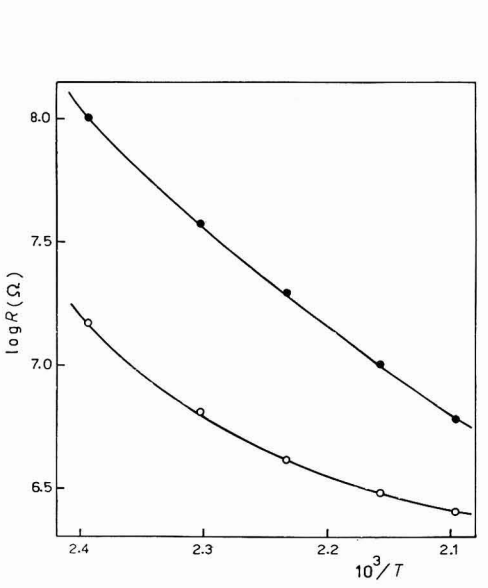

Fig. 2. Temperature-dependence of log R for typical soft-glass (○) and Pyrex (●) GRE's.

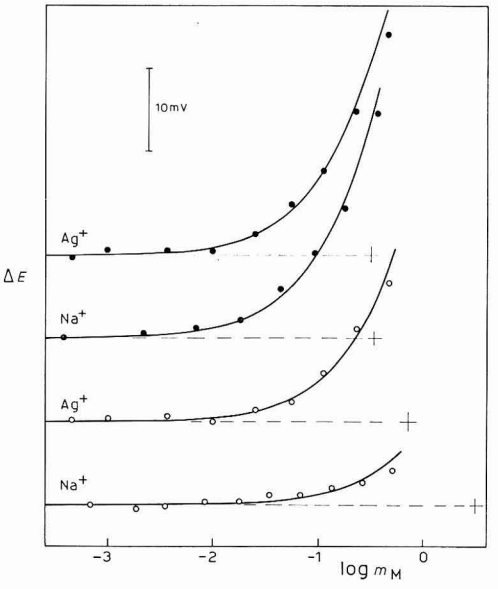

Fig. 3. E.m.f. of cell (3) as a function of the logarithm of the molality of added cation for soft-glass (○) and Pyrex (●) GRE's. The curves were calcd. from the exptl. points, excluding those for $m_M > 0.3$ mole kg^{-1}. (---), represent E*; (+), log m_M-values for which $k' m_M = 1$.

At 160°, typical values of the resistance were about 30 MΩ and 5 MΩ for Pyrex and soft-glass GRE's, respectively; plots of the temperature-dependence of log R are given in Fig. 2. The resistance of Pyrex GRE's was practically unaffected by heating at 300° in $(Li,K)NO_3$ for about 2 h, or after several days of aging above about 180°; the effect on soft-glass GRE's was much more marked, and the resistance dropped to about 0.1 MΩ (at 160°), or less. Chemical analysis showed that in these low-resistance electrodes, sodium ions were almost completely substituted by lithium ions; the lithium-containing glass was opaque and fragile.

Selectivity towards cations

To test the response of the electrodes towards various cations, the e.m.f. of the cell:

$$\mathrm{Pt}\,|\,\mathrm{Ag}\,|\,\begin{matrix}(Li,K)NO_3\\ AgNO_3\end{matrix}\,|\,\mathrm{glass}\,|\,\begin{matrix}(Li,K)NO_3\\ M(NO_3)_n\end{matrix}\,|\,\begin{matrix}\text{porous}\\ \text{diaphragm}\end{matrix}\,|\,\begin{matrix}(Li,K)NO_3\\ AgNO_3\end{matrix}\,|\,\mathrm{Ag}\,|\,\mathrm{Pt} \qquad (3)$$

was measured for varying concentrations of $M(NO_3)_n$, where M^{n+} was Na^+, Ag^+, Tl^+, Hg_2^{2+}, Hg^{2+}, Pb^{2+}, and Cd^{2+}.

The potential of Pyrex GRE's reached a stable value after about 15 min of immersion in the pure solvent. Soft-glass GRE's behaved similarly when aged, but required about 12 h to stabilize when used for the first time. After the additions of $M(NO_3)_n$, stable potential values were reached after about 10–20 min and remained constant (within ± 0.3 mV) for the time of measurement (30–40 min).

Typical results, obtained at 160°, are shown in Figs. 3 and 4, in which the difference between the initial e.m.f., obtained with the pure solvent, and the e.m.f. measured after each addition is plotted *vs.* the logarithm of the molality of the added nitrate. Only Ag^+, Na^+ and Pb^{2+} had an appreciable effect on soft-glass GRE's.*

The addition of $M(NO_3)_n$ to the middle compartment of cell (3) can affect the measured e.m.f. in three ways: (1) by varying the potential of the liquid junction with the right-hand compartment; (2) by lowering the activity of the solvent cations, Li^+ and K^+, by dilution and hence by altering indirectly, through the terms $k_K a_K$ and $k_{Li} a_{Li}$ in eqn. (1), the glass–melt junction potential; (3) by the direct effect of the added cation on the glass–melt potential (term $k_M a_M$ in eqn. (1)). The first two contributions should be negligible (less than 1 mV) at least up to 0.3 mole kg^{-1}, unless extreme deviations from ideality for the mixture of $M(NO_3)_n$ and $(Li,K)NO_3$ and very large differences in the mobility of M^{n+} and Li^+ and K^+ are assumed. Even at concentrations as high as 1 mole kg^{-1} the first two contributions should not exceed a few millivolts. It can therefore be assumed that up to 0.3 mole kg^{-1}, at least, the observed e.m.f. variations are due almost entirely to the direct effect of the added cation on the glass–melt junction potential.

For the case of the addition of a univalent cation, eqn. (1) can be rewritten as follows:

* According to LYALIKOV *et al.*[16], a glass electrode can be used as indicator electrode in connection with a Pt "reference" electrode in acid–base titrations in molten KNO_3. However, the addition to cell (3) of bases (KOH) or acids ($KHSO_4$ or HNO_3) in place of $M(NO_3)_n$ has no effect on the e.m.f., as could be anticipated (see also ref. 7). It appears likely that in LYALIKOV's work the glass electrode had a constant potential, while the "reference" Pt electrode (which apparently was immersed in the solution to be titrated) acted as an oxygen electrode, since it seems that air was not excluded from the titration cell.

$$E_j = \text{const.} + (RT/F) \ln (a_K + k_{Li}a_{Li} + k_M a_M)$$

Since in the concentration range explored, a_K and a_{Li} are constant, and a_M can be identified with the molality m_M of MNO_3, the e.m.f. of the cell can be written as follows

$$E = E^* + (RT/F) \ln (1 + k_M' m_M)$$

where E^* is the e.m.f. in the absence of solutes in the middle compartment and $k_M' = k_M/(a_K + k_{Li}a_{Li})$. The latter equation can be linearized:

$$\exp(EF/RT) = \exp(E^*F/RT) + \exp(E^*F/RT) k_M' m_M$$

By applying the least-squares method to this equation (introducing the proper weight factors, *i.e.*, $[(F/RT)\cdot\exp(EF/RT)]^{-2}$), the values of k_M' were obtained for the cases of Ag^+ and Na^+. As the term $k_M' m_M$ is never larger than unity, even in the most favourable cases, the values of k_M' are rather uncertain and show appreciable variations between individual GRE's; the values for the curves reported in Fig. 3, which can be considered as typical, are $k_{Ag}' = 3.1$ (Pyrex); 1.4 (soft-glass) and $k_{Na}' = 2.9$ (Pyrex); 0.3 (soft-glass).

It is easy to show, on the basis of the same general arguments leading to eqn. (1), that the dependence of E_j on m_M when M is a divalent cation is similar to that for a univalent cation. In fact, E_j should be independent of m_M for low m_M-values and should vary linearly with log m_M, with the Nernst slope, for high enough m_M-values. However, in this case it is not possible to express E_j by an explicit formula, valid also in the intermediate region where both the solvent cations and M^{2+} affect the E_j-value. The full lines for divalent cations in Fig. 4 have, therefore, no theoretical meaning and were drawn simply to visualize the behaviour of the GRE's.

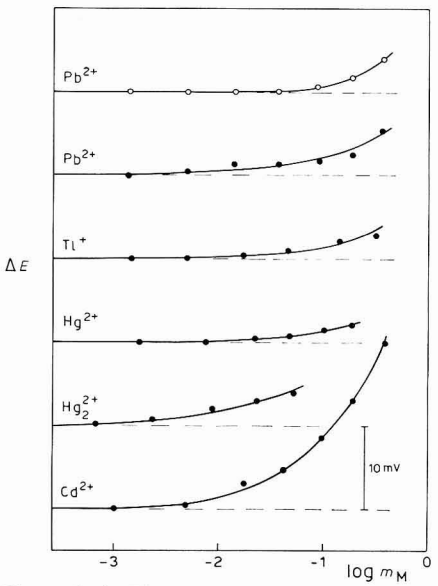

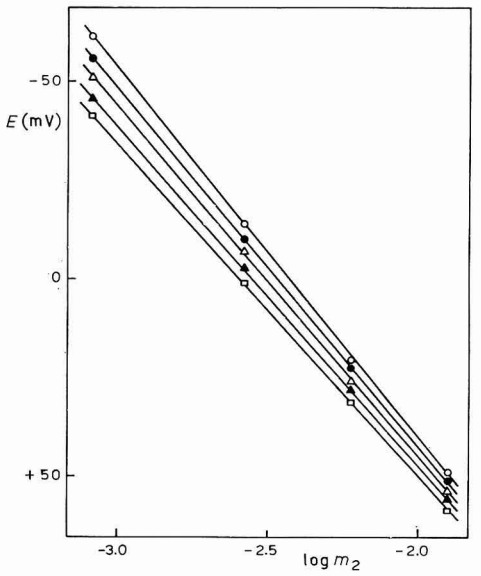

Fig. 4. As in Fig. 3. The curves are not calcd.

Fig. 5. Dependence of E on log m_2 for cell 2 at t: (□), 150°; (▲), 161°; (△), 174°; (●), 186°; (○), 199°. The straight lines were drawn with the Nernst slope.

The selectivity properties of Pyrex GRE's in molten $(Li,K)NO_3$ are appreciably different from those in molten NH_4NO_3. According to NOTZ AND KEENAN[7], the selectivity sequence in the latter solvent is: $Na^+ > Ag^+ > Li^+ > Hg^{2+} > Cd^{2+} > K^+ > Pb^{2+} > Tl^+$.

If this sequence were strictly applicable in $(Li,K)NO_3$, one would expect that none of the cations following Li^+ would affect the value of E_j, owing to the large amount of $LiNO_3$ present in the melt. From Fig. 4 it appears that this is not the case, particularly for Cd^{2+}.

NOTZ AND KEENAN have correlated their results with the data in water obtained by EISENMAN[6]; Pyrex glass can be considered as a Class X glass. In the case of soft-glass GRE's, such a correlation is made difficult by the complex composition of the glass employed. However, the higher alkali and alkaline-earth oxides contents and the lower Al_2O_3 and B_2O_3 contents with respect to Pyrex glass should bring the glass from the region of Class X to the region of Classes VII–IV, which are characterized by a high selectivity towards K^+ ions. This fact accords with the much smaller selectivity of soft-glass with respect to Pyrex GRE's for all cations in a melt rich in K^+ ions.

The selectivity properties of GRE's were found to be practically unaffected by aging and also, for soft-glass electrodes, by the consequent substitution of Na^+ by Li^+.

Stability and "standardization"

If GRE's of this kind are to be used in thermodynamic work, their potential *vs.* some "true" reference electrode, *e.g.*, the standard (1 mole kg^{-1}) silver electrode (SSE), must be known. This potential can be obtained by a "standardization" procedure which consists in measuring the e.m.f. of cell (2) for $AgNO_3$ concentrations in the external (right-hand) compartment varying between 10^{-3} and 10^{-2} mole kg^{-1}, *i.e.*, in a concentration range in which the GRE is unaffected by silver ions. In this concentration range the e.m.f. of the cell is given by

$$E = -(RT/F)\ln m_1 + E_a + (RT/F)\ln m_2 = E' + (RT/F)\ln m_2 \qquad (4)$$

where m_1 and m_2 are the silver ions concentrations inside and outside the glass bulb, and E_a is the asymmetry potential. The first two terms on the right-hand side of eqn. (4) are a constant, E', for each GRE at a given temperature, the E'-value of which can be obtained from a plot of E *vs.* $\log m_2$, and which must be subtracted from all potential values measured *vs.* the GRE in order to refer these values to the SSE.

The plots of E *vs.* $\log m_2$ (Fig. 5) were always straight lines with slope within 1% of the theoretical value (except for some Pyrex GRE's at low temperature).

The stability of the GRE's with time was tested by measuring the e.m.f. of cell (2) with constant silver nitrate content over periods up to 18 h, while the test for longer periods was effected by repeating the "standardization" procedure at various intervals. The "short term" stability was good for soft-glass GRE's, which gave e.m.f.-values constant within 0.5–1 mV in various tests over periods of 2–18 h; in similar tests, Pyrex GRE's gave variations from 1 to 5 mV.* The "long term"

* The E'-value of soft-glass GRE's used in $(Li,K)NO_3$ containing dissolved iodine at temperatures above about 190° can vary markedly (up to 20 mV in a 5-h period)[12]. The reasons for this were not elucidated.

stability was poor for both types of GRE's; the variation in one week could attain 10 mV, although, occasionally, aged soft-glass GRE's gave very constant values. Some of the GRE's (both Pyrex and soft-glass) were emptied, washed with water, dried and filled again with a solution having the same m_2-value; after this treatment, their E'-values were found unchanged within ± 2 mV.

CONCLUSIONS

Soft-glass GRE's have some distinct advantages over Pyrex GRE's. Their lower resistance makes the measurement less difficult, mainly because of the lower noise pick-up; their stability in time is generally better, and, most important, their sensitivity to dissolved cations is markedly lower, at least in solvents that do not contain Na^+ ions. When a very low resistance is required, the electrodes can be artificially aged by heating in $(Li,K)NO_3$ at about 300°, without impairing the other properties; however, in this case they become much more fragile.

For accurate e.m.f. measurements in thermodynamic work the GRE's must be standardized always immediately before and/or after each experiment. In this case their E'-value can be considered reliable within about ± 0.5 mV, if due care is exercised in the standardization procedure. For measurements of lower accuracy (*e.g.*, in voltammetric work) the standardization of GRE's needs to be controlled every 2–3 days, obviously the electrodes can be employed without standardization when only variations in e.m.f. during an experiment are of interest. Of course, the absence of a specific response of the glass to the cations to be investigated must be preliminarily verified in the particular solvent and in the range of concentrations employed.

It is worth noting here that the use of glass partitions in concentration cells of the type, for example,

$$\mathrm{M}\left|\begin{array}{c}\mathrm{MX}_n(\mathrm{C}_1)\\ \\ \mathrm{NaX}\end{array}\right|\mathrm{glass}\left|\begin{array}{c}\mathrm{MX}_n(\mathrm{C}_2)\\ \\ \mathrm{NaX}\end{array}\right|\mathrm{M} \qquad (5)$$

for obtaining activities or other thermodynamic data starting from the hypothesis that the glass–melt potential is determined only, *e.g.*, by Na^+ ions, can lead to serious errors, since it cannot be taken for granted *a priori* that the glass is not sensitive to M^{n+}, especially at high concentrations.

It is interesting to note that, according to ALABYSHEV *et al.*[17], evidence for the behaviour of a sodium glass electrode as a Na^+-sensitive electrode has been inferred from the fact that the cells:

$$\mathrm{Na} \mid \mathrm{glass} \mid \mathrm{Na+Cd}$$

$$\mathrm{Na} \mid \mathrm{glass} \mid \mathrm{NaNO_3} \mid \mathrm{glass} \mid \mathrm{Na+Cd} \qquad (6)$$

$$\mathrm{Na} \mid \mathrm{glass} \mid \mathrm{NaCl, CaCl_2, BaCl_2} \mid \mathrm{glass} \mid \mathrm{Na+Cd} \qquad (7)$$

have identical e.m.f.-values at each temperature. However, it is obvious that, apart from possible asymmetry potentials, the contributions of the glass–melt potentials cancel out in cells (6) and (7), even if these potentials are affected also by cations other than Na^+. It seems, therefore, that data obtained from cells of type (5) must be interpreted very cautiously in the absence of specific information on the behaviour of the glass employed.

ACKNOWLEDGEMENTS

The authors thank Professor L. RICCOBONI for his interest in this work. Glass analyses were kindly performed at the Stazione Sperimentale del Vetro, Murano, Venezia. This work was supported by the Italian National Research Council (C.N.R.).

SUMMARY

The behaviour of

$$\mathrm{Ag}\left|\begin{array}{c}(\mathrm{Li,K})\mathrm{NO_3}\\ \\ \mathrm{AgNO_3}\end{array}\right|\mathrm{glass}\Bigg|$$

half-cells has been investigated between 150 and 200° in view of their use as "reference electrodes" in molten $(\mathrm{Li,K})\mathrm{NO_3}$.

Electrodes made from soft-glass are better than Pyrex ones, having lower resistance, higher stability and lower sensitivity to solute cations. When used properly, these electrodes can give potential values accurate within ± 0.5 mV.

REFERENCES

1 A. F. ALABYSHEV, M. F. LANTRATOV AND A. G. MORACHEVSKII, *Reference Electrodes for Fused Salts*, The Sigma Press, Washington, D.C., 1965.
2 K. H. STERN, *Chem. Rev.*, 66 (1966) 355.
3 J. O'M. BOCKRIS, G. J. HILLS, D. INMAN AND L. YOUNG, *J. Sci. Instr.*, 33 (1956) 438.
4 D. INMAN, *J. Sci. Instr.*, 39 (1962) 391.
5 F. CONTI AND G. EISENMAN, *Biophys. J.*, 5 (1965) 247.
6 G. EISENMAN, *Advan. Anal. Chem. Instr.*, 4 (1965) 213.
7 K. NOTZ AND A. G. KEENAN, *J. Phys. Chem.*, 70 (1966) 662.
8 G. A. MAZZOCCHIN, G. G. BOMBI AND M. FIORANI, *Ric. Sci.*, 36 (1966) 338.
9 G. G. BOMBI, G. A. MAZZOCCHIN AND M. FIORANI, *Ric. Sci.*, 36 (1966) 573.
10 M. FIORANI, G. G. BOMBI AND G. A. MAZZOCCHIN, *Ric. Sci.*, 36 (1966) 580.
11 G. A. MAZZOCCHIN, G. G. BOMBI AND M. FIORANI, *J. Electroanal. Chem.*, 17 (1968) 95.
12 G. A. SACCHETTO, G. G. BOMBI AND M. FIORANI, *J. Electroanal. Chem.*, 20 (1969) 89.
13 G. G. BOMBI AND M. FIORANI, *Talanta*, 12 (1965) 1053.
14 G. G. BOMBI, R. FREDDI AND M. FIORANI, *Ann. Chim. (Rome)*, 56 (1966) 759.
15 D. J. G. IVES AND G. J. JANZ, *Reference Electrodes*, Academic Press, New York — London, 1961, p. 203 *et seq.*
16 YU. S. LYALIKOV, E. A. LEVINSON, G. I. TODOROVA AND V. V. NIKOLAEVA, *Uchenye Zapiski Kishinev. Gosudarst. Univ.*, 56 (1960) 91.
17 Ref. 1, p. 129.

Elsevier Sequoia S.A., Lausanne – Printed in The Netherlands

BEHAVIOUR OF TIN AS METAL–METAL PHOSPHATE ELECTRODE AND MECHANISM OF PROMOTION AND INHIBITION OF ITS CORROSION BY PHOSPHATE IONS

S. A. AWAD AND A. KASSAB
Chemistry Department, University College for Girls, Ain Shams University, Heliopolis, Cairo (U.A.R.)
(Received July 29th, 1968; in revised form, September 4th, 1968)

INTRODUCTION

No mention is made in the literature of the behaviour of metals as metal phosphate electrodes. In a recent study on lead[1], it has been found that within certain concentration ranges which depend on pH, this metal behaves as a lead–lead secondary phosphate electrode up to pH 8.7. At higher pH-values, it functions as a lead–lead tertiary phosphate electrode. Outside the concentration ranges that permit the thermodynamic response of potential to the concentration of a certain phosphate ion, the potential deviates either to more noble values owing to the inhibiting effect of phosphate ions on corrosion, or to more negative values indicating that phosphate ions can also enhance the corrosion of lead. An interesting fact that has arisen during the work is the inability of the tertiary phosphate ions to inhibit corrosion. It was felt of interest to extend this study to tin.

EXPERIMENTAL

The potential of the tin electrode was measured as a function of time within a period of 24 h, in aqueous phosphate solutions of concentrations varying between $5 \cdot 10^{-4}$ and 2 M. In order to prevent any variation in potential due to pH changes, the phosphate solutions were adjusted to definite pH-values, except in the case of tertiary phosphate solutions. Different series of solutions covering the pH range 1–13 were used; the composition of these has already been given[1]. The pH-values were checked with the hydrogen electrode and, when possible, with the quinhydrone electrode. AnalaR-grade reagents and conductivity water were used in all experiments.

The electrodes were prepared from rods 4 mm in diameter (Schering-Kahlbau Company). Before measurement, the electrode was abraded successively with 1, 0 and 00 grade emery paper, degreased with acetone and then washed thoroughly with water. Each experiment was carried out with a newly polished electrode and with a fresh portion of the solution.

A saturated calomel electrode was used as a reference electrode. The temperarure was maintained at 30° with an air thermostat controlled to $\pm$ 0.5°. All potentials were adjusted to the normal hydrogen scale.

RESULTS AND DISCUSSION

1. Behaviour of tin as metal phosphate electrode

Potential–time curves were constructed for the tin electrode in $5 \cdot 10^{-4}$–2 M phosphate solutions at different pH-values. The steady state potentials, otained 24 h after immersion, are plotted as a function of the logarithm of the molar concentration. Different relations were obtained which depend on the solution pH. In order to define the reactions taking place at the electrode, and thus governing its electrode behaviour, the experimentally observed potentials must be compared with the theoretical values calculated from thermodynamic data. As thermal data for the different tin phosphates are not available, the elucidation of the electrode reactions was based upon the slope of the potential–log C relations alone.

The lines obtained in solutions adjusted at pH 2.05 showed two linear portions: one covering the low concentration range up to 0.2 M with a slope of -15 mV/log C unit, and the other extending over the range 0.2–1 M with slope -60 mV. In the case of solutions buffered at pH 4.6, a similar behaviour was observed, but the curve corresponding to dilute solutions has a slope of only -8 mV (see Fig. 1). Also, in H_3PO_4–$HClO_4$ mixtures (pH $\approx$ 1.05), a slope of -15 mV was observed in the range, 0.05–1 M. Below 0.05 M, the potential was nearly constant.

The slope of -60 mV observed in concentrated solutions may be assigned to the formation of the primary phosphate:

$$Sn + 2\,H_2PO_4^- \rightarrow Sn(H_2PO_4)_2 + 2\,e \qquad (1)$$

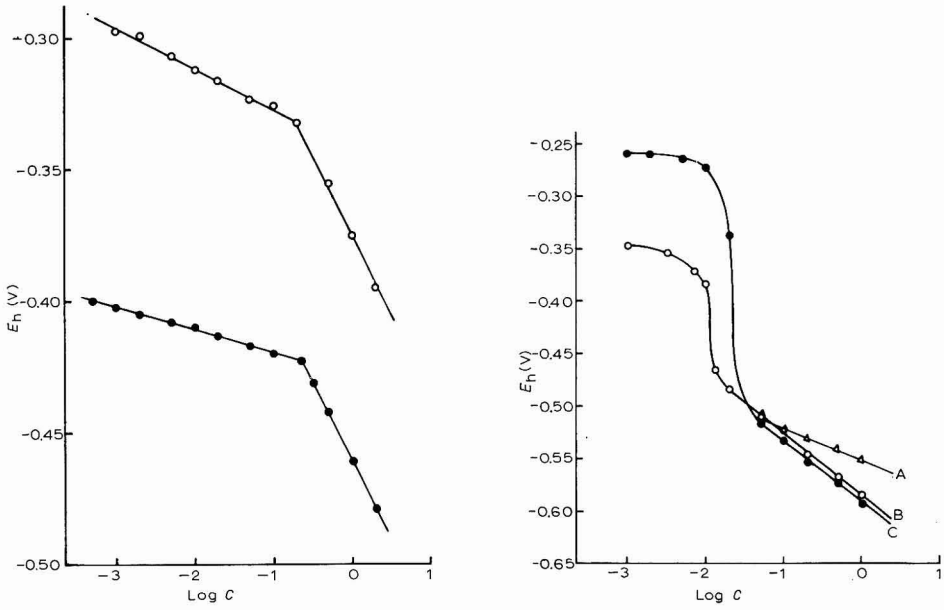

Fig. 1. Effect of concn. of: (○), (H_3PO_4+NaH_2PO_4) mixtures; (●), simple NaH_2PO_4, on the potential of tin.

Fig. 2. Effect of concn. of: (△), (NaH_2PO_4 + Na_2HPO_4) mixtures, pH not constant; (○), (NaH_2PO_4 + Na_2HPO_4) mixtures, pH constant; (●), simple Na_2HPO_4, on the potential of tin.

However, this possibility is excluded since the existence of the tin primary phosphate as an insoluble compound is not known. Moreover, the potential at a given concentration decreases by 80 mV as a result of an increase of pH from 2.05 to 4.6. This pH effect would not occur if the reacting species were $H_2PO_4^-$ ions. The formation of a secondary phosphate film according to:

$$Sn + HPO_4^{2-} \rightarrow SnHPO_4 + 2e \quad (2)$$

also does not account for the results, since it requires a slope of only -30 mV.

The greater slope observed in the present investigation may indicate the formation of a complex phosphate. Assuming the reaction to be:

$$Sn + 2HPO_4^{2-} \rightarrow Sn(HPO_4)_2^{2-} + 2e \quad (3)$$

the slope of -60 mV, is satisfactorily accounted for, since at constant pH the concentration of HPO_4^{2-} is proportional to that of $H_2PO_4^-$, and hence, $dE/d \log [HPO_4^{2-}] = dE/d \log [H_2PO_4^-]$. In order to predict the effect of pH associated with this reaction, it should be noted that the potential varies with pH inasmuch as the latter affects the HPO_4^{2-} concentration. Also, in a given primary phosphate solution the concentration of the secondary phosphate ion is inversely proportional to the hydrogen ion concentration, *i.e.*, $d\,pH = d \log [HPO_4^{2-}]$. It follows that $(dE/d\,pH)_{[H_2PO_4^-]} = dE/d \log [HPO_4^{2-}]$, and since the latter term is equal to $dE/d \log [H_2PO_4^-]$ the potential must decrease 60 mV per unit increase of pH. This value is twice that observed experimentally (31 mV).

To reconcile the slope of the potential–log C relation and the pH effect, it was suggested that the complex formed contains only one HPO_4^{2-} ion as follows:

$$Sn + H_2PO_4^- + HPO_4^{2-} \rightarrow Sn(H_2PO_4 \cdot HPO_4)^- + 2e \quad (4)$$

The electrode potential is then given by:

$$E = E_0 + (RT/2F) \ln \{[\text{complex}]/[H_2PO_4^-]\,[HPO_4^{2-}]\} \quad (5)$$

If the concentration of the complex is taken as nearly constant in the different phosphate concentrations, the expression for the electrode potential becomes:

$$E = E_0' - (RT/2F) \ln \{[H_2PO_4^-]\,[HPO_4^{2-}]\} \quad (6)$$

Owing to the direct proportionality, at constant pH, between the amount of secondary phosphate and the concentration of the primary phosphate, eqn. (6) is reduced to

$$E = E_0'' - (RT/2F) \ln [H_2PO_4^-]^2 \quad (7)$$

indicating a slope of -60 mV at 30°. With regard to the pH-dependence of potential, eqn. (6) requires that:

$$(dE/d\,pH)_{[H_2PO_4^-]} = dE/d \log [HPO_4^{2-}] = -30 \text{ mV at } 30°,$$

in excellent agreement with the experimental value. A summary of the above discussion is given in Table 1.

The smaller slopes observed in dilute solutions and in H_3PO_4–$HClO_4$ mixtures will be discussed below.

Measurements in equimolar solutions of primary and secondary phosphates showed relatively high potentials (-0.35 V) in solutions of concentration below 0.01

TABLE 1

DIFFERENT ELECTRODE COUPLES, THE CORRESPONDING E–log C SLOPES AND THE pH EFFECT ON POTENTIAL

Couple	*Slope* $= (dE/d \log [H_2PO_4^-])_{pH}$ *(mV)*	$(dE/d\ pH)_{[H_2PO_4^-]}$ *(mV)*
1 $Sn/Sn(H_2PO_4)_2$	−60	0
2 $Sn/SnHPO_4$	−30	−30
3 $Sn/[Sn(HPO_4)_2]^{2-}$	−60	−60
4 $Sn/[Sn(H_2PO_4 \cdot HPO_4)]^-$	−60	−30

M and will be discussed below. In 0.05–1 M solutions, a straight line with a slope of −30 mV was obtained (see Fig. 2, curve A). At first sight, it appears that the electrode reaction leads to the formation of a secondary phosphate film according to eqn. (2). This, however, was doubted as the complex $[Sn(H_2PO_4 \cdot HPO_4)]^-$ forms in solutions of lower pH, which thus contain smaller quantities of the secondary phosphate ions, and it seems, therefore, surprising that it does not form in the presence of appreciable quantitites of these ions. This contradiction may be due to the fact that, for equimolar solutions, the pH is not very constant; it changes, for example, from 6.02 in the 1 M mixture to 6.5 in the 0.2 M mixture. In solutions of pH adjusted exactly to 6.5 (by varying the ratio of primary to secondary phosphate), the potentials obtained gave a slope of −60 mV when plotted against the logarithm of the secondary phosphate concentration (see Fig. 2, curve B). However, no linear logarithmic relation was obtained on plotting the concentration of the primary phosphate. This slope indicates the formation of the tin secondary phosphate complex, $[Sn(HPO_4)_2^{2-}]$, according to eqn. (3). The marked change in slope due to slight variations in pH can be readily understood if the complex ion, $Sn(HPO_4)_2^{2-}$, represents the anion of a very weak acid, that can be called "phosphatostannous acid". Combination of this anion with a hydrogen ion results in the formation of the bi-ion, $HSn(HPO_4)_2^-$, to which we formerly gave the formula, $Sn(H_2PO_4 \cdot HPO_4)^-$, as deduced from the results in the pH range, 2.05–4.6. Therefore, the potential of the system, $Sn/Sn(HPO_4)_2^{2-}$, in the case when the pH is not quite constant, is superimposed by the system, $Sn/HSn(HPO_4)_2^-$, to an extent which increases gradually with phosphate concentration, owing to the decrease of pH in this direction. The net result is a gradual shift of potential to less negative values, and hence, a numerically smaller slope was observed (curve A). As evidence for the existence of complex tin phosphates, we have observed that the white precipitate formed on adding NaH_2PO_4 or Na_2HPO_4 to a stannous chloride solution dissolves in excess of the precipitating agent.

The results obtained in 0.05–1 M solutions of Na_2HPO_4, buffered at pH 8.7, coincide almost exactly with those observed in primary–secondary phosphate mixtures of constant pH (see Fig. 2, curve C). The same electrode reaction, *viz.*, the formation of the complex secondary phosphate, applies therefore to this series of solutions. As with the primary–secondary phosphate solutions, the potential below 0.01 M is exceptionally high (−0.25 V). A discussion of these high potentials will be given below.

The behaviour in secondary–tertiary phosphate mixtures is almost identical with that in simple tertiary phosphate solutions (see Fig. 3). In both series of solutions the potentials are also exceptionally high at low concentrations; in 0.001 M solutions

the potential is −0.2 V. On increasing the concentration above 0.01 *M*, the potential decreases rapidly to a value of *ca.* −0.82 V in molar solutions. During this sharp decrease we observed, however, slight potential maxima in solutions of 0.1–0.2 *M*. The absence of linear logarithmic relations in these series of solutions made it difficult to elucidate the electrode reaction. However, as will be shown below, the results obtained in concentrated solutions indicate a tin tertiary phosphate film.

2. Corrosion inhibition by phosphate ions

The exceptionally high potentials observed in dilute phosphate solutions of pH 6.5–12.9 were taken to represent metal/metal oxide potentials, on the basis that such low concentrations of phosphates are perhaps insufficient to give persistent phosphate films. From the free energy data[2], the standard potential of $Sn/Sn(OH)_2$ was calculated as −0.03 V. The potential in solutions of pH 8.7 is thus expected to be −0.552 V. The experimental value is, however, −0.26 V (see Fig. 2, curve C). The application of similar arguments to other solutions also indicated that the observed potentials cannot be attributed to an oxide film. The results are best explained on the basis of the inhibiting effect of phosphate ions on the corrosion of tin. Similar effects have already been observed in the case of steel[3] and zinc[4], whereby ennobling of the potential occurred at a definite phosphate concentration. The difficulty then arising is that further increase of concentration (above about 0.01 *M*) leads to a sharp decrease of potential which may be taken to indicate that phosphate ions also have a corrosive effect. It may be of interest to refer to the theory recently developed by BRASHER[3], that all anions are corrosive when found in large dilution, and become — or tend to be — inhibiting at high concentrations. It is, evident therefore that, even with a bifunctional nature, phosphate ions are not corrosive in 0.01 *M* solutions, so long as they behave as an inhibitor at lower concentrations. We tried to reconcile the inhibiting effect of phosphate ions and the sharp decrease of potential from the standpoint of the rates of the various electrode reactions.

The heterogenity of the surface, in the sense that some sites are anodic and others are relatively cathodic, is now a well established fact. At a metal corroding in aerated solutions, the following reactions proceed simultaneously:

(i) Anodic dissolution of the metal from the anodic areas

$$M \rightarrow M^{2+} + 2e \tag{8}$$

(ii) cathodic deposition of the metal ions at the cathodic areas

$$M^{2+} + 2e \rightarrow M, \tag{9}$$

(iii) cathodic reduction of oxygen at the cathodic areas

$$O_2 + 2\ H_2O + 4e \rightarrow 4\ OH^- \text{ (in alkaline solutions)} \tag{10}$$

(iv) and finally, the anodic evolution of oxygen at the anodic areas

$$4\ OH^- \rightarrow 2\ H_2O + O_2 + 4e \tag{11}$$

The rates of these reactions are represented, respectively, by:

$$V_1 = k_1(x)\ \exp(2\alpha EF/RT) \tag{12}$$

$$V_2 = k_2[M^{2+}]\ (1-x)\ \exp(-2(1-\alpha)EF/RT) \tag{13}$$

$$V_3 = k_3[O_2]\ (1-x)\ \exp(-\beta EF/RT) \tag{14}$$

$$V_4 = k_4[OH^-](x)\ \exp((1-\beta)EF/RT) \tag{15}$$

where k_1, k_2, k_3 and k_4 are the rate constants, x is the anodic fraction of the surface and $(1-x)$ the cathodic fraction; α and β are the fractions of the electrode potential, E, which accelerate the metal dissolution and reduction of oxygen, respectively, and $(1-\alpha)$ and $(1-\beta)$ correspond to the reverse reactions.

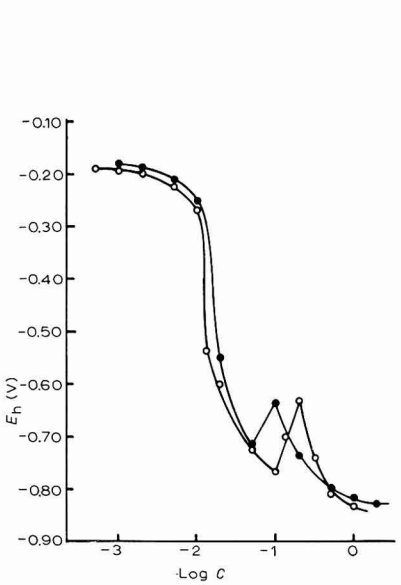

Fig. 3. Effect of concn. of: (●), (Na_2HPO_4 + Na_3PO_4) mixtures; (○), simple Na_3PO_4, on the potential of tin.

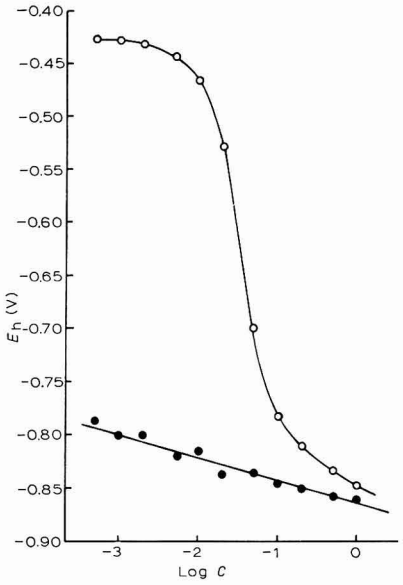

Fig. 4. Effect of concn. of Na_3PO_4 dissolved in: (○), 0.01 *N* NaOH; (●), 0.05 *N* NaOH, on the potential of tin.

Under stationary conditions, the metal corrodes at a rate, V_{corr}, equal to the net rate of metal dissolution, which is also equal to the net rate of reduction of oxygen; thus

$$V_{corr} = V_1 - V_2 = V_3 - V_4 \qquad (16)$$

The reduction of oxygen is often very slow compared to the metal dissolution. Thus, $(V_1 - V_2) \approx 0$, with the result that $V_1 \approx V_2$. This means that the potential approaches the reversible value of the metal/metal ion or metal/metal compound when a precipitating anion is present. In the latter case, the compound is precipitated on the anodic areas. For noble metals, on the other hand, reduction of oxygen proceeds at a higher rate than metal dissolution. Hence, $(V_3 - V_4) \approx 0$ and accordingly $V_3 \approx V_4$. The potential approaches, therefore, the reversible value of the oxygen electrode in the given solution. In many other cases, metal dissolution and reduction of oxygen proceed at comparable rates; the electrode thus acquires a potential which is appreciably more positive than that of the metal/metal ion system, and appreciably more negative than that of the oxygen electrode in the given solution. In this case the reverse reactions, *i.e.*, the deposition of metal ions and the anodic evolution of oxygen, are neglected, and

$$V_1 \approx V_3 = V_{corr} \qquad (17)$$

In view of the above argument we can proceed to explain the experimental

results. Thus, within certain concentration ranges tin behaves reversibly with respect to $HSn(HPO_4)_2^-$, $Sn(HPO_4)_2^{2-}$ or $Sn_3(PO_4)_2$, according to the pH of solution. This indicates that tin represents a case in which the redox reactions involving the metal predominate at the electrode surface, *i.e.*, $V_1 \approx V_2$. The potential shift in dilute solutions to less negative values, shows that the rates of the anodic reactions, *viz.*, the metal dissolution and evolution of oxygen, are being subjected to a decelerating effect. The latter reaction is already exceedingly slow, since the electrode potential is appreciably more negative than the reversible oxygen electrode potential. It follows, therefore, that the decelerating effect is associated with the metal dissolution and is most probably the decrease of ionic conductivity of a tin phosphate layer persisting on the anodic areas of the metal surface. The decrease of conductivity may be due to a decrease in the number of charge carriers or in their mobility, or in both. Apart from the reason for and mechanism of the decrease in conductivity, it is to be expected that, under these conditions, the rate of metal dissolution depends on the ionic conduction of the layer, in addition to its dependence on the electrode potential as shown by eqn. (12). The potential difference at the inner (metal/layer) interface must increase so that the potential gradient across the layer increases, and consequently the velocity of the charge carriers is enhanced. The result is that the measured potential, which is the difference between the metal and bulk of solution, increases. It follows that the rate of reduction of oxygen at the cathodic areas, which are not covered with the phosphate layer, is decreased, and hence, according to eqn. (16) the corrosion rate, $(V_3 - V_4)$, is diminished.

As will be discussed below, the ions responsible for the decrease of the layer conductivity are assumed to be adsorbed on the tin phosphate layer. Thus, under complete coverage with adsorbed ions, the ennobled potential becomes independent of concentration. This accounts for the fact that up to 0.002 M the potential remains almost constant (see Figs. 2 and 3). It is then possible that further increase of concentration permits adsorption on the cathodic sites. Assuming that reduction of oxygen proceeds more easily at the bare metallic areas than at those covered with the adsorbed phosphate ions, the rate of this reaction should decrease as a result of the decrease of $(1 - x)$, as eqn. (14) implies. In order to restore the equilibrium between the various electrode reactions, the potential must decrease, and hence the rate of metal dissolution, V_1, is again decreased. This means that the corrosion rate is once more diminished. The high potentials at low concentrations correspond, therefore, to the maximum inhibition through adsorption on the tin phosphate layer. At high phosphate concentrations, corrosion is inhibited through adsorption on both the phosphate layer (if it still persists) and the bare cathodic areas. It should be noted that the ennobling of potential prevented the measurement of reversible potentials, and the nature of the phosphate films formed in dilute solutions could not be identified.

3. Promotion of corrosion by phosphate ions

For an electrode subjected to the corrosive effect of an anion, the potential was found to vary with concentration according to:

$$E = a - b \log C \qquad (18)$$

where a and b are constants[3]. The small numerical slopes observed in phosphoric–perchloric acid solutions, as well as at low concentrations of phosphoric acid–primary

phosphate mixtures and of simple primary phosphate solutions (see Fig. 1), cannot be attributed to any of the tin phosphates. They are best explained on the basis that corrosion of tin is promoted under these conditions by the phosphate ions. To confirm this suggestion, the potential was measured in phosphate-free solutions of similar pH and were found to be -0.202 V at pH 2.05 and -0.258 V at pH 4.6. These potentials are *ca.* 100 and 140 mV less negative than the corresponding values in the most dilute phosphate solutions (see Fig. 1). Since the shift of potential to more negative values denotes an acceleration of the cathodic reduction of oxygen, the results indicate that the metal dissolves more easily in the phosphate solutions.

4. Mechanism of promotion and inhibition of corrosion by phosphate ions

It is important to note that the corrosion of tin is promoted by phosphate ions only under conditions preventing the persistence of a phosphate film. If it is assumed that adsorbed phosphate ions are capable of lowering the energy of activation of the ionisation of tin (reaction 8), corrosion promotion can be reasonably ascribed to adsorption of these ions on the bare anodic sites of the metal surface.

It is evident that for corrosion inhibition:

(i) The HPO_4^{2-} ion is an efficient corrosion inhibitor. Corrosion inhibition in primary–secondary phosphate mixtures (see Fig. 2), and in secondary–tertiary phosphate mixtures (see Fig. 3), may be due to the presence of that ion.

(ii) Tin is also ennobled in simple tertiary phosphate solutions (see Fig. 3), but the results may be ascribed to the presence of appreciable amounts of HPO_4^{2-} owing to the hydrolysis of PO_4^{3-} ions. To test whether the latter ions possess an inhibiting effect, measurements were made in tertiary phosphate solutions, which were made 0.01 *N* with respect to NaOH in order to suppress hydrolysis. The results (-0.425 V) showed a marked decrease of potential in dilute solutions (see Fig. 4). When the alkali concentration was increased to 0.05 *N*, no corrosion inhibition was observed. The potential followed a straight line with slope -21 mV, which probably indicates the formation of the tertiary phosphate according to:

$$3\,Sn + 2\,PO_4^{3-} \rightarrow Sn_3(PO_4)_2 + 6e \qquad (19)$$

The theoretical slope for such a reaction is -20 mV at 30°. It was concluded therefore, that the tertiary phosphate ion exhibits no inhibiting character.

It is now clear that the existence of a covering phosphate layer is insufficient for the inhibition of corrosion and it was concluded that corrosion inhibition is intimately associated with the nature of the interface between the semiconducting phosphate layer and solution. STANWORTH *et al.*[5] found that glasses in the P_2O_5–V_2O_5 system exhibit bulk electronic conduction, and are *n*-type semi-conductors. Recently, many more oxide glasses have been reported[6–9]. It is thus probable that a phosphate layer becomes inhibiting only if its surface can acquire a "semi-glassy" constitution, in which the tin, phosphorus and oxygen atoms are tightly bound with covalent linkages. It follows that the interface inhibits the transfer of tin ions to the solution, leading to decrease of ionic conduction of the phosphate layer, and, consequently, to the ennobling of potential. The semi-glassy constitution may be acquired through adsorption of the phosphate ions in a highly polymerised or condensed form. This suggests that the non-inhibiting character of the tertiary phosphate ion can be explained by the fact that, on adsorption, PO_4^{3-} ions exist in the simple ionic form. On the other hand, the

HPO_4^{2-} ion is readily condensable or polymerisable since it contains a hydrogen ion, and hence it is an inhibitor. The same argument applies also for the primary phosphate ion, but its behaviour depends on whether a phosphate film persists or not. In the former case it is corrosion inhibiting, while in the latter it is corrosion promoting. Lead[1] and tin represent the two types of behaviour.

The potential maxima observed in the case of secondary–tertiary phosphate mixtures and in simple tertiary phosphate solutions (see Fig. 3), may indicate that the layer/solution interface acquires a more complex structure and, hence, becomes more inhibiting. For example, a salt of formula, $Na_3H_3P_2O_8$, is crystallised from an equimolar solution of NaH_2PO_4 and Na_2HPO_4[10]. An ion of formula $HP_2O_8^{5-}$ may exist in a secondary–tertiary phosphate mixture. When found in appreciable amounts, such complex ions may increase the complexity of structure of the semi-glassy interface, and hence, the potential deviates to less negative values. After the complex ion has exhibited its maximum extra ennobling effect, there is normal decrease of potential — due to further adsorption on the bare cathodic areas — on further increase of concentration. The absence of a similar phenomenon in the case of primary–secondary phosphate mixtures is due to the fact that above 0.02 M, the phosphate layer dissolves as $Sn(HPO_4)_2^{2-}$ and it is thus impossible for the complex ions to manifest themselves by a shift in potential to less negative values.

For solutions in which the ions exhibit their inhibiting action, the potential values differed within $\pm$ 30 mV. This relatively low reproducibility is not surprising, but it is a familiar property of all surface processes because the characteristics of the surface are exceedingly sensitive to the pretreatment and handling of the electrode. This low reproducibility may, thus, support our proposal, that inhibition of corrosion with phosphate ions is due to adsorption. On the other hand, the reproducibility under conditions permitting thermodynamic behaviour (as manifested by linear potential–log C relations) was considerably high; the results differed within only ± 3 mV. It is, therefore, possible to calculate a reliable value for the free energy of formation of $Sn_3(PO_4)_2$. From Fig. 4, the standard potential of reaction (19) is -0.865 V, giving ΔG^0 for this reaction as -119.68 kcal. If ΔH and ΔG^0 of formation of PO_4^{3-} at 25° are taken as -306.9 and -245.1 kcal[11], the entropy change for the formation of this ion is -207.4 cal. Neglecting the variation of ΔS with temperature, the free energy of formation of PO_4^{3-} at 30° is -244.06 kcal, and accordingly, the free energy of formation of $Sn_3(PO_4)_2$ at that temperature is -607.8 kcal.

SUMMARY

The potential of the tin electrode in aqueous phosphate solutions was measured at 30° as a function of both pH and the electrolyte concentration. In concentrated solutions the electrode behaves reversibly with respect to certain tin compounds. Thus, in the pH range, 2.05–4.6, the electrode reaction in 0.2–1 M solutions involves the formation of $HSn(HPO_4)_2^-$, which is considered as the bi-ion of "phosphatostannous" acid. In the pH range, 6.5–8.7, the formation of the normal ion, $Sn(HPO_4)_2^{2-}$, governs the electrode potential in 0.05–1 M solutions. At higher pH, a tertiary phosphate layer persists on the electrode surface.

In dilute phosphate solutions, the results indicated either promotion or inhibition of corrosion of tin. The former effect was observed in the pH range, 2.05–4.6,

whereby the potential decreased by 8–15 mV per unit increase of log C. Corrosion inhibition was observed, on the other hand, at higher pH-values, whereby exceptionally high potentials were developed up to about 0.01 M. With further increase of concentration, the potential decreased sharply towards the values required by the above mentioned reversible couples.

Corrosion inhibition, manifested by the high potentials, was attributed to the adsorption of phosphate ions, on the surface of a persistent tin phosphate layer, in a highly polymerised or condensed form. The layer/solution interface acquires a "semi-glassy" constitution, which inhibits the transfer of tin ions to the solution. Adsorption on the bare cathodic areas as the concentration is further increased, was suggested to deaccelerate the cathodic reduction of oxygen, and hence, the potential decreases sharply leading to further corrosion inhibition. In the absence of a tin phosphate layer, adsorption of phosphate ions on the bare anodic areas accelerates the ionisation of the metal, perhaps through the reduction of the energy of activation of the process. This causes the corrosion of tin to be promoted.

Simple tertiary phosphate ions exhibit no inhibiting effect on corrosion. Therefore, above pH 12.5 (in which case the solutions contain only very small amounts of HPO_4^{2-}), the electrode behaves as $Sn/Sn_3(PO_4)_2$ over the whole concentration range studied. The free energy of formation of tin tertiary phosphate was calculated as -607.8 kcal.

REFERENCES

1 S. A. AWAD AND Z. A. ELHADY, *J. Electroanal. Chem.*, 20 (1969) 79.
2 W. M. LATIMER, *Oxidation Potentials*, Prentice Hall, Englewood Cliffs, N.J., 2nd ed., 1952, p. 149.
3 D. M. BRASHER, *Nature*, 193 (1962) 868.
4 V. K. GOUDA, M. G. A. KHEDR AND A. M. SHAMS EL DIN, *Corrosion Sci.*, 7 (1967) 221.
5 E. P. DENTON, H. RAWSON AND J. E. STANWORTH, *Nature*, 173 (1954) 1030.
6 J. D. MACKENZIE, *J. Am. Ceram. Soc.*, 47 (5) (1964) 211.
7 L. A. GRECHANIK, N. U. PETROVYKH AND V. G. KARPECHENKO, *Soviet Phys.-Solid State English Transl.*, 2 (1961) 1908.
8 A. F. IOFFE, *Polnoe Sobranie, Izd. Akad. Nauk SSSR*, 1 (1957) 407.
9 M. MUNAKATA, *Solid-State Electron.*, 1 (1960) 159.
10 FRITZ EPHRAIM, *Inorganic Chemistry*, Gurney and Jackson, 5th English ed., 1949, p. 732.
11 W. M. LATIMER, *Oxidation Potentials*, Prentice Hall, Englewood Cliffs, N.J., 2nd ed., 1952, p. 106.

Elsevier Sequoia S.A., Lausanne – Printed in The Netherlands

POLAROGRAPHY OF CARBON SUSPENSIONS

I. F. JONES* AND R. C. KAYE
Division of Pharmacy, Department of Pharmacology, University of Leeds (England)
(Received August 5th, 1968)

INTRODUCTION

Stirred suspensions of activated charcoal in aqueous electrolytes have been shown by MICKA[1,2] to depolarise the dropping mercury electrode. He recorded damped polarograms showing current peaks resembling polarographic maxima between −0.4 and −1.2 V from stirred suspensions of Carborafine activated charcoal in various electrolyte solutions. HALLUM AND DRUSHEL[3] have recorded cathodic waves of normal appearance in quiet suspensions of certain carbon blacks in dimethylformamide, using tetra-*n*-butylammonium iodide as supporting electrolyte. They suggested that the waves were due to the reduction of quinone-type compounds on the carbon surface. The presence of quinones and hydroquinones on the surfaces of some carbon blacks has been shown by GARTEN AND WEISS[4] to be the cause of some of the electrode reactions of these materials. STUDEBAKER *et al.*[5] have stated that as much as 18% of the oxygen found on carbon blacks may be present in a 1,4-quinone form.

The heavily damped polarograms recorded by MICKA[1,2] for charcoal (and also for some other suspensions) showed a high maximum-like cathodic current peak. At more negative potentials the current fell to a very low value, but not when excess electrolyte or gelatin was present. No explanation for this behaviour was suggested, but MICKA has explained the forms of the current peaks in terms of the adsorption forces between the charcoal particles and the mercury surface.

We now report the results of our investigation of the unusual polarographic properties of carbon suspensions.

EXPERIMENTAL

AnalaR grade mercury and chemicals were used where obtainable. The sample of sodium dithionite was supplied by Associated Chemical Companies Ltd. The activated charcoal was Norit NK, purified by removing acid-soluble material. Other forms of carbon used were graphite of unknown origin, carbon black obtained by deposition from a benzene flame, and powdered carbon rod of the type used for electrodes, supplied by Jencons of Hemel Hempstead.

Two types of polarographic cell were used. One was similar to that described by ILKOVIČ[6]. For the bulk electroreduction of charcoal a divided H-type cell was used. The capillary had a drop-time of 2.5 sec on closed circuit with no applied potential. Cell suspensions were deoxygenated and also stirred by bubbling oxygen-free nitrogen.

* Present address: The School of Pharmacy, Portsmouth College of Technology (England).

All experiments were carried out at room temperature which was always between 21 and 23°. Potentials were measured against a mercury pool anode or against saturated and normal calomel reference electrodes.

Current–time recordings were made by feeding cell currents into a single-stage current calibrated pre-amplifier and thence to one channel of a double-beam oscilloscope. Square wave output from an oscillator was fed into the second channel to provide a time-marker.

RESULTS AND DISCUSSION

Undamped polarograms for stirred buffered suspensions of activated charcoal were obtained at pH-values from 0 to 14 and also for stirred unbuffered suspensions in potassium chloride solutions of different strengths. An example is shown in Fig. 1. The

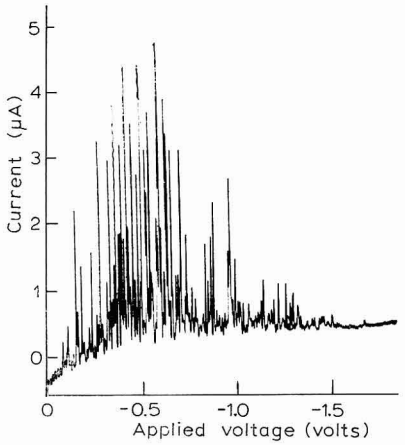

Fig. 1. Undamped polarogram of a stirred suspension of 0.01% activated charcoal in 0.1 *M* KCl soln.

high cathodic-current peaks are caused by the electrode reaction following the impact of charcoal particles on the drop surface. Although no electrical damping was used, the pen-recorder, because of its inertia, cannot follow the pulses due to individual particles. It behaves as an integrating device, each recorded peak being the result of several impacts. The variation of peak heights is due to random variation of the impact rate, which is convection—and not diffusion—controlled. The full heights of some of the peaks could not be recorded at the sensitivity used. With electrical damping a smoothed polarogram of the type shown by MICKA[1,2] was obtained. There was no obvious pH-shift of reduction potential between pH 0 and pH 7. Between pH 7 and pH 14 the potential became more negative.

Since the magnitude of the cathodic current depends on the rate of impact of particles with the mercury surface, the smaller reduction current at more negative potentials may be due to a lower impact rate. The oscillograph tracings of Fig. 2 show the correctness of this assumption. As the DME potential is made more negative than −650 mV (*vs.* SCE) there is a progressive decrease in the number of impacts during the life of one drop, although some individual current pulses are of the same magnitude as those recorded at less negative potential. The tracings obtained with

charcoal suspensions, compared with those obtained without charcoal, show that the electrocapillary zero is shifted to more negative potentials in the presence of charcoal.

Figure 3 shows more clearly the forms of the current pulses recorded with a faster time-base.

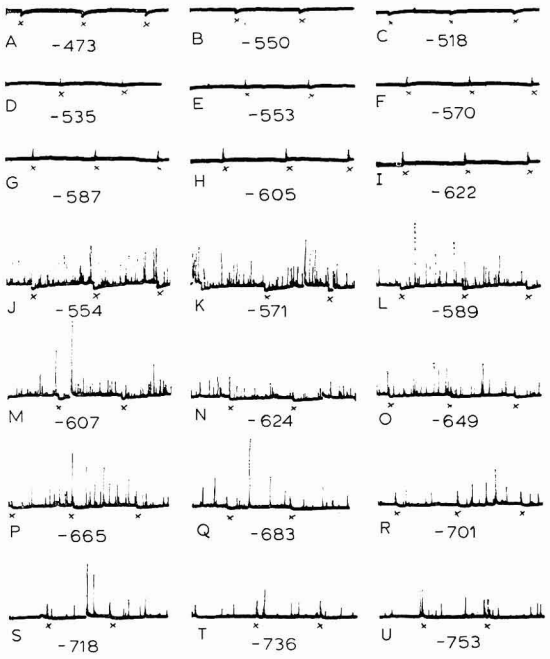

Fig. 2. Current–time tracings: (A–I), unstirred 0.1 *M* KCl soln.; (J–U), 0.01% unstirred suspension of activated charcoal in 0.1 *M* KCl recorded over several drop-lives. The mercury drop potential (mV) *vs.* SCE is shown for each tracing. The point of drop fall is indicated by X.

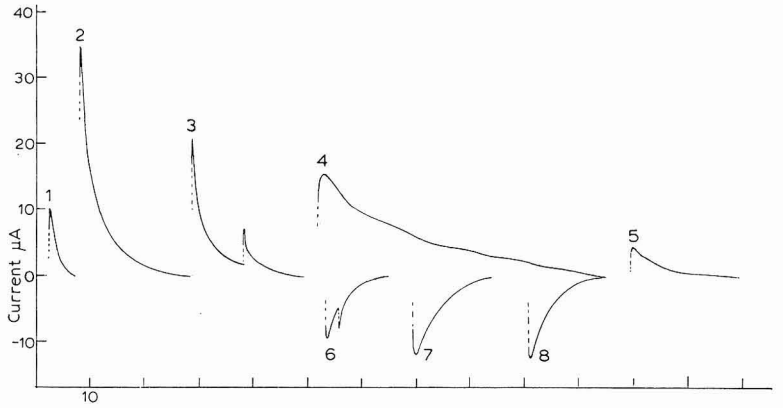

Fig. 3. Current–time tracings for unstirred 0.01% suspensions of activated charcoal in: (1–3), 0.1*N* HCl; (4 and 5), 0.1 *N* NaOH; (6–8), after reduction with sodium dithionite in 0.1 *N* NaOH. In tracings 3 and 6 two charcoal particles made impact with the drop surface in rapid succession. The time-scale is marked at 10-msec intervals.

The quantity of electricity used in the reduction of oxidant associated with single particles, calculated from the areas of the current–time oscillograph traces, varies between 0.0075 and 0. 373 μC. Current pulses, recorded oscillographically at intervals during static settling of charcoal suspension in the cell showed that the quantity of electricity required for reduction was related to particle size.

MICKA[1,2] has suggested that the oxidant associated with activated charcoal could be bound oxygen, but his attempt to remove this by outgassing at high temperature and low pressure was unsuccessful. Sodium sulphite is known to remove dissolved oxygen. Polarograms of charcoal suspensions containing sodium sulphite were therefore recorded. The pH of the suspension was made slightly alkaline to avoid decomposition of the sulphite. The charcoal current was unaffected by sulphite. However, the more powerful reducing agent, sodium dithionite, added in increasing amounts to a deoxygenated suspension of charcoal, progressively reduced the charcoal oxidant. The cathodic current peaks on the polarogram were then replaced by anodic peaks. This reversal of the charcoal current is shown in Fig. 4a, and by tracings 6–8 in Fig. 3. The charcoal in this case was partially reduced. For the complete chemical reduction of the oxidant contained in 20 mg of charcoal, 2 mg of sodium dithionite was required. All these experiments were carried out at pH 13 to avoid decomposition of dithionite.

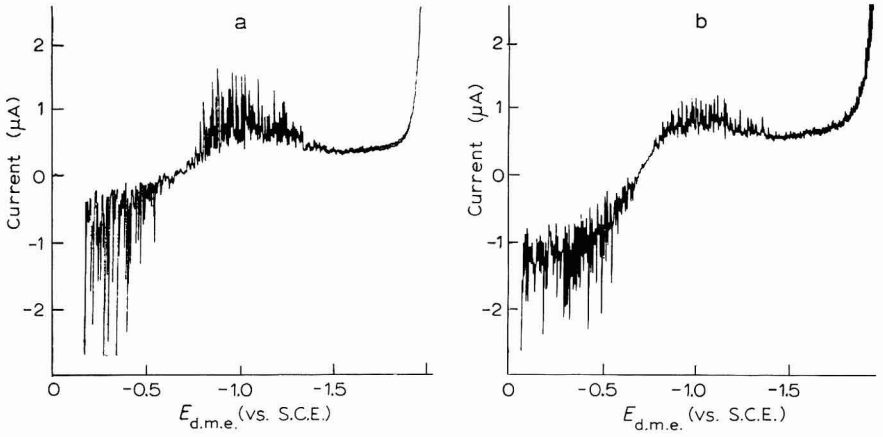

Fig. 4. Undamped polarograms of a stirred suspension of 0.01% activated charcoal in 0.1 *N* NaOH. (a), after partial reduction with sodium dithionite; (b), after partial electroreduction. Both polarograms show cathodic and anodic current peaks.

It was possible to centrifuge a suspension of dithionite-reduced charcoal and to wash the charcoal several times in absence of air. The polarogram of the re-suspended charcoal freed from dissolved dithionite was identical with that shown in Fig. 4. After the suspension had been exposed to air for a few hours all the charcoal was re-oxidised, only cathodic current being recorded on the polarogram. Re-oxidation was also achieved by adding oxygen-free methylene blue solution to a suspension of reduced charcoal.

Bulk electroreduction of activated charcoal was successfully achieved using

a divided H-cell. The cathodic and anodic compartments were joined by an agar–salt bridge. A normal calomel electrode of large area was used as anode. In the other compartment was a mercury pool cathode and there was also provision for the insertion of a dropping mercury electrode. A suspension of activated charcoal in 0.1 *M* potassium chloride solution was placed in the cathode compartment, deoxygenated, and electrolysis allowed to proceed at about −1000 mV (*vs.* NCE). The bulk reduction was interrupted at intervals and polarograms obtained. The cathodic current peaks were progressively reduced and replaced by anodic peaks. The polarogram of the partly reduced system (Fig. 4b) resembles that for the system partly reduced by dithionite (Fig. 4a). After exposure of the electrolytically-reduced charcoal suspension to air, all the anodic pulses disappeared and were replaced by cathodic pulses.

During the bulk reduction of charcoal suspensions, observations were made which led to an explanation of the diminished charcoal reduction at more negative potentials. At cathode potentials of about −1100 mV (*vs.* NCE) charcoal particles were seen to move slowly away from the salt-bridge side of the compartment to the other side, leaving a clear bright mercury surface at the salt-bridge side. No settling of charcoal particles occurred in this area. At −1500 mV, vigorous movement of the suspension was observed. The particles of charcoal were seen microscopically, in rapid movement along the surface of the mercury cathode in a direction away from the anode compartment. The stream of suspension was deflected upwards on striking the opposite wall of the compartment, thus setting up vigorous convection and stirring. The movement stopped when the cathode potential was reduced to about −1000 mV. Occasionally, the movement stopped spontaneously while the cathode was still maintained at more negative potential, but could be restarted by tapping the cell.

The phenomenon was observed more clearly by using a dilute suspension of coal of larger particle size to detect movement. Although the coal was not electroactive, the behaviour of the suspension was the same. The high velocity of the particles close to the mercury surface prevented contact of the particles with the mercury. This was established by observing the distance between a particle and its mirror image in the mercury. Although particle and image were sometimes very close they seldom coincided. Because of the high velocity of the particles in a horizontal plane they were unable to settle and establish contact with the mercury surface. However, a few of the biggest particles hit the mercury surface and rebounded several times before being swept upwards at the side of the cell. When the cathode was gradually made less negative there was a progressive reduction of stirring which finally became localised at the salt-bridge side of the cathode compartment before ceasing completely.

The movements described originated in the mercury; larger particles that had become trapped between the mercury and the sides of the vessel were seen to travel below the mercury surface in the opposite direction to those in suspension. All these movements are illustrated in Fig. 5a.

The mercury movement was greatly affected by the electrolyte concentration of the cell fluid. It diminished as the potassium chloride concentration was gradually increased from 0.01 to 1 *M*. It did not occur in saturated potassium chloride. Friction between the mercury and the vessel walls was also found to govern the movement of the mercury and hence the streaming of the suspension. The movements could be hindered by placing a little sharp sand in the cathodic compartment before introducing the mercury.

The mercury movement was examined more closely using a static mercury drop where the frictional effect was less. A short length of 2-mm bore glass tubing, with platinum wire sealed into one end, was slightly overfilled with mercury so that when it was inverted into the cell suspension, a static hanging mercury drop was formed. The cell contained 0.05 *M* potassium chloride with powdered coal to indicate movement. It was observed microscopically that streaming occurred over two ranges of

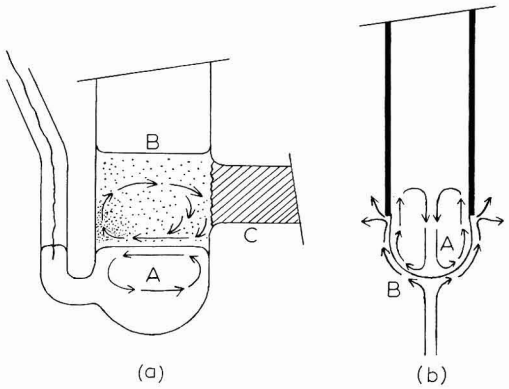

Fig. 5. Streaming of mercury and KCl soln. as observed (a), at the surface of a large mercury cathode; (b), at the surface of a static mercury drop. (A) mercury pool (a) or mercury drop (b); (B) KCl soln. with suspended coal particles to indicate movement; (C) salt–agar bridge connection to anodic compartment.

potential. The first was from 0 to −290 mV (*vs.* NCE). The streaming became slower as the potential approached the upper limit of this range and ceased at −290 mV. Streaming recommenced when the potential was increased to −900 mV. Beyond this point the streaming velocity increased markedly. At −1800 mV it was very vigorous and stirring of the mercury inside the tube containing it could be seen. This caused liquid to enter the mercury tube and rise to the top, slowly displacing mercury and causing the drop to fall. Several drops were formed in this way. It was observed microscopically that the coal particles were not able to establish contact with the mercury surface when streaming was proceeding vigorously.

The form of the streaming (Fig. 5b) was the same for both potential ranges over which it occurred, but it was less rapid on the positive side of the electrocapillary zero. As in the case of the large mercury cathode, the streaming of the aqueous suspension around the mercury drop was caused by movement of the mercury. Streaming around the drop also diminished with increasing electrolyte concentration and it was not observed in saturated potassium chloride solution. We found that the addition of 0.05% gelatin also reduced mercury movement and streaming.

The polarographic behaviour of other carbons

Stirred suspensions of graphite showed only slight peaks of cathodic current. This comparative inactivity was confirmed oscillographically. Powdered carbon rod, however, gave pronounced cathodic peaks but these were less than for activated charcoal. The height and number of the peaks were increased by further size reduction

of the carbon in an agate mortar. The carbon current could be eliminated by including sodium sulphite in the suspension. The sulphite was most effective when it was mixed intimately with the carbon in a mortar before adding the supporting electrolyte solution. Sulphite is known to remove dissolved oxygen, suggesting that in the case of this particular sample of carbon the electroactive material was loosely-held oxygen. This was confirmed by attaching the polarographic cell containing a carbon suspension, already deoxygenated by bubbling nitrogen, to a vacuum pump and pumping for 10 min. Gas was released from the carbon. After this treatment no cathodic current was recorded.

DISCUSSION

There are some differences between our experimental methods and results and those of other workers. MICKA[1,2] recorded only heavily damped polarograms and was therefore unable to detect charcoal reduction in unstirred suspensions. We were able to record on undamped polarograms charcoal reduction in quiet suspensions, but it was much less than in stirred suspensions. Oscillographic current–time recordings from unstirred suspensions also showed charcoal reduction but the particle impact rate was far less than in stirred suspensions. The supply of particles to the electrode is not diffusion-controlled and it is greatly increased by turbulence. The normal appearance of the polarographic waves recorded by HALLUM AND DRUSHEL[3] for quiet suspensions of carbon blacks is probably due to the colloidal size of the particles (8–10 mμ). These workers showed that the electrode reaction was in their case diffusion-controlled.

Our oscillographic current–time recordings showed that the current pulses due to reduction of individual particles reached their maximum values in about 1 msec, thereafter falling to zero over periods varying from 5 to 50 msec, depending on particle size and pH of the medium. Larger particles gave pulses with longer rise and decay times.

The particles are electrical conductors, hence rapid reduction of surface oxidant would be expected on impact with the mercury drop, giving rise to a high current pulse of short duration. The longer decay times recorded suggest a rate-determining process other than the electrode reaction itself. Such a process could be diffusion from the bulk of the solution to the particle surface of some material involved in the reduction process, probably hydrogen ions. This hypothesis is supported by the observation that the pulse heights were less and the decay times longer at high pH than at low pH (see Fig. 3).

The current could be due to reduction of hydrogen ions alone at the charcoal surface, the hydrogen overvoltage being very small for carbon. If so, similar behaviour would be expected of powdered carbon rod, but this was not found. Experiments with powdered carbon rod showed the reducible material in this case was loosely-held oxygen, the removal of which left an electroinactive material. If hydrogen ions are involved in the reduction of activated charcoal it must be through their participation in the reduction of material bound to the charcoal surface. This material could not be removed from activated charcoal by sulphite or by pumping, as in the case of powdered carbon rod, and could not therefore be loosely-held oxygen.

From the quantities of electricity represented by the oscillographically record-

ed current pulses, the number of reducible units per particle of charcoal was calculated. Assuming a 2-electron process, this number varied from $8 \cdot 10^{10}$ to $116 \cdot 10^{10}$ for particles in the 20–160 μ size range. The shape and surface area of the particle associated with any one current pulse could not be known with certainty. Assuming spherical particles for the purpose of calculating surface areas, the area occupied by a single reducible group ranged from 1.5 Å^2 to 7 Å^2. However, taking into account the shapes and porosities of the particles, the true surface areas must be many times greater than those used for this approximate calculation. Even so, the results seem to indicate a very high surface concentration of reducible groups. HALLUM AND DRUSHEL[3] have stated that the reducible surface groups of carbon blacks are quinone carbonyl groups, attached to graphite laminae projecting from the crystallite surfaces. The maximum distance between carbonyl groups in adjacent planes is 3.55 Å, which accords roughly with our calculated areas of the reducible groups. The diffusion current of about 3.4 μA recorded by HALLUM AND DRUSHEL[3] for a 4%-suspension of carbon black seems very low on the basis of the close packing of the quinone carbonyl groups indicated by our experimental results for a 0.01% suspension of activated charcoal. The observed reversibility of both chemical and electrical reduction processes is in accordance with the behaviour of a quinone–hydroquinone redox system. The thermodynamic irreversibility, shown by the wide separation of the cathodic and anodic currents recorded for the half-reduced system (Fig. 4, a and b), is to be expected when oxidant and reductant are bound to the charcoal surface and the electrode process is not diffusion-controlled.

Some of the results do not accord with the behaviour of a quinone–hydroquinone system. The redox potential of such systems is usually pH-independent at higher pH-values, at which the reductant is fully ionised. There was an indication of a shift of reduction potential to more negative values at high pH, but this may not be significant for the thermodynamically-irreversible system. If it be assumed that on account of the high availability of electrons in the graphitic laminae the bound reductant is not ionised at high pH, then both the pH–potential shift and the longer pulse decay time observed at high pH may be explained. The larger quantities of electricity used at high pH for the reduction of single particles remain unexplained.

The greatly diminished charcoal current at potentials more negative than about -1000 mV is due to the reduced ability of charcoal particles to make contact with the mercury surface. Turbulence in the suspension is necessary for a high impact rate. When vigorous streaming occurs at more negative potentials, turbulence at the drop surface is replaced by a relatively streamline flow. Thus, a boundary layer effect is created. The less vigorous streaming observed between 0 and -250 mV (*vs.* NCE) may also lead to decreased charcoal reduction over this potential range.

The streaming is induced by movement of mercury at the drop surface, which arises through variation of interfacial tension over the surface. This variation is due to a non-homogeneous electrical field, streaming being progressively suppressed by increasing electrolyte concentration. This accords with FRUMKIN'S[7,8] theory of polarographic maxima. In a homogeneous system, such as a solution, streaming can only result in an increased supply of oxidant to the electrode surface. In a non-homogeneous system, such as a suspension, the particles are swept along tangentially to the mercury surface and there is less chance of impact. This, and our observation of reduced streaming in the presence of gelatin, explain MICKA'S[1,2] recording of enhanced

charcoal current at more negative potentials when excess electrolyte or gelatin was present.

There seemed to be no fundamental differences between the streaming occurring on the negative side of the electro-capillary zero and that on the positive side, except that on the negative side the streaming became more vigorous as the difference between the electrode potential and that of the electrocapillary zero was increased. A corresponding difference of potential on the positive side of the electrocapillary zero could not be achieved before anodic oxidation of mercury intervened and terminated streaming.

SUMMARY

The polarographic behaviour of activated charcoal and two other forms of carbon have been studied. Activated charcoal suspensions give rise to a high cathodic current peak which is greatly enhanced by stirring. The diminished current on each side of the peak is shown to be due to the inability of particles to make contact with the DME at potentials removed from the electrocapillary zero of mercury. This inability arises from a boundary layer effect, produced by vigorous movement of the mercury surface and the liquid in contact with it.

The reducible groups on the charcoal surface can be reduced by sodium dithionite and also by bulk electroreduction. The cathodic current is then replaced on the polarogram by anodic current.

The quantities of electricity, calculated from oscillographic recordings of current pulses for single charcoal particles, show a very high surface concentration of reducible groups. The form of the pulses and the quantities of electricity they represent are pH-dependent, suggesting participation of hydrogen ions in the electroreduction process.

REFERENCES

1 K. Micka, *Collection Czech. Chem. Commun.*, 21 (1956) 647–651.
2 K. Micka, *Recent Advan. Polarography*, 3 (1960) 1182–1190.
3 J. V. Hallum and H. V. Drushel, *J. Phys. Chem.*, 62 (1958) 110–117.
4 V. A. Garten and D. E. Weiss, *Australian J. Chem.*, 8 (1955) 68–95.
5 M. L. Studebaker, E.W.D. Huffman, A.C. Wolfe and S. L. G. Nabors, *Ind. Eng. Chem.*, 48 (1956) 162–166.
6 D. Ilkovič, *Collection Czech. Chem. Commun.*, 8 (1936) 170.
7 A. Frumkin and B. Bruns, *Acta Physicochim. U.S.S.R.*, 1 (1934) 232.
8 B. Bruns, A. Frumkin, S. Jofa, L. Vanjukova and S. Zolotarevskaja, *Acta Physicochim. U.S.S.R.*, 9 (1938) 359.

ELECTROANALYTICAL CHEMISTRY AND INTERFACIAL ELECTROCHEMISTRY
Elsevier Sequoia S.A., Lausanne – Printed in The Netherlands

A STUDY OF THE FLUORIDE COMPLEXES OF CADMIUM BY A.C. AND D.C. POLAROGRAPHY

A. M. BOND
Department of Inorganic Chemistry, University of Melbourne, Parkville, 3052 Victoria (Australia)
(Received December 7th, 1967; in revised form, July 26th, 1968)

INTRODUCTION

The chloride, bromide and iodide complexes of cadmium have frequently been investigated polarographically but the only polarographic study of the fluorides of cadmium appears to be that by MESARIC AND HUME[1] who found evidence only for CdF^+. LEDEN[2], in what appears to be the only other study of cadmium fluorides (using the potentiometric method) demonstrated the existence of two cadmium fluoride complexes, CdF^+ and CdF_2. Both these studies indicated only very weak complex formation between fluoride and cadmium ions in aqueous solution. The polarographic method[3] for the evaluation of very weakly complexing species is limited by the precision with which small differences in $E_{\frac{1}{2}}$-values can be measured with changing ligand concentration. For the cadmium fluoride system, only small changes in $E_{\frac{1}{2}}$, of the order of a few millivolts, are observed even with large changes in fluoride concentration. Thus, for the polarographic interpretation of the cadmium–fluoride system any method for improving the precision of measurement of $E_{\frac{1}{2}}$-values would be extremely useful.

For cadmium it is known that summit potentials (E_s) obtained from a.c. polarography correspond to $E_{\frac{1}{2}}$-values[4]. This suggested that a.c. polarographic measurements could be used as an alternative to d.c. polarographic measurements with the possible advantage of an improvement in precision of measurements, as the accuracy and reproducibility of a.c. polarographic measurements (at least in analytical applications) are generally better than can be obtained by conventional d.c. polarography[5]. Although these results in analytical applications refer to current measurements only and not to potential measurements, E_s might as a result, be measured more accurately and reproducibly than $E_{\frac{1}{2}}$. This was thought to be possible because any polarogram obtained by the various polarographic techniques consists essentially of a graphical plot of potential *vs.* current, and the accuracy and reproducibility of E_s- or $E_{\frac{1}{2}}$-values obtained from this graph depend upon the accuracy and reproducibility with which both current and potential can be measured. Furthermore, GUPTA AND CHATTERJEE[6] have used E_s-values instead of $E_{\frac{1}{2}}$ to evaluate the cadmium–ammonia system with satisfactory results. They suggested that some of the advantages of this approach are that E_s can be determined more conveniently and accurately than $E_{\frac{1}{2}}$, and that E_s-measurements can be made more rapidly and with an improved all-round reproducibility, although no evidence is given in support of these claims.

Therefore, an investigation of the use of a.c. polarographic measurements in

the evaluation of the cadmium–fluoride system was undertaken with a view to obtaining accurate and reliable information as to the number and magnitude of the fluoride complexes. The technique of rapid polarography, which can be used in conjunction with both a.c. and d.c. polarography, was also examined because this gives higher accuracy and reproducibility, at least of current measurement, than conventional polarography.

EXPERIMENTAL

All chemicals used were of reagent-grade purity except sodium perchlorate which was of laboratory-reagent grade. The purity of the sodium perchlorate was checked by spot tests, which showed the absence of chloride, bromide, iodide, phosphate and sulphide. The concentrations of prepared sodium perchlorate solutions were determined analytically by precipitation of perchlorate as potassium perchlorate.

All measurements were made at $(30 \pm 0.1)^\circ$ and at an ionic strength of 1.0 maintained by sodium perchlorate.

Polarograms were obtained using the Metrohm Polarecord E 261. A.c. polarography was carried out using the Metrohm a.c. Modulator E 393 with an a.c. voltage of 10 mV, r.m.s. at 50 cycles/sec. To minimise cell impedance, the modulating a.c. voltage was applied through an auxiliary tungsten electrode. Rapid polarographic techniques and controlled drop-times were achieved with a Metrohm Polarographie-Stand E 354. The DME had a capillary constant, $m^{\frac{2}{3}} t^{\frac{1}{6}} = 2.64$ (in distilled water at zero applied potential *vs.* Ag/AgCl electrode). For the cyclic voltammetry, a Hewlett and Packard 3300-A function generator provided the triangular voltage which was applied through a potentiostat to a three-electrode cell, and the resulting traces were displayed on a Tektronix Type 502 dual beam oscilloscope. The working electrode consisted of a glass capillary J-tube filled with mercury.

Oxygen-free nitrogen was used to de-aerate the solutions.

The concentration of Cd^{2+} was approximately $8 \cdot 10^{-4}$ M; the ligand concentrations of fluoride are shown in the Tables.

RESULTS AND DISCUSSION

(*a*) *The polarographic method for determination of stability constants*

DEFORD AND HUME[3] have derived a method of mathematical analysis of the change in half-wave potential of a metal ion with changes in the concentration of complexing agent, which allows the identification of the successive complex ions formed and the determination of their formation constants.

Their expression can be represented as follows:

$$F_0(X) = \sum_j K_j C_x^j = \text{antilog } \{0.434\ (nF/RT)\ [(E_{\frac{1}{2}})_s - (E_{\frac{1}{2}})_c] + \log\ (I_s/I_c)\} \qquad (1)$$

where the symbol $F_0(X)$ is introduced for convenience to represent the experimentally measurable quantity on the right-hand side of the equation, β_j is the formation constant of the jth complex, C_x the concentration of the complex-forming substance and the subscripts s and c refer to the free ion and complexed ion, respectively.

The function, $F_1(X) = [F_0(X) - \beta_0]/C_x$ is now introduced by DEFORD AND HUME, where β_0 is the formation constant of the zero complex and is of course, unity.

If $F_1(X)$ is plotted against C_x and is extrapolated to $C_x=0$, then the value of $F_1(X)$ at the intercept equals β_1. Likewise, the value β_2 is given by the value of $F_2(X)$ at the intercept when the function $F_2(X)=[F_1(X)-\beta_1]/C_x$ is plotted against C_x and is extrapolated to $C_x=0$. The formation constants of higher complexes (if present) may be determined similarly.

As a consequence of the nature of the $F_j(X)$ functions, a plot of $F_j(X)$ *vs.* C_x for the last complex will be a straight line parallel to the concentration axis, and this allows the determination of the number of complexes.

(b) Errors in polarographic measurements of stability constants

The experimentally-measured quantity (right-hand side of eqn. (1)) can be simplified by neglecting the small term, log (I_s/I_c), to give an expression of the form:

$$F_0(X)=\text{antilog } -0.434\,(nF/RT)\,(\Delta E_{\frac{1}{2}}) \qquad (2)$$

which is often used in preference to the more exact expression of DEFORD AND HUME, *e.g.*, ref. 7.

It can be seen, therefore, that the reliability of the results obtained depends on the precision with which changes in half-wave potential can be measured. For large changes in $\Delta E_{\frac{1}{2}}$, small errors in the measurement of half-wave potentials are not especially significant. However, when $\Delta E_{\frac{1}{2}}$ is small, then the relative errors produced in $F_0(X)$ are rather large, and subsequent calculations of formation constants are subject to very large errors. For example, in a two-electron reduction such as for cadmium, at 30° $F_0(X)=\text{antilog } -33.28\,(\Delta E_{\frac{1}{2}})$. An optimistic error of 1 mV could be assumed in conventional d.c. polarographic half-wave potentials as used for evaluation of stability constants. This can be considered an optimistic estimate of the error because standard deviations found by FRANK AND HUME[8] in measuring $E_{\frac{1}{2}}$-values for the zinc–thiocyanate system were 0.6 mV from the $E_{d.e.}$ *vs.* log $[i/(i_d-i)]$ plot and 0.8 mV using their simpler method. Consideration of the cadmium–fluoride system shows that 0.5 *M* sodium fluoride produces a shift in $E_{\frac{1}{2}}$ of only 20 mV. This gives $F_0(X)=4.630$ from the simplified equation. However, $-(\Delta E_{\frac{1}{2}})$ could be 20 ± 2 mV. If $-(\Delta E_{\frac{1}{2}})=22$ mV, $F_0(X)=5.398$; if $-(\Delta E_{\frac{1}{2}})=18$ mV, $F_0(X)=3.972$. Thus, there is the possibility of large errors in $F_0(X)$ which are greatly magnified in subsequent calculations to obtain $F_1(X)$, $F_2(X)$ etc.; and stability constants of the higher complexes may contain very large errors.

(c) Experimental techniques for measuring changes in half-wave potential

Thus, any technique which enables $\Delta E_{\frac{1}{2}}$-values to be measured more accurately than by conventional d.c. polarography, will lead to improved calculations of the stability of complexes. The use of a.c. cadmium summit potentials which are known to coincide with d.c. cadmium half-wave potentials[4] seemed to be a promising technique at first sight, because of the simplicity with which E_s-values can be obtained directly from polarograms without the need of any further interpretation. In comparison, accurate $E_{\frac{1}{2}}$-values are evaluated by plots of log $[i/(i_d-i)]$ *vs.* $E_{d.e.}$ and precision of $E_{\frac{1}{2}}$-values depends on the accuracy with which the current as well as the potential can be measured from the polarogram. Thus, E_s-values should also be more reproducible, because E_s is obtained simply from the point of maximum current, which for a reversible a.c. wave is extremely well defined, being the point of symme-

try of the wave. In comparison, $E_{\frac{1}{2}}$ requires a knowledge of i_d, i and as well $E_{d.e.}$ to be defined for each value of i. These steps, and especially the definition of i_d, require extra interpretation and may lead to a lower reproducibility compared with that of the evaluation of E_s.

Examination of standard deviations in Tables 1 and 2 confirms that the reproducibility of E_s is considerably greater than $E_{\frac{1}{2}}$ evaluated by either log plots of $E_{d.e.}$ *vs.* log $[i/(i_d-i)]$ or by the simple method of FRANK AND HUME[8].

TABLE 1

STANDARD DEVIATIONS OF E_s. MEASUREMENTS MADE ON SOLUTIONS OF 0.5 *M* NaF/0.5 *M* $NaClO_4$ BY THE RAPID POLAROGRAPHIC METHOD WITH A SCAN RATE OF POTENTIAL OF 0.5 V PER MINUTE

Drop-time (sec)	$-E_s$ *(V vs. Ag/AgCl)*	$-E_s$ *av. (V)*	*Standard deviation* E_s *(V)*	*Half-band width (mV)*
0.32	0.5572, 0.5566 0.5576, 0.5574 0.5572	0.5572	0.0004	47 ± 1
0.24	0.5574, 0.5570 0.5578, 0.5576 0.5578	0.5575	0.0003	47 ± 1
0.16	0.5576, 0.5572 0.5568, 0.5572 0.5574	0.5572	0.0003	47 ± 1

Tables 1 and 2 also show that there is a constant difference of about 4 mV between E_s and $E_{\frac{1}{2}}$ in measurements at the various drop-times used. In the previous work which indicated that $E_{\frac{1}{2}}=E_s$[4], potentials were measured to only 0.01 V, and with measurements of this precision it can be seen that E_s and $E_{\frac{1}{2}}$ would coincide.

TABLE 2

STANDARD DEVIATIONS OF $E_{\frac{1}{4}}$. MEASUREMENTS MADE ON SOLUTIONS OF 0.5 *M* NaF/0.5 *M* $NaClO_4$ BY THE RAPID POLAROGRAPHIC METHOD WITH A SCAN RATE OF POTENTIAL OF 0.5 V PER MINUTE

Drop-time (sec)	$-E_{\frac{1}{4}}$ *(log plot)*[a] *(V vs. Ag/AgCl)*	$-E_{\frac{1}{4}}$ *av. (log plot)*[a]	*Standard deviation of* $E_{\frac{1}{4}}$ *(log plot)*	*Slope of log plot (mV)*	$-E_{\frac{1}{4}}$ *(simple method)*[b] *(V vs. Ag/AgCl)*	$-E_{\frac{1}{4}}$ *av. (simple method)*[b]	*Standard deviation of* $E_{\frac{1}{4}}$ *(simple method)*	$E_{\frac{1}{4}}-E_{\frac{1}{2}}$ *(mV)*
0.32	0.5612, 0.5612, 0.5597, 0.5605, 0.5608	0.5607	0.0006	31 ± 1	0.5598, 0.5614, 0.5622, 0.5606, 0.5610	0.5610	0.0009	31 ± 1
0.24	0.5608, 0.5603, 0.5618, 0.5607, 0.5614	0.5610	0.0007	31 ± 1	0.5620, 0.5614, 0.5606, 0.5624, 0.5608	0.5614	0.0008	31 ± 1
0.16	0.5599, 0.5608, 0.5612, 0.5613, 0.5613	0.5609	0.0006	31 ± 1	0.5624, 0.5604, 0.5606, 0.5610, 0.5612	0.5611	0.0008	31 ± 1

[a] Measured graphically by plot of $E_{d.e.}$ *vs.* log $[i/(i_d-i)]$.
[b] Measured by simple method of FRANK AND HUME[8].

Rapid polarographic techniques with controlled drop-times were used in conjunction with the measurements in Tables 1 and 2 at a potential scan rate of 0.5 V/min.

Under conditions of rapid polarography, results for both $E_{\frac{1}{2}}$ and E_s were more reproducible than with normal drop-times of 2–5 sec and at slower scan rates of 0.5 V/6 min. With the fast drop frequency of the rapid polarographic method, the mercury electrode appears almost stationary and the current deflections are therefore so small that damping can be dispensed with. This greatly facilitates interpretation of the current and of i_d, and hence $E_{\frac{1}{2}}$ measurements are more reproducible. Precision and reproducibility of E_s-values are also improved under the conditions of rapid polarography because at high drop rates and fast voltage scan rates, one drop uniquely defines the summit potential and the measurement of E_s requires no interpretation of the a.c. polarogram *i.e.*, in constructing a polarogram, it is possible to measure one point on the graph for every drop. At fast drop-times, points on the graph are extremely close together and one drop or point unambiguously defines E_s. However, at longer drop-times, points on the plot are farther apart and the maximum of the graph lying between two points has to be interpreted. This extra step lowers the reproducibility.

Analytical applications of a.c. polarography have already shown that the accuracy and reproducibility of measurements of the a.c. differential current ($i_{d\sim}$) are better than those of the d.c. diffusion current (i_d)[5]. Thus, whenever possible, it is preferable to use $i_{d\sim}$ instead of i_d.

(d) Justification for use of a.c. measurements in the polarographic method for determination of stability constants

The polarographic equation (1) used to determine stability constants is valid provided that:

(a) Nernstian conditions prevail, *i.e.*, the electrode reaction should be polarographically reversible.

(b) The complexed and uncomplexed species are in equilibrium under the experimental conditions.

(c) Only the uncomplexed species is electroactive at the d.c. potentials in question.

These conditions are fulfilled with the cadmium–fluoride system and a.c. polarographic measurements for this system will be valid provided they give the same $\Delta E_{\frac{1}{2}}$ and I_s/I_c ratio as d.c. polarographic measurements.

Several theoretical treatments have been used to calculate a relationship between E_s and $E_{\frac{1}{2}}$. These differ in the method of calculation, the approximations made in calculation, and the theoretical model of the mercury electrode used to derive the relationships. However, if the electrode process is diffusion-controlled, as in this work (linear calibration graphs in fluoride media of cadmium concentration *vs.* diffusion current) then the prediction of a treatment using the stationary plane model is $E_s = E_{\frac{1}{2}}^r$ where $E_{\frac{1}{2}}^r$ is the reversible polarographic half-wave potential[9]. However, spherical diffusion effects [10,11], and possibly some special effects introduced by rapid polarographic conditions (*e.g.* depletion), could cause E_s and $E_{\frac{1}{2}}^r$ to differ slightly as has been observed in this work.

Experimentally, a constant difference of about 4 mV has been found for an a.c. voltage of 10 mV, r.m.s. applied at 50 cycles/sec and under rapid polarographic

conditions as shown in Tables 1 and 2. If, however, either $E_s = E_{\frac{1}{2}}$, or $(E_s - E_{\frac{1}{2}})$ is constant, then the condition, $\Delta E_s = \Delta E_{\frac{1}{2}}$, will be satisfied.

In general, there is a good correlation between the a.c. polarographic summit potentials and the d.c. polarographic half-step potentials for cadmium under all polarographic conditions used, and the shift in the potentials of both E_s and $E_{\frac{1}{2}}$ on the addition of increasing amounts of fluoride was in the same direction and, within the limits of experimental error, of the same magnitude. This correlation was found to occur over all drop-times between 1.8 and 5.0 sec in conventional polarography, and at much faster controlled drop-times in rapid polarography. The absolute values of E_s and $E_{\frac{1}{2}}$ under all polarographic conditions were not in exact agreement, but in all cases, within the limits of experimental error, $\Delta E_{\frac{1}{2}} = \Delta E_s$, and hence results of E_s obtained by a.c. polarography can justifiably be used in polarographic theory for the determination of stability constants of the cadmium–fluoride system.

Since the concentration-dependence of the a.c. wave height ($i_{d\sim}$) for cadmium, up to a concentration of 10^{-3} M, was almost linear in fluoride media (as was the d.c. concentration-dependence of the diffusion current (i_d)) it was assumed that log (I_s/I_c), which is experimentally measured by the term log $[(i_d)_s/(i_d)_c]$, is equal to log $[(i_{d\sim})_s/(i_{d\sim})_c]$. As the term log (I_s/I_c) is very small for the cadmium–fluoride system, it was difficult to assess this equivalence experimentally, but within limits of experimental error, satisfactory agreement was obtained. It was assumed, therefore, that a complete treatment of the equation of DEFORD AND HUME is possible from results obtained by a.c. polarography.

(e) The cadmium–fluoride system

As a result of the studies of the various polarographic techniques for measuring $\Delta E_{\frac{1}{2}}$, the cadmium–fluoride system was studied by the rapid polarographic method with a controlled drop-time of 0.16 sec and a potential scan rate of 0.5 V/min. A comparison of $E_{\frac{1}{2}}$- and E_s-potentials for Cd^{2+} in 1.0 M of each of the electrolytes, $NaClO_4$, KNO_3, NaF, KF, showed excellent agreement but as the nitrate medium showed some evidence of nitrate complexing, $NaClO_4$ was used to maintain a constant ionic strength of 1.0 in preference. Fluoride was added as NaF. Although a.c. polarography can often be achieved without prior removal of oxygen, this was not possible with cadmium because E_s-values were slightly more negative in the presence of oxygen. This has been attributed to the formation of cadmium hydroxide in the presence of oxygen at the DME[4]. The negative shift, however, was less marked in the presence of fluoride which is consistent with the formation of fluoride complexes. $E_{\frac{1}{2}}$- and E_s- values were determined for each fluoride concentration on at least 3 separate runs. Reversibility was checked on all solutions by plots of $E_{d.e.}$ *vs.* log $[i/(i_d - i)]$, which were found to be linear with slope, 31 ± 1 mV, and by a.c.polarograms which had a half-band width of 47 ± 1 mV. Further confirmation of the reversibility of the system was obtained from cyclic voltammetry, where the difference in potential between the cathodic and anodic peaks was close to the value of $2 \cdot 0.028/n$ V expected for a reversible system at 25° [12]. Since E_s-values were considerably more reproducible than $E_{\frac{1}{2}}$, only data from a.c. measurements were used in subsequent calculations. Details of the calculations are listed in Table 3 and the graphical method of evaluation of DEFORD AND HUME[3] is shown in Fig. 1. The overall stability constants for the species CdF^+ and CdF_2 were found to be $\beta_1 = 5.8 \pm 0.2$ and $\beta_2 = 4 \pm 0.5$. Other workers have obtained values of

$\beta_1 = 2.9$, $\beta_2 = 3.4$[2] and $\beta_1 = 6.4 \pm 0.5$[1]. The percentage distribution of cadmium in the form of each species as a function of fluoride concentration (Fig. 2) shows that the predominant species over most of the concentration range studied is CdF^+. It is perhaps not surprising, therefore, that MESARIC AND HUME[1] using the d.c. polarographic method, over a lower fluoride concentration range reported only one species. In view of the slightly different ionic strengths and temperatures, the agreement for β_1 obtained by a.c. polarographic measurements and by conventional d.c. polarography[1] is satisfactory. The decreased error in β_1 of ± 0.2 compared with $\pm$ 0.5 obtained

TABLE 3

ANALYSIS OF $F_j(X)$ FUNCTIONS FOR Cd–F SYSTEM

C_x (M)	$-E_s$ (V vs. Ag/AgCl)	$i_{d\sim}$ (μA)	$F_0(X)$	$F_1(X)$	$F_2(X)$
0.00	0.5375	4.20	1	—	—
0.10	0.5435	4.10	1.622	6.220	4.20
0.20	0.5476	3.98	2.287	6.435	3.18
0.35	0.5531	3.92	3.544	7.271	4.20
0.50	0.5572	3.86	4.933	7.866	4.13
0.65	0.5604	3.72	6.527	8.503	4.16
1.00	0.5678	3.48	12.30	11.30	5.50

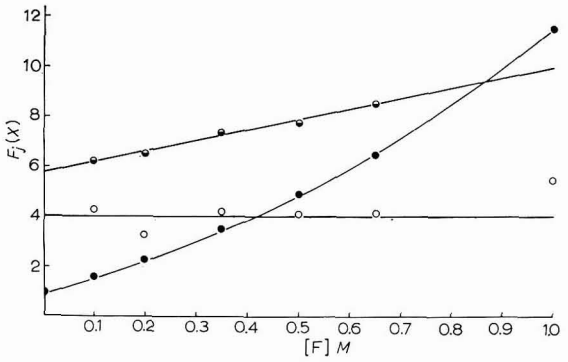

Fig. 1. $F_j(X)$ plots for Cd–F system. (●), $F_0(X)$; (◒), $F_1(X)$; (○), $F_2(X)$.

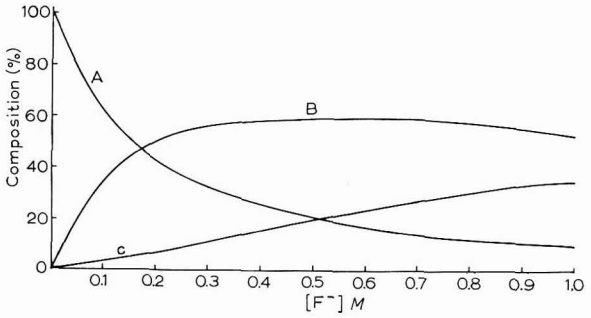

Fig. 2. Percentage distribution of various species present in Cd–F system. (A), Cd^{2+}; (B), CdF^+; (C), CdF_2.

by d.c. measurements, has been attributed to the increased precision of measurements of $\Delta E_{\frac{1}{2}}$ and demonstrates the usefulness of the a.c. method.

SUMMARY

A.c. polarographic measurements on aqueous solutions containing cadmium and fluoride ions have shown the existence of the species, CdF^+ and CdF_2, with stability constants (at 30° and an ionic strength of 1.0) of 5.8 and 4, respectively. Reproducibility studies of a.c. techniques as a means for measuring changes in half-wave potentials (upon which the polarographic method for the determination of stabilities is based) have shown that the results obtained from a.c. polarographic measurements should be more accurate than those obtained by conventional d.c. polarography.

REFERENCES

1 S. S. MESARIC AND D. N. HUME, *Inorg. Chem.*, 2 (1963) 1063.
2 I. LEDEN, Dissertation, Lund, 1943, p. 49.
3 D. D. DEFORD AND D. N. HUME, *J. Am. Chem. Soc.*, 73 (1951) 5321.
4 B. BREYER, F. GUTMAN AND S. HACOBIAN, *Australian J. Sci. Res.*, A3 (1950) 567.
5 B. BREYER AND H. H. BAUER, *Chemical Analysis*, Vol. 13, *Alternating Current Polarography and Tensammetry*, Interscience, New York/London, 1963, p. 128.
6 S. L. GUPTA AND M. K. CHATTERJEE, *J. Electroanal. Chem.*, 8 (1964) 245.
7 J. HEYROVSKY AND J. KUTA, *Principles of Polarography*, Academic Press, New York/London, 1966, pp. 152–155.
8 R. F. FRANK AND D. N. HUME, *J. Am. Chem. Soc.*, 75 (1953) 1736.
9 D. E. SMITH, in *Electroanalytical Chemistry*, Vol. 1, edited by A. J. BARD, Marcel Dekker, Inc., 1966, chap. I.
10 J. R. DELMASTRO AND D. E. SMITH, *Anal. Chem.*, 38 (1966) 169.
11 J. R. DELMASTRO AND D. E. SMITH, *Anal. Chem.*, 39 (1967) 1050.
12 P. DELAHAY, *New Instrumental Methods in Electrochemistry*, Interscience, New York/London, 1954, p. 137.

Elsevier Sequoia S.A., Lausanne – Printed in The Netherlands

SUPPORTING ELECTROLYTE EFFECT ON THE $[Ni(CN)_4]^{2-}$ ELECTROCHEMICAL REDUCTION

GIANCARLO TORSI AND PAOLO PAPOFF
Istituto Chimica Analitica dell'Università di Bari (Italy)
(Received February 19th, 1968; in revised form, August 5th, 1968)

It is known[1–4] that the Ni^{2+} ion forms in CN^- solutions the very stable complex, $[Ni(CN)_4]^{2-}$, which is essentially the only complex present even at a total concentration of CN^- lower than the stoichiometric value.

Under chemical or electrochemical reduction, this complex gives $[Ni_2(CN)_6]^{4-}$ which is slowly reoxidized by O_2 or water to $[Ni(CN)_4]^{2-}$. If a very strong chemical reducing agent is used, such as metallic potassium in liquid ammonia, the zerovalent $[Ni(CN)_4]^{4-}$ obtained is relatively stable in the absence of O_2 or water.

In the earlier polarographic studies[5,6], it was concluded that the Ni^{2+} complex is reduced with the uptake of one electron. According to HUME AND KOLTHOFF[7] the reduction is a two-electron process, the rate-controlling step being the electron transfer. From chronoamperometric measurements at constant current, DELAHAY AND MAMANTOV[8] concluded that the slow step is a preceding chemical reaction, while VLČEK[1,9] found that (from the dependence of the wave height and the half-wave potential on CN^- concentration, drop-time, and temperature) the reduction proceeds through two fast one-electron steps and the formation of an intermediate which undergoes many equilibria with the other species present. His conclusions were also supported by measurements both with the Kalousek commutator and oscillography.

Recently[10], a paper on $[Ni(CN)_4]^{2-}$ reduction at high CN^- concentration was published. From the conflicting data there was evidence of the influence of ionic strength. On this basis, it seemed worthwhile to study the ionic strength effect in order to gain a better knowledge of the mechanism of this reaction and to explain to some extent the contradictory results previously obtained.

In this paper, the results for the polarographic reduction of the nickel–cyanide complex (with different cations and concentrations of supporting electrolyte) are reported.

EXPERIMENTAL

All solutions were prepared from water twice-distilled over $KMnO_4$. Salts, of reagent-grade quality, were recrystallized and, when possible, heated at a temperature a little below the melting or the decomposition temperature. LiCN and CsCN were prepared from KCN on Dowex 50. The polarograms were obtained manually using a three-electrode cell and electronic control of the potential. The chronoamperometric measurements with linearly changing potential were made with a stationary mercury electrode and an apparatus constructed in this Institute.

The reference electrode was a SCE at $25 \pm 2°$. No correction was made for the liquid junction potential. The cell temperature was regulated at $\pm 0.1°$. The drop-time was mechanically controlled at 3 sec. The Ni^{2+} concentration was always $2 \cdot 10^{-4}$ M.

RESULTS AND DISCUSSION

Figure 1 shows the polarographic waves obtained at $[CN^-]/[Ni^{2+}] = 17$ for different KCl concentrations. It can be seen that the waves are shifted toward less negative potentials and the height of the plateau increases to a limiting value, as the K^+ concentration increases. In the case of potassium, the limiting value of the current is reached for a concentration about 0.1 N. At higher concentrations, a maximum appears which does not affect the limiting current value.

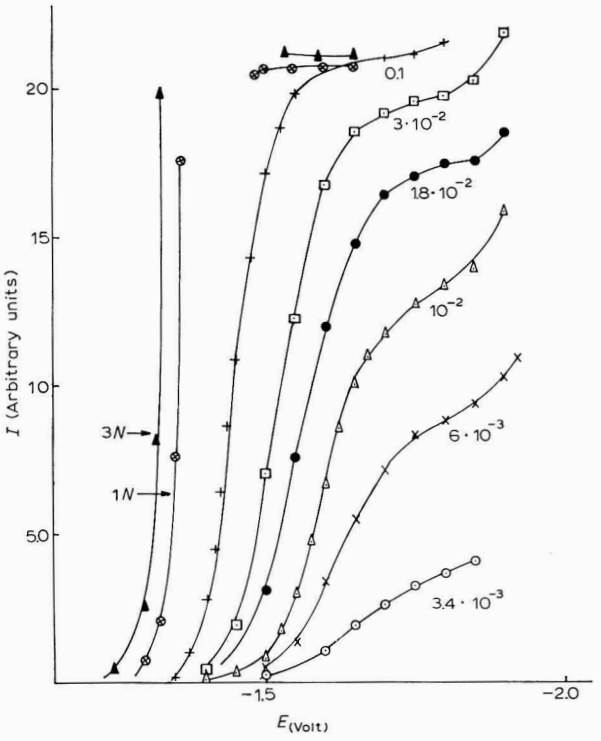

Fig. 1. $[Ni(CN)_4]^{2-}$ reduction polarograms at different K^+ concns. $[CN^-]/[Ni^{2+}] = 17$. The figures near each curve show the total concn. of K^+ obtained by adding KCl. The capacitive current has been subtracted by extrapolation.

In agreement with other authors, we found that there is some percent of kinetic contribution on the limiting current (Table 1). This contribution, the extent of which depends on the concentration of CN^-, is due to kinetic reoxidation of reduction products[1,9].

The curves of Fig. 1 are typical of a preceding chemical reaction[11]. The order of this reaction in respect to the Ni^{2+} ion was checked at a supporting electrolyte

concentration (10^{-2} *N* KCl) where the height of the wave is about half the limiting current; a very good proportionality between the height of the wave and the concentration of Ni^{2+} was found.

It is not possible from the polarographic curve analysis to ascertain whether the electron transfer is fast, even at high concentrations of supporting electrolyte where diffusion currents are obtained, owing to the presence here of a maximum. However a certain degree of electron transfer irreversibility can be assumed both from the half-wave potential-dependence on the supporting electrolyte cation type (see

TABLE 1

EFFECT OF $(CN)^-$ CONCENTRATION ON THE REDUCTION OF $[Ni(CN)_4]^{2-}$ FOR 1 AND $8 \cdot 10^{-3}$ *N* K^+ $T = 25°$, $c_{Ni^{2+}} = 2 \cdot 10^{-4}$ *M*

$c_{(CN)^-}$ (equiv./l)	i_{lim} (μA)	
	$c_{K^+} = 1$ equiv./l	$c_{K^+} = 8 \cdot 10^{-3}$ equiv./l
0	0.36*	
$1.2 \cdot 10^{-3}$	0.38	0.19
$2 \cdot 10^{-3}$	0.38	0.20
$4 \cdot 10^{-3}$	0.41	0.20
$6 \cdot 10^{-3}$	0.40	0.21
$8 \cdot 10^{-3}$	0.42	0.22
$1 \cdot 10^{-1}$	0.42	

* 0.1 *N* NH_4OH added

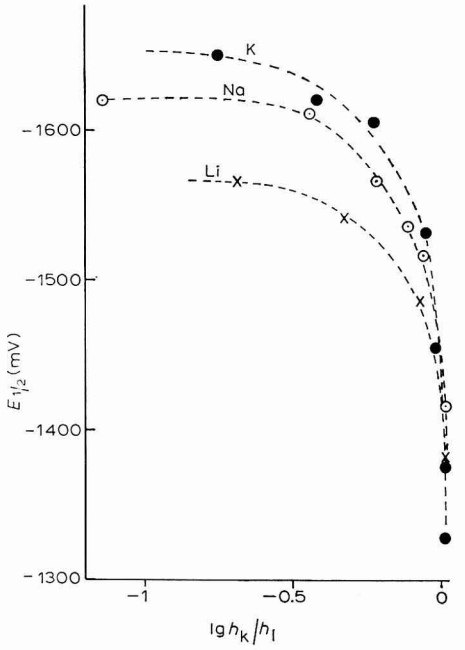

Fig. 2. Dependence of $E_{\frac{1}{2}}$ on log h_K/h_l for different concns. of supporting electrolyte. (●), K^+ salts; the concns. are (from left to right): $3.4 \cdot 10^{-3}$, $6 \cdot 10^{-3}$, 10^{-2}, $3 \cdot 10^{-2}$, 10^{-1}, $4 \cdot 10^{-1}$, 1 *M*. (○), Na^+ salts; the concns. are: 10^{-2}, $3 \cdot 10^{-2}$, $5 \cdot 10^{-2}$, $7.5 \cdot 10^{-2}$, 10^{-1}, $4 \cdot 10^{-1}$ *M*. (×), Li^+ salts; the concns. are: $6 \cdot 10^{-2}$, 10^{-1}, $4 \cdot 10^{-1}$, 1 *M*.

Fig. 2) and from the peak potential variation in chronoamperometric measurements. In the last case, in the range of 0.06 to 1 V scanning potential rate—which is comparable to the polarographic conditions—there is a small shift of the peak potential (about 15 mV) towards more negative potentials with increase in the scanning rate, even in 1 M KCl solutions (Fig. 3).

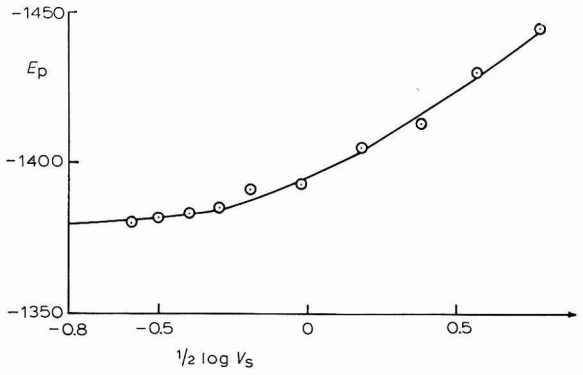

Fig. 3. Peak potential (E_p) *vs.* a function of potential scanning rate (v_s) in the chronoamperometric reduction of $[Ni(CN)_4]^{2-}$. $c_{Ni^{2+}} = 5 \cdot 10^{-4}$ M; $c_{CN^-} = 8.5 \cdot 10^{-3}$ M; $c_{KCl} = 1$ M.

Nevertheless, since in our case polarographic limiting currents measured at a potential far enough from the half-wave potential are used in the treatment of the data, it is reasonable to assume that under this condition the electron transfer is fast.

The Koutecký parameter, χ, for a kinetic current in the case of first-order reactions[11] has been calculated on the assumption that the kinetic contribution on the current is proportional to i both at low and high supporting electrolyte concentration (see Table 1). Since it was found that once the current is diffusion-controlled this current is independent of the supporting electrolyte concentration, the same i_D-value was used in the χ-calculations for all supporting electrolyte concentrations. The current data have been treated according to the theory of GIERST AND HURWITZ[12,13]. The simplest equation was used:

$$\chi = \chi_0 \exp(-zf\psi_0) \tag{1}$$

where z is the sum of the charges of all particles reacting to give the complex undergoing the reduction[14], $f = F/RT$, ψ_0 is the potential at the O.H.P. and $\chi = \sqrt{12/7}\, kKt$ (where k and K have the usual meaning of forward rate constant and equilibrium constant, and t is the drop-time).

Equation (1) holds only when the reaction layer thickness is small compared with the diffusion double layer (chemical reaction rate very fast, as was found in our case).

The χ-values were measured in some cases at constant $q = -22$ $\mu C/cm^2$ at which the corresponding current is practically no longer dependent on the potential.

In this case, since[15]

$$\psi_0 = \text{const.} + (1/Zf) \ln c \tag{2}$$

eqn. (1) can be written in the form:

$$\log \chi = \text{const.} - (z/Z) \log c \qquad (3)$$

where Z is the charge of the Z–Z supporting electrolyte and c its concentration in mole/l.

The E-values corresponding to $q = -22\ \mu C/cm^2$, at different supporting electrolyte concentrations were calculated as follows: from the data given by GRAHAME[16] for 0.1 M KCl or LiCl, the curves, q *vs.* E and q *vs.* $E - \psi_0$, were obtained. The latter curve is independent of the supporting electrolyte concentration[17] if no adsorption can be assumed. Once known, the $(E - \psi_0)$-value at $q = -22\ \mu C/cm^2$ for 0.1 M solutions, the ψ_0-values for the other concentrations of supporting electrolyte and the E-values at $q = -22\ \mu C/cm^2$, were obtained for any experimental concentration used.

Since the limiting current around the calculated E-value is not significantly dependent on the potential, the use of $\log \chi$ at constant q seems reasonable.

Figure 4a shows the function, $\log \chi$ *vs.* $\log c$, for Li^+, K^+, Cs^+. In the latter case, only one concentration ($1.1 \cdot 10^{-3}$ N) was tested since errors arising from too high a dilution at lower concentration would be quite significant and at higher concentration the maximum limiting current is reached quickly.

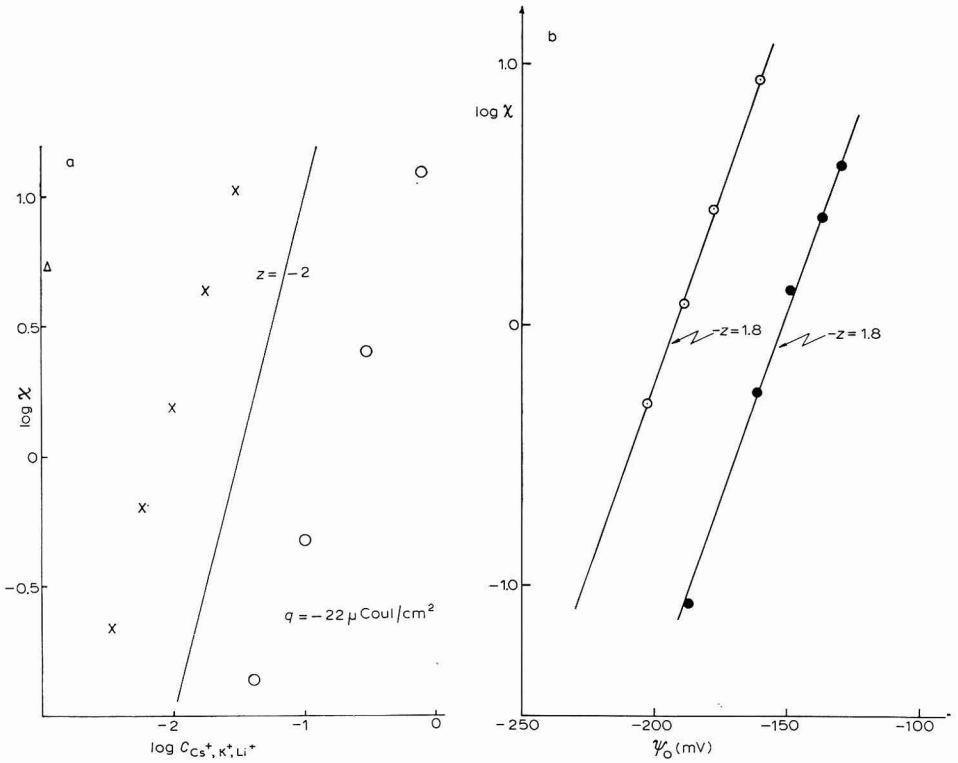

Fig. 4. Cation effect on $Ni(CN)_4^{2-}$ reduction. (a) The line has been drawn according to eqn. (3) with $z = -2$. Log χ *vs.* log cation concn. for different cation type. (○), Li; (×), K; (△), Cs. (b) Log χ *vs.* ψ_0 for different concns. of supporting electrolyte. (○), K^+ salts; (●), Na^+ salts.

For both Li^+ and K^+, the experimental points lie on straight lines the slope of which allows the value of z (-2) to be calculated (see eqn. (3)).

The small deviations observed at lower concentrations of supporting electrolyte, particularly in the case of the Li^+ salt, are probably due to some other alkaline cation impurities in the solution and a small amount of reducible H^+ ions.

In the case of Na^+ and K^+ salts, where ψ_0-values are available for many concentration values, the plot of log χ *vs.* ψ_0 was also used and fairly good straight lines were obtained (see Fig. 4b), with a slope corresponding to $z = -1.8$.

The value of $z = -2$ clearly excludes the possibility that the preceding chemical reaction may be an association among $[Ni(CN)_4]^{2-}$ and charged particles. Particularly, it excludes the possibility[18] of both an association with CN^- or Cl^-, and ion-pair formation with the cation of the supporting electrolyte. On the other hand, the dissociation of $[Ni(CN)_4]^{2-}$ with release of one $(CN)^-$ before the electron transfer, which would give $z = -2$, must be disregarded because of the very small effect of the $(CN)^-$ concentration on the polarographic wave, both in the case of high and low limiting current (Table 1). This effect may be explained according to VLČEK (see above) in terms of CN^- contribution on the catalytic reoxidation of the Ni^0 complex.

The suggestion of VLČEK[1] that the complex is reducible after an intramolecular rearrangement seems to be in accordance with all the experimental data even if a more likely scheme should be assumed, involving perhaps water molecules.

From the paper of PENNEMAN *et al.*[18], it may be presumed that aqueous tetracyanonickelate is essentially four-coordinated at CN^- concentration lower than 0.1 M. At higher cyanide concentrations, some $[Ni(CN)_5]^{3-}$ is formed, with the fifth cyanide group held much less strongly than the other four. In our experimental condition ($(CN)^-$ concentration lower than 10^{-2} M) it may be assumed that no other complexes other than one six-coordinated with two weakly bound water molecules is in equilibrium with the main tetra-coordinated complex, the former being involved in the electrochemical process.

As further support of this point of view, the $(CN)^-$ exchange rate for $[Ni(CN)_4]^{2-}$ is very likely of zero-order, as in the case of similar complexes[19].

With the assumption that $z = -2$, even in the case of the Cs^+ salt, the straight line from the corresponding log χ parallel to the other lines can be drawn. The difference between the values of log χ calculated for Cs^+ and Li^+ at the same concentration is about 4 orders of magnitude. The corresponding ψ_0-difference calculated from eqn. (1) is about 120 mV. The fact that the Gouy–Chapman theory explains rather satisfactorily the concentration-dependence of the polarographic wave height but not the dependence on cation type is verified for many other systems controlled either by the electron transfer or by a preceding chemical reaction. In the case of $[Ni(CN)_4]^{2-}$, the magnitude of the effect is very unusual. This can be explained to some extent by taking into account the high negative charge on the mercury and the double negative charge on the complex. Both conditions are too extreme for the Gouy–Chapman theory and, unfortunately, there are no other theories on the double layer to explain the experimental data[20].

The $[Ni(CN)_4]^{2-}$ behaviour can be explained according to the interpretation of GIERST *et al.*[21] of the cation influence on the electrode reaction based on the water organization around the ions.

As for the value of the product, kK, calculated at $\psi_0 = 0$ by extrapolation of

the log χ *vs.* ψ_0 curve, it must be pointed out that the extrapolation itself seems devoid of meaning owing to the large distance between the experimental points (confined in a small interval of ψ_0-values) and the extrapolated point. In addition, the very large difference between the k-values which would thus be found for different supporting-electrolyte cations, is rather difficult to explain from a kinetic point of view.

Hence, and by assuming a value of K equal to 10^{-2} (as the maximum value according to the experimental evidence that the limiting current at low concentration of supporting electrolyte tends to zero) a minimum value of $k = 10^{10}$ sec^{-1} may be found in the case of Li^+ salts.

SUMMARY

The reduction mechanism of $[Ni(CN)_4]^{2-}$ at the dropping mercury electrode was studied varying the concentration and the cation type of supporting electrolyte. It has been found that both have a strong effect on the limiting current, i_l, and the half-wave potential. This means that according to the experimental conditions, the electron transfer and/or a chemical reaction may be the rate-determining steps.

From the analysis of the limiting current data as a function of ψ_0, it was found that in the chemical reaction preceding the electron transfer, the sum of the charges of all the particles that react to give the electroactive complex is equal to -2.

Since in the experimental conditions used, the only complex present in the solution is the tetracyanonickelate ion with two negative charges, it results from $z = -2$ that this particle is reduced at the mercury electrode without any association. On the other hand, also the dissociation of $[Ni(CN)_4]^{2-}$, which is in accordance with $z = -2$, must be disregarded owing to the very small effect of the CN^- concentration on i_l. An intramolecular rearrangement as suggested by VLČEK may be considered responsible for the chemical rate-determining step.

The strong influence of the type of cation in the double layer region does not allow the correct determination of the equilibrium constant and the reaction rate constant, which must be very large.

REFERENCES

1 A. A. VLČEK, *Collection Czech. Chem. Commun.*, 22 (1957) 948.
2 A. L. VAN GEET AND D. N. HUME, *Inorg. Chem.*, 3 (1964) 523.
3 H. FREUND AND C. R. SCHNEIDER, *J. Am. Chem. Soc.*, 81 (1959) 4780.
4 J. S. COLEMAN, H. PETERSEN AND R. A. PENNEMAN, *Inorg. Chem.*, 4 (1965) 135.
5 N. V. EMELIANOVA, *Rec. Trav. Chim.*, 44 (1925) 528.
6 V. CAGLIOTI, G. SARTORI AND P. SILVESTRONI, *Atti Accad. Naz. Lincei, Rend. Classe Sci. Fis., Mat. Nat.*, 3 (1947) 448.
7 D. N. HUME AND I. M. KOLTHOFF, *J. Am. Chem. Soc.*, 72 (1950) 4423.
8 P. DELAHAY, *New Instrumental Methods in Electrochemistry*, Interscience Publishers, New York, 1962, p. 215.
9 A. A. VLČEK, *Collection Czech. Chem. Commun.*, 22 (1957) 1736.
10 HWANG AM KIM AND IL HYUN PARK, *Daehan Hwahak Hwoejee*, 9 (1965) 67.
11 J. KOUTECKÝ, *Collection Czech. Chem. Commun.*, 18 (1953) 597.
12 L. GIERST AND H. HURWITZ, *Z. Elektrochem.*, 64 (1960) 36.
13 H. HURWITZ, *Z. Elektrochem.*, 65 (1961) 178.
14 P. DELAHAY, *Double Layer and Electrode Kinetics*, Interscience Publishers, New York, 1965, p. 207.
15 P. DELAHAY, *Double Layer and Electrode Kinetics*, Interscience Publishers, New York, 1965, p. 42.

16 D. C. GRAHAME, *J. Electrochem. Soc.*, 98 (1951) 343.
17 D. C. GRAHAME, *Chem. Rev.*, 41 (1947) 441.
18 R. A. PENNEMAN, R. BAIN, G. GILBERT, L. H. JONES, R. S. WYHOLM AND G. K. W. REDDY, *J. Chem. Soc.*, (1963) 2266.
19 A. G. MACDIARMID AND N. F. HALL, *J. Am. Chem. Soc.*, 76 (1954) 4222.
20 P. DELAHAY, *Double Layer and Electrode Kinetics*, Interscience Publishers, New York, 1965, chap. 3.
21 L. GIERST, L. VANDENBERGHEN, E. NICOLAS AND A. FRABONI, *J. Electrochem. Soc.*, 113 (1966) 1025.

ELECTROANALYTICAL CHEMISTRY AND INTERFACIAL ELECTROCHEMISTRY
Elsevier Sequoia S.A., Lausanne – Printed in The Netherlands

POTENTIOMETRIC ESTIMATION OF POTASSIUM HYDROXOTETRACYANOTUNGSTATE(IV) AND DETERMINATION OF STANDARD POTENTIAL

KABIR-UD-DIN, A. A. KHAN AND M. AIJAZ BEG
Department of Chemistry, Aligarh Muslim University, Aligarh (India)

(Received May 29th, 1968; in revised form, July 2nd, 1968)

MIKHALEVICH AND LITVINCHUK synthesized potassium hydroxocyanotungstate(IV) and determined the purity by titrating potentiometrically with $K_3[Fe(CN)_6]$ or $KMnO_4$[1,2]. The standard potential for the change:

$$[W(CN)_8]^{3-} + e = [W(CN)_8]^{4-}$$

has been given as +0.57 V in the presence of KCl of unstated concentration (0°)[3] or +0.46 V at $\mu = 0$ (25°)[4]. When 4 CN^- groups are replaced by 4 OH^- groups, a value of $E_{W(IV)/W(V)} = -0.62$ V[5] in a saturated alkaline solution of the complex has been reported. In a detailed study of the redox properties of hydroxocyanotungstate-(IV), MIKHALEVICH AND LITVINCHUK[2] expressed the dependence of the redox potential on pH by the equation:

$$E_{ox/red} = E_0 + 0.029 \log[ox]/[red] + 0.116\ (7 - pH)$$

The equation shows that two electrons should be involved in the equilibrium process, but the proposed mechanism:

$$[W^{IV}(CN)_4(OH)_4]^{4-} \rightleftharpoons e + [W^{V}(CN)_4(OH)_4]^{3-}$$

$$[W^{V}(CN)_4(OH)_4]^{3-} \rightarrow e + WO_4^{2-} + 4\ HCN$$

suggests a one-electron reversible oxidation.

During the protonation stages of the tetrasubstituted complex according to the scheme[6]:

$$[W(CN)_4(OH)_4]^{4-} \underset{aq}{\overset{H^+}{\rightleftharpoons}} [W(CN)_4(OH)_3(H_2O)]^{3-} \underset{aq}{\overset{H^+}{\rightleftharpoons}} [W(CN)_4(OH)_2(H_2O)_2]^{2-}$$

(yellowish-brown) (lilac) (bluish-violet)

a significant change occurs in the basicity as well as in the redox potential. As the redox processes in the reaction are obscure, it was thought worthwhile to carry out a similar investigation to that for hydroxocyanomolybdate(IV)[7].

The present communication deals with (i) determination of potassium hydroxotetracyanotungstate(IV) using oxidants, I_2, $Cr_2O_7^{2-}$ and Ce(IV), and (ii) determination of E° for the existing redox couple in alkaline medium by the potential mediator method using $K_3[Fe(CN)_6]$ as the mediator.

EXPERIMENTAL

Preparation and purity of complex salts

Potassium tetrahydroxotetracyanotungstate(IV) tetrahydrate, $K_4[W(CN)_4(OH)_4] \cdot 4\ H_2O$. The crystalline yellow-brown complex was prepared electrolytically using the method of MIKHALEVICH AND LITVINCHUK[1,2]. All materials used were of A.R. grade (B.D.H.). The complex was kept over $CaCl_2$ in a vacuum desiccator. (Found: C, 9.02; N, 10.17; H, 2.01. Calcd. for $K_4W(CN)_4(OH)_4 \cdot 4\ H_2O$: C, 8.21; N, 9.57; H, 2.07%.) Its purity was determined potentiometrically by titrating with potassium ferricyanide.

Potassium hexacyanoferrate(III). The A.R. grade product was recrystallized from water and air-dried. The iron content of the complex was determined iodometrically as Fe(III)[8].

All other reagents used were A.R. grade or Merck reagent-grade. The complex salt solutions were stored in coloured bottles wrapped in black paper. Triply-distilled water was used throughout the work.

Apparatus

A Pye Precision Vernier potentiometer (Cat. No. 7568) in conjunction with a ballistic galvanometer and lamp and scale arrangement was used for potential measurements. A saturated calomel electrode was used as a reference and a bright platinum electrode as the indicator electrode. A side-tube from the reference electrode with porous end-plate, filled with KNO_3 (satd.)–agar was used to connect the two halves of the cell.

All measurements were made in a darkened room. The temperature was maintained within $\pm 0.1°$ in a Townson and Mercer thermostat. All operations were carried out under a nitrogen atmosphere. Cylinder nitrogen was used after passage through chromous chloride and alkaline pyrogallol solutions.

RESULTS AND DISCUSSION

Determination with alkaline iodine

For the potentiometric determination of potassium tetrahydroxotetracyanotungstate(IV) with iodine, the galvanic circuit was as follows:

$$Pt^- \mid K_4[W(CN)_4(OH)_4] \,\vdots\, KNO_3 \,\vdots\, KCl\ Hg_2Cl_2 \mid Hg^+$$
(satd.)

The titrations were carried out in 1 *M* KOH at 30° with 0.1 *M* iodine. The intensity of the reddish-violet colour of the solution decreased as the titration proceeded. A sharp jump in potential was observed on adding one equivalent of the oxidant and the solution became colourless. A typical curve is shown in Fig. 1A. The potential break at the equivalence point was about 0.248 V for 0.05 ml of oxidant in the titration of 2 m*M* hydroxocyanide in 1 *M* potassium hydroxide with 0.1 *M* iodine solution. Only direct titrations (hydroxocyanide solution in the cell) are possible.

The redox reaction may be represented as:

$$[W^{IV}(CN)_4(OH)_4]^{4-} + I_2 \rightleftharpoons [W^{VI}(CN)_4(OH)_4]^{2-} + 2\ I^- \qquad (1)$$

The equilibrium constant (K) for the above reaction, using $E°_{I_2/I^-} = +0.5355$ V[9] and $E°_{[W(CN)_4(OH)_4]^{2-}/[W(CN)_4(OH)_4]^{4-}} = -0.7177$ V (as described below), was calculated as $1.184 \cdot 10^6$. This high value indicates that at equilibrium, almost all the $[W(CN)_4(OH)_4]^{4-}$ is oxidized to $[W(CN)_4(OH)_4]^{2-}$ by iodine.

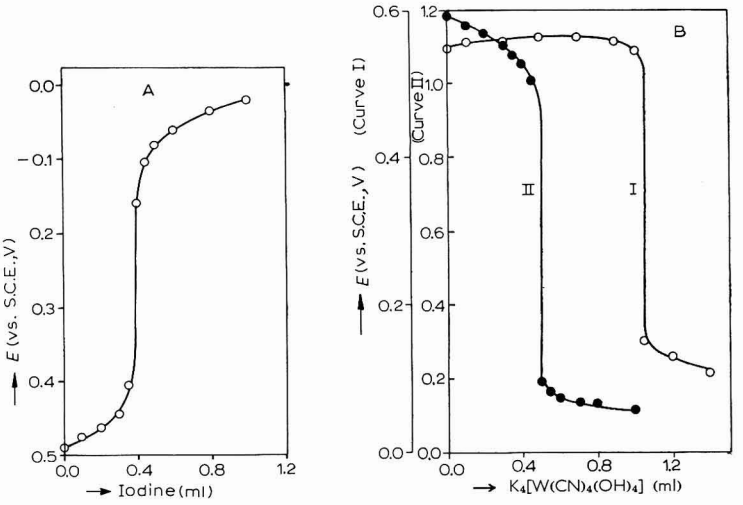

Fig. 1. (A), Potentiometric titration of 2 mM $K_4W(CN)_4(OH)_4$ in 1 M KOH with 0.1 M iodine. (B), Potentiometric titration with 0.1 M $K_4W(CN)_4(OH)_4$ of: (I), 1.75 mM $K_2Cr_2O_7$ in 4 M H_2SO_4; (II), 5 mM $Ce(SO_4)_2$ in 4 M H_2SO_4.

Determination with acid potassium dichromate

Direct titrations of hydroxocyanide with $K_2Cr_2O_7$ are not possible in acid medium because of the reaction between hydroxocyanide and acid. A solution of $K_2Cr_2O_7$ in 4 M H_2SO_4 was taken in the titration cell and was titrated with 0.1 M hydroxocyanide. The solution was decolourized owing to reduction of $K_2Cr_2O_7$. Any hydroxocyanide added after the equivalence point is decomposed by the acid content of the reaction mixture. A potential break of 0.40 V/0.05 ml was obtained. The results of a typical titration are shown in Fig. 1B, curve I.

Determination with acid cerium(IV) sulphate

Since direct titrations were again impossible, $Ce(SO_4)_2$ in a medium of 4 M H_2SO_4 was titrated with hydroxocyanide. At the equivalence point, a jump in potential of 0.818 V/0.05 ml was observed (see Fig. 1B, curve II).

The difference in the behaviour of the various oxidants towards potassium hydroxocyanotungstate(IV) is self evident. Only those oxidants with a high oxidation potential gave large inflexions at the equivalence point.

The amounts of oxidants consumed in all the titrations correspond stoichiometrically to the oxidation of hydroxocyanotungstate(IV) to (VI):

$$K_4[W^{IV}(CN)_4(OH)_4] \rightleftharpoons K_2[W^{VI}(CN)_4(OH)_4] + 2\,e \qquad (2)$$

The methods are accurate to $\pm 0.01\%$.

Determination of E°

The potential mediator method[10] was used in this determination. Hydroxocyanide (20 ml of 2.5 mM) was titrated with 0.1 M $K_3[Fe(CN)_6]$. After each addition, the potential was measured at the bright platinum electrode. Titrations were continued until a sudden change in potential was observed. Experiments were carried out with varying concentrations of KOH (0.1–3.0 M).

The value of E° was determined using the relationship:

$$E = E^\circ - RT/nF \ln [t/(t_c - t)]$$

where E is the electrode potential, t the amount of oxidant added at any point during the titration, t_c, the amount of oxidant added at the equivalence point and R, T, F and n have their usual significance. The mean values of E°, determined graphically by plotting $\log[t/(t_c - t)]$ *vs.* electrode potential (Fig. 2) at varying KOH concentrations, are recorded in Table 1.

It can be seen from Fig. 2 that the slope of the various straight lines is approximately -0.03, so that n, the number of electrons taking part in the equilibrium process, is equal to 2, confirming the proposed redox mechanism:

$$[W^{IV}(CN)_4(OH)_4]^{4-} \rightleftharpoons e + [W^{V}(CN)_4(OH)_4]^{3-} \rightleftharpoons [W^{VI}(CN)_4(OH)_4]^{2-} + 2e \quad (3)$$

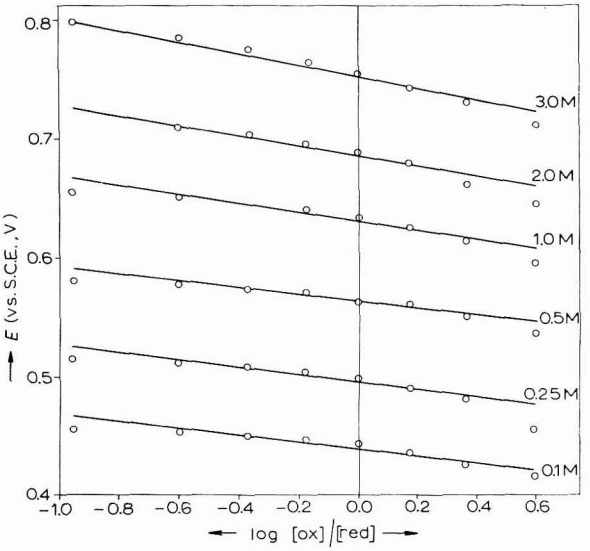

Fig. 2. Plot of electrode potential *vs.* log[ox]/[red] at varying KOH concn.

TABLE 1

VALUES OF E° (*vs.* NHE) AT VARYING CONCENTRATIONS OF KOH (μ = 3.1)

KOH concn. (M)	*E° (from plot) (V)*	*KOH concn. (M)*	*E° (from plot) (V)*
0.10	−0.6752	1.0	−0.7177
0.25	−0.6827	2.0	−0.7237
0.50	−0.7007	3.0	−0.7397

The effect of KOH concentration on the $E°$-value of the system may be interpreted in a similar manner to that proposed by KOLTHOFF[11] for the effect of HCl concentration on the ferro–ferricyanide system. On the basis of these considerations the equation:

$$E_{ox/red} = E° - [RT/nF] \ln [ox]/[red][KOH]^{\alpha} \quad (4)$$

holds instead of the usual equation

$$E = E° - [RT/nF] \ln [ox]/[red]$$

TABLE 2

VALUES OF $E°$ (*vs.* NHE) AT DIFFERENT TEMPERATURES (μ = 1.535)

Temp. (°K)	$E°$	*Temp.* (°K)	$E°$
298	−0.7015	313	−0.7501
303	−0.7127	318	−0.7803
308	−0.7419	323	−0.8050

For a fixed value of [ox]/[red], a plot of E *vs.* log [KOH] results in a straight line the slope of which gives the value of $\alpha = 1.5$. Thus, the equation representing the effect of KOH on the redox couple is:

$$E_{ox/red} = E° - [RT/nF] \ln [ox]/[red][KOH]^{1.5} \quad (5)$$

Effect of ionic strength and calculation of thermodynamic quantities

The ionic strength was adjusted with KNO_3 solution. Experiments carried out at different ionic strengths show that the oxidation potential decreases with increase in ionic strength.

$E°$ was determined at different temperatures (Table 2) in the range, 298–323°K at intervals of 5°. These values were used to calculate $\Delta G°$, $\Delta H°$ and $\Delta S°$ for the system at various temperatures; the values at 298°K are 32.4 kcal mole^{-1}, 22.6 kcal mole^{-1} and 184 cal deg.$^{-1}$ mole^{-1}, respectively.

ACKNOWLEDGEMENT

We thank Dr. S. M. F. RAHMAN for providing the facilities for this work and the C.S.I.R., New Delhi (India), for the award of a Junior Fellowship to one of us (K.U.).

SUMMARY

The potentiometric determination of tetrapotassium tetrahydroxytetracyanotungstate(IV) using I_2, $Cr_2O_7^{2-}$ and Ce(IV) as oxidants is reported. Studies relating to the determination of the oxidation potential ($E°$) by the potential mediator method for W(IV)–W(VI) hydroxocyanide complex ion couple in alkaline medium are described. The $E°$-value depends on the concentration of KOH and the relation-

ship, $E = E^\circ - [RT/nF]$ ln [ox]/[red][KOH]$^{1.5}$ has been found to hold for the couple. The thermodynamic quantities, ΔG°, ΔH° and ΔS°, have also been calculated.

REFERENCES

1 K. N. MIKHALEVICH AND V. M. LITVINCHUK, *Zh. Neorgan. Khim.*, 4 (1959) 1775.
2 K. N. MIKHALEVICH AND V. M. LITVINCHUK, *Zh. Neorgan. Khim.*, 9 (1964) 2391.
3 O. COLLENBERG, *Z. Physik. Chem.*, 109 (1924) 353.
4 H. BAADSGARD AND W. D. TREADWELL, *Helv. Chim. Acta*, 38 (1955) 1669.
5 K. N. MIKHALEVICH AND V. M. LITVINCHUK, *Nauchn. Zap. L'vovsk. Politekhn. Inst., Ser. Khim. Tekhnol.*, 50 (1958) 16.
6 V. M. LITVINCHUK AND K. N. MIKHALEVICH, *Ukr. Khim. Zh.*, 25 (1959) 563.
7 KABIR-UD-DIN, A. A. KHAN AND M. AIJAZ BEG, *J. Electroanal. Chem.*, 18 (1968) 187.
8 A. I. VOGEL, *Quantitative Inorganic Analysis*, Longmans-Green and Co., New York, 1951, p. 356.
9 W. M. LATIMER, *The Oxidation States of the Elements and their Potentials in Aqueous Solutions*, Prentice-Hall, New York, 1953, p. 63.
10 S. GLASSTONE, *Introduction to Electrochemistry*, D. Van Nostrand Company, Princeton, N.J., 1942, p. 276.
11 I. M. KOLTHOFF, *Chem. Weekblad*, 16 (1919) 1406.

ELECTROANALYTICAL CHEMISTRY AND INTERFACIAL ELECTROCHEMISTRY
Elsevier Sequoia S.A., Lausanne – Printed in The Netherlands

PHOSPHORORGANISCHE VERBINDUNGEN. 61[1]. POLAROGRAPHISCHE UNTERSUCHUNG QUARTÄRER PHOSPHONIUM- UND ARSONIUMSALZE

LEOPOLD HORNER UND JÜRGEN HAUFE*
Institut für Organische Chemie, Universität Mainz (Deutschland)
(Eingegangen am 13 Mai 1968; revisioniert am 29 Juli 1968)

EINLEITUNG

Die kathodische Abspaltung eines Liganden von quartären Phosphonium- und Arsoniumsalzen an der Quecksilber- oder Bleielektrode hat der präparativen phosphor- und arsenorganischen Chemie neue Wege erschlossen. Mit Hilfe dieser Methode konnten erstmalig optisch aktive tertiäre Phosphine und Arsine dargestellt werden, deren Verwendung ein vertieftes Verständnis für den Mechanismus vieler phosphor- und arsenorganischer Reaktionen vermittelte[2].

An Hand der quantitativen Bestimmung der an der Quecksilberkathode gebildeten Reaktionsprodukte hatten wir zwei Haftfestigkeitsreihen aufgestellt, die damals acht phosphorständige[3] und neun am Arsen gebundene Liganden[4] umfassten. In der Zwischenzeit haben wir diese Haftfestigkeitsreihen mit der gleichen Methodik weiter ausgebaut[5]. Die so ermittelten Reihen haben jedoch den Nachteil, dass sie die Liganden nur in ihrer relativen Bindungsstärke untereinander ordnen aber kein quantitatives Mass für die Bindungsstärken vermitteln. Ein quantitativer Vergleich der Ligandenhaftfestigkeit erschien jedoch umso dringlicher, als auch die Korrosionsschutzwirkung der Phosphonium- und Arsoniumsalze gegenüber Eisen in saurem Medium eine Abhängigkeit von der Natur der Liganden erkennen liess, die mit der Stellung der Liganden in den Haftfestigkeitsreihen parallel ging[6]. In der Hoffnung, für die Haftfestigkeit der Liganden ein quantitatives Mass zu finden, haben wir polarographisch unter stets gleichen Bedingungen die Halbstufenpotentiale einer grossen Zahl von Phosphonium- und Arsoniumsalzen bestimmt.

ERGEBNISSE

Oniumsalze mit P[4,5–15], As[4,9], I[16], Sb[17–19], S[20–27], als Zentralatom sind schon häufig polarographisch untersucht worden. Die gefundenen Halbstufenpotentiale lassen sich jedoch nur schwer vergleichen, da fast alle Autoren bei unterschiedlichen Bedingungen gearbeitet und daher auch unterschiedliche Werte erhalten haben. Die Kenntnis der Abhängigkeit der Halbstufenpotentiale von den Milieubedingungen ist umso entscheidender, als die Reduktionsvorgänge an der Quecksilberkathode irreversibel sind, und die für reversible Prozesse gültigen Beziehungen nur mit Vorbehalt verwendet werden dürfen. Die Halbstufenpotentiale mussten deshalb unter sorgfältig einzuhaltenden stets gleichen Bedingungen bestimmt werden. Zusammenfassend kann

* Auszug aus der Dissertation, J. HAUFE, Univ. Mainz, 1966.

festgestellt werden, dass die Halbstufenpotentiale abhängen: (i) von der Depolarisatorkonzentration, (ii) von der Temperatur, (iii) von der Tropfgeschwindigkeit, (iv) von der Höhe des Quecksilberniveaus und (v) von Art und Konzentration des Maximumdämpfers.

Die Interpretation der Polarogramme ist schwierig, weil oft mehrere Stufen auftreten. Die positiver liegenden Stufen entsprechen wahrscheinlich der Umwandlung der quartären Phosphonium- und Arsoniumsalze in die tertiären Phosphine bzw. Arsine, die negativer liegenden Stufen lassen auf einen reduktiven Abbau der tertiären zu sekundären Verbindungen schliessen[10]. Ob es sich hierbei um Ein- oder Zwei-Elektronenübergänge handelt, kann mit Hilfe der logarithmischen Analyse der Polarogramme nicht entschieden werden. Die quartären Oniumsalze können nach Auskunft unserer Messmethode an der Quecksilberkathode über folgende irreversibel (vergleiche jedoch[11]) verlaufende Prozesse abgebaut werden:

$$\begin{array}{ccc} R_4P^{(+)} & \xrightarrow[(1)]{+e} & R_4P\cdot \xrightarrow[(2)]{+e} R_4P{:}^{(-)} \\ & \downarrow{\scriptstyle (3)} & \downarrow{\scriptstyle (4)} \\ & R_3P + R\cdot & \xrightarrow[(5)]{+e} R_3P + R^{(-)} \\ & \downarrow{\scriptstyle (6)} & {\scriptstyle (7)}\downarrow{\scriptstyle +H^{(+)}} \\ & R_3P + \tfrac{1}{2}(R.R) & R_3P + RH \end{array}$$

An Stelle von zwei hintereinander geschalteten Einelektronenübergängen könnten die Oniumionen aber auch in einem Schritt zwei Elektronen aufnehmen.

Der Reaktionsweg (1), (3) könnte dann als bewiesen gelten, wenn das aus $R_4P\cdot$ hervorgehende Radikal $R\cdot$ in Gestalt der Dimerisierungs- oder Disproportionierungsprodukte quantitativ gefasst werden könnte. Da $R_4P\cdot$ und $R\cdot$ an der Quecksilberoberfläche jedoch adsorbiert sind, steht auch einem weiteren Übergang eines Elektrons auf diese beiden Radikale gemäss Schritt (2) oder (5) nichts im Wege. Die Entscheidung, ob der Abbau über die Stufen (1), (3), (5) und (7) oder über (1), (2), (4) und (7) verläuft, ist auf polarographischem Wege nicht möglich. Die wenigen bisher bekannten Beispiele, bei denen die Produktenanalyse einen Rückschluss auf die Kathodenvorgänge erlaubt, sollen in einem anderen Zusammenhang besprochen werden[5]. Die spärlichen Angaben der Literatur sind z.Teil widerspruchsvoll.

WAWZONEK UND WAGENKNECHT[10] geben für Tetraphenylphosphoniumchlorid (40) in Dimethylformamid zwei Einelektronenübergänge an, während MATSUO[12] für die gleiche Verbindung in Wasser einen Zweielektronenübergang findet. Das Trimethylphenylphosphoniumion (15) soll nach COLICHMAN[7] an der Quecksilberkathode im alkoholischen Medium in zwei Einelektronenübergängen abgebaut werden. MATSCHINER UND ISSLEIB[11] beobachten beim Triphenylbenzylphosphoniumchlorid (11) mit Hilfe des Kalousek-Umschalters in wässriger Lösung für die erste Stufe einen reversiblen Einelektronenübergang, der von einer nachgelagerten chemischen Reaktion begleitet ist. Nach unserer heutigen Kenntnis ist es auch unter Berücksichtigung der an der Quecksilberkathode gebildeten Reaktionsprodukte unmöglich, einen verbindlichen und einheitlichen Reaktionsmechanismus für die kathodische Spaltung aufzustellen. Wir haben noch kein quantitatives Mass für die Reaktionsschritte (1) und (2) und die Ligandenablösung (3) und (4), umso weniger, als die Zwischenverbindungen an der Quecksilberoberfläche adsorbiert sind und sich wahrscheinlich nur die

TABELLE 1

POLAROGRAPHISCHE UNTERSUCHUNG EINIGER PHOSPHONIUMSALZE IN WÄSSRIGER LÖSUNG ($10^{-3}M$)

Phosphoniumbromid		*Lit.***	*Stufe*	$-E_{\frac{1}{2}}$ *(V)*	i_d *(μA)*	n_1	n_2
Methyltriphenyl-	(1)	28	1	1.862	2.60	2.7	1.1
Cyclohexyltriphenyl-	(2)	32	1	1.859	2.94	1.6	
			2	2.092	0.28	1.2	
Äthyltriphenyl-	(3)	3	1	1.837	1.79	3.1	
			2	1.970	0.80	1.7	
iso-Propyltriphenyl-	(4)	30	1	1.833	1.56	9.1	1.2
			2	2.092	2.14	0.7	
n-Propyltriphenyl-	(5)	30	1	1.822	1.36	2.3	
			2	1.962	0.72	1.4	
			3	2.075	0.14	2.2	
n-Butyltriphenyl-	(6)	3	1	1.802	1.16	2.1	
			2	1.984	1.22	1.2	
2-Butyltriphenyl-	(7)	5	1	1.769	1.38	6.3	
			2	2.086	1.20	1.0	
iso-Butyltriphenyl-	(8)	30	1	1.720	1.26	2.4	
			2	2.039	1.28	0.6	
tert-Butyltriphenyl-	(9)	3	1	1.657	0.86	2.0	
			2	2.041	0.54	2.2	
Allyltriphenyl-	(10)	28	1	1.626	2.10	1.4	
			2	1.775	0.20	0.9	
			3	2.065	0.45	2.2	
			4	2.468	1.35	2.1	
Benzyltriphenyl-*	(11)	31	1	1.552	2.80	1.3	
Cyanomethyltriphenyl-*	(12)	33	1	1.301	1.62	0.9	
			2	2.051	0.84	0.9	
Benzhydryltriphenyl- $c < 10^{-3}\,M$	(13)	34	1	1.271	0.58	1.3	
			2	2.067	0.13	2.2	
Dimethyldiphenyl-	(14)	29	1	2.087	4.38	1.3	
Trimethylphenyl-	(15)	7	1	2.271	5.10	0.9	
Diäthyldiphenyl-	(16)	29	1	2.031	2.58	2.1	0.7
4-Brom-*n*-butyltriphenyl-	(17)	35	1	1.160	0.46	0.4	
			2+3	1.766	2.25	3.4	
			4	2.151	1.25	0.6	
Methylen-bis-triphenyl-	(18)	36	1	1.195	2.50	0.8	
			2	1.817	0.95	1.7	
			3	1.932	1.19	2.7	
Dimethylen-bis-triphenyl-	(19)	37	1	1.475	2.50	1.9	
			2	2.064	2.70	2.2	
Trimethylen-bis-triphenyl-	(20)	37	1	1.307	0.40	2.7	
			2	1.712	5.40	2.1	
			3	2.054	1.00	2.0	
Tetramethylen-bis-triphenyl-	(21)	35	1	1.798	8.80	1.8	
			2	2.058	0.90	2.1	
Pentamethylen-bis-triphenyl-	(22)	38	1	1.807	5.04	3.6	
Hexamethylen-bis-triphenyl-	(23)	38	1	1.822	4.75	1.8	
			2	2.000	1.10	0.8	

(Fortsetzung auf der folgenden Seite)

TABELLE 1 (Fortsetzung)

Phosphoniumbromid		*Lit.***	*Stufe*	$-E_{\frac{1}{2}}$ *(V)*	i_d *(μA)*	n_1	n_2
Oktamethylen-bis-triphenyl-	(24)		1	1.732	3.70	2.3	
			2	1.971	1.50	1.2	
Dekamethylen-bis-triphenyl-	(25)	38	1	1.715	1.25	0.9	
$c < 10^{-3}M$			2	1.916	0.65	2.2	
			3	2.073	0.45	—	
Dodekamethylen-bis-triphenyl-	(26)		1	1.664	1.50	2.7	
$c < 10^{-3}M$			2	1.944	2.50	0.9	
n-Propyl-tri-*p*-anisyl	(27)	39	1	1.934	0.68	0.7	
			2	2.109	1.12	0.9	
			3	2.364	0.90	0.7	
n-Propyl-tris-dimethylamino-	(28)	39	1	1.653	0.43	0.3	
			2	2.111	0.82	0.7	
Methyl-tris-dimethylamino-	(29)	40	1	1.642	0.31	0.3	
			2	2.098	0.64	0.7	
Benzyl-tris-dimethylamino-	(30)	41	1	1.637	0.17	0.5	
			2	2.230	2.65	0.3	
Benzyl-tris-N-trimorpholino-	(31)	42	1	1.627	0.31	—	
			2	2.206	6.40	0.4	
Methyl-tris-*p*-dimethylaminophenyl-	(32)	43	1	1.697	0.17	—	
Benzyl-tris-*p*-dimethylaminophenyl-	(33)	39	1	1.279	0.36	0.8	
$c < 10^{-3}M$			2	1.886	0.21	—	
p-Hydroxyphenyltriphenyl-*	(34)	46	1	1.900	2.40	0.7	
			2	2.046	0.50	3.0	
p-Anisyltriphenyl-	(35)	44	1	1.835	1.26	1.4	
			2	1.988	0.26	1.8	
			3	2.128	0.56	1.9	
p-Aminophenyltriphenyl-	(36)	46	1	1.801	0.88	2.0	
			2	1.916	0.34	1.3	
			3	2.144	0.30	2.3	
			4	2.473	1.56	1.2	
p-Dimethylaminophenyltriphenyl-	(37)	44	1	1.777	2.60	2.1	0.7
			2	2.091	0.41	1.1	
p-Tolyltriphenyl-	(38)	44	1	1.692	2.50	2.0	0.8
			2	2.073	0.26	1.7	
m-Tolyltriphenyl-	(39)	44	1	1.684	2.28	2.0	0.7
			2	2.066	0.46	1.9	
Tetraphenyl-	(40)	44	1	1.680	2.80	2.1	0.6
			2	2.068	0.15	1.5	
o-Tolyltriphenyl-	(41)	44	1	1.678	2.12	2.0	0.3
			2	2.061	0.21	1.8	
p-Benzhydrylphenyltriphenyl-	(42)	45	1	1.668	0.60	1.0	0.6
$c < 10^{-3}M$							
p-Cumyltriphenyl-	(43)	44	1	1.654	2.78	1.7	0.7
			2	2.056	0.40	1.3	
p-Carbohydroxyphenyltriphenyl-	(44)	44	1	1.630	1.10	0.6	0.2
			2	2.346	27.0	0.6	

TABELLE 1 (Fortsetzung)

Phosphoniumbromid		*Lit.***	*Stufe*	$-E_{\frac{1}{2}}$ *(V)*	i_d *(μA)*	n_1	n_2
1-Naphthyltriphenyl-	(45)	44	1	1.439	0.88	3.5	1.1
			2	1.781	0.50	0.9	
			3	2.054	0.45	1.9	
			4	2.326	1.70	0.8	
			5	2.488	1.30	2.0	
2-Naphthyltriphenyl-	(46)	44	1	1.554	1.80	2.0	
			2	1.653	0.75	1.4	
			3	2.049	0.44	1.4	
			4	2.207	1.00	1.1	
			5	2.325	2.20	1.0	
			6	2.494	1.65	1.4	
p-Biphenylyltriphenyl-	(47)	44	1	1.527	1.70	2.4	0.9
			2	1.655	0.35	1.1	
			3	2.076	0.29	1.6	
			4	2.279	1.30	1.0	
			5	2.490	4.70	1.2	
p-Nitrophenyl-triphenyl- $c < 10^{-3}M$	(48)	47	1	0.454	2.90	3.1	1.5
			2	1.502	1.35	1.1	
			3	1.831	0.65	2.0	
			4	2.118	0.50	1.8	
p-Phenylen-bis-triphenyl-	(49)	44	1	1.155	0.40	1.6	
			2	1.269	0.08	1.5	
			3	1.477	1.24	1.2	
			4	1.667	2.48	1.6	
			5	2.069	0.24	1.5	
			6	2.435	4.70	3.1	
p-Trifluormethylphenyltriphenyl-	(50)		1	1.410	7.85	1.1	
			2	2.077	0.35	2.2	
			3	2.323	7.90	0.7	
			4	2.482	1.20	3.3	
p-Phenylsulfophenyltriphenyl-	(51)	5	1	1.227	2.06	1.8	1.3
			2	1.677	0.65	3.1	
			3	1.954	1.15	1.3	
			4	2.083	0.17	1.3	
			5	2.350	1.65	1.4	
			6	2.490	1.05	2.0	
Di-*p*-tolyldiphenyl-	(52)	5	1	1.695	2.48	1.5	0.9
			2	2.092	1.18	0.9	
Tri-*p*-tolylphenyl-	(53)	5	1	1.727	2.60	2.1	1.2
			2	2.071	0.32	3.0	
Di-*p*-anisyldiphenyl-	(54)	5	1	1.790	0.98	1.3	
			2+3	1.954	3.12	—	
Tri-*p*-anisylphenyl-	(55)	5	1	1.848	1.30	1.2	
			2	2.006	0.22	2.1	
			3	2.128	0.74	2.9	
Tri-*p*-tolyl-*p*-cumyl-	(56)	5	1	1.713	2.50	2.2	0.6
			2	2.004	0.46	2.5	
			3	2.455	0.28	1.6	

* Phosphoniumchlorid

** Die angeführte Literatur bezieht sich auf die Herstellung der Salze

Reaktionsschritte (6) und (7) nicht an der Quecksilberoberfläche abspielen. Für die Bildung des Radikals $R_4P\cdot$ sprechen präparative Befunde: z.B. die Bildung radikalischer Kombinationsprodukte[5]. Die Entstehung einer rotbraunen, kurzlebigen oxydationsempfindlichen Verbindung auf der Quecksilberkathode schreiben wir dagegen dem Anion R_4P^- zu. Unsere eigenen Ergebnisse über die Polarographie der Phosphoniumsalze in wässriger Lösung enthält Tabelle 1. Tabelle 1 zeigt, dass von den 56 untersuchten Phosphoniumsalzen nur acht eine einzige Reduktionsstufe, 29 zwei Stufen, 9 drei Stufen, 5 vier Stufen und 5 fünf bzw. sechs Stufen haben.

Wir glauben nicht fehl zu gehen, wenn wir die erste, im allgemeinen auch am stärksten ausgeprägte Reduktionsstufe dem reduktiven Abbau der Phosphoniumsalze zu den tertiären Phosphinen zuordnen. Für die zweite niedrigere Stufe, die meist zwischen -2.03 und -2.08 V liegt, machen wir den reduktiven Abbau der tertiären Phosphine zu den sekundären Phosphinen verantwortlich. Die übrigen Reduktionsstufen sind relativ leicht zu erklären bei folgenden am Triphenylphosphin P-ständigen Liganden: 4-Brom-*n*-butyl (17), *p*-Trifluormethylphenyl (50), *p*-Biphenylyl (47), 1- (45) und 2-Naphthyl (46), *p*-Nitrophenyl (48), *p*-Phenylsulfophenyl (51) und *p*-Phenylen (49). In allen Fällen werden durch Halogen, Nitrogruppen oder aromatische Kerne zusätzliche Elektronen verbraucht. Beim Allyltriphenylphosphoniumion (10) kann man die beiden ersten Stufen dem Übergang zu tertiärem Phosphin, die dritte Stufe der weiteren Reduktion des Triphenylphosphins und die vierte der Absättigung der Allylgruppe zur Propylgruppe zuordnen. Schwierig ist die Interpretation der zusätzlichen Stufen bei den Bis-phosphoniumsalzen und allen Phosphoniumionen, die Liganden mit Elektronendonatoren wie OCH_3, NH_2, CH_3 am Aromaten tragen.

Die logarithmische Analyse der Polarogramme deckt bei den Phosphonium- und Arsoniumsalzen keine aussagekräftigen Zusammenhänge über die Zahl der von der Kathode auf das Substrat übergehenden Elektronen auf, da die Kathodenprozesse irreversibel verlaufen. Bei einigen Salzen der Tabelle 1 sind zwei verschiedene Werte für n, n_1 und n_2 angegeben. Das ist immer dann der Fall, wenn die Auftragung von $-E$ gegen log $[i/(i_d-i)]$ eine abgeknickte Gerade ergibt. Weitere Einzelheiten können dem Versuchsteil entnommen werden. Bei den acht Phosphoniumsalzen mit nur einer einzigen Reduktionsstufe dürfte es sich um Zweielektronenübergänge handeln. Auch für das Trimethylphenylphosphoniumbromid (15) finden wir im Gegensatz zu COLICHMAN[27] nur eine Stufe.

Eine ins einzelne gehende Analyse der Daten in Tabelle 1 ist fast unmöglich. Deshalb wird auch auf die Veröffentlichung der bei allen Salzen bei niederen Konzentrationen ($0.7\cdot10^{-3}$, $0.4\cdot10^{-3}$ und $0.2\cdot10^{-3}M$) gewonnenen Halbstufenpotentiale und Diffusionsströme verzichtet. Zwei Beispiele werden weiter unten besprochen. Einige sich abzeichnende Zusammenhänge sollen anschliessend besprochen werden.

Alkyltriphenylphosphoniumsalze

In Tabelle 1 sind die Salze (1)–(13) nach der Grösse ihrer Halbstufenpotentiale geordnet. Unter Berücksichtigung der früheren präparativen Befunde[5] erkennt man, dass die Haftfestigkeit der aliphatischen Liganden mit dem Halbstufenpotential der Phosphoniumsalze abnimmt. Trägt man die Halbstufenpotentiale gegen die σ^*-Konstanten von Taft auf, so findet man keine lineare Abhängigkeit. Lediglich Methyl (1), Benzyl (11) und Benzhydryl (13) ergeben eine Gerade mit der Steigung $\varrho^* = +1.46$ V. GRIMSHAW UND RAMSEY[14] finden bei den am Benzylrest substituierte Triphenyl-

benzylphosphoniumchloriden $\varrho = +0.23 \pm 0.07$ V. Dieser Wert muss von dem hier gefundenen abweichen, da die Autoren nicht die Taft'sche σ^*-, sondern die Hammett'sche σ-Substitutionskonstante benutzen und in methanolischer Lösung arbeiten.

In Tabelle 2 werden die Halbstufenpotentiale von sechs strukturell systematisch abgewandelten Phosphoniumsalzen verglichen.

Die Halbstufenpotentiale verschieben sich bei Ersatz eines Phenylrestes durch einen Alkylrest um ungefähr gleiche Beträge zu negativeren Werten.

Der Anstieg des Diffusionsstromes mit zunehmender Substitution durch Methylgruppen ist auf die Vergrösserung des Diffusionskoeffizienten der kleiner werdenden Phosphoniumionen zurückzuführen.

TABELLE 2

ABHÄNGIGKEIT DER HALBSTUFENPOTENTIALE EINIGER PHOSPHONIUMSALZE MIT SYSTEMATISCH ABGEWANDELTER SUBSTITUTION AM PHOSPHOR

Phosphoniumbromid		$-E_{\frac{1}{2}}$ *(V)*	$\Delta(-E_{\frac{1}{2}})$ *(V)*	i_d/c *(μA/mM)*
Tetraphenyl-	(40)	1.680	0.182	2.80
Methyltriphenyl-	(1)	1.862		2.60
			0.225	
Dimethyldiphenyl-	(14)	2.087		4.38
			0.184	
Trimethylphenyl-	(15)	2.271		5.10
Tetraphenyl-	(40)	1.680	0.156	2.80
Äthyltriphenyl-	(3)	1.836		1.79
			0.195	
Diäthyldiphenyl-	(16)	2.031		2.58

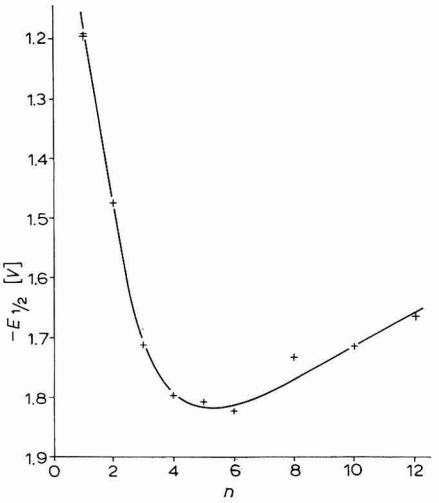

Abb. 1. Abhängigkeit der Halbstufenpotentiale von Bis-phosphoniumsalzen (18)–(26) $[(C_6H_5)_3P\text{-}(CH_2)_n\text{-}P(C_6H_5)_3]Br_2$ von der Zahl der CH_2-Gruppen, n.

Alkyliden-bis-phosphoniumsalze

Die Abhängigkeit der Halbstufenpotentiale vom Abstand der geladenen Zentren in α,ω-n-Alkylen-bis-triphenylphosphoniumsalzen (18)–(26) zeigen Tabelle 1 und Abb. 1.

Man sieht, dass die Vergrösserung des Abstandes der polaren Gruppen das Halbstufenpotential senkt, dass bei $n=4$, 5 und 6 ein Minimum erreicht wird und mit zunehmender Länge der Alkylidenkette die Halbstufenpotentiale wieder ansteigen. Für das Minimum der Halbstufenpotentiale machen wir konformativ bedingte Effekte beim Entladungsvorgang der Bis-phosphoniumsalze in der Doppelschicht der Quecksilberoberfläche verantwortlich. Vom Halbstufenpotential aus beurteilt, sollten die Entladungsvorgänge bei den Bis-phosphoniumsalzen mit $n=4$, 5 und 6 ähnlich sein wie bei den Alkyltriphenylphosphoniumsalzen, deren Halbstufenpotentiale ebenfalls zwischen -1.8 und -1.9 V liegen (s.Tabelle 1).

Gemischt substituierte Phosphoniumsalze

Tabelle 1 enthält noch eine Reihe schwer reduzierbarer Phosphoniumsalze (27)–(33) mit drei *p*-Anisyl-, Dimethylamino-, N-Morpholino- oder *p*-Dimethylaminophenyl-Gruppen als Liganden am Phosphor. Während Phosphoniumsalze mit drei der oben genannten Gruppen und einem Benzyl- oder Propylrest noch gut erkennbare Halbstufenpotentiale haben, liegen die der Salze mit einem Methylrest schon im Leitsalzanstieg.

Aryltriphenylphosphoniumsalze

Bei einigen Tetraarylphosphoniumsalzen kann man polarographisch vier oder mehr Stufen beobachten; dies bedeutet, dass vier und mehr Reduktionsschritte an der Quecksilberkathode ablaufen.

Die Halbstufenpotentiale der Aryltriphenylphosphoniumsalze (34)–(51) sind in Tabelle 1 zusammengestellt. Die Halbstufenpotentiale, gegen die Hammettschen σ-Werte[48] aufgetragen, liefern nur eine grobe Beziehung. Für ϱ errechnet sich $+0.291 \pm 0.191$ V. Diese Halbstufenpotentiale vermitteln aber keine eindeutige Auskunft darüber, welcher Rest reduktiv vom Phosphor abgelöst wird. Präparativ ist es jedoch wichtig, dass Reste, die das Halbstufenpotential zu positiveren Werten verschieben, leichter reduktiv abgespalten werden als solche, die ein negativeres Potential bedingen.

Abhängigkeit der Halbstufenpotentiale vom Lösungsmittel

Da von einigen Phosphoniumsalzen aus Löslichkeitsgründen keine 10^{-3} *M* wässrigen Lösungen hergestellt werden können, werden diese in 90-% Methanol polarographiert. In Tabelle 3 sind die Halbstufenpotentiale von sechs Phosphoniumsalzen

TABELLE 3

VERGLEICH DER HALBSTUFENPOTENTIALE EINIGER IN WASSER UND IN 90-% METHANOL VERMESSENER PHOSPHONIUMSALZE $[(C_6H_5)_3PR]X$ (X = Cl, Br)

R		$-E_{\frac{1}{2}}(V)$		$\Delta(-E_{\frac{1}{2}})$
		H_2O	90% CH_3OH	(V)
Methyl	(1)	1.862	2.068	0.206
Äthyl	(3)	1.837	2.013	0.176
Benzyl	(11)	1.552	1.826	0.274
p-Aminophenyl	(36)	1.814	2.063	0.249
p-Dimethylaminophenyl	(37)	1.777	2.063	0.286
Phenyl	(40)	1.680	1.946	0.266

zusammengestellt, die in Wasser und in 90% Methanol bei einer Konzentration von 10^{-3} *M* vermessen worden sind.

In Durchschnitt liegen die Halbstufenpotentiale in 90% Methanol um 0.243 V ±0.034 V niedriger als in Wasser. Substrahiert man diesen Betrag von den Halbstufenpotentialen der allein in 90% Methanol vermessenen Salze, die in reinem Wasser nicht genügend löslich sind, so sollte man angenähert die Halbstufenpotentiale dieser Salze in Wasser erhalten. Diese Umrechnung haben wir für vier Phosphoniumsalze vorgenommen (Tabelle 4).

TABELLE 4

UMGERECHNETE HALBSTUFENPOTENTIALE EINIGER IN 90% METHANOL GEMESSENER PHOSPHONIUMSALZE ($[C_6H_5)_3PR]X$ ($10^{-3}M$; X = Cl, Br) FÜR WASSER ALS LÖSUNGSMITTEL

R		$-E_{\frac{1}{2}}$ (*V*)	
		in 90% CH_3OH (gef.)	*in H_2O (ber.)*
Benzhydryl	(13)	1.562	1.319
p-Benzhydrylphenyl	(42)	1.918	1.675
p-Nitrophenyl	(48)	0.552	0.309
9-Fluorenyl[34]	(57)	1.508	1.265

TABELLE 5

POLAROGRAPHISCHE UNTERSUCHUNG EINIGER ARSONIUMSALZE IN WÄSSRIGER LÖSUNG (10^{-3} *M*)

Arsoniumbromid		*Lit.**	*Stufe*	$-E_{\frac{1}{2}}$ (*V*)	i_d (*μA*)	n_1	n_2
Methyltriphenyl-	(58)	49	1	1.498	1.04	0.7	
			2	1.775	0.35	0.8	
			3	2.081	0.48	1.6	
			4	2.378	0.30	1.0	
Äthyltriphenyl-	(59)	50	1	1.489	1.12	0.9	
			2	2.054	1.08	1.3	
o-Tolyltriphenyl-	(60)	5	1	1.389	1.70	0.9	0.3
			2	2.062	0.19	1.7	
m-Tolyltriphenyl-	(61)	51	1	1.384	1.64	0.8	0.3
			2	2.070	1.04	0.9	
p-Tolyltriphenyl-	(62)	52	1	1.382	1.82	0.9	0.3
			2	2.041	0.54	1.8	
Tetraphenyl-	(63)	53	1	1.377	2.02	1.0	0.3
			2	2.060	0.40	1.8	
p-Cumyltriphenyl-	(64)	5	1	1.364	2.20	0.8	0.2
			2	2.038	0.34	2.2	
p-Biphenylyltriphenyl	(65)	5	1	1.224	0.84	1.1	
			2	1.416	0.62	0.5	
			3	2.048	0.42	0.9	
			4	2.330	1.74	1.2	
Benzyltriphenyl-	(66)	54	1	1.213	2.83	0.5	0.3
			2	2.057	0.51	2.1	
			3	2.356	0.83	0.7	
			4	2.470	0.24	2.1	

* Die angeführte Literatur bezieht sich auf die Herstellung der Salze

Die umgerechneten Werte zeigen eine ausreichende Übereinstimmung mit den in Wasser bei geringerer Konzentration bestimmten Halbstufenpotentialen (s. Tabelle 1).

Halbstufenpotentiale einiger Arsoniumsalze

Tabelle 5 enthält die Halbstufenpotentiale von neun Arsoniumsalzen.

Im Vergleich zu den Phosphoniumsalzen sind die Halbstufenpotentiale der entsprechend substituierten Arsoniumsalze um *ca.* 0.3 V nach positiveren Werten verschoben. Auch bei den Arsoniumsalzen beobachtet man in Abhängigkeit vom Liganden ein- und zweistufige Reduktionsvorgänge. Die erste Reduktionsstufe (−1.2 bis −1.5 V) ordnen wir der Umwandlung des quartären Arsoniumsalzes in das tertiäre Arsin zu; die negativer liegende Stufe (−2.04 bis −2.08 V) könnte für die Reduktion der tertiären Arsine zu sekundären Arsinen verantwortlich sein[10]. Präparativ konnte aber dieser weitergehende reduktive Abbau noch nicht nachgewiesen werden.

Vergleich der gefundenen Halbstufenpotentiale mit Literaturwerten

Wie bereits eingangs erwähnt, beeinflussen die Messbedingungen die Lage der Halbstufenpotentiale erheblich. In Tabelle 6 sind die unter unseren jetzigen "Standardbedingungen" gefundenen Werte den übrigen Literaturwerten gegenübergestellt.

TABELLE 6

VERGLEICH DER HALBSTUFENPOTENTIALE EINIGER PHOSPHONIUM- UND ARSONIUMSALZE IN WASSER MIT ANDEREN LITERATURWERTEN

Oniumsalze		$-E_{\frac{1}{2}}$ (V)		
		Diese Arbeit	*Ref. 4*	*Andere Autoren*
$[(C_6H_5)_3PCH_3]^+$	(1)	1.862	2.153	
$[(C_6H_5)_3P\text{-}tert\text{-}C_4H_9]^+$	(9)	1.656	1.735	
$[(C_6H_5)_3PCH_2C_6H_5]^+$	(11)	1.552	1.658	
$[(C_6H_5)_3PCH_2CN]^+$	(12)	1.301		1.581[11]
$[(C_6H_5)_3PCH_2P(C_6H_5)_3]^{2+}$	(18)	1.195		1.331[11]
$[(C_6H_5)_4P]^+$	(40)	1.680	1.733	1.226[12]
$[(C_6H_5)_3P\text{-}o\text{-}tolyl]^+$	(41)	1.678	1.720	
$[(C_6H_5)_3AsCH_3]^+$	(58)	1.520	1.600	
$[C_6H_5)_3AsC_2H_5]^+$	(59)	1.489	1.560	
$[(C_6H_5)_4As]^+$	(63)	1.377	1.340	1.37[12]
$[(C_6H_5)_3AsCH_2C_6H_5]^+$	(66)	1.213	1.090	

BESCHREIBUNG DER VERSUCHE

Apparatur

Die Messungen werden an einem Polarograph Metrohm-Polarecord E 261 ausgeführt, der mit einem Rapidstand (Tropfkontrolleinrichtung E 354 S) und einem *iR*-Kompensator E 446 ausgerüstet ist.

Mit der Rapidpolarographie-Einrichtung können alle Polarogramme mit der schnellen Registriergeschwindigkeit des Polarographen (1 Min pro Spannungsdurchlauf) aufgenommen werden. Weitere Vorteile dieser Methode sind[56]:

(a) Der Grenzstrom einer polarographischen Stufe verläuft nahezu parallel

zum Grundstrom, da die Tropfzeit nicht mehr potentialabhängig ist. Dadurch lassen sich bei höheren Empfindlichkeiten kleine Stufen noch genauer vermessen.

(b) Durch die kurze Tropfzeit (0.2 sec) kann auf eine Dämpfung der kleinen Tropfenzacken verzichtet werden; es tritt daher keine durch die Dämpfung bedingte Verzerrung der Kurve auf.

Schwierigkeiten entstehen jedoch bei Potentialen unter -2.0 V, weil sich die optimale Einstellung der Klopfimpulsstärke kaum finden lässt. Das Quecksilber beginnt dann aus der Kapillare auszulaufen, ohne zu tropfen, oder es gehorcht dem Klopfimpuls nicht mehr und beginnt mit natürlicher Tropfzeit zu tropfen.

Da der Innenwiederstand der Polarographiezelle ziemlich hoch ist (1450 Ω), wird bei allen Messungen während der Aufnahme der Polarogramme der Spannungsabfall in der Lösung $E=iR$ automatisch korrigiert.

Sämtliche Polarogramme in wässriger und methanolischer Lösung werden mit zwei Silber–Silberchlorid-Elektroden (Metrohm EA 420) in gesättigter Kaliumchlorid-Lösung aufgenommen. Um zu verhindern, dass Kaliumchlorid-Lösung in die Polarographiezelle eindiffundiert, in der das Kaliumion eine Stufe ergeben würde, wird zwischen das Elektrodensystem und die Polarographiezelle (Metrohm EA 664) noch eine Salzbrücke mit 0.1 *M* Tetra-*n*-butylammoniumbromid-Lösung[10] eingeschaltet.

Eichung der Messanordnung

Um sicher zu gehen, dass der Polarograph ohne Fehler arbeitet, wird zu Beginn eines jeden Messtages eine $1.25\cdot10^{-3}$ *M* Lösung von RbCl polarographiert[57,58]. Als Grundelektrolyt dient eine 0.1 *M* Lösung von Tetra-*n*-butylammoniumbromid (TBA), die 0.05% Triton X-100 (Octylphenyldecaäthylenglykoläther, Serva-Entwicklungslabor, Heidelberg) als Maximumdämpfer enthält.

Zur Verdrängung von gelöstem Sauerstoff spült man die Lösung 10 Min mit Reinstickstoff. Gemessen wird bei $25.0\pm0.2°$.

Folgende Werte werden gefunden:

Wässrige Lösung: $E_{\frac{1}{2}}=-2.092$ V ±0.003 V (22 Messungen); 90-% Methanol: $E_{\frac{1}{2}}=-1.985$ V ±0.003 V (5 Messungen). Bei der Polarographie einer wässrigen $0.5\cdot10^{-3}$ *M* TlCl-Lösung wird unter sonst gleichen Bedingungen als Mittelwert von acht Messungen $E_{\frac{1}{2}}$ zu -0.421 V ±0.004 V gefunden. Addiert man zu diesen Werten -43 mV, so erhält man die auf die gesättigte Kalomelelektrode bezogenen Werte von -2.135 ±0.003 V (-2.118 ±0.005 V) für Rb^+ und -0.464 ±0.004 V (-0.460 $\pm$ 0.005 V) für Tl^+ (Literaturwerte[57] in Klammern).

Die Fehlergrenze liegt hier und bei den Oniumsalzen bei $\pm$ 0.005 V.

Die Zahl n der an der Quecksilberkathode auf das Substrat übergegangenen Elektronen wird durch logarithmische Analyse[57,59] der polarographischen Kurven bestimmt. Am Beispiel des Polarogramms des Tetraphenylphosphoniumbromids (40) seien einige für Oniumsalze typische Besonderheiten erläutert. Im Polarogramm dieser Verbindung treten zwei Stufen auf, von denen die erste wesentlich höher ist als die zweite.

Abbildung 2 zeigt die erste Stufe des Tetraphenylphosphoniumbromids (40).

Bei der logarithmischen Analyse der ersten Stufe des Tetraphenylphosphoniumbromids (40) erhält man zwei Kurvenäste verschiedener Steigung (Abb. 3).

Für den ausgezogenen Teil der Kurve findet man für die Zahl n der ausgetauschten Elektronen $n_1=2.11$ und für den gestrichelten Kurventeil, $n_2=0.62$. Zwei mögliche

Erklärungen bieten sich an: (1) Es könnte sich um zwei Prozesse handeln, deren Halbstufenpotentiale jedoch so nahe beieinander liegen, dass die beiden Stufen nicht mehr getrennt werden. (2) Es handelt sich um einen quasi-irreversiblen Reduktionsschritt[55,57].

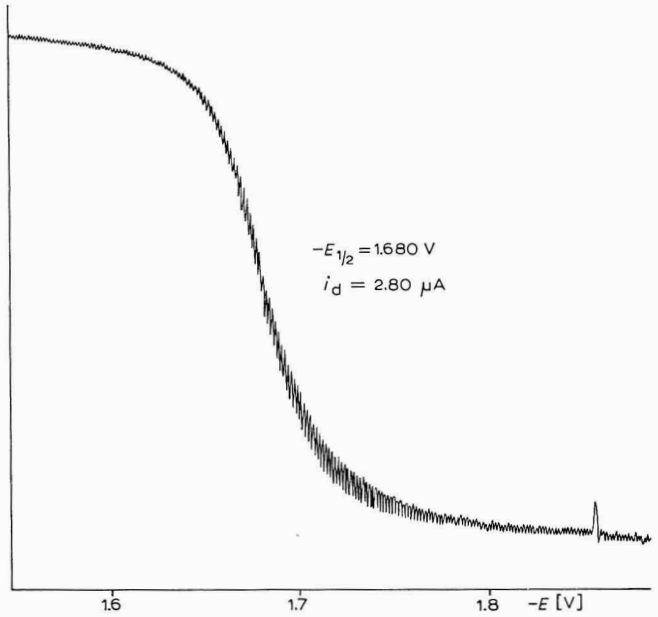

Abb. 2. Polarogramm der ersten Stufe des Tetraphenylphosphoniumbromids (40). Depolarisatorkonzentration: 10^{-3} M; Grundelektrolyt: 0.1 M Tetra-n-butylammoniumbromid; Maximumdämpfer: 0.05% Triton X-100; Lösungsmittel: Wasser; Temperatur: 25.0°±0.2°; Rapidpolarographie (t = 0.2 sec); iR-Korrektur.

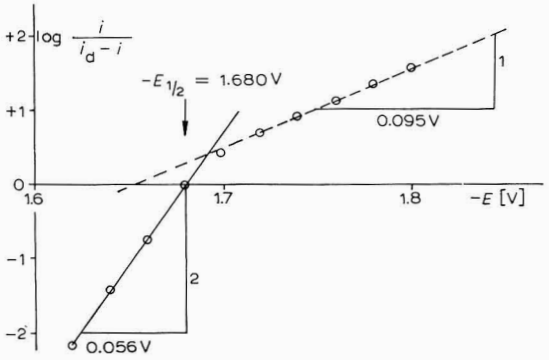

Abb. 3. Logarithmische Analyse der ersten Stufe des Tetraphenylphosphoniumbromids (40).

Abhängigkeit der Halbstufenpotentiale von den einzelnen Parametern

Einfluss der Konzentration. Da sich die Halbstufenpotentiale der Oniumsalze mit der Konzentration ändern, werden die Polarogramme bei vier genau eingestellten Konzentrationen aufgenommen.

In dieser Arbeit sind jedoch nur die bei der höchsten Konzentration erhaltenen Ergebnisse zusammengestellt. Beim Tetraphenylphosphoniumbromid (40) erhält man bei Variation der Konzentration die in Tabelle 7 zusammengestellten Werte für die Halbstufenpotentiale und Diffusionsströme. Zwischen den Halbstufenpotentialen und dem Logarithmus der Konzentration besteht in diesem Falle eine lineare Beziehung. Bei anderen Oniumsalzen ergibt sich sehr oft keine Proportionalität zwischen Halbstufenpotential und Konzentration.

TABELLE 7

ABHÄNGIGKEIT DES HALBSTUFENPOTENTIALS UND DES DIFFUSIONSSTROMES VON DER KONZENTRATION AN TETRAPHENYLPHOSPHONIUMBROMID (40) IN WASSER

c (mM)	$-E_{\frac{1}{2}}$ (V)	i_d (μA)	i_d/c ($\mu A \cdot l/mM$)
0.2	1.716	0.60	3.00
0.4	1.702	1.19	2.98
0.7	1.680	1.98	2.82
1.0	1.680	2.80	2.80

TABELLE 8

ABHÄNGIGKEIT DES HALBSTUFENPOTENTIALS UND DES DIFFUSIONSSTROMES VON DER KONZENTRATION AN BENZYLTRIPHENYLPHOSPHONIUMCHLORID (11) IN WASSER UNTER STANDARDBEDINGUNGEN

c (mM)	$-E_{\frac{1}{2}}$ (V)	i_d (μA)	c (mM)	$-E_{\frac{1}{2}}$ (V)	i_d (μA)
0.1	1.588	0.35	0.7	1.562	2.20
0.3	1.584	0.93	0.9	1.556	2.68
0.5	1.570	1.53	1.1	1.554	3.08

Am Beispiel des Benzyltriphenylphosphoniumchlorids (11) wird der Einfluss der verschiedenen Parameter untersucht. Die Abhängigkeit des Halbstufenpotentials von der Konzentration unter Standardbedingungen zeigt Tabelle 8.

Standardbedingungen: Leitsalz: 0.1 M in Wasser; Depolarisator: 10^{-4}–10^{-3} M Oniumsalz, meist $0.7 \cdot 10^{-3}$ M; Temperatur: 25.0°±0.2°; Dämpfung: 0; Bezugselektrode: Silberchlorid-Elektrode in gesättigter Kaliumchloridlösung; Rapidpolarographie: t=0.2 sec; Höhe des Quecksilberniveaus: 56 cm; Maximumdämpfer: 0.05% Triton X-100; iR-Korrektur.

Variation der Tropfzeit (t). Den Zusammenhang zwischen Tropfzeit einerseits und Halbstufenpotential und Diffusionsstrom andererseits unter Standardbedingungen am Beispiel des Benzyltriphenylphosphoniumchlorids (11) zeigt Tabelle 9. Zwischen dem Halbstufenpotential und log t besteht eine lineare Beziehung, $\Delta E_{1/2}/\Delta \log t = +76$ mV.

Variation der Temperatur. Tabelle 10 zeigt den Einfluss der Temperatur auf das Halbstufenpotential und den Diffusionsstrom des Benzyltriphenylphosphoniumchlorids (11) unter Standardbedingungen. $E_{\frac{1}{2}}$ und i_d zeigen eine von der Temperatur lineare Abhängigkeit $\Delta E_{\frac{1}{2}}/\Delta T = +2.24$ mV/Grad, $\Delta i_d/\Delta T = +0.0387$ μA/Grad.

Variation der Maximumdämpfer-Konzentration (Triton X-100). Tabelle 11 lehrt, dass oberhalb eines Prozentgehaltes von 0.03 an Maximumdämpfer die Werte $E_{\frac{1}{2}}$ und i_d konstant sind.

TABELLE 9

ABHÄNGIGKEIT DES HALBSTUFENPOTENTIALS UND DES DIFFUSIONSSTROMES VON DER TROPFZEIT t UNTER STANDARDBEDINGUNGEN BEI BENZYLTRIPHENYLPHOSPHONIUMCHLORID (II)

t (sec)	$-E_{\frac{1}{2}}$ (V)	i_d (μA)	t (sec)	$-E_{\frac{1}{2}}$ (V)	i_d (μA)
0.16	1.568	2.10	0.32	1.546	2.36
0.20	1.560	2.22	2.30	1.504	3.02
0.24	1.554	2.22	2.80	1.504	3.26
0.28	1.550	2.24			

TABELLE 10

ABHÄNGIGKEIT DES HALBSTUFENPOTENTIALS UND DES DIFFUSIONSSTROMES VON DER TEMPERATUR UNTER STANDARDBEDINGUNGEN BEI BENZYLTRIPHENYLPHOSPHONIUMCHLORID (II)

T(°C)	$-E_{\frac{1}{2}}$ (V)	i_d (μA)	T (°C)	$E_{\frac{1}{2}}$ (V)	i_d (μA)
20.2	1.567	1.98	40.1	1.521	2.62
24.9	1.561	2.12	49.6	1.501	3.10
31.6	1.539	2.40			

TABELLE 11

ABHÄNGIGKEIT DES HALBSTUFENPOTENTIALS UND DES DIFFUSIONSSTROMES VON BENZYLTRIPHENYLPHOSPHONIUMCHLORID (II) VON DER KONZENTRATION AN MAXIMUMDÄMPFER UNTER STANDARDBEDINGUNGEN

$c_{Trit.}$ (%)	$-E_{\frac{1}{2}}$ (V)	i_d (μA)	$c_{Trit.}$ (%)	$-E_{\frac{1}{2}}$ (V)	i_d (μA)
0.01	1.628	2.88	0.075	1.558	2.18
0.03	1.568	2.26	0.10	1.556	2.10
0.05	1.560	2.22			

TABELLE 12

ABHÄNGIGKEIT DES HALBSTUFENPOTENTIALS UND DES DIFFUSIONSSTROMES EINER WÄSSRIGEN 10^{-3} M BENZYLTRIPHENYLPHOSPHONIUMCHLORID-LÖSUNG (II) VON DER HÖHE DES QUECKSILBERNIVEAUS BEI DER RAPID-POLAROGRAPHIE UND DER NORMALEN POLAROGRAPHIE

h (cm)	*Rapid-Pol.* (t=0.2 sec)		*normale Pol.*	
	$-E_{\frac{1}{2}}$ (V)	i_d (μA)	$-E_{\frac{1}{2}}$ (V)	i_d (μA)
26			1.483	3.05
32	1.560	1.95	1.489	3.25
38	1.560	2.10	1.490	3.70
44	1.560	2.50	1.490	3.95
50	1.560	2.75	1.499	4.40
56	1.556	3.35	1.501	4.55
62	1.556	3.35	1.501	4.55
68	1.557	3.50	1.500	4.35

Diese hohe Maximumdämpfer-Konzentration lässt auf das Vorliegen von Adsorptionsvorgängen an der Elektrode schliessen.

Variation der Höhe des Quecksilberniveaus (h). Den Einfluss der Höhe des Quecksilberniveaus und der Tropfgeschwindigkeit auf Halbstufenpotential und

Diffusionsstrom bei einer Konz. von 10^{-3} *M* Benzyltriphenylphosphoniumchlorid (11) zeigt Tabelle 12. Zwischen $h^{\frac{1}{2}}$ und i_d einerseits und log h^{-1} und $E_{\frac{1}{2}}$ andererseits bestehen lineare Beziehungen: Rapidpolarographie ($t=0.2$ sec): $\Delta i_d/\Delta h^{\frac{1}{2}} = +0.735$ μA/cm$^{\frac{1}{2}}$. Normale Polarographie: $\Delta i_d/\Delta h^{\frac{1}{2}} = 0.825$ μA/cm$^{\frac{1}{2}}$; $\Delta E_{\frac{1}{2}}/\Delta \log h^{-1} = +34$ mV. Die Halbstufenpotentiale der in den Tabellen 1 und 5 angegebenen Verbindungen werden ebenfalls unter Standardbedingungen (s.S. 257) bestimmt. Zur Absicherung dieser Daten werden immer zwei Polarogramme angefertigt.

Polarographie in Methanol

Phosphoniumsalze in Methanol. Phosphoniumsalze, die in Wasser nicht ausreichend löslich sind, werden in einer Lösung von Methanol–Wasser (90:10) unter Standardbedingungen polarographiert. Die Einstellung der Rapidelektrode ist in diesem Lösungsmittelgemisch manchmal zeitraubend, da das Quecksilber sehr leicht zu rinnen beginnt.

Die Ergebnisse der polarographischen Messungen in 90% Methanol sind in Tabelle 13 zusammengestellt.

TABELLE 13

POLAROGRAPHISCHE UNTERSUCHUNG EINIGER PHOSPHONIUMSALZE ($10^{-3}M$) IN 90-% METHANOL

Phosphoniumbromid		*Stufe*	$-E_{\frac{1}{2}}$ (*V*)	i_d (*μA*)	n_1	n_2
Methyltriphenyl-	(1)	1	2.068	4.35	1.0	
Äthyltriphenyl-	(3)	1	0.907	0.90	1.0	
		2	2.013	4.55	0.9	
Benzyltriphenyl-	(11)	1	1.826	4.35	1.2	
Benzhydryltriphenyl-	(13)	1	1.562	3.65	0.9	
p-Aminophenyltriphenyl-	(36)	1	2.063	4.15	0.6	
p-Dimethylaminophenyltriphenyl-*	(37)	1	2.063	3.55	1.2	
Tetraphenyl-	(40)	1	1.946	3.70	1.3	
p-Benzhydrylphenyltriphenyl-*	(42)	1	1.918	2.90	0.8	
p-Nitrophenyltriphenyl-	(48)	1	0.552	7.00	1.3	
		2	1.739	2.55	1.0	
		3	2.076	5.05	1.5	
9-Flurenyltriphenyl-	(57)	1	1.508	3.00	0.6	0.3

* Phosphoniumchlorid

DANKSAGUNG

Die vorliegende Untersuchung wurde durch Mittel des Bundeswirtschaftsministeriums gefördert. Herrn Dr. D. BEHRENS von der Dechema sei für die wirksame Hilfe bei der Beschaffung von Mitteln herzlich gedankt.

ZUSAMMENFASSUNG

Die Halbstufenpotentiale einer Anzahl quartärer Phosphonium- und Arsoniumsalze werden unter Standardbedingungen bestimmt und deren Abhängigkeit von der Konzentration des Depolarisators, der Temperatur, der Tropfgeschwindigkeit, der

Höhe des Quecksilberniveaus und der Konzentration des Maximumdämpfers (Triton X-100) festgestellt. Die Halbstufenpotentiale geben aber keine Auskunft darüber, welche Liganden und in welchem Verhältnis die Liganden abgespalten werden. Die bisherigen Befunde sprechen dafür, dass Liganden als Radikale (Aufnahme von einem Elektron) und als Anionen (Aufnahme von zwei Elektronen) abgespalten werden.

SUMMARY

The half-wave potentials of a number of quaternary phosphonium and arsonium salts are determined under standard conditions, and their dependence on the concentration of the substrate, the temperature, the drop rate, the height of the mercury head, and the concentration of the capillary-active substance (Triton X-100) is established. It is not possible to deduce from the half-wave potentials which ligands, and in what proportion these ligands, are reductively cleaved. The results suggest that ligands are split off as radicals (transfer of one electron) and as anions (transfer of two electrons).

LITERATUR

1 60. Mitteil.: L. HORNER, R. LUCKENBACH UND W. D. BALZER, *Tetrahedron Letters*, 27 (1968) 3157. Sehe auch 14. Mitteil. unserer Serie: *Studien zum Vorgang der Wasserstoffübertragung*; 13. Mitteil.: L. HORNER UND H. NEUMANN, *Chem. Ber.*, 98 (1965) 3462.
2 L. HORNER, *Helv. Chim. Acta*, Fasciculus extraordinarius Alfred Werner, (1967) 93.
3 L. HORNER UND A. MENTRUP, *Ann. Chem.*, 646 (1961) 65.
4 L. HORNER, F. RÖTTGER UND H. FUCHS, *Chem. Ber.*, 96 (1963) 3141.
5 57. Mitteil.: L. HORNER UND J. HAUFE, *Chem. Ber.*, 101 (1968) 2903.
6 L. HORNER UND F. RÖTTGER, *Korrosion*, 16 (1963) 57.
7 E. L. COLICHMAM, *Anal. Chem.*, 26 (1954) 1204.
8 M. SHINAGAWA, H. MATSUO UND H. NEZU, *Japan Analyst*, 5 (1956) 20.
9 H. MATSUO, *J. Sci. Hiroshima Univ. Ser. A*, 22 (1958) 281.
10 S. WAWZONEK UND J. H. WAGENKNECHT, *Polarography 1964*, herausgegeben von G. J. HILLS, Macmillan, London, 1966.
11 H. MATSCHINER UND K. ISSLEIB, *Z. Anorg. Allgem. Chem.*, 354 (1967) 60.
12 H. MATSUO, *J. Sci. Hiroshima Univ. Ser. A*, 22 (1958) 51.
13 J. H. WAGENKNECHT UND M. M. BAIZER, *J. Org. Chem.*, 31 (1966) 3885.
14 J. GRIMSHAW UND J. S. RAMSEY, *J. Chem. Soc.*, B (1968) 63.
15 J. M. SAVEANT UND M. VEILLARD-RAYER, *Bull. Soc. Chim. France*, (1967) 2415.
16 E. L. COLICHMAN UND H. P. MAFFEI, *J. Am. Chem. Soc.*, 74 (1952) 2744.
17 M. SHINAGAWA, H. MATSUO UND H. OKASHITA, *Japan Analyst*, 7 (1958) 219.
18 H. E. AFFSPRUNG UND A. B. GAINER, *Anal. Chim. Acta*, 27 (1962) 578.
19 M. D. MORRIS, P. S. MCKINNEY UND E. C. WOODBURY, *J. Electroanal. Chem.*, 10 (1965) 85.
20 E. L. COLICHAM UND D. L. LOVE, *J. Org. Chem.*, 18 (1953) 40.
21 M. FINKELSTEIN, R. C. PETERSEN UND S. D. ROSS, *J. Electrochem. Soc.*, 110 (1963) 422.
22 P. ZUMAN UND S. TANG, *Collection Czech. Chem. Commun.*, 28 (1963) 829.
23 J. H. WAGENKNECHT UND M. M. BAIZER, *J. Electrochem Soc.*, 114 (1967) 1095.
24 A. LÜTTRINGHAUS UND H. MACHATZKE, *Ann. Chem.*, 671 (1964) 165.
25 J. M. SAVEANT, *Compt. Rend.*, 257 (1963) 448
26 J. M. SAVEANT, *Compt. Rend.*, 258 (1964) 585.
27 S. TANG AND P. ZUMAN, *Collection Czech. Chem. Commun.*, 28 (1963) 1524.
28 G. WITTIG UND U. SCHÖLLKOPF, *Chem. Ber.*, 87 (1954) 1318.
29 A. MICHAELIS UND A. LINK, *Ann. Chem.*, 207 (1881) 193.
30 A. MICHAELIS UND H. v. SODEN, *Ann. Chem.*, 229 (1885) 295.
31 K. FRIEDRICH UND H. G. HENNING, *Chem. Ber.*, 92 (1959) 2756.
32 H. J. BESTMANN UND O. KRATZER, *Chem. Ber.*, 96 (1963) 1899.
33 G. P. SCHIEMENZ UND H. ENGELHARD, *Chem. Ber.*, 94 (1961) 578.
34 L. HORNER UND E. LINGNAU, *Ann. Chem.*, 591 (1955) 135.
35 A. MONDON, *Ann. Chem.*, 603 (1957) 115.

36 F. RAMIREZ, N. B. DESAI, B. HANSEN UND N. MCKELVIE, *J. Am. Chem. Soc.*, 83 (1961) 3539.
37 G. WITTIG, H. EGGERS UND P. DUFFNER, *Ann. Chem.*, 619 (1958) 10.
38 A. KOTTLER, H. SCHEFFLER UND G. WERNER, *DBP 941, 193*; *C. A.*, 52 (1958) 14678 g, h.
39 R. SINGER, Dissertation, Universität Mainz, 1966.
40 A. H. COWLEY UND R. P. PINNELL, *J. Am. Chem. Soc.*, 87 (1965) 4454.
41 *Houben-Weyl, Methoden der organischen Chemie*, 12/1, Enke, Stuttgart, 1963, S. 347.
42 F. RÖTTGER, Dissertation, Universität Mainz, 1962.
43 G. P. SCHIEMENZ, *Chem. Ber.*, 98 (1965) 65.
44 L. HORNER, G. MUMMENTHEY, H. MOSER UND P. BECK, *Chem. Ber.*, 99 (1966) 2782.
45 H. HOFFMANN UND P. SCHELLENBECK, *Chem. Ber.*, 99 (1966) 1134.
46 L. HORNER, H. HOFFMANN, H. G. WIPPEL AND G. HASSEL, *Chem. Ber.*, 91 (1958) 52.
47 L. HORNER UND H. HOFFMANN, *Chem. Ber.*, 91 (1958) 45.
48 H. H. JAFFÉ, *Chem. Rev.*, 53 (1953) 191; L. P. HAMMETT, *Chem. Rev.*, 17 (1935) 125; D. H. MCDANIEL UND H. C. BROWN, *J. Org. Chem.*, 23 (1958) 420; C. C. PRICE UND R. H. MICHEL, *J. Am. Chem. Soc.*, 74 (1962) 3652.
49 W. STEINKOPF UND G. SCHWEN, *Ber. Dtsch. Chem. Ges.*, 54 (1921) 2969.
50 F. FUCHS, Diplomarbeit, Universität Mainz, 1960.
51 F. G. MANN UND J. WATSON, *J. Chem. Soc.*, (1947) 505.
52 R. LYON UND F. G. MANN, *J. Chem. Soc.*, (1942) 666.
53 J. CHATT UND F. G. MANN, *J. Chem. Soc.*, (1940) 1192.
54 F. F. BLICKE, H. H. WILLARD UND J. T. TARAS, *J. Am. Chem. Soc.*, 61 (1939) 88.
55 H. MATSUDA UND Y. AYABE, *Ber. Bunsenges. Physik. Chem.*, 63 (1959) 1164.
56 H. W. NÜRNBERG UND G. WOLFF, *Chem.-Ing. Tech.*, 37 (1965) 977.
57 J. HEYROVSKÝ UND J. KŮTA, *Grundlagen der Polarographie*, Akademie-Verlag, Berlin, 1965.
58 W. A. PLESKOW, *Zh. Fiz. Khim.*, 22 (1948) 351.
59 J. TOMEŠ, *Collection Czech. Chem. Commun.*, 9 (1937) 12.

Elsevier Sequoia S.A., Lausanne – Printed in The Netherlands

ELECTROCHEMISTRY OF AQUODIETHYLLEAD(IV) ION

MICHAEL D. MORRIS
Department of Chemistry, The Pennsylvania State University, University Park, Pa. 16802 (U.S.A.)
(Received August 26th, 1968)

Tin and lead form a number of partially alkylated derivatives in which the central metal atom may be bonded to one, two, or three organic groups. These are usually prepared[1] as the halides, which are covalent in the solid phase and in most organic solvents, but which dissociate in aqueous solution to hydrated ions capable of acidic hydrolysis[2]. The electrochemistry of the aquo-ions derived from the tin compounds has been extensively studied recently[3–6], but little is known about the electrochemistry of the aquo-ions derived from lead alkyls.

COSTA[7] has reported that trialkyllead halides show two one-electron waves in 30% isopropanol, but did not identify the products of the reactions. In very early work, however, HEIN AND KLEIN prepared hexaethyldilead by reduction of triethyllead bromide on a lead cathode[8] and presumably the same type of radical coupling occurs in the reduction of trialkyllead halides at the dropping mercury electrode. KORSHUNOV AND MALYUGINA[9] reported that triethyllead hydroxide is reduced polarographically, first to hexaethyldilead and then to unspecified products of a second one-electron transfer.

FRIEDLINE AND TOBIAS[10] have shown that the aquodimethyllead(IV) cation has a linear carbon–lead–carbon skeleton and undergoes acidic hydrolysis, with a first pK_a apparently larger than 7. Structurally, the ion resembles the aquodialkyltin(IV) ions, which also have linear skeletons[2]. However, the aquodialkyltin(IV) ions behave as acids of pK_a 3.0–3.5[2,3], in contrast to the much weaker acidity of the organolead analogue.

Despite the structural similarities of the two ions, the electrochemistry of the aquodiethyltin(IV) cation, which undergoes a reversible, two-electron transfer, followed by polymerization of the resulting diradicals[3,4], is quite different from that of the aquoidethyllead(IV) cation, reported in the present communication.

EXPERIMENTAL

For polarographic experiments, a Wenking potentiostat, equipped with a conventional operational amplifier integrator potential scan, was employed. Cyclic voltammetric experiments were performed on a Heath polarograph. Triangular potential sweeps were obtained from a Hewlett-Packard 202A signal generator. Controlled potential electrolyses were performed with the Wenking potentiostat. An operational amplifier difference integrator [11] was used to integrate the electrolysis current, measured as the iR drop across a precision resistor in series with the coulometric cell.

Mercury analyses were carried out by atomic absorption spectrometry[11]. The diethylmercury to be assayed was extracted from the aqueous sample into a known

amount of 2-heptanone and the mercury absorbance (2537 Å line) was measured in an air–acetylene flame on a Perkin-Elmer model 303 atomic absorption spectrometer. Diphenylmercury dissolved in 2-heptanone previously saturated with 0.5 *M* perchloric acid was used to prepare calibration curves.

Diethyllead diacetate (m.p. 124°–125°) was prepared for us by Dr. G. M. VAN DER WANT, Organisch Chemisch Instituut, T.N.O., Utrecht, and was used as received. Diphenylmercury (City Chemical Corp., New York, m.p. 124–126°) was used as received. Triton X-100 (Hartman-Leddon Corp., Philadelphia), was used as received. All other reagents were of A.C.S. reagent grade. Distilled water was used to prepare all solutions.

RESULTS

A polarogram of $1.0 \cdot 10^{-4}$ *M* diethyllead(IV) cation in 0.5 *M* perchloric acid is shown as Fig. 1 and the polarographic behavior in acid solution is summarized as Table 1. Conventional logarithmic analysis[12] of the rising portion of the wave shows it to be irreversible. The limiting current is diffusion-controlled (proportional to the square root of mercury height) and proportional to depolarizer concentration over the entire range investigated.

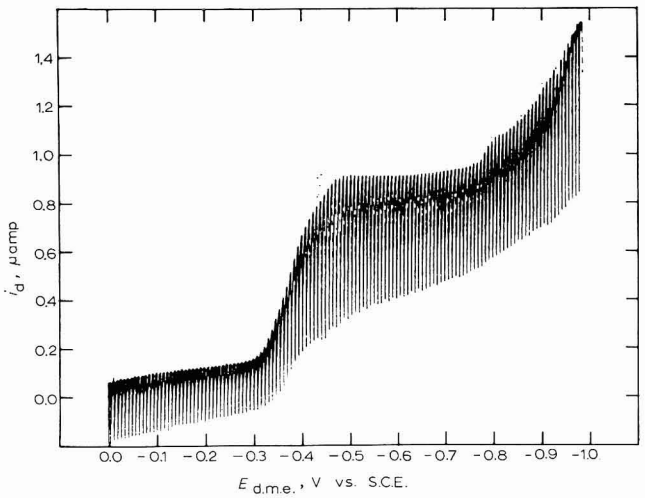

Fig. 1. Polarogram of $1.01 \cdot 10^{-4}$ *F* $(C_2H_5)Pb^{2+}$ in 0.5 *F* $HClO_4$. $4 \cdot 10^{-4}$% Triton X-100 present as maximum suppressor.

The pH-dependence of the half-wave potential is depicted in Fig. 2. The slope of the straight line segment of the curve in the pH-dependent region is 25 mV/pH unit. The extrapolation of this portion of the curve intercepts the acid solution half-wave potential baseline at pH 4.2.

Exhaustive controlled potential electrolysis at −0.70 V *vs.* SCE of aquodiethyllead(IV) cation solutions in 0.5 *F* $HClO_4$ gave an apparent *n*-value of 1.96 ± 0.07, independent of initial depolarizer concentration. The organometallic products were

identified by mass spectrometry as tetraethyllead and diethylmercury. The cathode contained lead metal.

Assay of the diethylmercury content of the electrolyzed solutions showed that diethylmercury was a minor product of the reactions. These results, summarized as

TABLE 1

POLAROGRAPHY OF AQUODIETHYLLEAD(IV) CATION IN 0.5 *F* PERCHLORIC ACID[a,b]

$(C_2H_5)_2Pb^{2+}$ $(F \cdot 10^{-4})$	$E_{\frac{1}{2}}$ (*V vs. SCE*)[c]	i_d (*A*)	$(C_2H_5)_2Pb^{2+}$ $(F \cdot 10^{-4})$	$E_{\frac{1}{2}}$ (*V vs. SCE*)[c]	i_d (*A*)
1.09	−0.370	0.73	10.9	−0.377	7.6
2.17	−0.375	1.47	21.7	−0.383	15.2
5.43	−0.377	3.73			

[a] Capillary characteristics, $m = 1.79$ mg/sec, $t = 4.2$ sec. [b] $4 \cdot 10^{-4}$% Triton X-100 as maximum suppressor. [c] All measurements ± 0.005 V.

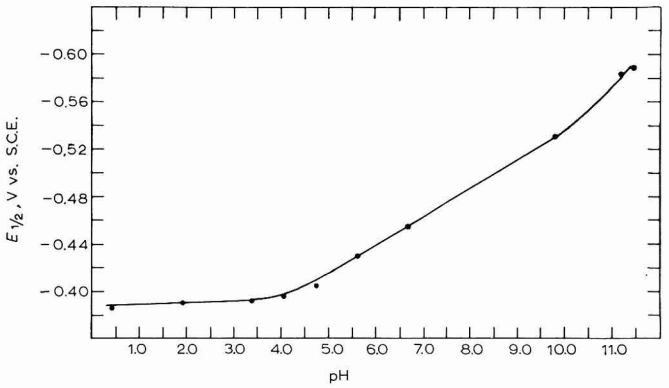

Fig. 2. Dependence of $E_{\frac{1}{2}}$ of $1.01 \cdot 10^{-4}$ *F* $(C_2H_5)_2Pb^{2+}$ on pH. Ionic strength, 0.5. $4 \cdot 10^{-4}$% Triton X-100 present as maximum suppressor.

TABLE 2

ANALYSIS OF ELECTROGENERATED DIETHYLMERCURY[a]

Et_2Pb^{2+} *taken* $(moles \cdot 10^{-5})$	Et_2Hg *found* $(moles \cdot 10^{-5})$	Et_2Hg/Et_2Pb^{2+}	Et_2Pb^{2+} *taken* $(moles \cdot 10^{-5})$	Et_2Hg *found* $(moles \cdot 10^{-5})$	Et_2Hg/Et_2Pb^{2+}
1.00	0.39	0.39	6.2	1.28	0.20
2.03	0.48	0.24	10.0	1.20	0.12
4.00	0.98	0.25	14.2	1.10	0.08

[a] Electrolysis at a large mercury pool. $E = -0.070$ V *vs.* SCE. Supporting electrolyte, 100 ml 0.5 *F* $HClO_4$ containing $4 \cdot 10^{-4}$% Trition X-100 as maximum suppressor.

Table 2, show that diethylmercury is the ultimate reduction product of 8–40% of the diethyllead(IV) cation. The mercury assays are reproducible to about ±10%. The large errors are caused in part by leakage of volatile diethylmercury from the coulometric cell and in part by the inherent difficulties of working with the very small quantities involved.

Cyclic voltammetry of the aquodiethyllead(IV) system was carried out at a hanging mercury drop electrode. A typical cyclic voltammogram is shown as Fig. 3. The main system is the inorganic lead(II)–lead amalgam system, which is irreversi-

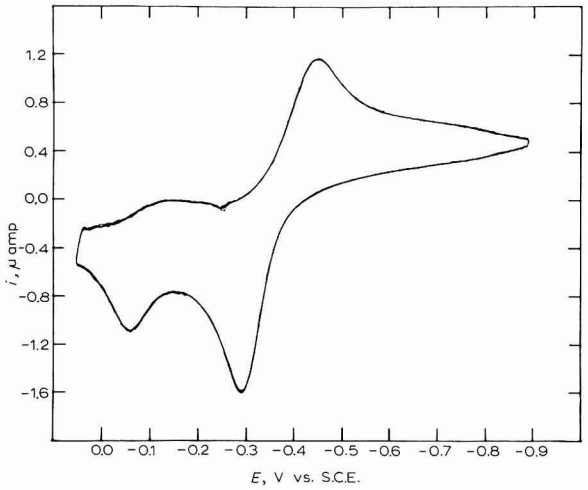

Fig. 3. Cyclic voltammogram of $1.01 \cdot 10^{-4}$ F $(C_2H_5)_2Pb^{2+}$ in 0.5 F $HClO_4$, $4 \cdot 10^{-4}$% Triton X-100. Sweep rate, 0.2 V/sec (0.1 Hz).

ble at the Triton X-100 concentration employed. Because this reduction occurs at almost the same potential as that of the aquodiethyllead(IV) cation, it masks the reduction of the latter ion. When the parent metal of an organometallic ion is formed as a reduction product, its concentration rapidly builds up in the diffusion layer until peaks for the inorganic ion become larger than those for the organometallic system[11]. The smaller pair of waves at -0.075 V and -0.12 V appears to be an adsorption–desorption system, probably due to diethylmercury. The well-defined anodic wave has a height proportional to the 2/3 power of the potential sweep rate. The cathodic wave is too ill-defined to measure.

DISCUSSION

The experimental results show that the aquodiethyllead(IV) cation undergoes a two-electron reduction. Stoichiometrically, this is equivalent to the formation of a diethyllead(II) diradical, an organolead analogue of a carbene. The diradical would be expected to be very unstable, as are the diradicals formed by the electroreduction of the aquodiethyltin(IV) cation[4].

Two decay paths, disproportionation and transmetallation are open to the diethyllead(II) diradical and both reactions are observed. The course of the electrode process may be represented, then, by eqns. (1)–(3).

$$Et_2Pb^{2+} + 2\,e \rightarrow Et_2Pb: \qquad (1)$$

$$2Et_2Pb: \rightarrow Et_4Pb + Pb^0 \qquad (2)$$

$$Et_2Pb: + Hg \rightarrow Et_2Hg + Pb^0 \qquad (3)$$

The assay of the coulometric products shows that the relative amount of diethylmercury, the product of the transmetallation reaction, decreases as the initial concentration of depolarizer increases. That is, disproportionation, a reaction second-order in organolead species, becomes more important with increasing bulk concentration and

concomitant increasing surface concentration of the transient diradical. Transmetallation remains the minor decay path, accounting for only 40% of the aquodiethyllead(IV) radical consumed at an initial concentration of $1 \cdot 10^{-4}$ *M*. Presumably, at the limit of infinite dilution, when the electrogenerated radicals would be infinitely far apart on the electrode surface, transmetallation would be the only observed decay path.

The electrochemical work sheds little light on the structure of the intermediate diradical. However, the transmetallation reaction observed in this system is quite similar to well studied non-electrochemical electrophilic substitutions at carbon–metal bonds[13]. In particular, the electrochemical follow-up reaction resembles the isotopic exchange between dialkylmercury or diarylmercury and metallic mercury.

In the isotopic exchange reaction, two alkyl or aryl groups are transferred simultaneously and a cyclic transition state has been invoked[13,14]. The major arguments for the cyclic transition state are that the use of optically active organomercury compounds leads to complete retention of configuration and that no redistribution of alkyl or aryl groups occurs when unsymmetrical organomercurials (*e.g.*, RHgR') are employed as substrates. Such a cyclic transition state, structure I, is likely in the transmetallation electrogenerated organometallic diradicals. This type of intermediate has been invoked to explain similar follow-up reactions in the electroreduction of the diphenylthallium(III) cation[11]. It is possible that the diethyllead(II) diradical decays by loss

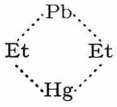

(I)

of ethyl radicals, one at a time, to form transient ethylmercury(I) radicals, which rapidly disproportionate. While this possibility cannot be excluded at present, there is no reason to suppose that the electrochemical transmetallation should proceed by a different path than the non-electrochemical analogue. Experiments with mixtures of dialkyllead(IV) cations and unsymmetrical dialkyllead(IV) cations, designed to confirm or reject structure I, are in progress. These will be reported in a subsequent communication.

The decay reactions of the diethyllead(II) diradical are quite different from those of the electrogenerated diethyltin(II) diradical, which undergoes rapid polymerization[4,6]. Polydialkyllead compounds are extremely unstable; the few examples known are observable only at liquid nitrogen temperatures[15]. This fact reflects the weakness of lead–lead bonds relative to tin–tin bonds. Consequently, electrogenerated dialkyllead radicals must decay by other paths than polymerization. Since the bond energies (measured on the fully methylated compounds) of the lead–carbon bond, 31 kcal/mole[16] and the mercury–carbon bond, 27 kcal/mole[17], are comparable, transmetallation is as likely as disproportionation for the decay of the organolead radical. On the other hand, the tin–carbon bond is considerably stronger, 54 kcal/mole[16] than the mercury–carbon bond, and transmetallation is a less likely path than polymerization for the decay of dialkyltin(II) diradicals.

Electron transfer into a diethyllead(IV) ion is slower than into the tin analogue. Consequently, diethyllead(IV) polarograms are irreversible.

Since diethyllead(IV) polarograms are irreversible, it is unlikely that the pH-

dependent shift of half-wave potential in the system is a simple measure of the acid-dissociation constant of the parent aquo-ion. The extrapolation of the pH *vs.* $E_{\frac{1}{2}}$ potential curve to the acid solution baseline occurs at pH 4.2. For a reversible system, this pH would be numerically equal to pK_a of the depolarizer[18]. In the present system, this interpretation may not be correct, since the wave shape observed depends somewhat on the buffer. FRIEDLINE AND TOBIAS[10] estimate pK_a of the dimethyllead(IV) ion as 7.4 or less, considerably larger than our tentative estimate of 4.2. In neither study, however, has a definitive measure of this important property of the ion been possible.

ACKNOWLEDGEMENTS

We wish to thank Dr. G. M. VAN DER WANT, Organisch Chemisch Instituut, T.N.O., Utrecht and Dr. J. HONEYCUTT, The Ethyl Corporation, Baton Rouge, for gifts of organolead compounds. The generous support of the National Science Foundation (grant GP-6164) is also acknowledged.

Part of this material was presented to the Division of Analytical Chemistry, American Chemical Society, 155th National Meeting, San Francisco, April, 1968.

SUMMARY

Aquodiethyllead(IV) ion undergoes a two-electron reduction at the dropping mercury electrode. $E_{\frac{1}{2}}$ is -0.37 V *vs.* SCE in acidic solution and becomes more negative with a slope of 25 mV/pH unit in neutral and alkaline buffers. The diradical initially formed decays rapidly by disproportionation to tetraethyllead and lead metal and by transmetallation to diethylmercury. Disproportionation is the major decay path over the accessible concentration range.

REFERENCES

1 G. E. COATES AND K. WADE, *Organometallic Compounds*, Vol. 1, Methuen and Co., London, 1967, pp. 430–496.
2 R. S. TOBIAS, *Organometal. Chem. Rev.*, 1 (1966) 93.
3 M. D. MORRIS, *Anal. Chem.*, 39 (1967) 476.
4 M. D. MORRIS, *J. Electroanal. Chem.*, 16 (1968) 569.
5 M. DEVAUD, P. SOUCHAY AND M. PERSON, *J. Chem. Phys.*, 64 (1967) 646.
6 M. DEVAUD, *Compt. Rend.*, Ser. C, 263 (1966) 1269.
7 G. COSTA, *Ann. Chim. (Rome)*, 40 (1950) 541.
8 F. HEIN AND A. KLEIN, *Chem. Ber.*, 71B (1938) 2381.
9 I. A. KORSHUNOV AND N. I. MALYUGINA, *J. Gen. Chem. USSR Eng. Transl.*, 31 (1961) 982.
10 C. E. FRIEDLINE AND R. S. TOBIAS, *Inorg. Chem.*, 5 (1966) 354.
11 J. S. DIGREGORIO AND M. D. MORRIS, *Anal. Chem.*, 40 (1968) 1286.
12 J. HEYROVSKÝ AND J. KŮTA, *Principles of Polarography*, Academic Press, Inc., New York, 1966, p. 205.
13 F. G. THORPE, *Studies on Chemical Reactivity and Structure*, edited by J. H. RIDD, John Wiley and Sons, Inc., New York, 1966, p. 247.
14 D. R. POLLARD AND J. V. WESTWOOD, *J. Am. Chem. Soc.*, 88 (1966) 1404.
15 L. C. WILLEMSENS, *Organolead Chemistry*, International Lead Zinc Research Organization, New York, 1964, p. 45.
16 L. C. WILLEMSENS, *Organolead Chemistry*, International Lead Zinc Research Organization, New York, 1967, p. 63.
17 J. J. EISCH, *The Chemistry of Organometallic Compounds*, The MacMillan Co., New York, 1967, p. 63.
18 D. R. CROW AND J. V. WESTWOOD, *Quart. Rev. London*, 19 (1965) 57.

ELECTROANALYTICAL CHEMISTRY AND INTERFACIAL ELECTROCHEMISTRY
Elsevier Sequoia S.A., Lausanne – Printed in The Netherlands

POLAROGRAPHIC INVESTIGATION OF METAL ACETYLACETONATES

VI. COBALT(II) ACETYLACETONATES*

BOŽENA ĆOSOVIĆ AND MARKO BRANICA
Department of Physical Chemistry, Institute "Ruder Bošković", Zagreb, Croatia (Yugoslavia)
(Received July 29th, 1968)

INTRODUCTION

The polarographic reduction of cobalt(II) in perchlorate solutions in the absence of complexing agents results in one irreversible two-electron wave, which is strongly influenced by the potential of the electrode double layer[1,2]. By increasing the concentration of the supporting electrolyte, a kinetic control in the mass transfer is observed. The decrease in the limiting current is caused by the change in the ψ-potential of the electrode double layer and was first reported by GIERST for the reduction of divalent nickel[3–5]. According to GIERST, hydrated nickel, as well as divalent cobalt, should be partially dehydrated before the electrode process proceeds. The rate of dehydration increases on raising the negative ψ-potential, which, however, falls with increase in the concentration of the supporting electrolyte.

The reduction mechanism of divalent cobalt in the presence of complexing ligand is strongly dependent on the nature of the ligand and on the stability of the primary product, which means that the electrode process proceeds either in two separate steps giving monovalent cobalt as a relatively stable product of the first step, or in only one two-electron reduction process[6,7]. The effect of acetylacetone on the polarographic behaviour of iron(III)[8], copper(II)[9,10], uranyl[11–13], indium(III)[14–15], and nickel(II)[16] has already been studied. The degree of complexation in aqueous solution and the characteristics of the electrode processes were deduced from the results obtained by the d.c., a.c., s.w., and pulse polarography.

In order to find a correlation between the electrode behaviour of cobalt(II) and its species present in an aqueous solution of acetylacetone, the above mentioned polarographic techniques were used. A scheme for the reaction mechanism is proposed.

EXPERIMENTAL

Polarographic measurements were carried out using conventional polarographs as described in previous papers[14,15]. A Radiometer PO4 polarograph was used in connection with the Drop Life Timer DLTI. Barker's Merwyn-Harwell square wave polarograph Mark III and Southern-Harwell MK II pulse polarograph were also used. The degree of the reversibility of the electrode process was proved by the Kalousek

*Taken from the Ph.D. Thesis of B. Ćosović, *Faculty of Science, University of Zagreb*, December, 1967.

commutator[17]. All stock solutions ($Co(NO_3)_2$, acetylacetone, sodium perchlorate, Britton–Robinson buffer) were prepared from analytical-grade chemicals, and the techniques used were as already described[14,15].

RESULTS

The limiting and peak currents of cobalt(II) reduction in the presence of acetylacetone obtained applying the d.c., a.c., and s.w. techniques, are presented in Fig. 1. A decrease in current was observed at concentrations of free ligand above 10^{-4} *M*.

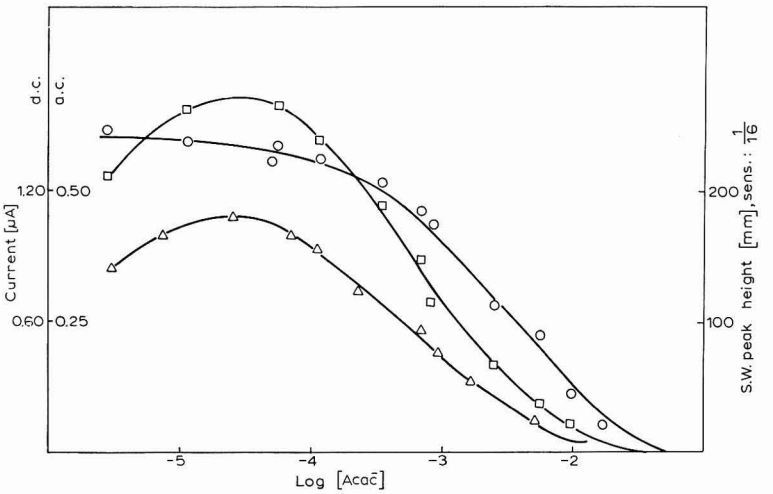

Fig. 1. D.c. limiting currents (○), a.c. (□) and s.w. (△) peak heights *vs.* free ligand concn. Soln. contained: $5 \cdot 10^{-4}$ *M* $Co(NO_3)_2$, 0.04 *M* HAcac, 0.5 *M* $NaClO_4$ and phosphate buffer.

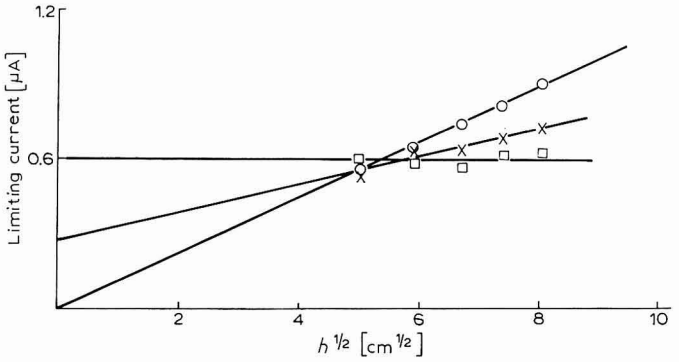

Fig. 2. Dependence of limiting current on mercury column height, at pH-values: (○), 6.50; (×), 7.79; (□), 8.14. Soln. as for Fig. 1.

The dependence of the limiting current on the mercury column height (Fig. 2) indicates that there could be a kinetic control in the mass transfer.

The degree of reversibility of the electrode process was examined with the aid of the Kalousek commutator[17] (circuit I). Normal and commutated polarograms for

the reduction of cobalt(II) in perchlorate solutions in the absence and in the presence of acetylacetone are given in Figs. 3 and 4, respectively. As no anodic wave can be recognized in a wide potential range, it can be concluded that both processes are totally irreversible.

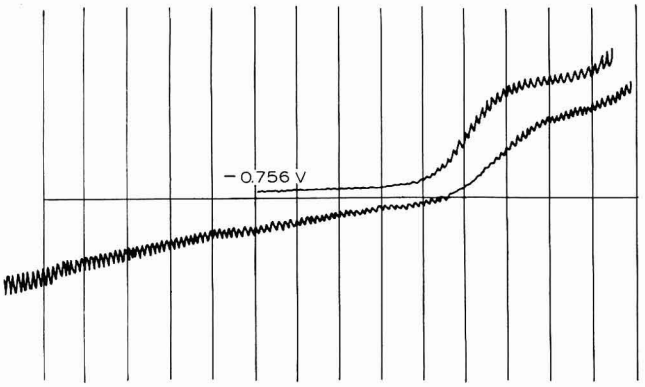

Fig. 3. Normal and commutated polarograms of Co(II) obtained with Kalousek commutator (circuit I) in soln. containing: $5 \cdot 10^{-4}$ *M* $Co(NO_3)_2$, 0.5 *M* $NaClO_4$ and Britton–Robinson buffer, pH = 6. Auxiliary potential, $E_2 = -1.425$ V (*vs.* SCE), 108 mV/scale unit, sensitivity 1/30, $f =$ 12.5 c/sec.

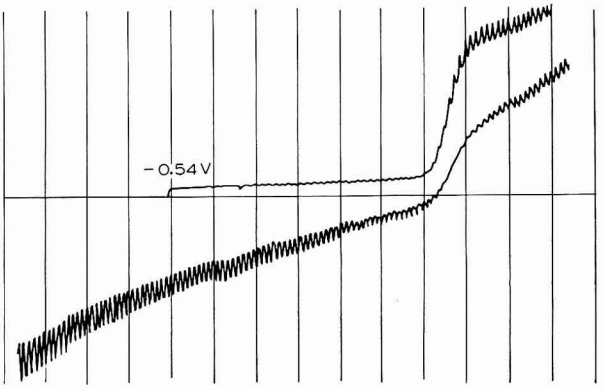

Fig. 4. Normal and commutated polarograms of Co(II) obtained using the Kalousek commutator (circuit I) in soln. containing: $5 \cdot 10^{-4}$ *M* $Co(NO_3)_2$, 0.01 *M* HAcac, 0.5 *M* $NaClO_4$ and Britton–Robinson buffer, pH = 6. Auxiliary potential, $E_2 = -1.400$ V (*vs.* SCE), 108 mV/scale unit, sensitivity 1/30, $f = 12.5$ c/sec.

Since the electrode processes take place at the negatively charged mercury surface, the nature and the concentration of the cations present can be expected to have a large effect on the polarographic waves measured. In order to check this possibility, systems were prepared in which the concentration of sodium perchlorate was varied. No other cations were used, in order to avoid the precipitation or formation of strong complexes with the acetylacetonato ions. Preliminary d.c. measurements indicated the double wave behaviour of cobalt(II). Since the resolution of the d.c. waves obtained was unsatisfactory, a pulse polarograph was used in further experiments.

The peak heights of the corresponding derivative pulse polarograms obtained at various concentrations of the supporting electrolyte and of the complexing ligand are given in Fig. 5.

In sodium perchlorate solutions of concentration above 0.1 M (free ligand concentration between 10^{-4} and 10^{-7} M) two reduction waves were observed. The first, *i.e.*, the more positive wave, increased with increase in free ligand concentration and could be ascribed to the reduction of the cobalt(II)monoacetylacetonato complex; the second more negative wave, which decreased under the same conditions, coincided with the wave of the cobalt(II)aquo complex.

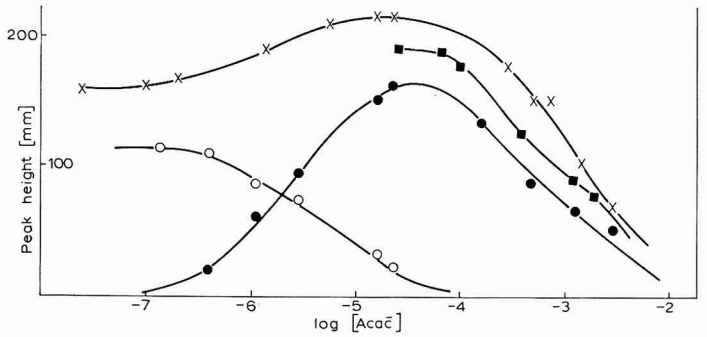

Fig. 5. Effect of concns. of sodium perchlorate and free ligand on height of derivative pulse polarograms (pulse amplitude, 7 mV) obtained by reduction of $2.5 \cdot 10^{-4}$ M Co(II) in aq. $5 \cdot 10^{-3}$ M HAcac and Britton–Robinson buffer. (×), 0.1; (■), 0.5; (●), (1st wave) 1.5; (○), (2nd wave) 1.5 M $NaClO_4$. Sens.: $\frac{1}{5} \times \frac{1}{8}$.

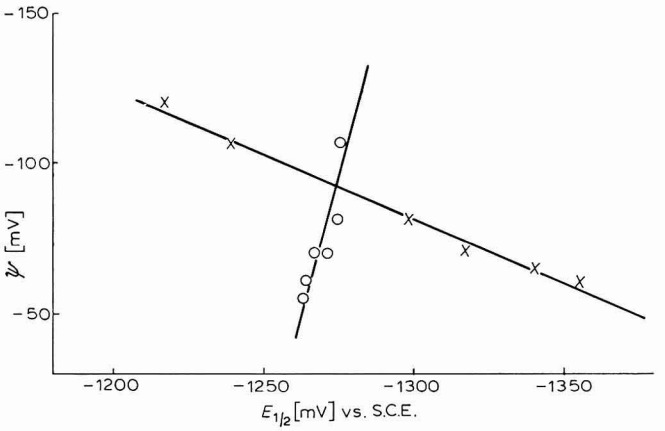

Fig. 6. Relationship between half-wave potential, $E_{\frac{1}{2}}$, and ψ-potential of electrode double layer for the polarographic reduction of $2.5 \cdot 10^{-4}$ M $Co(NO_3)_2$ in Britton–Robinson buffer pH 6.6 in: (×), $NaClO_4$ soln.; (○), $NaClO_4$ soln. + $5 \cdot 10^{-3}$ M HAcac.

In order to explain the double wave behaviour of Co(II) at higher concentrations of the supporting electrolyte, the effect of the electrode double layer on each wave was investigated separately. Measurements were carried out in pure perchlorate solution and in the presence of acetylacetone; the composition of the latter solution was chosen so as to give only one cobalt(II)monoacetylacetonato wave. The ψ-potential values

were taken from Tables calculated by RUSSELL[18] (on the basis of GRAHAME's experimental results) for sodium fluoride solution, but (assuming the absence of specific adsorption of both electrolytes) they could also be used in the case of sodium perchlorate.

In Fig. 6 the half-wave potentials of the waves of cobalt(II)aquo (curve 1) and cobalt(II)monoacetylacetonato (curve 2) complexes are plotted against the corresponding ψ-potentials. In both cases, straight lines were obtained which could be described by the following equation[19]:

$$\Delta E_{\frac{1}{2}} = (1 - z/\alpha n)\Delta\psi \qquad (1)$$

Assuming that the charge, z, of the reacting particles could be $+1$ or $+2$, the corresponding transfer coefficients were calculated. The following combinations were evaluated for the two-electron reduction of cobalt(II) in pure perchlorate solution:

$z = +1 \quad \alpha n = 0.30$
$z = +2 \quad \alpha n = 0.60$

and in the presence of acetylacetone

$z = +1 \quad \alpha n = 1.31$
$z = +2 \quad \alpha n = 2.62$

Using the method proposed by GIERST *et al.*[20], *i.e.*, following the relative change of the apparent rate constant, which is caused by the change of the ψ-potential of the double layer, the same parameters (z and αn) were recalculated. After graphical deduction of the charging current component, i/i_d plots were constructed and log $\chi_1 = f(E)$ plots were established using the values tabulated by WEBER AND KOUTECKY[21]. However, as only the relative changes of the apparent rate constant are of interest, the comparison between the rate constants has been based on log χ_1-values[20]. The next step was to select for each system a "median" potential, for which all log χ_1-values have been calculated, and then to plot these against the corresponding ψ-potentials. The results obtained are shown in Fig. 7. The charge numbers of the reacting particles and the transfer coefficients have been established from the slope of the straight lines obtained using the following relation[20]:

$$\Delta \ln \chi_1 / \Delta\psi = (\alpha n - z)F/RT \qquad (2)$$

Assuming, again, that $z = +1$ or $z = +2$, the following combinations were calculated for the reduction of cobalt(II) in perchlorate solution

$z = +1 \quad \alpha n = -0.40$
$z = +2 \quad \alpha n = 0.60$

and in an aqueous solution of acetylacetone

$z = +1 \quad \alpha n = 1.31$
$z = +2 \quad \alpha n = 2.32$

Comparing the results obtained by both methods with the αn-values calculated from the logarithmic analysis of the waves and corrected for the double layer effect, the following combinations were taken to be valid:

$z = +2 \quad \alpha n = 0.60$ Co(II) in $NaClO_4$ solution
$z = +1 \quad \alpha n = 1.30$ Co(II) in $NaClO_4$ + acetylacetone solution.

The nature and the kinetics of the chemical reaction, that causes the observed decrease in the wave height (Fig. 1) were next investigated. The measurements were, therefore, repeated at various controlled drop-times. The experimental results, which correspond to the apparent dissociation curves, are shown in Fig. 8. The logarithmic slope of the curves[22]:

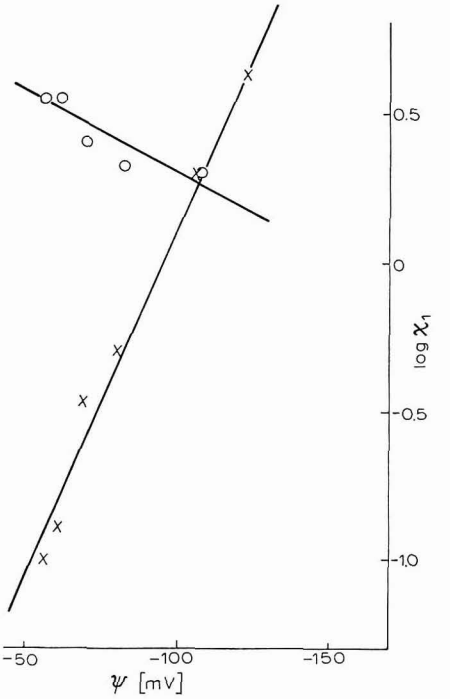

Fig. 7. Logarithmic values of KOUTECKY's χ_1 function, calcd. for polarographic reduction of $2.5 \cdot 10^{-4}$ *M* $Co(NO_3)_2$ in Britton–Robinson buffer pH 6.6 in: (×), $NaClO_4$ soln.; (○), $NaClO_4$ + $5 \cdot 10^{-3}$ *M* HAcac *vs.* ψ-potential of the electrode double layer.

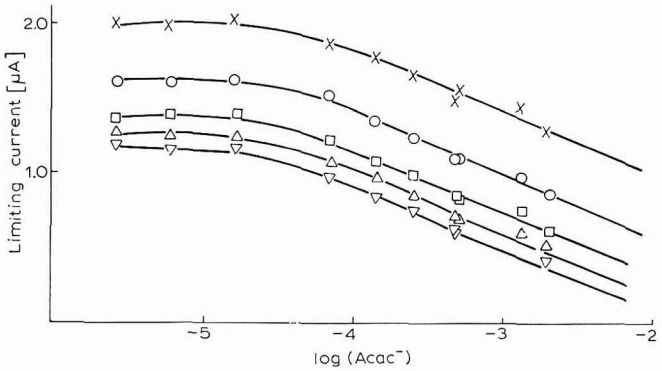

Fig. 8. Time-dependence of "polarographic dissociation curves" obtained for reduction of $5 \cdot 10^{-4}$ *M* $Co(NO_3)_2$ in aq. 0.02 *M* HAcac + 0.1 *M* $NaClO_4$ + Britton–Robinson buffer. *t*: (▽), 0.20; (△), 0.32; (□), 0.50; (○), 1.00; (×), 2.86 sec.

$$\Delta\log[i_1/(i_d-i_1)]/\Delta\log[X] = -m+k-\tfrac{1}{2} \quad (3)$$

was found to be $-\frac{1}{2}$, which implies that m and k should be equal (m is the coordination number of the highest complex prevailing in the solution, and k is the coordination number of the electroinactive complex causing the kinetic control in the mass transfer). The coordination number, m, was evaluated using the following equation[23]:

$$\Delta\log[i_1 i/(i_1-i)]/\Delta\log[X] = -m+q \quad (4)$$

where i is the current at a constant potential and q is the coordination number of the electroactive species which is assumed to be 1, considering that the charge number of the reacting particle is, $z=+1$, Since the above equation was found to be equal to -1, m was taken as 2.

The dissociation of the diacetylacetonato–cobalt(II) complex was taken, therefore, as the reaction preceding the electron transfer.

In the general equation of the kinetic wave[24]:

$$[i_1/(i_d-i_1)] = 0.886\sqrt{(\varrho/\sigma)t} \quad (5)$$

ϱ and σ were substituted according to the definition:

$$\varrho = k_d$$

$$\sigma = \Sigma[I]/\Sigma[A] = K_1 \cdot K_2[Acac^-]^2/(1+K_1[Acac^-]) \quad (6)$$

The thermodynamic stability constants $(K_1)_{\mu=0}$ and $(K_2)_{\mu=0}$ determined potentiometrically by IZATT *et al.*[25] were converted to the concentration constants[26,27] (for ionic strength of the solution investigated) $K_1 = 1.063 \cdot 10^5$, $K_2 = 8.37 \cdot 10^3$ and then introduced into the equation of the kinetic wave.

The values of the rate constants, k_d and k_r obtained are presented in Table 1.

TABLE 1

RATE CONSTANTS, k_d and k_r, FOR THE CHEMICAL REACTION PRECEDING THE REDUCTION OF COBALT-(II)

t (*sec*)	[*Acac*$^-$] at $i_1 = i_d/2$ (*M*)	k_d (*sec*$^{-1}$)	k_r (*mole*$^{-1}$ *l sec*$^{-1}$)
1.00	$3.02 \cdot 10^{-3}$	32.1	$2.69 \cdot 10^5$
0.50	$1.45 \cdot 10^{-3}$	30.1	$2.57 \cdot 10^5$
0.32	$9.13 \cdot 10^{-4}$	30.0	$2.51 \cdot 10^5$
0.20	$6.03 \cdot 10^{-4}$	30.0	$2.51 \cdot 10^5$
		30.9 ± 0.1	$(2.6 \pm 0.1) \cdot 10^5$

DISCUSSION

On the basis of the experimental results, the following scheme for the reaction mechanism can be given:

$$Co(H_2O)_6^{2+} \rightleftharpoons CoAcac^+ \underset{k_d}{\overset{k_r}{\rightleftharpoons}} CoAcac_2$$

$$\alpha n = 0.60 \qquad\qquad \alpha n = 1.30$$

$$Co(Hg) \qquad\qquad Co(Hg)$$

Depending on the composition of the solution, cobalt(II)aquo and/or cobalt(II)monoacetylacetonato complexes participate in the electrode process giving one or two polarographic waves. These waves are strongly affected by the ionic strength of the supporting electrolyte. The difference in the values of charge numbers between the reducible species (cobalt(II)aquo and cobalt(II)monoacetylacetonato complexes) and between their transfer coefficients caused a shift of their wave potentials in opposite directions, when the concentration of the supporting electrolyte was increased.

Cobalt(II)diacetylacetonate was found to be a non-reducible species in the potential range from mercury anodic oxidation to the reduction potential of the supporting electrolyte. Since the equilibrium between the cobalt(II)monoacetylacetonato and diacetylacetonato complex was found to be insufficiently mobile, the rate constants could be determined by the polarographic method. Although the nature of the equilibrium between the other two species, cobalt(II)aquo and cobalt(II)monoacetylacetonato complexes, could not be accurately determined, the existence of a sluggish equilibrium was assumed.

The effect of the electrode double layer on the rate of the chemical reaction coupled with the electron transfer was not investigated although a change in the height of the kinetic wave when the concentration of the electrolyte was varied has been observed. However, since the thickness of the reaction layer calculated on the basis of the rate constants determined (k_d and k_r) is much greater than that of the diffuse double layer, other effects of the ionic strength should be expected.

No proof for the reduction mechanism of cobalt(II) involving $Co(H_2O)_5OH^+$ as the reacting particle has been obtained. However, as detailed investigations were not carried out in a wider pH range, no final conclusion regarding this possibility[1,2] could be drawn. The value of the transfer coefficient, $\alpha = 0.30$, which we obtained for the two-electron reduction of cobalt(II) in perchlorate solution is in good agreement with that reported by CHICKRYZOVA AND LYALIKOV[28] ($\alpha = 0.35$) obtained under similar conditions (pH 6.8–6.9).

SUMMARY

The polarographic behaviour of cobalt(II) has been studied with respect to the composition of an aqueous solution of acetylacetone, using various polarographic techniques. The electrode process in pure perchlorate solution as well as in the presence of acetylacetone has been shown to be irreversible. The transfer coefficient, $\alpha = 0.30$, and the charge number of the reducible species, $z = +2$, are found to be valid for the reduction of cobalt(II) in pure perchlorate solution and in an aqueous solution of 10^{-2} M acetylacetone at pH < 4.5. In aqueous solutions of acetylacetone of pH > 4.5, the transfer coefficient was: $\alpha = 0.65$ and the charge number $z = +1$; these values correspond to the reduction of the cobalt(II) monoacetylacetonato species.

The double wave behaviour of cobalt(II) observed in the presence of acetylacetone at concentrations of the supporting electrolyte above 0.1 M is explained by the effect of electrostatic forces in the electrode double layer.

In solutions where the ligand concentration is above 10^{-4} M, the limiting current has a kinetic character caused by a slow dissociation of cobalt(II)diacetylacetonato to the monoacetylacetonato complex. The rate constants of the chemical reaction

have been calculated:

$k_d = (30.9 \pm 0.1)\ \text{sec}^{-1}$

$k_r = (2.6 \pm 0.1)\ 10^5 \text{mole}^{-1}\ \text{l sec}^{-1}$.

ACKNOWLEDGEMENT

Measurements with the Kalousek commutator were carried out at the "J. Heyrovský" Polarographic Institute in Prague. The authors would like to express their thanks to Dr. J. MAŠEK and his colleagues for making the facilities available and also for helpful discussions.

REFERENCES

1 E. VERDIER AND F. ROUELLE, *Compt. Rend.*, 259 (1964) 1856.
2 E. VERDIER AND F. ROUELLE, *J. Chim. Phys.*, 62 (1965) 297.
3 L. GIERST AND H. HURWITZ, *Z. Elektrochem.*, 64 (1960) 36.
4 L. GIERST, *Transactions of the Symposium on Electrode Processes* edited by E. YEAGER, J. Wiley and Sons, New York, 1961, p. 109.
5 J. DANDOY AND L. GIERST, *J. Electroanal. Chem.*, 2 (1961) 116.
6 A. A. VLČEK, *Z. Elektrochem.*, 61 (1957) 1014.
7 A. A. VLČEK, *Z. Physik. Chem. (Leipzig), Sonderheft*, (1958) 143.
8 M. PETEK AND M. BRANICA, *J. Polarog. Soc.*, 9 (1963) 1.
9 M. PETEK, LJ. JEFTIĆ AND M. BRANICA, *Polarography 1964, Proc. 3rd Int. Conf. Southampton*, edited by G. J. HILLS, Vol. 1, pp. 491–504.
10 M. PETEK, J. KŮTA AND M. BRANICA, *Collection Czech. Chem. Commun.*, 32 (1967) 3510.
11 LJ. JEFTIĆ AND M. BRANICA, *Croat. Chem. Acta*, 35 (1963) 203.
12 LJ. JEFTIĆ AND M. BRANICA, *Croat. Chem. Acta*, 35 (1963) 211.
13 M. BRANICA AND J. KŮTA, *Collection Czech. Chem. Commun.*, 31 (1966) 2833.
14 B. ĆOSOVIĆ AND M. BRANICA, *J. Polarog. Soc.*, 12 (1966) 5.
15 B. ĆOSOVIĆ AND M. BRANICA, *J. Polarog. Soc.*, 12 (1966) 97.
16 B. ĆOSOVIĆ, M. VERŽI AND M. BRANICA, to be published.
17 M. KALOUSEK, *Collection Czech. Chem. Commun.*, 13 (1948) 105.
18 C. D. RUSSELL, *J. Electroanal. Chem.*, 6 (1963) 486.
19 J. J. TONDEUR, A. DOMBERT AND L. GIERST, *J. Electroanal. Chem.*, 3 (1962) 225.
20 L. GIERST, D. VANDENBERGHEN, E. NICOLAS AND A. FRABONI, *J. Electrochem. Soc.*, 113 (1966) 1025.
21 J. WEBER AND J. KOUTECKÝ, *Chem. Listy*, 49 (1955) 562; *Collection Czech. Chem. Commun.*, 20 (1955) 980
22 J. KORYTA, *Chem. Listy*, 51 (1957) 1544; *Collection Czech. Chem. Commun.*, 23 (1958) 1408.
23 J. KORYTA, *Electrochem. Acta*, 1 (1959) 26.
24 J. KOUTECKÝ, *Collection Czech. Chem. Commun.*, 18 (1953) 597.
25 R. M. IZATT, W. C. FERNELIUS AND B. P. BLOCK, *J. Phys. Chem.*, 59 (1955) 235.
26 R. M. IZATT, CH. G. HASS, JR., B. P. BLOCK AND W. C. FERNELIUS, *J. Phys. Chem.*, 58 (1954) 1133.
27 R. A. ROBINSON AND R. H. STOKES, *Rastvory Elektrolytov*, translated Izd. Inos. Lit., Moskva, 1963; original *Electrolyte Solutions*, Butterworths, London, 1959, p. 541.
28 E. G. CHICKRYZOVA AND YU. S. LYALIKOV, *Izv. Nauk Moldavsk. SSSR*, 12 (1961) 3.

ELECTROANALYTICAL CHEMISTRY AND INTERFACIAL ELECTROCHEMISTRY
Elsevier Sequoia S.A., Lausanne – Printed in The Netherlands

THE USE OF COMPLEX-FORMING REAGENTS IN THE POLAROGRAPHIC ANALYSIS OF INORGANIC SUBSTANCES
XIV*. POLAROGRAPHIC BEHAVIOUR OF ETHYLENEDISULPHURDIACETIC ACID IN THE PRESENCE OF A MERCURY SALT

DESANKA SUŽNJEVIĆ
Faculty of Science, Department of Physical Chemistry, University of Belgrade (Yugoslavia)
JAN DOLEŽAL
Department of Analytical Chemistry, Charles University, Prague (Czechoslovakia)
MILOSLAV KOPANICA
J. Heyrovský Polarographic Institute, ČSAV, Prague (Czechoslovakia)
(Received July 13th, 1968; in revised form, August 5th, 1968)

Ethylenedisulphurdiacetic acid (I) was first prepared by RAMBERG AND TIBERG[1]

HOOC–H_2C–S–CH_2–CH_2–S–CH_2COOH (I)

but so far little attention has been given to its chelate-forming abilities; literature data are sparse and only of a qualitative nature. Recent studies based on potentiometric and spectrophotometric measurements have shown that this reagent forms 1:1 metal:ligand chelates with some divalent metals[2–4].

In the present paper the polarographic behaviour of mercuric ions in the presence of ethylenedisulphurdiacetic acid (H_2Z) is described with a view to finding the molar ratio of the chelate-forming substance and determining the stability constant of the resulting chelate by means of polarographic data.

EXPERIMENTAL

Apparatus

Polarograms were recorded with a Metrohm Polarecord E-261 and with an H-type polarographic cell with a large separate saturated mercury sulphate electrode. An electrode of large (4.5 cm^2) active surface was prepared to prevent its polarization. pH-values were measured with a Radiometer pH-meter PHM 4 using a glass electrode as reference electrode. For conductivity measurements, a Radiometer conductivity-meter CDM-2 was used in connection with an ultrathermostat.

Reagents

Ethylenedisulphurdiacetic acid was prepared by PODLAHA[4]. Other solutions used were prepared from reagent-grade chemicals.

Buffer solutions (Britton–Robinson; acetic acid–sodium acetate; borate–

* No. XIII of this series: J. DOLEŽAL AND O. GÜRTLER, *Talanta*, 15 (1968) 299.

phosphate) were prepared from reagent-grade chemicals according to recommended procedures. The ionic strength was kept constant ($\mu = 0.1$) using potassium nitrate or sodium perchlorate solutions.

RESULTS AND DISCUSSION

A well-developed anodic wave with half-wave potential -200 mV *vs.* saturated mercury sulphate electrode (at pH 5–6) was observed in buffered solutions containing H_2Z. This wave corresponded to the oxidation of mercury from the dropping mercury electrode in the chelate-forming medium. The limiting current resulted from diffusion of the ligand to the electrode surface. After the addition of mercuric salt to the buffered solution of H_2Z, this wave became cathodic in character with the same half-wave potential and also with the diffusion character of the limiting current (Fig. 1). The diffusion nature of the limiting current was established by the dependence of the heights of the waves on the height of the mercury reservoir. A linear function was found between the square root of the height of mercury reservoir and the wave heights of both types of waves described for different values of pH and for several different concentrations of the substances investigated. In the investigation of the dependence of the half-wave potentials of the waves on the pH, the potential of the reference electrode was controlled by measurement of the half-wave potential of the reduction wave of Tl^+ ions in ammoniacal medium. The results have shown that the potential of the reference electrode remained constant during the experiments and therefore it was unnecessary to use the three-electrode system[5].

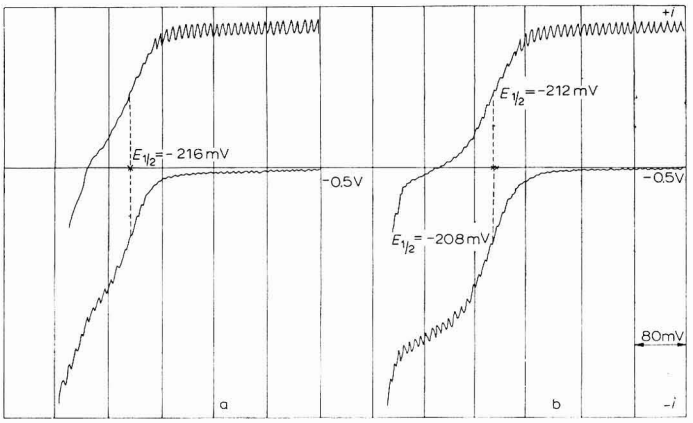

Fig. 1. Anodic and cathodic polarographic waves of H_2Z and its mercuric chelate. $2 \cdot 10^{-3}$ *M* H_2Z; $1 \cdot 10^{-3}$ *M* HgZ_2; borate–phosphate buffer soln. at pH: (a), 8.58; (b), 5.59.

The dependence of the half-wave potential of both anodic and cathodic waves upon the pH was investigated in the pH-ranges of universal Britton–Robinson buffer solution, acetic acid–sodium acetate, and borate–phosphate buffer solutions (see Fig. 2, with two curves obtained by the analysis of anodic and cathodic waves). In both cases the dependences followed the same function. In acid medium up to about pH 4, the half-wave potential changed linearly towards negative potentials.

The slope of this part of the curve was about 60 mV for unit change of pH. Above pH 4, the half-wave potentials remained constant up to about pH 8.5. At higher pH-values, the anodic and cathodic waves were insufficiently developed for the results to be utilizable.

The concentration-dependence of the anodic diffusion current of H_2Z at different pH-values with different buffer solutions is linear over a wide range of H_2Z concentration (see Fig. 3a). The dependence of the cathodic diffusion current is also linear over a wide range of concentration of the mercuric chelate (Fig. 3b).

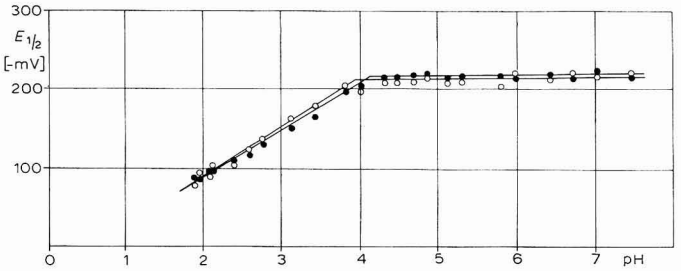

Fig. 2. Dependence of the half-wave potential of anodic (○) and cathodic (●) waves on pH (Britton–Robinson buffer soln., $\mu = 0.1$), $2 \cdot 10^{-3}$ *M* H_2Z, 0.004% gelatine, $1 \cdot 10^{-3}$ *M* HgZ_2^{2-}, 0.004% gelatine.

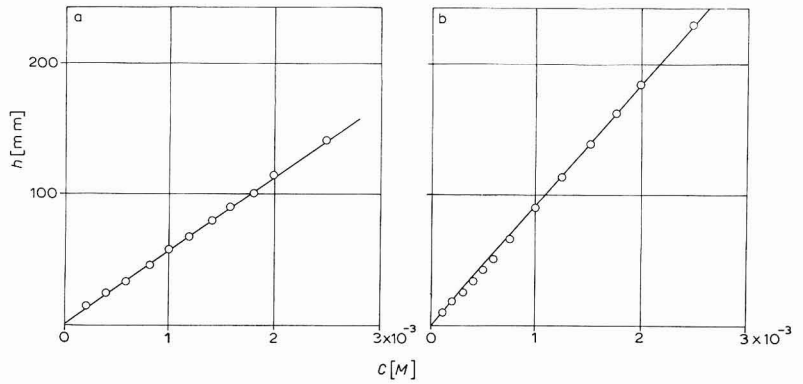

Fig. 3. Dependence of wave heights on concn. (a), anodic waves in acetic acid–acetate buffer soln. (pH = 3.80); (b), cathodic waves in Britton–Robinson buffer (pH = 3.29).

The composition of the chelate resulting from the reaction between H_2Z and Hg^{2+} ions was determined by an amperometric titration. Titration curves were obtained by recording polarographic waves corresponding to a series of solutions maintained at a constant concentration of Hg^{2+} ions, but with different concentrations of H_2Z in a buffer solution of identical pH. In a second series, the concentration of H_2Z was kept constant and the concentration of Hg^{2+} ions varied. The equivalence points resulting from these series of measurements were found to be the same. The results have shown that at the equivalence point, the molar ratio, Hg^{2+}:Z, was 1:2. The slopes of the linear branches produced by the change of cathodic and anodic wave heights did not differ considerably. It is evident, therefore, that the species

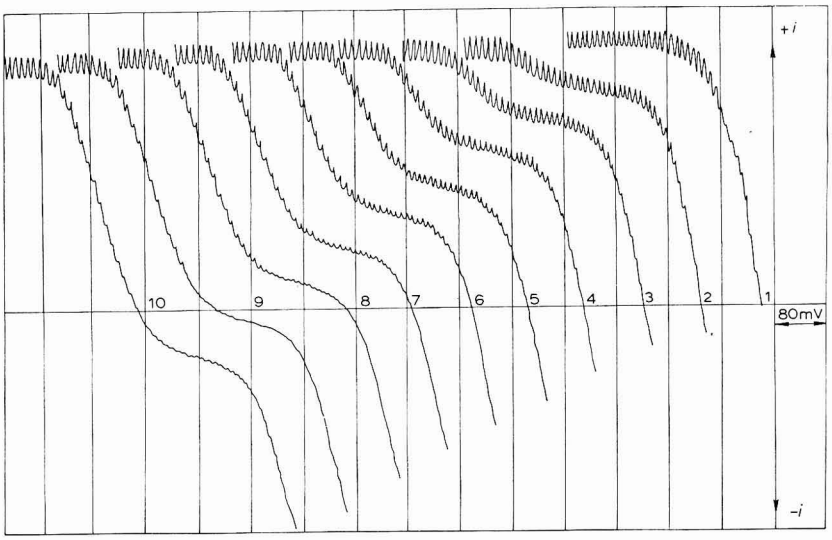

Fig. 4. Amperometric titration of $Hg(NO_3)_2$ with H_2Z. (1), $3 \cdot 10^{-3}$ *M* $Hg(NO_3)_2$, 0.004% gelatine acetic acid–acetate buffer (pH = 3.66); (2–10), addition of 0.1 ml 0.1 *M* H_2Z for each curve

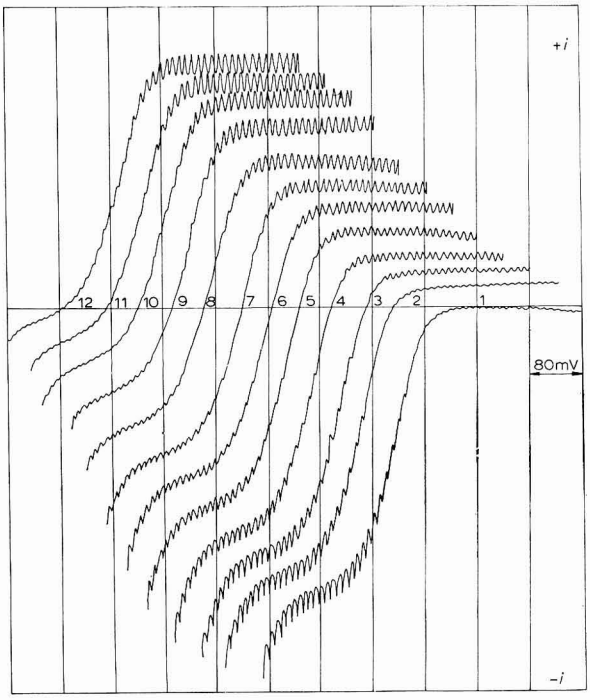

Fig. 5. Amperometric titration of H_2Z with $Hg(NO_3)_2$. (1), $2 \cdot 10^{-3}$ *M* H_2Z, 0.004% gelatine, Britton–Robinson buffer soln. (pH = 3.29); (2–12), addition of 0.1 ml 0.01 *M* $Hg(NO_3)_2$ for each curve.

which take part in diffusion in each case have a similar diffusion coefficient. Figures 4 and 5 show the amperometric titration curves obtained.

Job's continuous variation method was applied to the system studied and confirmed the results obtained by amperometric titrations.

Logarithmic analysis[6,7] of the anodic and cathodic waves (dependence of log $[\bar{i}^2/(\bar{i}_d-\bar{i})]$ *vs.* E for the cathodic, and log $[(\bar{i}_d-\bar{i})/\bar{i}^2]$ *vs.* E for the anodic wave, respectively) gave straight lines with slopes of 30 mV. These findings confirm the reversibility of the corresponding electrode process and the two-electron reduction (oxidation) character of this reaction. The reversibility of the electrode process was further verified by oscillopolarographic measurements[8].

The results have shown that the polarographic behaviour of the mercury chelate of H_2Z is less complicated in comparison with the polarography of the Hg–EDTA chelate[11,12]. In view of the values of the dissociation constant of H_2Z ($pK_1=3.17$ and $pK_2=3.82$)[4] and the pH-dependence of the half-wave potential of the waves studied (Fig. 2), the formation of the 1:2 chelate may be represented by the following reactions.

$$Hg^{2+}+2\ H_2Z \rightleftharpoons HgH_{(4-n)}Z_2^{(2-n)}+nH^+ \quad (1)$$

and

$$Hg^{2+}+2\ Z^{2-} \rightleftharpoons HgZ_2^{2-} \quad (2)$$

Reaction (1) is valid at pH-values below 4, reaction (2) at pH-values above 4. The stability constant of the HgZ_2^{2-} chelate is defined as

$$K_{HgZ_2}=[HgZ_2^{2-}]/[Hg^{2+}][Z^{2-}]^2 \quad (3)$$

where the concentration of the anion depends on pH. The pH-dependence was formulated generally by SCHWARZENBACH[9] by introducing the α_H coefficient, which for H_2Z is defined as

$$\alpha_H=1+[H^+]/K_1+[H^+]^2/K_1K_2 \quad (4)$$

where K_1 and K_2 are the dissociation constants of H_2Z. With the use of the α_H coefficient the concentration of the anion reagent $[Z^{2-}]'$ is given by the equation

$$[Z^{2-}]'=\alpha_H[Z^{2-}] \quad (5)$$

Because the electrode process studied was found to be reversible, the value of the stability constant of the HgZ_2 chelate was determined from the dependence of the half-wave potential of the waves upon the pH. As in the case of the Hg–EDTA chelate[10–12], an equation was derived which gives the relation between the half-wave potential and pH for the cathodic wave:

$$E_{\frac{1}{2}}=E^0+0.029\log(D_k^{\frac{1}{2}}/D_A^{\frac{1}{2}})+0.029\log\alpha_H-0.029\log K_{HgZ_2} \quad (6)$$

where E^0 is the standard Hg^{2+}/Hg potential, D_k the diffusion coefficient of the chelated mercury ions, D_A the diffusion coefficient of the ligand and α_H is defined by eqn. (4). The stability constant of the HgZ_2 chelate was determined using eqn. (6). The data for the half-wave potentials corresponding to various pH-values are summarized in Table 1. All measurements were carried out at a constant ionic strength of 0.1. The diffusion coefficients, D_k and D_A, are approximately the same as was concluded by the change of anodic and cathodic waves during the amperometric

titrations. The average value of the stability constant of the HgZ_2 chelate was found to be $\log K_{HgZ_2} = 13.82 \pm 0.2$.

The results given in Table 1 show that the stability constant, K, has a constant value in the pH-interval up to pH 3. At pH-values above 3, there is a definite tendency for $\log K$-values to increase with increase in pH. This increase may be explained by the fact, that hydroxo complexes of mercury(II) are also formed in a solution of

TABLE 1

HALF-WAVE POTENTIALS OF THE CATHODIC WAVE AT DIFFERENT pH-VALUES AND THE CORRESPONDING LOG K-VALUES CALCULATED ACCORDING TO EQUATION (6)

pH	$E_{\frac{1}{2}}$ *(mV vs. NHE)*	*log K*	*pH*	$E_{\frac{1}{2}}$ *(mV vs. NHE)*	*log K*
1.90	509	13.21	2.85	431	13.24
1.95	493	13.76	3.05	419	14.34
2.10	489	13.65	3.55	395	14.88
2.10	486	13.55	3.80	383	14.72
2.25	481	13.66	4.15	367	15.10
2.35	481	13.38	4.70	363	15.10
2.50	473	13.38	5.15	351	15.45
2.60	455	13.89	5.75	347	15.58

pH above 3. If the stability of the hydroxo complex of mercury(II) is (according to RINGBOM[13]) expressed by the value of $\log \alpha_{Hg(OH)}$, this parameter is equal to *ca.* 2 at pH 4 and *ca.* 6 at pH 6. At a relatively small stability of the HgZ_2 chelate, its formation is more influenced by the existence of the hydroxo complex than, for example, the formation of the Hg–EDTA chelate. In the polarographic study of the stability of the Hg–EDTA chelate[12] (carried out as in the present case), the slight increase of the $\log K$-values obtained was observed only at pH-values above 8, owing to the relatively high stability of the Hg–EDTA chelate ($\log K_{HgEDTA} = 21.6$).

ACKNOWLEDGEMENT

The authors wish to express their gratitude to Dr. J. PODLAHOVÁ and Dr. J. PODLAHA, Department of Inorganic Chemistry, Charles University, Prague for kind provision of the reagent sample and for helpful discussion.

SUMMARY

Polarographic cathodic and anodic waves corresponding to the reduction of mercuric ions from the chelate of ethylenedisulphuridiacetic acid, and the anodic oxidation of mercury in the presence of this reagent, were studied. In both cases the waves are well-developed and produced by reversible two-electron electrode processes limited by diffusion. The molar ratio, metal:ligand was found to be 1:2 using the amperometric titration technique, and Job's method of continuous variations carried out with potentiometric and conductivity measurements. From the dependence of the half-wave potential of the waves upon the pH, the stability constant of the HgZ_2 chelate was determined as $\log_{10} K = 13.82 \pm 0.2$.

REFERENCES

1 L. RAMBERG AND A. TIBERG, *Ber.*, 47 (1914) 730.
2 K. SUZUKI AND K. YAMASAKI, *J. Inorg. Nucl. Chem.*, 24 (1962) 1093.
3 G. SAINI, G. OSTACOLI, E. CAMPI AND N. CIBARIO, *Gazz. Chim. Ital.*, 91 (1961) 242.
4 J. PODLAHA, Habil. Thesis, Chem. Dept., Charles University, Prague, 1968.
5 A. A. VLČEK, *Collection Czech. Chem. Commun.*, 19 (1954) 862.
6 J. TOMEŠ, *Collection Czech. Chem. Commun.*, 9 (1937) 12.
7 J. J. LINGANE, *J. Am. Chem. Soc.*, 61 (1939) 976.
8 R. KALVODA, *Techniques of Oscillographic Polarography*, Elsevier, Amsterdam, 1965.
9 G. SCHWARZENBACH, *Die komplexometrische Titrationen*, Enke Verlag, Stuttgart, 1955, p. 8.
10 B. MATYSKA AND I. KÖSSLER, *Collection Czech. Chem. Commun.*, 16 (1951) 221.
11 J. GOFFART, G. MICHEL AND G. DUYCKAERTS, *Anal. Chim. Acta*, 9 (1953) 184.
12 B. MATYSKA, J. DOLEŽAL AND D. ROBALOVÁ, *Collection Czech. Chem. Commun.*, 21 (1956) 107.
13 A. RINGBOM, *Complexation in Analytical Chemistry*, Interscience Publishers, New York, 1963, p. 44.

ELECTROANALYTICAL CHEMISTRY AND INTERFACIAL ELECTROCHEMISTRY
Elsevier Sequoia S.A., Lausanne – Printed in The Netherlands

DIE POLAROGRAPHISCHE REDUKTION VON SOLOCHROMVIOLETT RS UND DER MECHANISMUS DER KOMPLEXBILDUNG MIT ALUMINIUM IN METHANOLISCHER LÖSUNG

L. HOLLECK, J. M. ABD EL KADER UND A. M. SHAMS EL DIN
Chemisches Institut der Hochschule, Bamberg (Deutschland)
(Eingegangen am 13 Juli, 1968)

Solochromviolett RS (SVRS) (I) wurde von WILLARD UND DEAN[1] als geeignetes Reagenz für die indirekte polarographische Bestimmung von Aluminium in wässriger Lösung empfohlen.

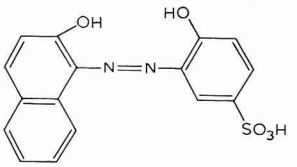

(I)

In Acetatpuffer von pH 4.6 liefert die Verbindung eine einzige Reduktionsstufe. In Gegenwart von Al^{3+} spaltet diese Stufe in zwei Teile auf: der erste Teil entspricht der Reduktion des überschüssigen Farbstoffes, der nicht reagiert hat, während die zweite Teilstufe—um etwa 200 mV zu negativeren Potentialen verschoben—dem an Al^{3+} gebundenen Teil des Farbstoffes entspricht. Das Anwachsen der Höhe dieser Stufe und/oder eine entsprechende Verminderung der Stufenhöhe für die freie Verbindung sind dem Al^{3+}-Gehalt der Lösung direkt proportional. Zur Erhöhung der Empfindlichkeit der Bestimmung schlugen FLORENCE u. a.[2] kürzlich die Verwendung der Oxydationsstufen von SVRS und seines Al-Komplexes an der rotierenden Graphit-Elektrode vor. Beide Verbindungen liefern gut ausgebildete Stufen, die unter geeigneten Bedingungen um etwa 350 mV getrennt sind. Bei der Oxydation bilden sich die entsprechenden Azoxyverbindungen.

Obgleich das polarographische Verhalten von SVRS oder ähnlicher Farbstoffe (X) verschiedentlich untersucht wurden[1-7] und ihre Reaktion mit Al^{3+} mehrfach zur analytischen Anwendung gelangte[8-10], lassen sich die Ergebnisse verschiedener Autoren z.T. nicht miteinander vereinbaren. Während z.B. DEAN UND BRYAN[3] sowie PERKINS UND REYNOLDS[4] die Reduktion des freien Farbstoffes als den Übergang von zwei Elektronen pro Molekül ansehen (entsprechend der Bildung des Hydrazo-Derivats), liefern die Untersuchungen von FLORENCE[6,7] Hinweise dafür, dass vier Elektronen an dem Vorgang beteiligt sind, wobei unter Bruch der N–N-Bindung die beiden entsprechenden Amine gebildet würden. Dabei wurde eine rasche Disproportionierung der als unbeständige Zwischenstufe gebildeten Hydrazoverbindung angenommen[6]. Auch die Zusammensetzung des gebildeten Al-Komplexes ist umstritten. DEAN[1,3], FLORENCE[2] und COATES[11] nehmen einen Komplex AlX_2 an. Ähnliche Zusammensetzungen werden auch den Solochrom-Komplexen von Zn und

Ni[3], der Lanthaniden[7] sowie den Komplexen von Al mit anderen *ortho*-dihydroxy-Azoverbindungen[12–14] zugeschrieben. Es existieren jedoch auch Hinweise[3,4], wonach sich in Lösungen höherer pH-Werte auch ein anderer Komplex, nämlich Al^{3+}:3 X, bilden soll. Auch dafür, dass das an Al^{3+} gebundene SVRS bei negativeren Potentialen reduziert wird als die freie Verbindung, sind verschiedene z.T. unbefriedigende Erklärungen gegeben worden. Die ursprüngliche Annahme, dass die Komplexbildung das Farbstoffmolekül in der *cis*-Form festlegt, während das freie Molekül in der *trans*-Form vorliegt[1], wurde später aufgrund sterischer Überlegungen verworfen[3,4]. Daneben wurden andere Erklärungen angegeben[3], die nicht weiter diskutiert werden sollen.

Im Hinblick auf den Mangel an Übereinstimmung wurde angesichts der Erfahrungen, die an unserem Institut in einer Reihe von Untersuchungen über das polarographische Verhalten substituierter Azoverbindungen sowohl in wässrigem[15,16] wie nicht-wässrigem Medium[17] gewonnen wurden, die Reduktion von SVRS und seines Aluminium-Komplexes in methanolischen Lösungen verfolgt. Bei der Untersuchung anderer organischer Verbindungen in diesem Medium[18–20] hatte es sich gezeigt, dass Zusätze von Protonendonatoren sowie solcher Stoffe, die Protonen-Transferprozesse katalysieren, bei der Klärung des Reduktionsmechanismus hilfreich sein können.

EXPERIMENTELLES

Bei den vorliegenden Untersuchungen wurde eine einfache polarographische Zelle benutzt, bei der ein seitlicher Ansatz durch eine feinporige Glasfritte abgeschlossen war. Letztere stellte die Verbindung zu der (wässrigen) KCl-Lösung einer grossflächigen gesättigten Kalomelelektrode (GKE) her, in welche die Zelle in der Weise eintauchte, dass das Niveau der Flüssigkeit in der Zelle etwa 1 cm oberhalb demjenigen in der Kalomelelektrode blieb. Hierdurch wurde ein Eindringen von Wasser in die Zelle weitgehend vermieden. Die Entlüftung der Lösung erfolgte mit reinem Stickstoff. Als Leitelektrolyt diente 0.1 *M* LiCl in reinem Methanol (E. Merck, Darmstadt). Technisches SVRS (Dr. Th. Schuchardt, München) wurde aus 50%igem Methanol umkristallisiert. Wasserfreies $AlCl_3$ (Merck) wurde in Methanol gelöst. Als Protonendonator diente Benzoesäure, als Katalysator für Protonen-Transferprozesse N,N-Dimethyl-*p*-phenylendiamin (DMPD) mit der Konzentration $2.5 \cdot 10^{-4}$ *M*. Wenn nicht anders angegeben, erfolgten die Untersuchungen mit $1 \cdot 10^{-3}$ *M* SVRS, bei Zimmertemperatur von 20–21°.

ERGEBNISSE UND DISKUSSION

Kurve 1 der Abb. 1 gibt die polarographische Reduktion von $1 \cdot 10^{-3}$ *M* SVRS in reinem Methanol (Leitelektrolyt, 0.1 *M* LiCl) wieder. Die Verbindung wird in drei aufeinanderfolgenden Stufen reduziert, deren Halbstufenpotentiale −0.57, −0.78 und −0.98 V (GKE) betragen. In Abwesenheit anderer Zusätze geht der ersten Stufe ein kleines Maximum vorauf, das durch 0.04 Gew.-% Triphenylphosphinsulfid unterdrückt werden kann.

Alle drei Stufen von SVRS in Methanol sind diffusionsbestimmt, wie aus der Abhängigkeit der Stufenhöhe von der Hg-Niveauhöhe hervorging. Ein Vergleich der Gesamthöhe der drei Stufen von SVRS mit derjenigen einer gleich konzentrierten Lösung von Azoxybenzol unter ähnlichen Bedingungen[20] führt zu dem Schluss, dass

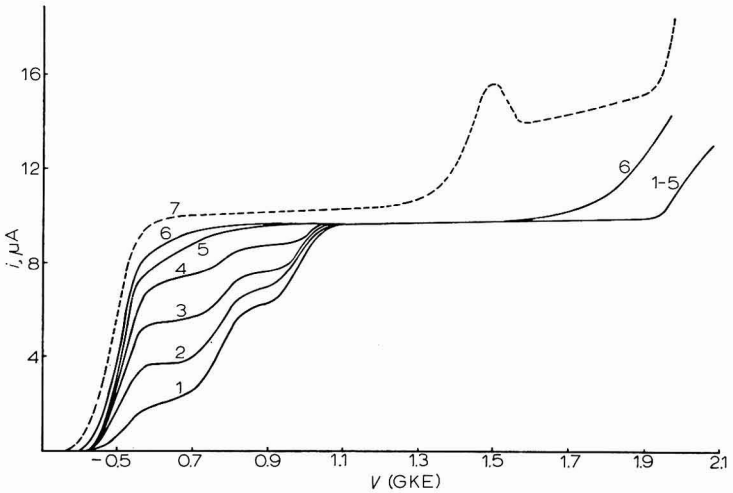

Abb. 1. Wirkung von Benzoesäure-Zusatz auf die polarographischen Strom–Spannungs-Kurven von $1 \cdot 10^{-3}$ *M* SVRS in Methanol (0.1 *M* LiCl). (1), 0; (2), 0.5; (3), 1.0; (4), 1.5; (5), 2.0; (6), $3.0 \cdot 10^{-3}$ *M* Benzoesäure; (7), wie (6) + $2.5 \cdot 10^{-4}$ *M* DMPD.

am Gesamtvorgang vier Elektronen pro Molekül SVRS beteiligt sind. In dieser Beziehung stimmen die vorliegenden Untersuchungen mit denen von FLORENCE[6,7] überein. Demnach führt die Reduktion zur Bildung der beiden Amine. Zusammen mit der Tatsache, dass die Höhe der einzelnen Stufen jeweils nicht dem Austausch einer ganzen Zahl von Elektronen entspricht, lässt dieser Befund kaum Zweifel, dass es sich um die Reduktion einer Substanz handelt, die in verschiedenen Dissoziationsstufen vorliegt. Ähnliche Verhältnisse wurden für 4-Carboxyazobenzol beobachtet[17], wo das Polarogramm aus zwei getrennten Stufen besteht; die erste Stufe entspricht der Reduktion der nicht ionisierten Form, die zweite derjenigen des Anions.

Die im weiteren geschilderten Ergebnisse unterstützen die Folgerung, dass die Protonen der beiden *ortho*-ständigen Hydroxygruppen am Reduktionsvorgang beteiligt sind. Dies ist wie folgt zu formulieren:

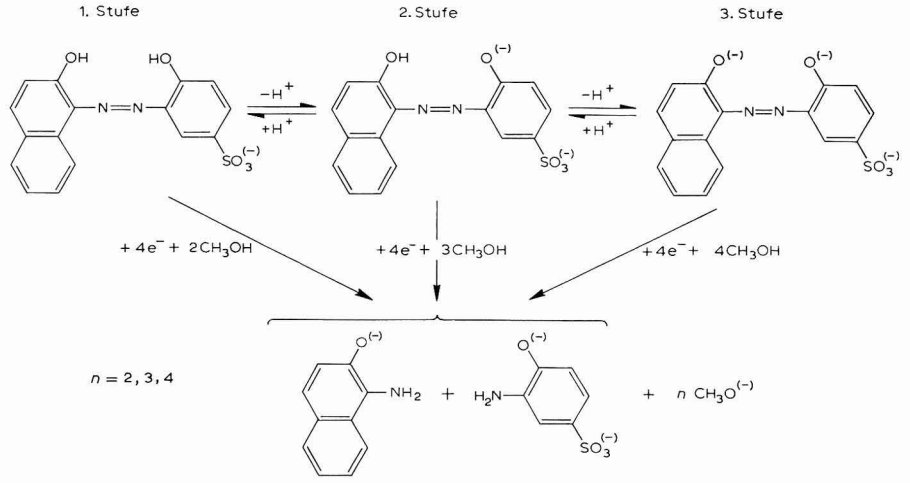

Dass SVRS in methanolischer Lösung in drei Dissoziationsstufen vorliegt, konnte durch Untersuchungen nachgewiesen werden, bei denen die Lösung mit bestimmten Mengen Benzoesäure als Protonendonator versetzt wurde. Wie aus den Kurven 2–5 der Abb. 1 hervorgeht, wächst die Höhe der ersten Stufe bei Erhöhung der Säurekonzentration auf Kosten der beiden anderen. Bei einer Konzentration von $2 \cdot 10^{-3}$ *M* Benzoesäure (dem Doppelten der SVRS-Konzentration) erfolgt die Reduktion in einer einzigen Stufe bei dem Potential der ursprünglichen ersten Stufe. Bei weiterer Erhöhung der Säuremenge verschiebt sich die Stufe leicht zu positiveren Potentialen (Kurve 6 in Abb. 1 für $3 \cdot 10^{-3}$ *M* Benzoesäure), wobei zugleich der Endanstieg eher erfolgt. Die Reduktion von SVRS in einer einzigen Stufe bei genügendem Säuregehalt zeigt, dass hierdurch die Dissoziation der beiden OH-Gruppen unterdrückt wird. Die Tatsache, dass zwei Äquivalente Benzoesäure erforderlich sind, um die Reduktion in einer einzigen Stufe ablaufen zu lassen, während die Bildung der beiden Amine insgesamt vier Protonen erfordert, führt zu dem Schluss, dass die beiden Protonen der Oxygruppen des Farbstoffes auch weiterhin bei dem Prozess verbraucht werden.

N,N-Dimethyl-*p*-phenylendiamin (DMPD), das sich in vorhergehenden Untersuchungen[17,19,20] als sehr wirksamer Katalysator von Protonen-Transferprozessen erwiesen hatte, verursacht hier nur die Unterdrückung des Maximums der ersten Stufe von SVRS, während die Reduktionspotentiale aller drei Stufen nicht in messbarem Umfange beeinflusst werden. Selbst in Gegenwart von Benzoesäure ist die Wirkung von DMPD nur recht gering. Diese Befunde zeigen, dass der Zusatzstoff nicht stark —wie in anderen Fällen[17,20]—an der Elektrodenoberfläche adsorbiert wird, und zwar sehr wahrscheinlich wegen der bevorzugten Adsorption der oxydierten Form des Depolarisators. Dagegen katalysiert der DMPD-Zusatz die Reduktion des in der Lösung vorliegenden Säureüberschusses: Kurve 7 der Abb. 1 zeigt, dass der bei der Reduktion von SVRS nicht verbrauchte Säureanteil eine gut ausgebildete Stufe mit $E_{\frac{1}{2}} = -1.4$ V (GKE)[19] ergibt, die in Abwesenheit des Zusatzstoffes (Kurve 6) nicht beobachtet wird. DMPD wird demnach an der Elektrodenoberfläche stärker adsorbiert als die Reduktionsprodukte von SVRS.

Mit Al^{3+} reagiert SVRS in methanolischer Lösung unter Bildung des charakteristischen violett gefärbten Komplexes. Das polarographische Verhalten dieser Mischungen wies gewisse Besonderheiten auf und wurde daher detaillierter untersucht. Wegen der offenkundig vereinfachten Verhältnisse bei Vorliegen nur einer einzelnen Stufe des Komplexbildners wurden die Untersuchungen hauptsächlich mit Lösungen durchgeführt, die—neben den beiden reagierenden Stoffen—zwei Äquivalente Benzoesäure pro Farbstoffmolekül enthielten. Weiterhin wurde festgestellt, dass die Gestalt der Polarogramme von der Gegenwart oder Abwesenheit von DMPD in der Lösung abhängt; die Verhältnisse in diesen beiden Fällen werden daher getrennt diskutiert. Um der Übersichtlichkeit der Darstellung willen werden die in Lösungen mit $2.5 \cdot 10^{-4}$ *M* DMPD erhaltenen Ergebnisse zuerst betrachtet.

Wie im Falle wässriger Lösungen[1,3,4,6] wurde festgestellt, dass die Bildung des Al–SVRS-Komplexes auch in Methanol bei Zimmertemperatur ziemlich langsam erfolgt. Die Kurven in Abb. 2 zeigen den Fortgang der Reaktion zwischen $1 \cdot 10^{-3}$ *M* SVRS und $3 \cdot 10^{-4}$ *M* Al^{3+} im Verlaufe von 24 Stunden. Man sieht, dass die ursprüngliche Stufe des Komplexbildners in zwei Teile aufspaltet, deren Gesamthöhe jedoch praktisch gleich der Höhe der ursprünglichen Stufe bleibt. Zufolge des Halbstufenpotentials und in Analogie mit wässrigen Lösungen[1] entspricht die erste Stufe der

Reduktion des freien, nicht in Reaktion getretenen Farbstoffes. Die um etwa 300 mV zu negativeren Potentialen verschobene zweite Stufe gehört zur Reduktion der Azogruppe im Al-Komplex. Eine dritte Stufe, die den beiden vorhergehenden noch aufgesetzt ist, stellt die gleichzeitige Reduktion des bis dahin nicht in Reaktion getretenen Al^{3+} (vgl. Kurve 6, Abb. 2) und des beim Zerfall des Komplexes infolge Reduktion freigesetzten Al^{3+} dar.

Es ergab sich, dass 24-stündiges Stehen der Lösung bei Raumtemperatur für

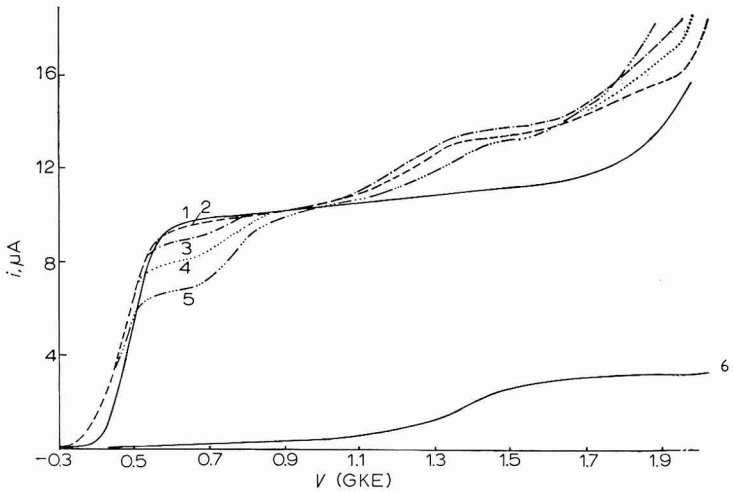

Abb. 2. Polarographische Kurven, die den zeitlichen Ablauf der Reaktion zwischen $1 \cdot 10^{-3}$ *M* SVRS + $2 \cdot 10^{-3}$ *M* Benzoesäure (1) und $3 \cdot 10^{-4}$ *M* Al^{3+} (6) bei Zimmertemperatur anzeigen, jeweils nach: (2), 0.25; (3), 2; (4), 6; (5), 24 Stunden.

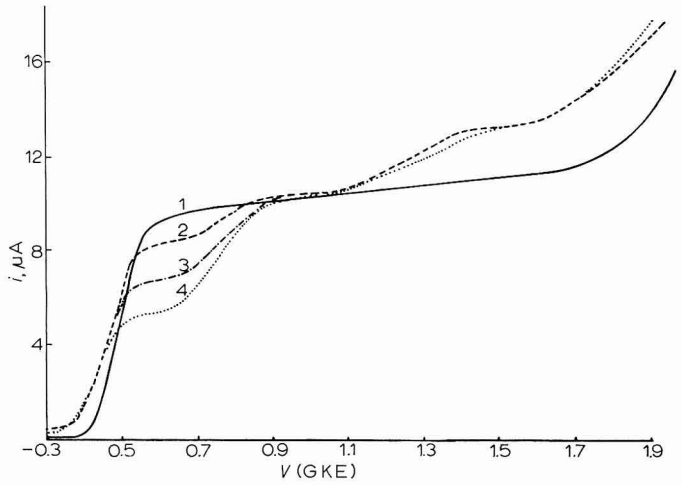

Abb. 3. Polarographische Strom–Spannungs-kurven von: (1), $1 \cdot 10^{-3}$ *M* SVRS + $2 \cdot 10^{-3}$ *M* Benzoesäure + $2.5 \cdot 10^{-4}$ *M* DMPD; (2)–(4), + $3 \cdot 10^{-4}$ *M* Al^{3+} nach 10 Min Erwärmung bei steigenden Temperaturen bis nahe dem Siedepunkt.

den vollständigen Ablauf der Komplexbildung nicht ausreichte. Die Wirkung einer Temperaturerhöhung der Lösung zur Beschleunigung der Reaktion wurde untersucht. Die Kurven der Abb. 3 zeigen den Grad der Komplexbildung nach jeweils 10 Min Erwärmung bei von Kurve 2–4 bis zum Siedepunkt wachsenden Temperaturen. Alle Polarogramme wurden jeweils 60 Min nach der Vermischung der Reagenzien (einschliesslich der Erwärmungszeit) bei Zimmertemperatur registriert. Eine verlängerte Erwärmung der Lösung erbrachte keine weitere Verminderung der Stufenhöhe des freien Farbstoffes. Bei den im folgenden beschriebenen Versuchen wurden die Lösungen daher 15 Min auf 60° erwärmt.

Die Kurven in Abb. 4 zeigen, dass die Verminderung der Stufenhöhe des freien Farbstoffes und die entsprechende Erhöhung derjenigen des Al-Komplexes der Al^{3+}-Konzentration in der Lösung proportional sind, solange ein Überschuss des Komplexbildners vorliegt. Die Bindung zwischen Al^{3+} und SVRS erfolgt in einem Molverhältnis sehr nahe bei 2 SVRS : 1 Al^{3+}; in dieser Hinsicht scheint der in Methanol gebildete Komplex die gleiche Struktur zu haben, wie sie für wässrige Lösungen niedrigen pH-Wertes allgemein angenommen wurde.

Nach PERKINS UND REYNOLDS[4] wird der Al–SVRS-Komplex durch Verdrängung der beiden Protonen der Hydroxylgruppen des Farbstoffes und unter Übernahme eines Elektronenpaares von den Stickstoffatomen der in Resonanz befindlichen Azogruppe gebildet, wodurch sich für Al^{3+} die Koordinationszahl 6 einstellt. Wir formulieren die Reaktion wie folgt:

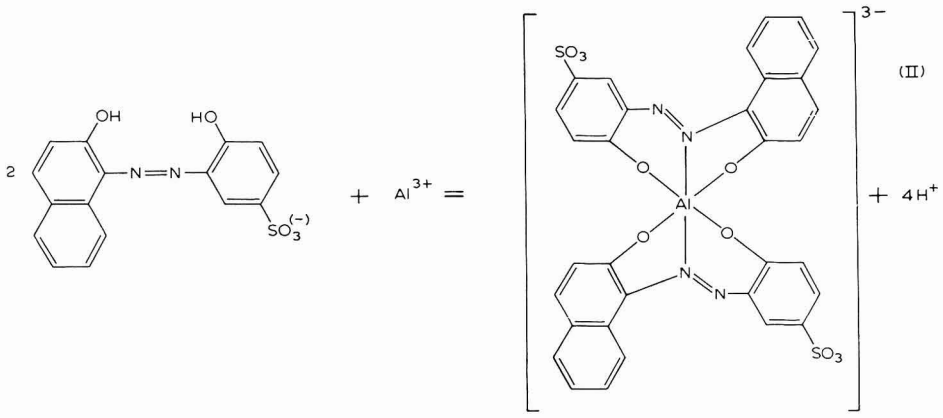

Wie bereits erwähnt, ist mit der Reduktion von SVRS der Bruch der N–N-Bindung unter Bildung der beiden entsprechenden Amine verbunden. Da die Gesamthöhe der in Gegenwart von Al beobachteten zwei Stufen mit der Stufenhöhe von SVRS allein praktisch identisch ist, muss geschlossen werden, dass die Reduktion des Al-Komplexes ebenfalls zur Amin-Stufe erfolgt. Durch diese Zerstörung des komplexbildenden Moleküls wird das Al^{3+} freigesetzt, das—im Gegensatz zu wässrigen Lösungen—im Bereich der dritten Stufe der Kurven in Abb. 4 reduziert wird. Sofern bei Säureüberschuss in Gegenwart von DMPD auch Wasserstoff entladen wird, erfolgt dies ebenfalls im gleichen Potentialbereich bei etwa -1.4 V[19].

Das gleiche Bild, wie oben beschrieben, wird grundsätzlich auch mit DMPD-

freien Lösungen beobachtet. Hier wird jedoch ausserdem eine bei etwa −0.05 V beginnende Vorstufe registriert (Abb. 5), die bei Zimmertemperatur und bei Konstanz aller experimentellen Parameter mit der Reaktionszeit wächst. Bei einer Erwärmung für die Dauer von 15 Min bis nahe dem Siedepunkt ist die Vorstufenhöhe eine lineare Funktion des Al-Gehalts der Lösung. Da das Ausmass der Komplexbildung, gemessen an der Höhe der Al–SVRS-Stufe, praktisch ebenso wie in Gegenwart von DMPD unter sonst gleichen Bedingungen ist, entwickelt sich die Vorstufe offenbar auf Kosten der Stufe des freien Farbstoffes und stellt demnach eine erleichterte Reduktion des letzteren dar.

Die Ursache der Vorstufe ist leicht zu verstehen, wenn man in Betracht zieht,

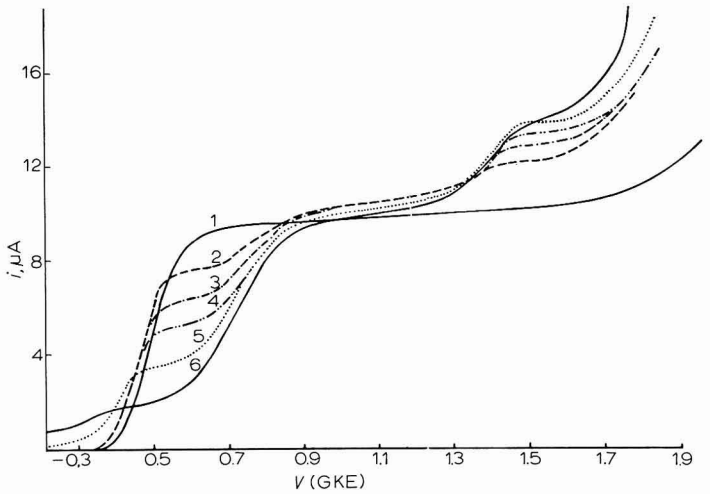

Abb. 4. Polarographische Kurven (der vorerwärmten Lösungen) von $1 \cdot 10^{-3}$ *M* SVRS + $2 \cdot 10^{-3}$ *M* Benzoesäure + $2.5 \cdot 10^{-4}$ *M* DMPD mit: (1), 0; (2), 1.0; (3), 2.0; (4), 3.0; (5), 4.0; (6), $5.0 \cdot 10^{-4}$ *M* Al^{3+}.

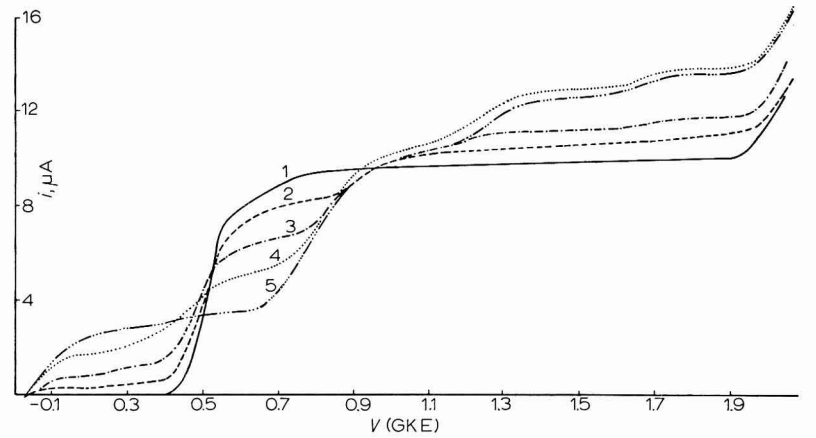

Abb. 5. Wie Abb. 4, jedoch ohne DMPD-Zusatz.

dass bei der Komplexbildung eine entsprechende Menge HCl (Reaktion II) gebildet wird. Diese Säure—stärker als Benzoesäure—verstärkt das Protonenangebot des Mediums und verursacht eine beträchtliche Positivierung des Reduktionspotentials. Dass dies tatsächlich der Fall ist, wurde durch Untersuchungen bewiesen, bei denen HCl anstelle von $AlCl_3$ der Reaktionslösung ($1 \cdot 10^{-3}$ *M* SVRS + $2 \cdot 10^{-3}$ *M* Benzoesäure) zugesetzt wurde. Bei einem Zusatz von $5 \cdot 10^{-4}$ *M* HCl entwickelt sich die Vorstufe bei -0.05 V und ihre Höhe beträgt ein Viertel der ursprünglichen Stufe. Die Höhe der Stufe wächst linear mit der Konzentration der Mineralsäure, bis bei $2 \cdot 10^{-3}$ *M* HCl die Reduktion wieder bei diesem positiven Potential in einer einzigen Stufe erfolgt.

Bemerkenswert ist die Beobachtung, dass die Vorstufe bei einem Zusatz von nur $2.5 \cdot 10^{-4}$ *M* DMPD vollständig verschwindet, wobei stattdessen eine gut ausgebildete zweite Stufe um -1.4 V entsteht. Letztere entspricht der durch den Zusatzstoff katalysierten Wasserstoffentwicklung.

Die obigen Ergebnisse zeigen, dass DMPD, das gewöhnlich als Katalysator für Protonen-Transferprozesse wirkt, in Gegenwart starker Säuren eine inhibierende Wirkung ausübt. Ähnliche Verhältnisse wurden kürzlich bei der Reduktion von Azoxybenzol in methanolischer Lösung[20] beobachtet. Das Verhalten wurde damit erklärt, dass eine Protonen-Übertragung in Gegenwart von DMPD nur über die protonisierte Form des letzteren erfolgt. Wegen des relativ stark basischen Charakters der Dimethylamino-Gruppe ist jedoch zu erwarten, dass der pK_S-Wert der protonisierten Form des DMPD grösser als derjenige der freien starken Säure ist. Infolgedessen kann anstelle einer Katalyse Inhibition erfolgen[20].

Abgesehen von der Entwicklung der Vorstufe auf Kosten der Stufe des freien Farbstoffes, zeigen die Polarogramme von Al–SVRS in Abwesenheit von DMPD qualitativ das gleiche Bild wie in Gegenwart des Zusatzes. Es ist jedoch zu bemerken, dass die katalysierte H^+-Stufe des HCl in Gegenwart von DMPD bei Potentialen auftritt, die mit denjenigen vergleichbar sind, bei denen die Reduktion der Al^{3+}-Ionen erfolgt, die durch die Zerstörung des komplexbildenden Moleküls freigesetzt werden (dritte Stufe der Polarogramme in Abb. 4 und 5), so dass beide Prozesse an der gleichen Stelle in Erscheinung treten. Infolgedessen müsste unter sonst gleichen experimentellen Bedingungen (Konzentration an Al^{3+}, Erwärmungszeit und -temperatur) die in Gegenwart von DMPD beobachtete dritte Stufe grösser sein als die entsprechende in Abwesenheit des Zusatzes. Dass dies tatsächlich der Fall ist, geht aus einem Vergleich der Kurven in Abb. 4 und 5 hervor.

Die polarographische Untersuchung der Komplexbildung in nichtwässriger Lösung—hier am Beispiel des Systems Al^{3+}/Solochrom in Methanol veranschaulicht—bietet beträchtliche Vorzüge gegenüber derjenigen in wässriger Lösung. So gestattet sie ein deutlicheres Verständnis der Rolle, die das H^+-Ion bei der Reduktion des komplexbildenden Agens und/oder seines Metallkomplexes spielt. Solche Effekte lassen sich in wässriger Lösung wegen der Verwendung gepufferter Grundelektrolyte gewöhnlich nicht so klar veranschaulichen. Ausserdem kann die Verwendung geeigneter grenzflächenaktiver Stoffe (Katalysatoren oder Inhibitoren) die Klärung des Elektrodenprozesses und die Aufstellung eines Reaktionsmechanismus erleichtern.

Dem Bundesministerium für Wirtschaft wird für die Unterstützung der Arbeiten gedankt, der Alexander von Humboldt-Stiftung für ein Stipendium (A.M.S.).

ZUSAMMENFASSUNG

Solochromviolett RS (SVRS) wird polarographisch in wasserfreiem Methanol (0.1 *M* LiCl) in drei wohldefinierten diffusionsbestimmten Stufen reduziert. Die Stufen entsprechen der Reduktion der undissozierten, teilweise und vollständig dissoziierten Form des Depolarisators. Die Gesamthöhe der drei Stufen entspricht dem Übergang von vier Elektronen pro Farbstoffmolekül. Zusatz eines Protonendonators (Benzoesäure) bewirkt die Vereinigung der drei Stufen zu einer einzigen, sobald zwei Äquivalente Säure pro Mol Farbstoff in der Lösung vorliegen.

Al^{3+} bildet mit SVRS einen 1 : 2-Komplex. Der an Al^{3+} gebundene Anteil des Farbstoffes wird bei negativeren Potentialen als der nicht gebundene reduziert. Eine dritte Stufe entspricht der Reduktion des bei der Zerstörung des Komplexes freigesetzten Al^{3+} und gegebenenfalls einer zusätzlichen Wasserstoffabscheidung. In Abwesenheit von DMPD entwickelt sich bei positiveren Potentialen eine Vorstufe, die der erleichterten Reduktion von SVRS in Gegenwart der bei der Komplexbildung freigesetzten Säure zugeschrieben wird; DMPD inhibiert die Ausbildung der Vorstufe.

Zusatzstoffe, die als Inhibitoren oder als Katalysatoren von Elektrodenprozessen bzw. -teilprozessen wirksam sind, führen auch hier zu detaillierteren Aussagen über den Reduktionsmechanismus bzw. die Struktur des Depolarisators.

SUMMARY

Solochrome Violet RS (SVRS) is reduced polarographically in anhydrous 0.1 *M* LiCl methanolic solutions in three well-defined, diffusion-controlled waves. The waves are due to the reduction of the undissociated, partially, and totally dissociated forms of the depolarizer. The total height of the three waves corresponds to the transfer of 4 electrons/dye molecule. The addition of a proton donor (benzoic acid) causes the three waves to coalesce into one when two equivalents of acid/equivalent of dye are present in the solution.

Al^{3+} combines with SVRS to form a 1:2 complex. The part of the dye bound to Al^{3+} is reduced at more negative potentials. A third wave represents the reduction of Al^{3+} set free after complex destruction and, in presence of excess acid, also hydrogen evolution. In the absence of DMPD, a prewave develops at more positive potentials and is related to the enhanced reduction of SVRS in the presence of the acid set free during complex formation. DMPD inhibits the development of the prewave.

Additives acting as inhibitors or catalysts of electrode processes (or parts of the latter) prove to be useful also in this case for a more detailed elucidation of reduction mechanisms and the structure of the depolarizer, respectively.

LITERATUR

1 H. H. WILLARD UND J. A. DEAN, *Anal. Chem.*, 22 (1950) 1264.
2 T. M. FLORENCE, F. J. MILLER UND H. E. ZITTEL, *Anal. Chem.*, 38 (1966) 1065.
3 J. A. DEAN UND H. A. BRYAN, *Anal. Chim. Acta*, 16 (1957) 87, 94.
4 M. PERKINS UND G. F. REYNOLDS, *Anal. Chim. Acta*, 18 (1958) 616; 19 (1958) 54, 194.
5 G. F. REYNOLDS, *Z. Anal. Chem.*, 173 (1960) 24.
6 T. M. FLORENCE, *Australian J. Chem.*, 18 (1965) 609.
7 T. M. FLORENCE UND G. H. AYLWARD, *Australian J. Chem.*, 15 (1962) 65.
8 E. SONNTAG, *Kohasz. kapok*, 95 (1962) 523.

9 M. PERKINS UND G. F. REYNOLDS, *Anal. Chim. Acta*, 18 (1958) 625.
10 E. GÖRLICH UND H. PREZEWTOCKA, *Chem. Anal. (Warsaw)*, 6 (1961) 685.
11 E. COATES UND B. RIGG, *Trans. Faraday Soc.*, 58 (1962) 2058.
12 B. A. COONEY UND J. H. SAYLOR, *Anal. Chim. Acta*, 21 (1959) 276.
13 T. M. FLORENCE, *Anal. Chem.*, 34 (1962) 496.
14 T. M. FLORENCE UND D. B. IZARD, *Anal. Chim. Acta*, 25 (1961) 386.
15 L. HOLLECK, A. M. SHAMS EL DIN, R. M. SALEH UND G. HOLLECK, *Z. Naturforsch.*, 19b (1964) 161.
16 L. HOLLECK UND G. HOLLECK, *Polarography 1964, (Proc. 3rd Intern. Congr. Polarog.)*, edited by G. J. HILLS, MacMillan, London, 1966.
17 L. HOLLECK, D. JANNAKOUDAKIS UND A. WILDENAU, *Electrochim. Acta*, 12 (1967) 1523.
18 D. JANNAKOUDAKIS UND A. WILDENAU, *Z. Naturforsch.*, 22b (1967) 118.
19 D. JANNAKOUDAKIS, A. WILDENAU UND L. HOLLECK, *J. Electroanal. Chem.*, 15 (1967) 83.
20 L. HOLLECK UND A. M. SHAMS EL DIN, *Electrochim. Acta*, 13 (1968) 199.

Elsevier Sequoia S.A., Lausanne – Printed in The Netherlands

ADSORPTION BEHAVIOUR OF QUINOLINE, 2- AND 4-METHYLQUINOLINE AT MERCURY–SOLUTION AND AT AIR–SOLUTION INTERFACES

I. ELECTROCAPILLARY CURVES, SURFACE TENSION AND SURFACE POTENTIAL

SILVANO BORDI AND GIORGIO PAPESCHI
Istituto di Chimica fisica, Università di Firenze (Italy)
(Received July 9th, 1968)

Electrocapillary studies on the adsorption of organic compounds at the mercury–solution interface have been carried out by BLOMGREN AND BOCKRIS[1], CONWAY AND BARRADAS[2–4], PARSONS AND PARRY[7], KAGANOVICH AND GEROVICH[8], FRUMKIN AND DAMASKIN[5,6,14], and others*. They obtained very interesting results either in the experimental work or in the theory of the electric double layer with and without adsorbed organic species.

The adsorption of organic molecules on metal interfaces plays a very important part in the action of corrosion inhibitors, electrocrystallization modifiers, and electrode reaction modifiers. Moreover, the change in the adsorption of certain compounds with the concentration and with the electrode charge is of use in understanding their action in several biochemical reactions.

The adsorption on the mercury electrode can be studied easily and quantitatively by measuring the interfacial tension between the electrode and the electrolyte. Furthermore, it is possible to compare the adsorption behaviour of organic molecules on mercury and on solid metal electrodes when the rational electrode potentials[9] are considered.

The use of heterocyclic organic compounds as iron corrosion inhibitors was recently investigated in our laboratory. The results showed that it was necessary to carry out adsorption studies in order to understand the inhibitive effect of certain organic molecules during corrosion reactions.

In the present study the results obtained for neutral aqueous solutions of quinoline, 2-methylquinoline and 4-methylquinoline (π-electron-deficient substances)

TABLE 1

	Dipole moment (μ)	*Ionization constant* (pK_a)
Quinoline	2.20	4.9
2-Methylquinoline	1.95	5.4
4-Methylquinoline	2.52	5.2

*We are indebted to our colleague, Dr. F. Pratesi, for translations of the Russian papers.

are presented and discussed. Table 1 gives the dipole moments and the pK_a-values[10] of the organic molecules considered.

The interfacial tension, γ_{Hg}, of the mercury–solution interface was measured as a function of potential and organic species concentration using 1 N KNO_3 as the supporting electrolyte.

The surface tension, γ, and the surface potential, ΔV, were obtained in the same concentration range and provided information concerning the adsorption behaviour at the free surface of the aqueous solutions.

EXPERIMENTAL

A. Mercury–solution interface

Capillary electrometer. A modified Lippmann electrometer was designed and built. With this apparatus (see Fig. 1) the interfacial tension was determined from the depression on the mercury in contact with the solution in a Pyrex glass capillary of the capillary electrometer.

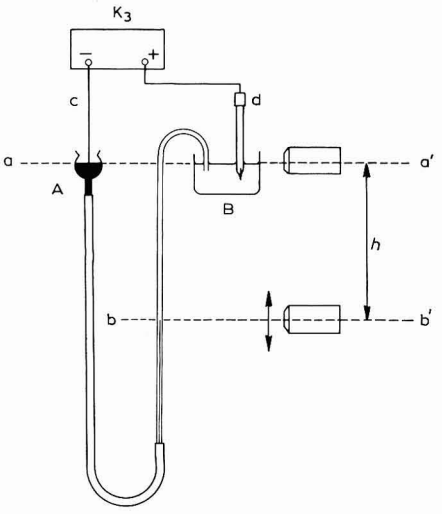

Fig. 1. Capillary electrometer.

The difference in level, h, (Fig. 1) was measured precisely. The level a–a' was in the same plane as the mercury surface in reservoir A and the solution surface in cell B. The level b–b' was in the plane through the mercury meniscus in the capillary. In order to obtain the best precision, two parallel microscope systems were used: one aimed at the level a–a', the other at the level b–b'. The distance between the two microscopes was varied using a high precision screw, and all distances, h, between the two levels were measured with an accuracy of 0.001 cm.

The negative electrode (c) consisted of a Pt wire in contact with the mercury in reservoir A. A normal calomel electrode (d) was used for all experiments and was immersed in the test solution. The electric contact between the normal calomel electrode

and the solution was secured through a very narrow asbestos bridge sealed into the glass at the tip of the electrode.

Procedure. The cell and auxiliary glassware were cleaned with a chromic–sulphuric cleaning solution and washed with triply-distilled water; they were then placed in a hot steam jet and washed again before using, with fresh triply-distilled water. Oxygen-free nitrogen was bubbled through the solution in the cell after which the capillary was placed in the solution. Reservoir A was moved upward until mercury drops were discharged from the capillary and when reservoir A was lowered the solution entered the capillary. At this point the normal calomel electrode was placed in the electrometer cell. When the mercury A and solution B levels were on the same plane, the position of the meniscus in the capillary at different polarization values was determined.

TABLE 2

Interfacial tension				*Interfacial tension*			
E_{NCE} (*V*)	KNO_3 1 *N* this work (dyn cm^{-1})	KNO_3 1 *N* Craxford and McKay (dyn cm^{-1})	Δ	E_{NCE} (*V*)	KNO_3 1 *N* this work (dyn cm^{-1})	KNO_3 1 *N* Craxford and McKay (dyn cm^{-1})	Δ
0	375.72	—		0.7	418.24	418.2	0
	383.10	—			415.65	415.7	−0.2
0.1	389.94	—		0.8	412.53	412.7	−0.2
	396.03	396.2	−0.2		408.80	409.0	−0.2
0.2	401.50	401.5	0	0.9	404.62	404.7	−0.1
	406.45	406.4	0		399.98	400.1	−0.1
0.3	410.48	410.4	+0.1	1.0	394.66	394.7	0
	414.21	414.0	+0.2		388.73	—	
0.4	416.94	416.8	+0.1	1.1	382.41	—	
	419.07	419.1	0		375.72	—	
0.5	420.59	420.5	+0.1	1.2	368.72	—	
	421.43	421.2	+0.2		361.19	—	
0.6	421.28	421.1	+0.2	1.3	353.44	—	
	420.14	420.2	−0.1				

The polarizing circuit was of the potentiometric type, and all potentials were measured with a Leeds and Northrup K3 potentiometer to ±0.01 mV. The range of potentials, 0–1100 mV, was traversed at 50-mV intervals. In this range the organic substances were electro-inactive as verified with polarograms performed from +100 to −1300 mV *vs.* NCE.

The electrometer was calibrated first with 1 *N* KNO_3 assuming the electrocapillary maximum to be 421.2 dyn cm^{-1} as found by CRAXFORD AND MCKAY[11]. The results obtained in several runs were found to be reproducible to ±0.2 dyn cm^{-1} along the entire range of the electrocapillary curves. In Table 2 our values for 1 *N* KNO_3 are compared with the values of CRAXFORD AND MCKAY.

B. Air–solution interface

Tensiometer. The surface tension of the air–solution interface was measured at constant temperature as a function of concentration of quinoline, 2- and 4-methylquinoline with a DuNouy tensiometer. n-Hexane ($\gamma = 18.4$) and chlorobenzene ($\gamma = 33.2$) were used to calibrate the tensiometer.

Surface potential apparatus. The surface potential at the air–solution interface was measured as a function of the concentration of quinoline, 2- and 4-methylquinoline by the ionizing electrode method. The radioactive source was ^{241}Am (half life of 458 years) which emits only α-radiation and the intensity of which was 0.5 mcurie.

The difference in potential across the reference calomel electrode and a gold electrode placed between the radioactive source and the solution surface was measured with a Keithley 602 electrometer of input impedance above $10^{14}\ \Omega$.

MATERIALS

Mercury was purified by treatment with hot concentrated NaOH solution followed by washing in triply-distilled water and distillation in an all-Pyrex glass apparatus under 18 mm Hg pressure. It was then passed many times through diluted (5%) HNO_3 solution in a long glass tube. Finally, it was redistilled after a further washing with triply-distilled water.

Distilled water was twice distilled over alkaline permanganate in a Pyrex glass apparatus, the final distillation being carried out in two interconnected glass stills where oxygen-free nitrogen bubbled during ebullition. The conductivity of the water obtained was $0.6 \cdot 10^{-6}\ \Omega^{-1}\ cm^{-1}$. All solutions were prepared from this water.

Merck's G.R. quality KNO_3 was used without further purification. Fluka's AG.Buchs S.G. quality quinoline, 2- and 4-methylquinoline was distilled at atmospheric pressure. The purified substances boiled (760 mm Hg) at 236, 246 and 262°, respectively.

RESULTS

A. Electrocapillary curves

The electrocapillary curves were obtained at $19 \pm 1°$ in 1 N KNO_3 with quinoline, 2- and 4-methylquinoline added to obtain various concentrations ranging from 0.1 to 30 mM for quinoline, and from 0.05 to 9 mM for the other two substances. The ranges were limited by the low solubility of the compounds.

The electrocapillary curves show that the quinoline, 2- and 4-methylquinoline are strongly adsorbed on the mercury. The alternative plots of the lowering of the interfacial tension, $\Delta\gamma_{Hg}$, *vs.* E (Figs. 2, 3, 4) as a function of the concentration are more significant and very clearly illustrate a similar adsorption behaviour for the three organic species.

On the assumption that this adsorption was reversible, the Gibbs equation may be used to calculate the surface excess:

$$\Gamma = -\frac{1}{2.303\,RT}\left(\frac{\Delta\gamma_{Hg}}{\Delta \log c}\right)_{E,T}$$

where Γ is the surface excess, R the gas constant, T the absolute temperature, γ_{Hg} the interfacial tension and c the concentration.

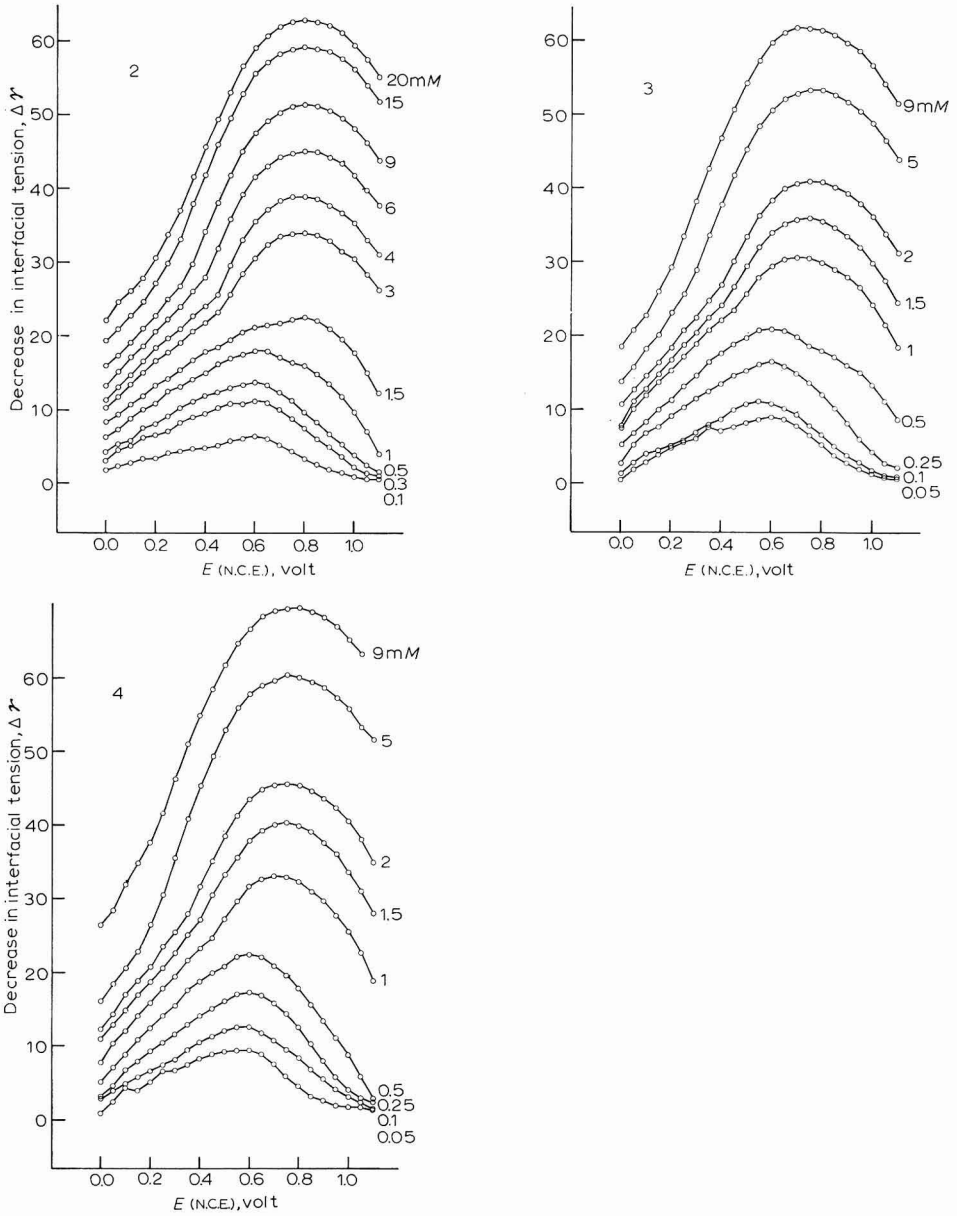

Figs. 2–4. Dependence of $\Delta\gamma$ upon the potential, E (NCE) at different concn., c (mM). (2), quinoline; (3), 2-methylquinoline; (4), 4-methylquinoline.

Smooth curves were drawn through γ–log c coordinates and the quantities $(\Delta\gamma_{Hg}/\log c)_E$ were evaluated graphically.

In Figs. 5, 6 and 7 the surface excess is plotted against the concentration at different values of E. For quinoline, 2- and 4-methylquinoline, the values of Γ_{max} were found to be $6.5 \cdot 10^{-10}$, $6.09 \cdot 10^{-10}$ and $6.57 \cdot 10^{-10}$ mole cm^{-2}, respectively.

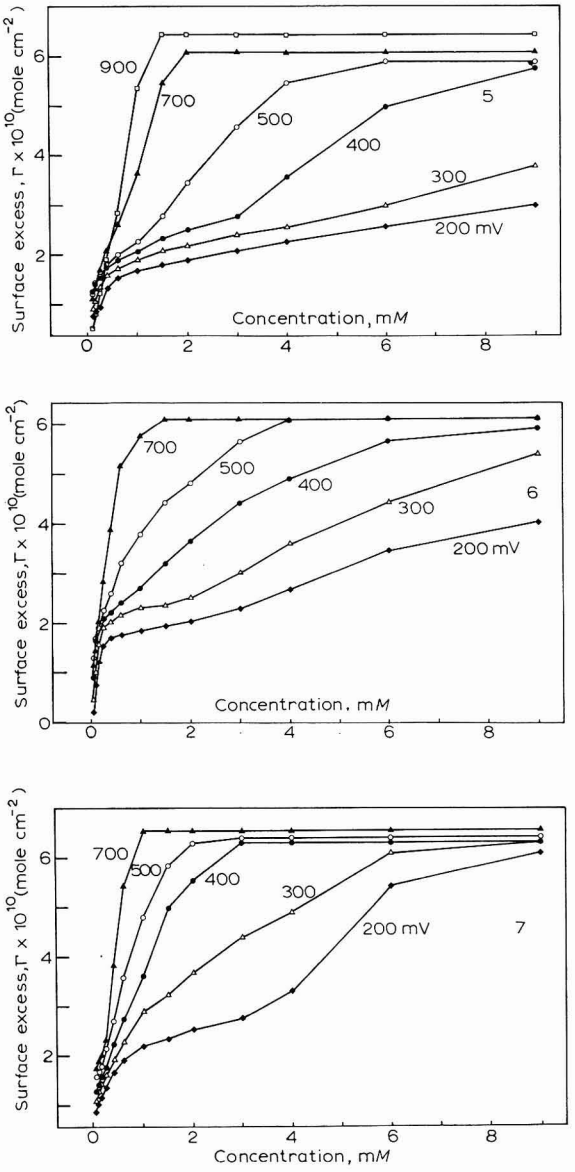

Figs. 5–7 Dependence of surface excess upon the concn. in the presence of 1 *N* KNO_3 at different *E* (NCE). (5), quinoline; (6), 2-methylquinoline; (7), 4-methylquinoline.

B. Surface tension

Surface tension values determined as a function of concentration by the ring method at a constant temperature of 18.0° are shown in Fig. 8 for quinoline, 2- and 4-methylquinoline. All solutions contained 1 *N* KNO_3 as supporting electrolyte.

The surface excess (Fig. 9b) at the air–solution interface was obtained as before by a graphical method using the Gibbs adsorption equation.

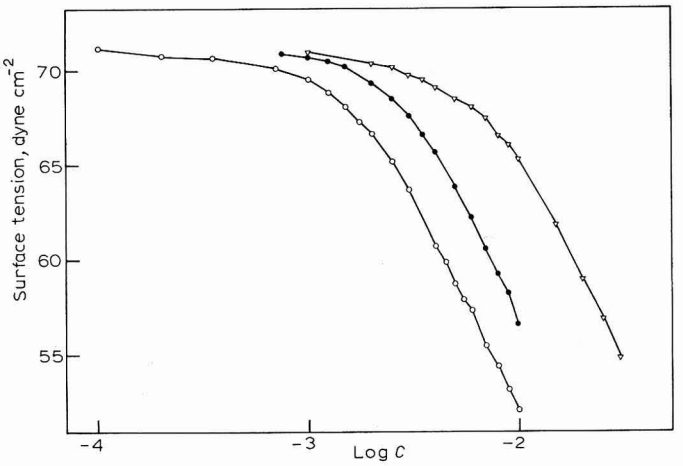

Fig. 8. Surface tension as function of log (concn.) for: (▽), quinoline; (●), 2-methylquinoline; (○), 4-methylquinoline in the presence of 1 N KNO_3.

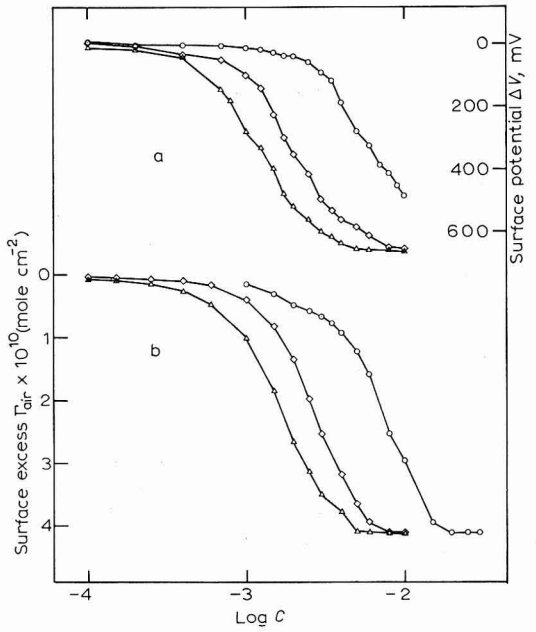

Fig. 9. (a), Surface potential, ΔV (mV); (b), surface excess Γ (mole cm^{-2} · 10^{-10}) for: (○) quinoline; (◇), 2-methylquinoline; (△) 4-methylquinoline *vs.* log (concn.). All solns. contained 1 N KNO_3.

C. Surface potential

Several runs of surface potential measurements on aqueous solutions of quinoline, 2- and 4-methylquinoline using 1 N KNO_3 as supporting electrolyte were carried out in the same concentration ranges and at a room temperature of 18–19°. Good reproducibility was obtained, and Fig. 9a shows a plot of surface potential *vs.* log c for the compounds tested.

DISCUSSION

The experimental results show a strong adsorption of quinoline, 2- and 4-methylquinoline at the mercury–solution and air–solution interfaces.

The shape of electrocapillary curves shows that this adsorption, when 1 N KNO_3 is used as the supporting electrolyte, leads to a large shift in the point of zero charge in the direction of more positive potentials ($\Delta E = 270$, 320 and 330 mV for quinoline, 2- and 4-methylquinoline, respectively); the lowering of the interfacial tension, $\Delta\gamma_{Hg}$, is 51.3 dyn cm^{-1} for quinoline, 62.0 dyn cm^{-1} for 2-methylquinoline and 69.3 dyn cm^{-1} for 4-methylquinoline (9 mM is the maximum concentration considered).

A more detailed examination leads to the result that for low concentrations, the shift of p.z.c. is slight since the lowering of the curves is nearly the same on anodic and cathodic sides. As the concentration is increased, the values of ΔE increase rapidly whereas the interfacial tension lowering becomes larger on the descending branch than on the ascending branch of the electrocapillary curves.

In order to represent this phenomenon more clearly it is convenient to consider the interfacial tension lowering, $\Delta\gamma_{Hg}$, as a function of the potential for different values of the concentration (Figs. 2, 3, 4).

Let us consider for simplicity, and discuss in particular, the case of quinoline. Only slight differences for the values of $\Delta\gamma_{Hg}$ and E can be found for the other substances, while the general behaviour is quite similar.

It can be seen from Fig. 2 that two families of curves of parabolic form are obtained from the experimental data. The curves of the first family, for low concentrations, have their maxima near the value of E_{max}. The curves of the second family have their maxima shifted 200 mV towards negative potentials, and are those for concentrations above about 1 mM. We can assume for the moment that this behaviour correlates to an adsorbate reorientation related to the concentration.

Figure 10 (related to 4-methylquinoline) shows that the lower the concentration, the more negative the potential at which the organic molecules undergo reorientation. Therefore, the change in the molecular orientation at the mercury solution interface depends on the concentration and is controlled by the potential.

The Γ/c curves at different potentials given in Figs. 5, 6 and 7 have an unusual shape. At low negative potentials a plateau is observed near $2.4–2.5 \cdot 10^{-10}$ mole cm^{-2}. As the concentration increases and the potential becomes more negative, this plateau disappears and a second plateau is formed at $6.6 \cdot 10^{-10}$ for quinoline and 4-methylquinoline, and at $6.1 \cdot 10^{-10}$ mole cm^{-2} for 2-methylquinoline.

The values of surface excess corresponding to the two plateaux and the relative molecular areas are shown in Table 3 for all three compounds.

The value of $2.4–2.5 \cdot 10^{-10}$ mole cm^{-2} corresponds to a molecular area of 65–68 $Å^2$, and the value of $6.1–6.6 \cdot 10^{-10}$ mole cm^{-2} to a molecular area of 25.1–27.1 $Å^2$.

The areas occupied by a quinoline molecule were estimated by BLOMGREN AND BOCKRIS[1] from molecular models to be 25 $Å^2$ if vertically oriented, and 60$Å^2$ when arranged in a planar position.

On the basis of the experimental results it is possible to explain the adsorption behaviour of quinoline and its methyl derivatives as follows.

In dilute solutions the adsorbed molecules are arranged with the plane of the ring parallel to the mercury surface when the mercury charge is positive or negative, *i.e.*, for low concentrations the organic molecules interact with the metallic phase mainly by way of π-electrons: the complete disappearance of adsorption occurs when the mercury surface assumes a sufficiently negative charge.

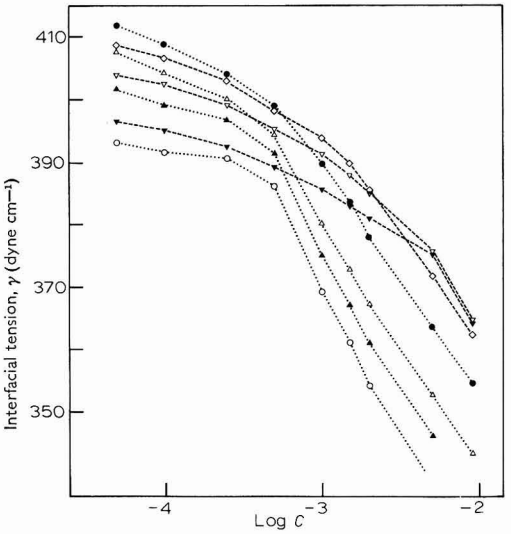

Fig. 10. Effect of 4-methylquinoline concn. on the interfacial tension at different values of E (NCE): (▼), 200; (▽), 300; (◇), 400; (●), 600; (△), 800; (▲), 900; (○), 1000 mV.

TABLE 3

	$\Gamma_{max} \cdot 10^{-10}$ mole cm^{-2}		Å^2/molecule	
	Planar	*Vertical*	*Planar*	*Vertical*
Quinoline	2.5	6.6	65	25.1
2-Methylquinoline	2.4	6.1	68	27.1
4-Methylquinoline	2.5	6.6	65	25.1
Quinoline[1]	2.8	6.5	60	25

A monolayer with the molecules lying flat is formed at $\Gamma = 2.4\text{–}2.5 \cdot 10^{-10}$ mole cm^{-2} and accounts for the first step in the isotherms.

When the concentration exceeds a certain value which is slightly different for each of the three compounds, along the ascending branch of the electrocapillary curves (where the mercury charge is positive) the interaction between π-electrons and metallic surface is strong enough so that the organic molecules lie flat in the adsorbed monolayer. As the positive charge on the mercury is reduced, however, and along the descending branch where the mercury side of the interface acquires an increasingly larger negative charge, the orientation of the organic molecules will change either because of the weakening of the π-bond interaction with the mercury, or because of the interaction of the dipole moment with the charged metal.

A closely-packed film with the molecules vertically oriented is achieved when the surface excess attains the value of $6.1\text{–}6.6 \cdot 10^{-10}$ mole cm^{-2} (Table 3).

The shift of the point of zero charge *vs.* the logarithm of the concentration of the surface active substances is given in Fig. 11a and the change of the p.z.c. shift with the surface excess, $\Gamma_{Hg}^{(e=0)}$, is given in Fig. 12. The first plot shows that a sudden

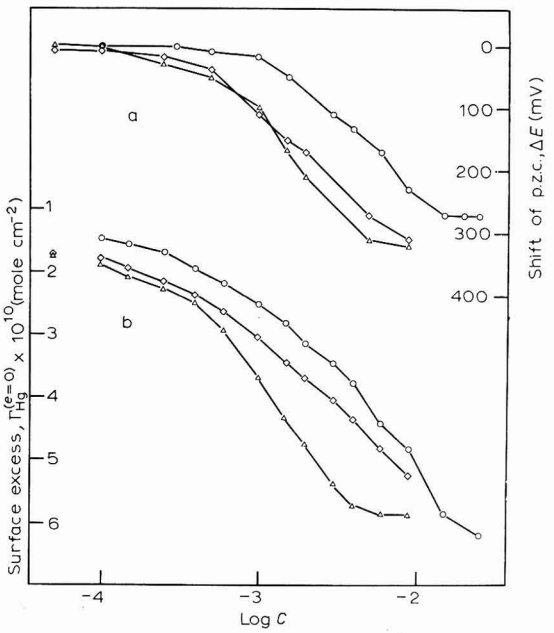

Fig. 11. (a), Shift of p.z.c., ΔE (mV); (b) surface excess $\Gamma_{Hg}^{(e=0)}$ (mole cm$^{-2}\cdot 10^{-10}$) for (○), quinoline; (◇), 2 methylquinoline; (△), 4-methylquinoline *vs.* log (concn.). All solns. contained 1 *N* KNO_3.

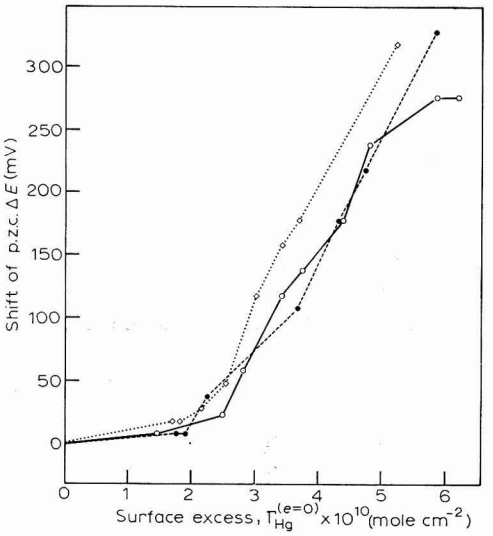

Fig. 12. Dependence of the shift of the p.z.c. upon the surface excess at the mercury–solution interface. (○), quinoline; (◇), 2-methylquinoline; (●), 4-methylquinoline.

increase occurs in the change of p.z.c. potential at about 1 mM for quinoline and a few tenths of a mM less for the other two compounds. Many authors consider that this abrupt change is due to new molecular orientation subsequent to the increase in concentration[2,4]. The plots of Fig. 12 show that a critical surface concentration exists at which the p.z.c. shift value rises sharply. After this point (about $2.5 \cdot 10^{-10}$ mole cm^{-2}), ΔE increases.

A comparison between the data obtained for the three heterocyclic compounds shows that there are slight differences in their adsorption at the mercury–solution interface. The deviations noted can be related to :

(i) the different π-electron density due to the different position of the methyl group in the heterocyclic ring;

(ii) the different dipole moments;

(iii) the presence in the 2- and 4-methylquinoline molecule of the hydrophobic methyl group which makes their adsorption greater than that of quinoline.

Information on the adsorption behaviour of quinoline, 2-and 4-methylquinoline at the air–solution interfaces was obtained from the surface tension (γ_{air}) and the surface potential (ΔV) data.

In Fig. 8 are given the changes in the surface tension of these substances with varying log (concentration) and in Fig. 9b are shown the respective adsorption isotherms (*vs.* log c). The maximum value of Γ ($=4.1 \cdot 10^{-10}$ mole cm^{-2}, which is the same for all three compounds considered) corresponds to a molecular area of about 40 Å^2. This value is 10–15 Å^2 larger than that found for the same substances at the mercury–solution interface, but it is consistent, according to FOWKES[12], if we consider that there is one water molecule (10 Å^2) for every organic molecule in the adsorbed surface monolayer.

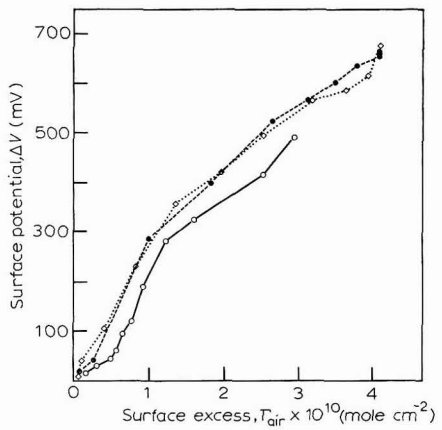

Fig. 13. Dependence of the surface potential upon the surface excess at the air–solution interface. (○), quinoline; (◇), 2-methylquinoline; (●), 4-methylquinoline.

It is of particular significance that the shapes of the Γ_{air}/log c and ΔV/log c curves are similar (Fig. 9a,b). The dependence of the surface potential, ΔV, upon the surface excess, Γ_{air}, at the air–solution interface is shown in Fig. 13 and is linear to the first approximation. A similar dependence has been found by FRUMKIN[8,13]

for saturated aliphatic compounds, like butylamine and n-propylalcohol, at the air–solution interface.

When mercury is polarized at the electrocapillary maximum potential, it may be supposed that the mercury–solution interface is an uncharged interface ($q=0$). On this assumption, a comparison is made between the behaviour of the molecular adsorption at the air–solution and at the uncharged mercury–solution interface. The surface excess, Γ_{air} and $\Gamma_{Hg}^{(e=0)}$, respectively, are plotted in Figs. 9 and 11b *vs.* log (concentration). Table 4 shows the value of the limiting adsorption for the two interfaces and the relatively molecular areas.

TABLE 4

	Mercury–solution		*Air–solution*	
	$\Gamma_{Hg}^{(e=0)} \cdot 10^{-10}$ *(mole cm^{-2})*	*Å^2/ molecule*	$\Gamma_{Hg}^{(e=0)} \cdot 10^{10}$ *(mole cm^{-2})*	*Å^2/ molecule*
Quinoline	6.2	26.6	4.1	40.2
2-Methylquinoline	5.3	31.1	4.1	40.2
4-Methylquinoline	5.9	27.9	4.1	40.2

It is evident that the adsorption behaviour at the two interfaces shows some differences. Generally speaking, the surface activity of the quinoline and methylderivatives at the interface with mercury is somewhat higher than at the interface with air. Furthermore it should be noted that the organic molecules adsorb on the metal only after displacing solvent molecules from the interface. Thus a closely-packed film of the surface-active substances without water molecules is formed on the mercury, whereas at the air–solution interface organic molecules and water dipoles are in a ratio of 1:1 in the adsorption film. The stronger adsorption energy of the organic species on the metal can be due to a sort of image energy which does not exist at the solution free surface, and it can be favoured by a van der Waals interaction between the adsorbed molecules and the mercury. Moreover, the bond between the metal phase and the π-electrons of the aromatic ring, which can even alter the molecular setting during the adsorption, is not observable at the air–solution interface.

In this paper we have referred only to the experimental results on the adsorption behaviour at two different interfaces of some heterocyclic surface-active substances. A detailed investigation of some interesting aspects of the adsorption behaviour observed during this study will be the subject of a subsequent report.

ACKNOWLEDGEMENTS

Part of the experimental work was performed by us in the Department of Chemistry at Kent State University (U.S.A.), and we should like to express our thanks to Professor R. R. MYERS (Chairman) for laboratory facilities and for his interest in this work. We gratefully acknowledge help and advice from Professor R. J. RUCH.

We are also indebted to the C.N.R. of Italy for the award of a maintenance grant in the U.S.A. during the tenure of which part of this research was carried out.

We wish to thank Dr. R. PARSONS (University of Bristol, England) for helpful discussion on the subject of this paper during his recent visit to our laboratories.

SUMMARY

A modified Lippmann electrometer was designed and built and used to obtain electrocapillary curves by varying the concentration of aqueous solutions of quinoline, 2-methylquinoline and 4-methylquinoline using 1 N KNO_3 as supporting electrolyte.

Measurements of surface tension, with the ring method, and surface potential, with the ionizing method, were obtained over the same concentration range at the free solution surface.

Comparison was made in terms of the surface excess and the molecular area, between the adsorption behaviour of the organic species at the mercury–solution and air–solution interfaces.

REFERENCES

1 E. Blomgren and J. O'M. Bockris, *J. Phys. Chem.*, 63 (1959) 1475.
2 B. E. Conway and R. G. Barradas, *Electrochim. Acta*, 5 (1961) 319.
3 B. E. Conway, R. G. Barradas, P. G. Hamilton and J. M. Parry, *J. Electroanal. Chem.*, 10 (1965) 485.
4 R. G. Barradas and P. G. Hamilton, *Can. J. Chem.*, 43 (1965) 2468.
5 A. N. Frumkin, R. I. Kaganovich and E. Bit Popova, *Dokl. Akad. Nauk SSSR*, 141 (1961) 670.
6 A. N. Frumkin and B. B. Damaskin, *International Congress of Polarography, London*, Butterworths, London, 1967.
7 J. Parry and R. Parsons, *J. Electrochem. Soc.*, 113 (1966) 992.
8 R. I. Kaganovich and V. M. Gerovich, *Elektrokhimiya*, 2 (1966) 977.
9 D. C. Grahame, *Chem. Rev.*, 41 (1947) 441.
10 A. Albert, *Heterocyclic Chemistry*, University of London, The Athlone Press, London, 1959. A. L. McClellan, *Tables of Experimental Dipole Moment*, W. H. Freeman, San Francisco, London, 1963.
11 S. R. Craxford and A. C. McKay, *J. Phys. Chem.*, 39 (1935) 545.
12 F. M. Fowkes, *J. Phys. Chem.*, 66 (1962) 385.
13 A. N. Frumkin, B. B. Damaskin and A. A. Survila, *Electrokhimiya*, 1 (1965) 738.
14 A. N. Frumkin and B. B. Damaskin, *Modern Aspects of Electrochemistry*, Vol. III, edited by J. O'M. Bockris and B. E. Conway, Butterworths, London, 1964.

ELECTROANALYTICAL CHEMISTRY AND INTERFACIAL ELECTROCHEMISTRY
Elsevier Sequoia S.A., Lausanne – Printed in The Netherlands

POLAROGRAPHIC, CONDUCTOMETRIC AND POTENTIOMETRIC STUDIES ON POLYETHYLENEIMINE

T. M. H. SABER AND A. M. SHAMS EL DIN
Laboratory of Electrochemistry and Corrosion, National Research Centre, Dokki, Cairo (U.A.R.)
(Received July 15th, 1968)

INTRODUCTION

The effect of variations in the concentration of gelatin on the polarographic hydrogen wave of sulphuric acid in lithium sulphate was recently studied[1]. In minute amounts ($\simeq 1 \cdot 10^{-3}$ wt-%) the additive suppressed the maximum of the wave completely without, however, affecting its reduction potential. As the concentration of gelatin was raised, the entire wave shifted, first towards more positive potentials (catalysis) and then back to cathodic potentials (inhibition). In the region of inhibition, another maximum of somewhat peculiar characteristics appeared[1], and the limiting diffusion current progressively decreased with increase in additive concentration[1,2]. A mechanism accounting for these observations was proposed based on protonation of the nitrogen groupings of the additive.

However, owing to the complex chemical structure of gelatin, a quantitative treatment of the results was rather difficult. Also, the decrease in the limiting current of the hydrogen wave with increased additive concentration is expected to depend on the type and purity of the gelatin sample used. It was, therefore, of interest to establish whether the effects described above for gelatin could also be obtained with other polymeric nitrogen-containing substances of definite molecular structure. A study of the surface-active properties of polyethyleneimine (PEI), $-[-CH_2CH_2NH-]_{\overline{n}}$, was undertaken, from which it appeared that not all the imino-groupings of the additive function catalytically. Distinction could be made between weakly protonated, catalytically-active groups, on one hand, and strongly protonated, catalytically-inactive groups, on the other. The two types are present in a ratio of *ca.* 1:1. The same conclusion was also reached from conductometric and potentiometric measurements. The study establishes also the feasibility of the polarographic technique for studying certain properties of polyelectrolytes in solution which as far as we are aware, has not yet been attempted.

EXPERIMENTAL

The polyethyleneimine (PEI) used was supplied by The Chemirad Corp. (New Jersey, U.S.A.) as an aqueous solution containing *ca.* 50 wt-% active material. Elemental chemical analysis showed it to contain 54 wt-% of PEI. The polymer had an average molecular weight of 30000 (suppliers information) corresponding to $n \simeq 700$

in $-[-CH_2CH_2NH-]_{\overline{n}}$. A stock solution of 0.054 *M* PEI was prepared by analytical dilution, molarity being calculated on the basis of the monomer unit.

The effect of PEI on the hydrogen wave of sulphuric acid, and forward and backward amperometric titration of the acid with the imine, were carried out in a supporting electrolyte of 0.16 *M* sodium sulphate. Polarograms were recorded on a type PO 3h Radiometer Polarograph at appropriate sensitivity. All solutions were de-aerated by bubbling a stream of purified hydrogen gas through them for *ca.* 15 min before tracing the polarograms. Measurements were carried out at room temperature, 23–25°.

The conductivity of PEI–H_2SO_4 mixtures of different compositions was measured on a Leeds and Northrup, Jones-type conductivity bridge connected with a Radiometer Oscilloscope (OSG 41 a) as a null-point detector. Conductivity measurements were carried out at 25 ± 0.001°; conductivity water was used in the preparation of the solutions.

PEI in 0.16 *M* sodium sulphate solutions was also titrated potentiometrically

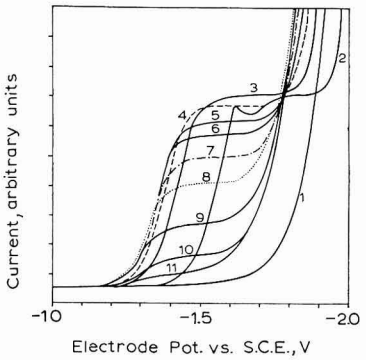

Fig. 1. Effect of PEI additions on the hydrogen wave of $1.92 \cdot 10^{-3}$ *N* H_2SO_4 in 0.16 Na_2SO_4. (1), Supporting electrolyte + $1.08 \cdot 10^{-4}$ *N* PEI; (2), 0; (3), $1.08 \cdot 10^{-4}$; (4) $2.16 \cdot 10^{-4}$; (5), $4.32 \cdot 10^{-4}$; (6), $6.48 \cdot 10^{-4}$; (7), $1.08 \cdot 10^{-3}$; (8), $1.51 \cdot 10^{-3}$; (9), $2.16 \cdot 10^{-3}$; (10), $2.59 \cdot 10^{-3}$; (11), $3.02 \cdot 10^{-3}$ *N* PEI.

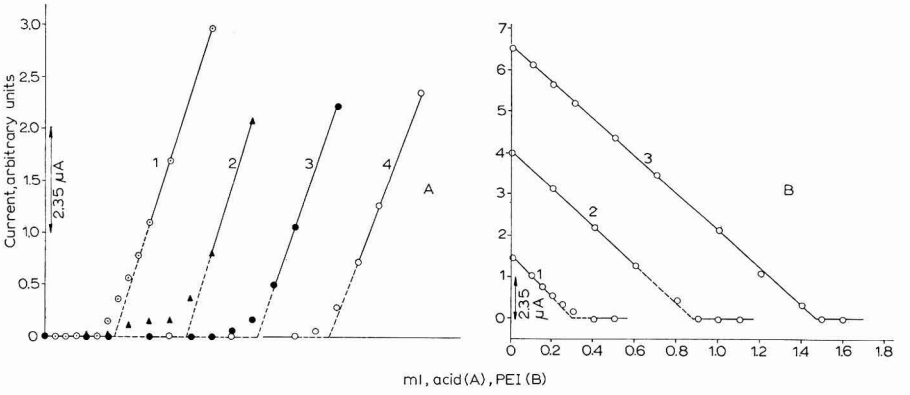

Fig. 2. Amperometric forward (A) and backward (B) titration of PEI (0.054 *N*) with H_2SO_4 (0.0192 *N*). (A). (1), 0.5; (2), 1.0; (3), 1.5; (4), 2.0 ml PEI/25 ml soln. (B). (1), 0.5; (2), 1.5; (3), 2.5 ml H_2SO_4/25 ml soln.

against sulphuric acid. A Metrohm pH-meter type E 353 and a combined glass electrode were used to follow the titration.

Most of the amperometric and all conductometric and potentiometric titrations were carried out at constant volumes. Quantities of the two reactants were mixed and diluted to a definite volume with water. Portions of these solutions were then used to measure the electrical property searched. Series B of the amperometric titration experiments (Fig. 2), however, were carried out by adding portions of the acid to known volumes (10 ml) of PEI–Na_2SO_4 solutions. Corrections for the added volumes were made according to standard procedures[3].

RESULTS AND DISCUSSIONS

A well-developed, diffusion-controlled hydrogen wave is recorded in a solution of composition: 0.16 *M* Na_2SO_4 + $1.92 \cdot 10^{-3}$ *N* H_2SO_4 Fig. 1, (curve 2). The wave is preceded by a small maximum which is easily suppressed by PEI. With the smallest addition of the compound ($1.08 \cdot 10^{-4}$ *N* PEI) the maximum is completely eliminated and the reduction wave shifts, as a whole, *ca.* 120 mV towards positive potentials (Fig. 1, curve 3). Apparently, the additive exerts a catalytic action on the proton discharge reaction. Higher concentrations of PEI shift the wave further towards less negative values but induce, at the same time, a decrease in the limiting current which is linearly proportional to the additive concentration. The hydrogen wave completely disappears when the solution is $3.024 \cdot 10^{-3}$ *N* with respect to PEI. The decrease in the height of the hydrogen wave is not due to a corresponding increase in the bulk viscosity of the solution as more polymer is added. This was ascertained by titrating a solution of $4.32 \cdot 10^{-3}$ *N* PEI in 0.16 *M* Na_2SO_4 with 0.0192 *N* H_2SO_4 in an Ubbelohde 3-bulb viscometer. No detectable change in the solution viscosity was measured.

The catalytic effect of N-containing organic compounds is related to the readiness with which a free proton in solution adds to the lone pair of electrons of the nitrogen atom to form the protonated form, BH^+ (B is the catalyst molecule). The reduction of BH^+ adsorbed on the electrode surface by a sequence of reactions such as[4,5]:

$$B_{ads} + H^+ \rightarrow BH_{ads}^+$$

$$BH_{ads}^+ + e^- \rightarrow BH_{ads} \rightarrow B_{ads} + \tfrac{1}{2}H_2$$

is said to be easier than that of the free proton, H_3O^+, and leads to a decrease in the overpotential necessary for the evolution of hydrogen. The magnitude of the catalytic effect depends upon both the adsorbability and acid strength of the cation[5], BH^+.

The catalytic effect of PEI has certain interesting features. Thus, irrespective of the decrease in the limiting current of the hydrogen wave, the displacement of its half-wave potential towards positive values increases asymptotically with the concentration of the additive. In this respect PEI differs from gelatin[1] where catalysis attained its maximum value in a solution $8.0 \cdot 10^{-3}$ wt-% with respect to the additive. Above this concentration, there was inhibition and the wave moved once again towards negative potentials. Also, judging by the extent of wave displacement towards positive potentials PEI is a stronger catalyst than gelatin for the evolution of hydrogen. This difference is evidently due to the smaller molecular volume and higher basicity of PEI and probably also stronger adsorbability. As with gelatin, the decrease in the limiting current of the hydrogen wave on addition of PEI indicates that part of the

reducible protons are masked and transformed into a polarographically-inactive form. Here, however, the decrease is directly proportional to the additive concentration which suggests that this property can be applied for the amperometric determination of PEI in solution. In Fig. 2 curves are given representing both the "forward (A)" and "backward (B)" titration of the acid by the imine. Both sets of curves show reasonably sharp equivalence points which are directly proportional to the concentration of PEI (acid) in solution thus strongly recommending the amperometric technique for the rapid analysis of PEI solutions.

In addition, the curves of Fig. 1 show that although PEI combines with the acid to yield a polarographically-non-reducible species (*i.e.*, in which the protons are no longer free) the latter is responsible for catalyzing the discharge of the remaining part of the acid. Since catalysis involves the labile exchange of protons between the solution and the additive, it must be concluded that the catalytically-active centres in PEI are not those responsible for the diminution in the height of the hydrogen wave. This may more readily be understood when the stoichiometry of the reaction between the acid and PEI is considered. Owing to the use of sodium sulphate in a relatively high concentration as a supporting electrolyte, free H_3O^+ ions, are unlikely to be present in solution and equilibrium is mainly in favour of HSO_4^- formation. The height of curve 2 of Fig. 1 corresponds, therefore, to the reduction of $1.92 \cdot 10^{-3}$ *M* HSO_4^-. This wave completely disappears when the solution is made $3.024 \cdot 10^{-3}$ *M* with respect to PEI. Accordingly, the two substances react in the molar ratio, 0.6 $HSO_4^-(H^+)$: PEI. This results is consistent both in forward and backward titration experiments (Fig. 2), and in solutions where the acid or base concentration is varied by a factor of three, and indicates, therefore, that this molecular ratio is real. Apparently, this ratio corresponds to the formation of the structure $-CH_2-CH_2-NH_2^+-CH_2-CH_2-NH-CH_2-CH_2-NH_2^+-$, in which the imino-groupings of PEI are alternatively free and protonated. In such a form the protons are strongly attached to the nitrogen atoms and are not reduced at the mercury electrode. Conformational variations in the PEI chains upon protonation, established by NMR studies[6], might be responsible (at least in part) for the difference between the ratio of PEI:H^+ actually determined and that assigned to the above structure. The protonation of one particular nitrogen atom in the PEI chain changes its character form one of electron- donating to that of electron-attracting. This causes a considerable reduction in the electron density on the neighbouring nitrogen atom. Also, owing to steric and/or electrostatic effects, strong protonation of these intermediate imino-groupings is unlikely to take place. Catalysis of the hydrogen evolution is evidently the result of electron transfer to the weakly protonated groups adsorbed on the electrode surface. As already discussed above, catalysis (*i.e.*, shift of the wave towards positive potentials) increases with increase in PEI concentration until the hydrogen wave completely disappears. Retardation of the hydrogen evolution reaction by large amounts of the additive—as is the case with gelatin[1]—was not observed in the present study. Whether this is due to the relatively smaller molecular weight and hence lower blocking efficiency of PEI, or to the fact that inhibition sets in at still higher additive concentrations at which the hydrogen wave would have completely disappeared, cannot be decided.

It was of interest to establish whether distinction between strongly and weakly protonated imino-groups in PEI chains could be confirmed by electrometric methods other than polarography. One apparent approach was to measure the mobility of the

hydrogen ion in PEI–acid solutions. The results of these measurements are given in Fig. 4 as conductometric titration curves for increasing PEI concentrations. These curves are formed of two linear segments. Along the lower portions, the conductivity of the solutions varies only slightly with additions of acid, indicating that the acid is

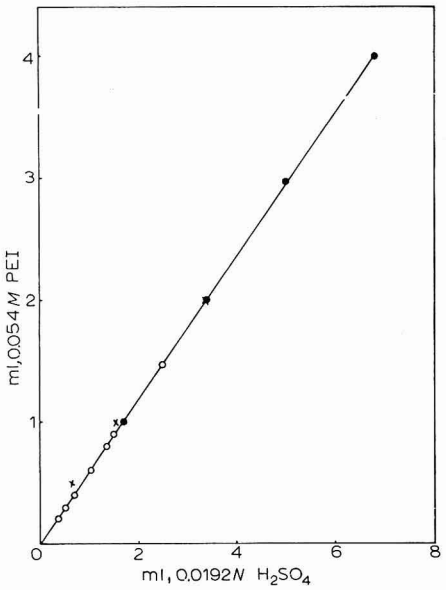

Fig. 3. Relation between PEI and H_2SO_4 volumes at the inflexion points. (○), Amperometric; (●), conductometric; (×), potentiometric.

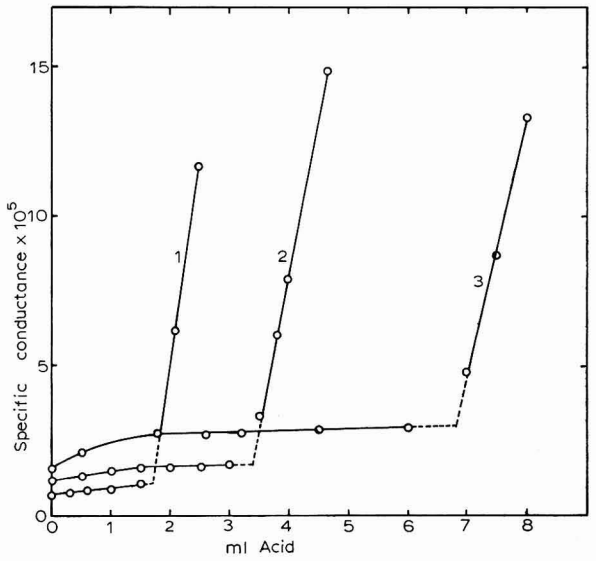

Fig. 4. Conductometric titration of PEI (0.054 *N*) with H_2SO_4 (0.0192 *N*). (1), 1.0; (2), 2.0; (3), 4.0 ml PEI/50 ml soln.

strongly bound to the PEI chains. At the upper parts of the curves, the conductivity increases linearly with the acid concentration. The slope of the conductivity–volume curve at this stage of neutralization is, however, less than that measured in the absence of PEI showing that the mobility of the acid is somewhat restricted in the presence of the imine. Since the neutralization of PEI at these dilutions does not measurably affect the bulk viscosity of the solution, the decreased conductivity indicates that the acid is weakly bound to the protonated PEI chains. The two lines of the titration curves of Fig. 4 intersect at sulphuric acid volumes that are strictly proportional to the concentration of PEI in solution. The ratio between the volumes of the two reagents is exactly the same as determined amperometrically (see corresponding points in Fig. 3).

Polythyleneimine was also titrated potentiometrically with H_2SO_4, using the glass indicator electrode. Some results of this series of measurements are given by the curves of Fig. 5, in which the progress of the titration is expressed in terms of the degree of neutralization, α. As expected for weak polybase electrolytes, the titration curves extend over a much wider range of pH than corresponds to the Henderson–Hasselbach equation for the neutralization of an ordinary monoacid base, *viz.*, $pH = pK + \log [\alpha/(1-\alpha)]$. Here, as α increases, the remaining basic groups progressively become

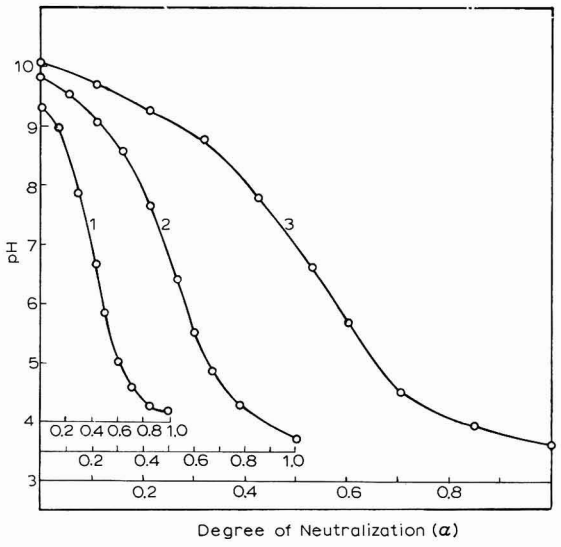

Fig. 5. Potentiometric titration of PEI (0.054 *N*) with H_2SO_4 (0.0192 *N*) in presence of 0.16 *M* Na_2SO_4. (1), 0.5; (2), 1.0; (3), 2.0 ml PEI/25 ml soln.

weaker as a result of the growing positive charge on the polyion. The most interesting feature of the curves of Fig. 5 is that the points of their maximum inflexion occurs at $\alpha = 0.60$–0.62, and correspond, therefore, to that found by the amperometric and conductometric techniques (Fig. 3). Following these points, the pH of the solution changes slowly to lower values as more acid is added. In this respect, the curves of Fig. 5 differ from those given by SHEPHERD AND KITCHENER [7] for the same compound: the inflexion at $\alpha \simeq 0.5$ is not so clear. This may be due to the fact that SHEPHERD AND

KITCHENER used a PEI sample of a much shorter average chain length ($n \simeq 35$–40) than that of the present investigation. With these relatively small molecules, the primary, more basic, $-NH_2$ end groups affect the course of the neutralization reaction in such a manner that up to $\leqslant \alpha$ 0.06, the simple Henderson–Hasselbach equation describes the titration curve, with a constant apparent pK equal to 9.0. KATCHALSKY's theory[8] of polyelectrolytes was found to account for the part of the curve between 0.3 $< \alpha <$ 0.5 for a pK of 10.0. The theory failed, however, to describe the conditions at advanced stages of neutralization. Around $\alpha = 0.9$, the groups appeared to be about 2 pH-units weaker than predicted. This was explained by taking into consideration the electrostatic interaction between neighbouring –NH– groups.

With the PEI sample used in the present investigation ($n = 700$–1000) the role of the $-NH_2$ end groupings can be neglected since their abundance does not exceed *ca.* 3/mil of the total basic-groups. However, the distinct inflexion at $\alpha \simeq 0.6$ indicates that a marked change in the basicity of the polymer took place at this particular composition. The fact that the same reacting ratio was reached using a number of measuring techniques leaves little doubt that the imine-groups are not protonated to the same extent. Distinction can be made between strongly protonated, non-conducting, polarographically-inactive groups, on one hand, and weakly protonated, conducting, catalytically-active groups, on the other. The present investigation establishes also the feasibility of the polarographic technique for the study of the properties of basic polyelectrolytes in solution. Further work on other substances along these lines is in progress.

SUMMARY

The effect of polyethyleneimine (PEI) on the hydrogen wave of sulphuric acid in 0.16 M sodium sulphate is examined over a wide concentration range. In small amounts the additive suppresses the maximum of the wave and shifts its reduction potential towards more positive values (catalysis). Higher concentrations of PEI cause a diminution in the height of the limiting current of the wave, which is proportional to the amount of the additive. This allows the development of an amperometric procedure for the determination of PEI in solution. The hydrogen wave completely disappears at the molar ratio. α, (H^+:PEI) of 0.6. Distinction can be made between strongly protonated, polarographically-inactive imino groups, on one hand, and weakly protonated, catalytically-active groups, on the other. The same conclusion was also reached from conductometric and potentiometric titration experiments. The conductivity curves of PEI–H_2SO_4 mixtures exhibit distinct inflexions at $\alpha = 0.6$. Below this value, the conductivity is practically independent of H_2SO_4 additions, indicating strong binding by PEI. Above $\alpha = 0.6$, the conductivity increases linearly with acid concentration and suggests weak binding. The potentiometric titration curves have their maximum point of inflexion also at $\alpha = 0.6$ indicating a marked change in the basicity of the polyelectrolyte at this composition.

REFERENCES

1 L. HOLLECK, J. M. ABD EL KADAR AND A. M. SHAMS EL DIN, *J. Electroanal. Chem.*, 17 (1968) 401.
2 W. HANS AND W. JENSCH, *Z. Elektrochem.*, 56 (1952) 648.

3 I. M. KOLTHOFF AND J. J. LINGANE, *Polarography*, Interscience, New York, 2nd ed., 1952, p. 888.
4 M. VON STACKELBERG AND H. FASSBENDER, *Z. Elektrochem.*, 62 (1958) 834.
5 M. VON STACKELBERG, W. HANS AND W. JENSCH, *Z. Elektrochem.*, 62 (1958) 839.
6 K. J. LIU, personal communication.
7 E. J. SHEPHERD AND J. A. KITCHENER, *J. Chem. Soc.*, (1956) 2448.
8 A. KATCHALSKY AND O. SPITNIK, *J. Polymer Sci.*, 2 (1947) 432; A. KATCHASLKY, O. KUNZLE AND W. KUHN, *J. Polymer Sci.*, 5 (1950) 283; A. KATCHALSKY AND S. LIFSON, *J. Polymer Sci.*, 11 (1953) 409; A. KATCHALSKY, N. SHAVIT AND H. EISENBERG, *J. Polymer Sci.*, 13 (1954) 69; S. LIFSON AND A. KATCHALSKY, *J. Polymer Sci.*, 13 (1954) 43.

Elsevier Sequoia S.A., Lausanne – Printed in The Netherlands

POLAROGRAPHIC MAXIMUM SUPPRESSING ABILITY OF MALATHION IN NON-AQUEOUS AND AQUEOUS SYSTEMS

E. LADÁNYI AND D. N. RĂDULESCU
Institute of Hygiene, Cluj (Rumania)
(Received July 13th, 1968)

The organophosphorus insecticide, (O,O-dimethyl S-(1,2-dicarboethoxyethyl) dithiophosphate), known as malathion, malathon, mercaptothion, carbofos, or carbetox, is polarographically inactive, and is, therefore, determined polarographically by indirect methods[1-3].

Since malathion shifts the half-wave potential, $E_{\frac{1}{2}}$, of some substances such as maleic and fumaric acids, oxygen and hydrogen peroxide, JURA concluded that there is adsorption of malathion which forms a film on the dropping mercury electrode surface[1]. NANGNIOT using a cathode-ray polarograph of linear tension-sweep in aqueous methanol–HCl medium, obtained 3 adsorption peaks for malathion and considered that this confirmed the adsorbability of malathion on the dropping mercury electrode[4,5].

According to present knowledge of the effects produced on polarographic curves by adsorbed electro-inactive substances[6-8], malathion should behave as a typical surface-active substance and as such should suppress the polarographic maxima of the first kind[9]. It was decided to study the effect of malathion on such a polarographic maximum and to investigate the use of the expected effect for analytical purposes.

Since it is known[5] that malathion hydrolyses very easily at all pH-values other than 5.26[10], its effect on the maximum was investigated in non-aqueous conditions. Using a solvent-supporting electrolyte system of ammonium trimethylphenyl chloride in benzene–methanol, we found that in non-aqueous conditions malathion does not suppress the benzoyl peroxide maximum unless there is a short contact with a medium permitting hydrolysis of malathion. We studied, therefore, the relation between the degree of suppression, the initial malathion concentration, and the water-contact time with and without atmospheric contact.

APPARATUS AND MATERIALS

A Heyrovský LP-60 type polarograph with an electronic recording system was used. A dropping mercury electrode (DME) served as cathode and the reference electrode consisted of mercury of the bottom of a Novak-type electrolysis vessel. The capillary constants found in doubly-distilled water at 0 V gave $mt = 0.0116$ g. The composition of the solvent-supporting electrolyte system was 2% ammoniumtrimethylphenyl chloride in benzene–methanol (1:3). The maximum-producing depolarizer was 0.5% benzoyl peroxide in the given solvent-supporting electrolyte system. The avail-

able insecticides were: 100% malathion (Dutch product) and 100% carbetox (Rumanian product) both of technical grade. The pH was measured with a Clamann Grahnert MV-11 pH-meter.

EXPERIMENTAL

The investigation was based on measurements of the height of the maximum before and after the addition of the insecticide in the polarographic cell. Purified N_2 was bubbled for 10 min through a mixture of 5 ml of solvent-supporting electrolyte and 0.2 ml benzoyl peroxide solution. The current–voltage curve was then recorded between 0 and -0.6 V with a sensitivity of $1.8 \cdot 10^{-3}$ A/mm, and the drop-time adjusted to 3 sec at 0 V in the given system. The insecticide (100 μg/ml) was then added in the same cell, being either dissolved in a benzene–methanol (1:3) mixture or dispersed in water (pH = 7.1) by vigorous shaking for 5 min. The added volume assured a concentration range of 0–8 μg/ml in the cell. After 2-min de-aeration the current–voltage curve was recorded again under the same conditions. The results were expressed in degree of suppression, h_1/h_0, as $f(c_0)$ and f(time) where h_0 and h_1 are the maxima heights before and after the addition of the insecticide. The degree of suppression–contact-time dependence was studied at $24 \pm 0.5°$ with and without atmospheric contact. In order to follow the effect of the latter, the volumetric flasks were kept in a thermostat which assured a constant relative vapour pressure above the solution so that it was unnecessary to adjust them to the initial volume.

RESULTS

The behaviour of benzoyl peroxide in the system described led us to prefer it to the oxygen maximum which is poorly reproducible and thus less suitable for

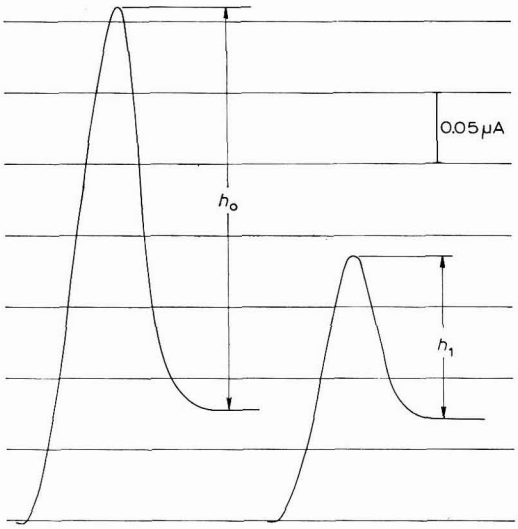

Fig. 1. Benzoyl peroxide maximum in benzene–methanol (1:3) before and after suppression.

analytical purposes. Moreover, there are data to show[10], that organic peroxides have a stabilizing action on malathion.

In the given system, benzoyl peroxide has $E_{\frac{1}{2}} = 0.075$ V (*vs.* the Hg pool) giving a sharp maximum (Fig. 1) the height of which depends exponentially on its concentration. For concentrations > 150 μg/ml, the logarithmic dependence has a linear pattern (Fig. 2). The peak potential, E_{peak}, (but not $E_{\frac{1}{2}}$) depends also on the peroxide concentration, becoming more negative with increase of the latter. Thus, for 193 μg/

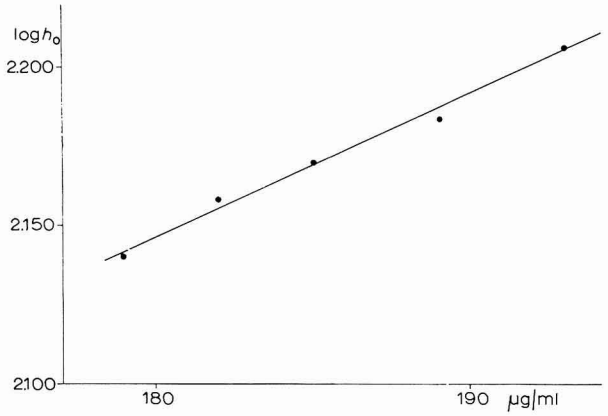

Fig. 2. Maximum height–benzoyl peroxide concn. dependence.

TABLE 1

REPRODUCIBILITY OF THE BENZOYL PEROXIDE MAXIMUM*

Preparation	*Maximum height (h_0) (mm)*			*Rel. error of recording (%)*	*Rel. error of preparation (%)*
	Recording				
	1	*2*	*3*		
1	158	158	158	0	0.3
2	162	158	158	1.1	0.5
3	158	160	156	0.8	0.3
4	159	159	—	0	0.3
5	159	159	159	0	0.3
6	158	158	158	0	0.3
				0.32	0.35

* 1.93 μg benzoyl peroxide/ml in benzene–methanol (1:3).

TABLE 2

EFFECT OF WATER TRACES ON THE MAXIMUM HEIGHT

Contact-time (h)	h_1/h_0									
	Doubly-distilled H_2O					*Drinking H_2O*				
ml added:	*0*	*0.1*	*0.2*	*0.3*	*0.4*	*0*	*0.1*	*0.2*	*0.3*	*0.4*
0	1.0	0.88	0.80	0.72	0.64	1.0	0.90	0.79	0.72	0.64
24	1.0	0.89	0.81	0.72	0.64	1.0	0.89	0.80	0.72	0.62

ml, $E_{peak} = -0.20$ V; for 536 μg/ml, -0.37 V. The reproducibility of the maximum is excellent both for repeated recordings of the same solution and solutions prepared on different occasions (Table 1).

As observed, traces of water affect the maximum height but this cannot be attributed to the peroxide concentration change since equal quantities of water and benzene–methanol mixture produce different decreases in the max. height (Fig. 3). The phenomenon may be explained by the change of the structure of the electrical double layer in the presence of water. Since doubly-distilled and drinking water produced the same decrease in the maximum height, foreign ions do not affect it. Also, the decrease of the maximum remains constant in time (Table 2).

In non-aqueous conditions, (Table 3 and Fig. 4, curves A'B') neither the Dutch nor Rumanian malathion (added in microgram quantities) suppress the maximum and its height remains unchanged independent of the contact-time of the insecticide with the benzene–methanol mixture. Under identical conditions no suppressing effect could be obtained even with hundred times more (273 μg/ml; 360 μg/ml) malathion. In contact with doubly-distilled water from which dissolved CO_2 had not been eliminated (pH = 5.6) malathion of the same concentration range again had no suppressing effect (Table 3 and Fig. 4, curves A'B').

TABLE 3

BEHAVIOUR OF MALATHION IN NON-AQUEOUS AND AQUEOUS MEDIA

No. i.	*Maximum suppressing conditions*		*Degree of suppression* $(h_1/h_0)_{corr}$*							
	Medium	*Contact-time*	*Concn. of insecticide in cell (μg/ml)*							
			0.44	*1.73*	*1.88*	*2.94*	*3.70*	*4.47***	*5.45*	*7.15*
1	BM	2 min	1.00	1.00	—	1.00	—	1.00	—	—
1'	BM	24 h	1.00	1.00	—	1.00	—	1.00	—	—
2	$(H_2O)_{DD}$	2 min	—	—	1.00	—	1.00	—	1.00	1.00
2'	$(H_2O)_{DD}$	24 h		—	1.00	—	1.00	—	1.00	1.00
3	$(H_2O)_{Dr}$	2 min	—	—	1.00	—	1.00	—	1.00	1.00
3'	$(H_2O)_{Dr}$	24 h	—	—	0.89	—	0.83	—	0.79	0.77

BM = Benzene–methanol (1 : 3)
$(H_2O)_{DD}$ = Doubly-distilled water with dissolved CO_2 (pH = 5.6)
$(H_2O)_{Dr}$ = (Drinking water (pH = 7.1)
* $(h_1/h_0)_{corr} = (h_1/h_0)_i + (1.00 - (h_1/h_0)_{H_2O})$ or $(h_1/h_0)_i + (1.00 - (h_1/h_0)_{B-M})$
** 2.85 μg (Dutch) + 1.62 μg (Rumanian) malathion/ml.

The situation is quite different if malathion is in contact with drinking water (pH = 7.1). Immediately after the contact (about 2 min), there is no evidence of any suppressing effect and the log $(h_1/h_0 \cdot 100)_{corr}$ values lie on the curve for non-aqueous conditions (Table 3 and Fig. 4). With increase in contact-time, the maximum begins to be suppressed and after 24 h the suppression is already considerable. There is a proportionality between the degree of suppression and the initial malathion concentration (log $h_1/h_0 \cdot 100)_{corr}$ being a linear function of c_0 (Table 3 and Fig. 4, curve B'').

These observations suggest that it is not malathion which adsorbs on the DME surface but a hydrolytic decomposition product and this causes the suppression of the benzoyl peroxide maximum and all the other phenomena described, characteristic

of surface-active substances[1,3-5]. The authors who suggested that malathion was adsorbed on the DME surface, carried out their experiment at pH-values very different from 5.26, *i.e.*, under conditions favourable for hydrolysis[1,5]. On the other hand, SOHR obtained (in potassium chloride) adsorption waves also for phosphorus esters without sulphur[11] which contradicts NANGNIOT's presumption[4] that the $-\overset{|}{\underset{\diagup\diagdown}{P}}-S-$ or $-\overset{|}{\underset{\|}{P}}-S$ (S) grouping is responsible for the adsorption of phosphorus esters on the DME.

Therefore, by following the change of the degree of suppression as a function of time we could study the kinetics of malathion hydrolysis (Fig. 5). The degree of suppression–time-dependence follows an exponential curve which decreases to a

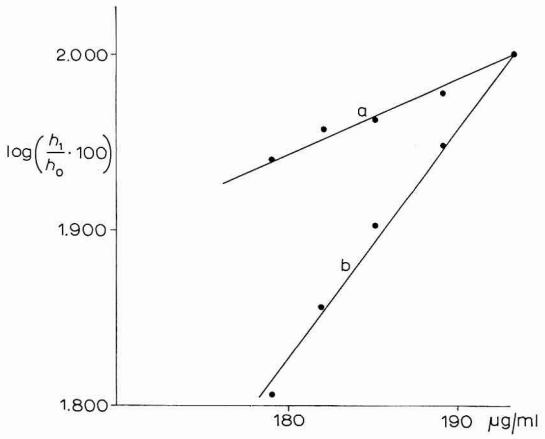

Fig. 3. The effect of the nature of the diluent on the magnitude of the benzoyl peroxide maximum. Added to the benzene–methanol (1 : 3) soln. of benzoyl peroxide: (a), Benzene–methanol (1 : 3); (b), Doubly-distilled or drinking water.

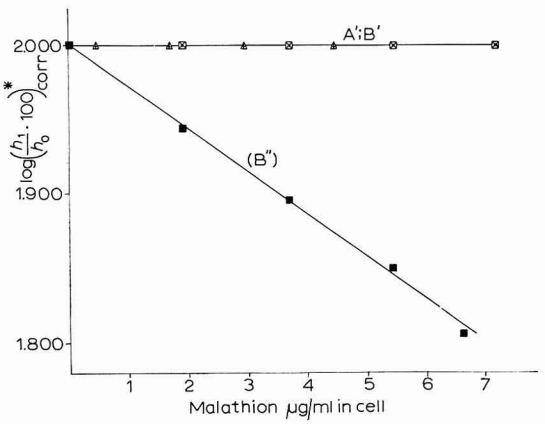

Fig. 4. Effect of medium in which malathion is stored on the benzoyl peroxide maximum height; a concentration and contact-time dependence log $(100h_1/h_0)_{corr}$ = log $(100h_1/h_0)_i$ + [2.000 − log $(100h_1/h_0)_{H_2O \text{ or } B-M}$]
Time: (△, □, ●) 2 min; (+, ×, ■) 24 h. Medium: (△, +) B–M; (□, ×) $(H_2O)_{DD}$, (●, ■) $(H_2O)_{Dr}$.

constant value (Fig. 5). Atmospheric contact favours the speed of hydrolysis (Fig. 6). If it is assumed that the reaction does not stop at an equilibrium, the final value of the degree of suppression corresponds to the completely hydrolysed insecticide. Thus,

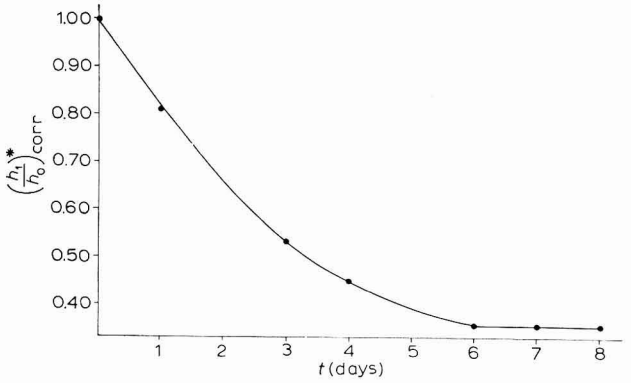

Fig. 5. Degree of suppression–contact-time dependence of malathion. Malathion concn.: 100 μg/ml water (pH = 7.1); 4 μg/ml in polarographic cell; $t = 24 \pm 0.5°$; atmospheric contact.

$$(h_1/h_0)_{corr} = (h_1/h_0)_i + 1.00 - (h_1/h_0)_{H_2O}$$

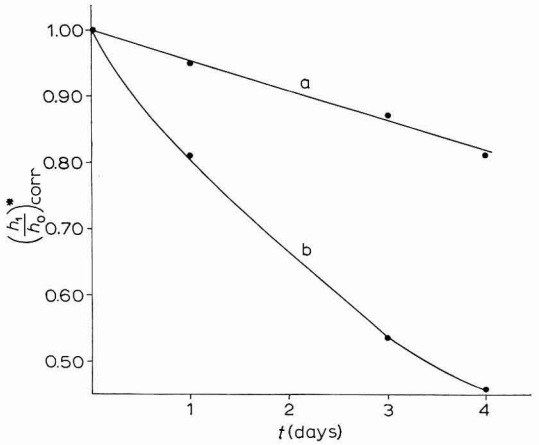

Fig. 6. Effect of atmospheric contact on the degree of suppression–water contact-time dependence of malathion. (a), without; (b), with atmospheric contact.

$$^*(h_1/h_0)_{corr} = (h_1/h_0)_i + 1.00 - (h_1/h_0)_{H_2O}$$

when h_1/h_0 changes from 1.00 to a constant value (Fig. 5) unhydrolysed malathion varies between 100 and 0% of its initial concentration c_0. Since h_1/h_0 depends exponentially on c_0, the unhydrolysed malathion concentration at any time is given by the logarithm of the h_1/h_0-values. Figure 7 represents the kinetic curve of malathion hydrolysis at pH = 7.1 at 24° with atmospheric contact. Its analysis shows that the reaction is pseudo-first-order (Fig. 8). The rate constant for the above experimental conditions is $K = 0.253$ days^{-1}.

Our findings are indirectly confirmed by some authors who studied the toxicity

of malathion on human and animal organisms. They concluded that malathion kept in drinking and river water loses its toxicity[12] with increased speed in contact with the atmosphere[12,15–17]; the hydrolysis of its ester groups is responsible for its detoxication [13,14]. Also, we found that fish used in toxicological experiments[12] survived in a malathion–water system prepared 6 days earlier although the initial malathion concentration was 100 μg/ml, *i.e.*, over the toxic level[12].

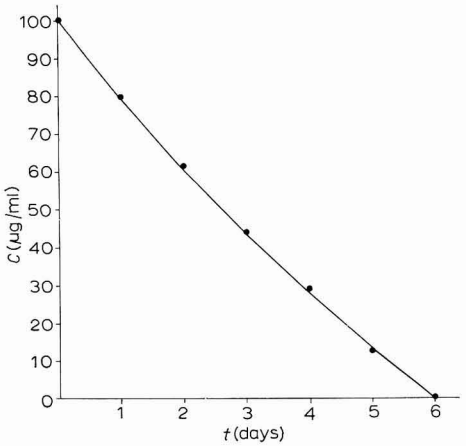

Fig. 7. Kinetics of malathion hydrolysis.

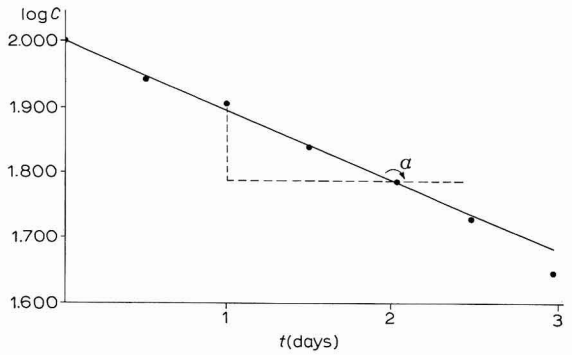

Fig. 8. Logarithmic analysis and rate constant determination of malathion hydrolysis.

CONCLUSIONS

The experimental data suggest that only hydrolysed malathion adsorbs on the DME and this suppresses the polarographic maximum of benzoyl peroxide. The quantitative relationships between the degree of suppression, initial concentration, and contact-time with the medium favouring hydrolysis, enables polarography to be used for analytical purposes and kinetic studies.

SUMMARY

The effect of malathion on the stable, reproducible polarographic maximum of benzoyl peroxide in non-aqueous and hydrolysis-favourable conditions suggests that malathion itself is not adsorbed on the DME, but that a hydrolytic decomposition product causes the appearance of phenomena characteristic of surface-active substances. Using the quantitative relationships established between the degree of maximum suppression and the speed of malathion hydrolysis, we studied polarographically (at pH=7.1, 24° and with atmospheric contact) the malathion hydrolysis kinetics. In these conditions the reaction is of pseudo-first-order with a rate constant, $K=0.253$ days^{-1}.

REFERENCES

1 W. H. JURA, *Anal. Chem.*, 27 (1955) 525.
2 I. PRAT AND D. BODIN, *Mem. Serv. Chim. Etat Paris*, 41 (1957) 243.
3 P. H. MARTENS AND P. NANGNIOT, *Mededel. Landbouwhogeschool Opzoekingsstat. Staat Gent*, deel XXIV, No. 3–4 (1959) 948.
4 P. NANGNIOT, *Mededel. Ghent Rijksfac. Landbouwwetensch.*, 31, 3 (1966) 447.
5 P. NANGNIOT, *Anal. Chim. Acta*, 31 (1964) 166.
6 J. HEYROVSKÝ, *Collection Czech. Chem. Commun.*, Suppl. II. 19 (1954) 58.
7 J. HEYROVSKÝ, F. ŠORM AND J. FOREJT, *Collection Czech. Chem. Commun.*, 12 (1947) 11.
8 J. KŮTA, *Modern Aspects of Polarography*, edited by T. KAMBARA, Plenum Press, New York, 1966, p. 62.
9 J. PROSZT, K. GYÖRBIRO AND V. CIELSZKY, *Polarográfia*, Akadémia, Budapest, 1964, p. 160.
10 W. O. NEGHERBON, *Handbook of Toxicology*, Vol. III, Saunders, Philadelphia, 1959, p. 452.
11 H. SOHR, *Chem. Zvesti*, 16 (1962) 316.
12 N. W. GHELBERG, L. COSTIN AND S. NAGY, *Igiena Bucharest*, 17 (1968) 81.
13 W. C. DAUTERMAN AND A. R. MAIN, *Toxicol. Appl. Pharmacol.*, 9 (1966) 408.
14 S. P. MURPHY, *J. Pharmacol. Exp. Therap.*, 156,2 (1967) 352.
15 M. ELMINA AND S. DE GOUVELA, *Garcia Orta*, 13 (1965) 139.
16 D. E. COFFIN, *J. Assoc. Offic. Agr. Chemists*, 49 (1966) 1018.
17 W. DELMON AND LA HUE, *U. S. Dept. Agr. Marketing Res. Rept. 768*, 1966.

Elsevier Sequoia S.A., Lausanne – Printed in The Netherlands

SHORT COMMUNICATIONS

A chronocoulometric method with dropping electrode for adsorption study

Introduction

The determination of equilibrium properties of the electrical double layer is barely possible if organic ions with a strong surface activity are adsorbed at the electrode. If an equilibrium coverage of the electrode, which would be considerably smaller than unity, had to be attained it would be necessary to use a rather low concentration of the surfactant. Under these conditions the adsorption equilibrium does not establish for very long. The measurement of interfacial tension with a capillary electrometer is not practicable[1].

Another approach to double-layer structure in this situation is the investigation of its effect on electrode reactions using i–t curves with the mercury dropping electrode (see *e.g.* ref. 2). Here two effects are observed: the blocking of the electrode by the adsorbed film[3,4] and the electrostatic effect of the adsorbed ions[2]. In the case of strong adsorption, the surface concentration of the surfactant may depend only on its diffusion to the surface of the electrode[5]

$$\Gamma(t) = 7.36 \cdot 10^{-4} c_A D_A^{\frac{1}{2}} t^{\frac{1}{2}} \quad (1)$$

where c_A is concentration of the surfactant, D_A its diffusion coefficient and t the time elapsed from the start of drop formation. KŮTA *et al.*[2] described the electrostatic effect by the Frumkin formula and assumed that the potential difference in the diffuse double layer, φ_2, depends on relative coverage of the electrode, $\theta = \Gamma/\Gamma_m$, according to the equation:

$$\varphi_2 = \varphi_{2,0} + k\theta \quad (2)$$

where Γ_m is the maximum surface concentration, $\varphi_{2,0}$ the electrical potential difference in the diffuse double-layer in absence of adsorption and k a constant.

Principle of the method

The method proposed in the present paper aims at a direct determination of the dependence of the surface charge on time, under conditions of strong, diffusion-controlled adsorption when eqn. (1) is valid. Thus, if $q(t)$ and $\Gamma(t)$ are known, the electrical potential difference in the diffuse double layer may be directly calculated as a function of time using the Gouy–Chapman model. The relationship between q and θ may verify Frumkin's equation[5]

$$q = q^0 + \theta(q^1 - q^0) \quad (3)$$

where q^0 is the electrode charge in the absence of the surface active substance and q^1 is the charge under full coverage of the electrode.

Experimental

Our method is based on integration of the instantaneous charging current at the dropping electrode at constant potential. We call it a "chronocoulometric method" in spite of the fact that in its experimental arrangement it differs from the method proposed by ANSON[7]. The integrating circuit is shown in Fig. 1. The current is amplified in the operational amplifier A_1 and its output potential is fed to the integrator A_2. The resulting Q–t curve is recorded with a fast-response recorder.

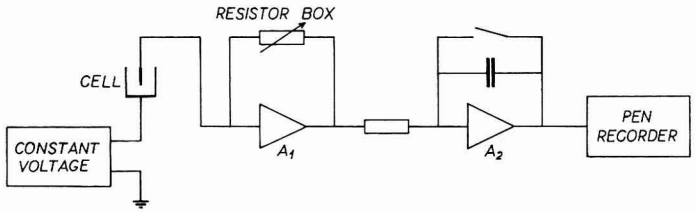

Fig. 1. The integrating circuit.

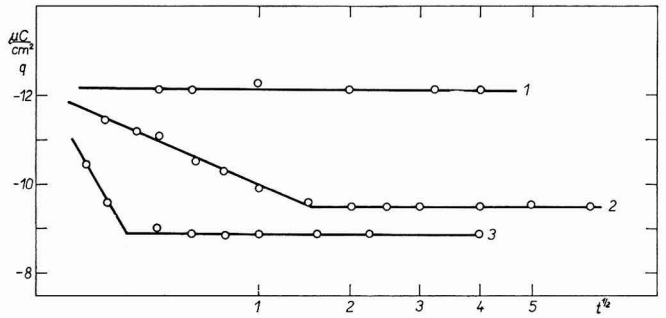

Fig. 2. q–t curves in 0.1 M KCl. Concns. of $(C_4H_9)_4NCl$: (1), $6 \cdot 10^{-5}$; (2), 10^{-4}; (3), $3 \cdot 10^{-4}$ M. $E = -1.170$ V *vs.* NCE.

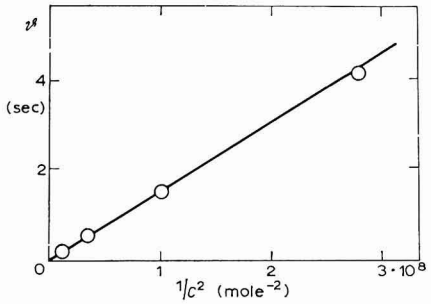

Fig. 3. Dependence of time of coverage, θ, on c_A^{-2} (θ is the value of t for Γ_m according to eqn. (1)).

The main obstacles of the method are residual currents of the order of 10^{-8} A which are observed at the potential of zero charge even if all electroactive substances have been removed from the solution using deaeration with a stream of very pure argon and pre-electrolysis with a gold electrode. These residual currents were considerably decreased if for the dropping electrode a conical capillary tube was used

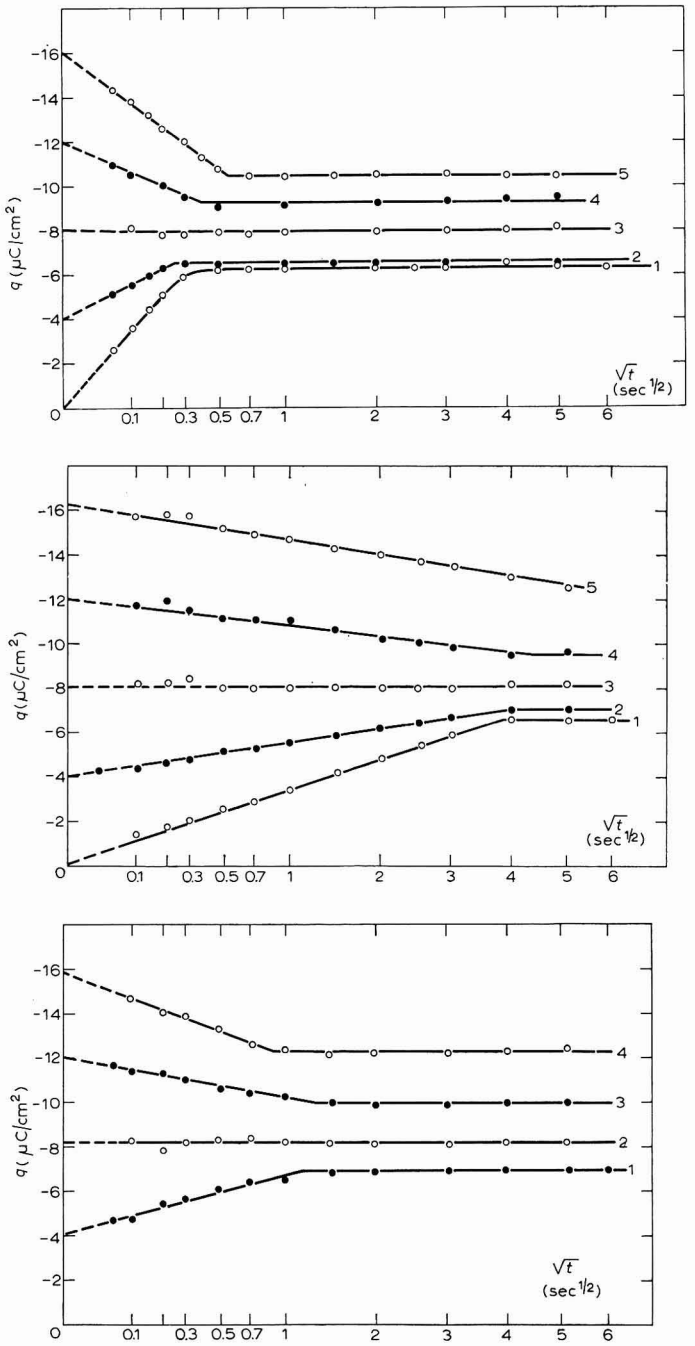

Figs. 4–6. q–t dependencies. Fig. 4 and Fig. 5: 1 M KCl + $2 \cdot 10^{-4}$ M $(C_4H_9)_4NCl$ and 1 M KCl + $6 \cdot 10^{-5}$ M $(C_4H_9)_4NCl$ resp., at electrode potentials *vs.* NCE (1), −0.478; (2), −0.595; (3), −0.768; (4), −0.998; (5), −1.239 V. Fig. 6: 0.02 M KCl + 10^{-4} M $(C_4H_9)_4NCl$ at electrode potentials (1), −0.673; (2), −0.846; (3), −1.076; (4), −1.317 V.

as recommended by DE LEVIE[8] and COOKE *et al.*[9]. The conical part was about 10 mm long and the original diameter of 0.09 mm decreased to 0.02 mm. Under these conditions, residual currents of 10^{-9}–$2 \cdot 10^{-9}$ A were obtained at the potential of electrocapillary zero. The charge–time curves were, if necessary, corrected for these residual currents.

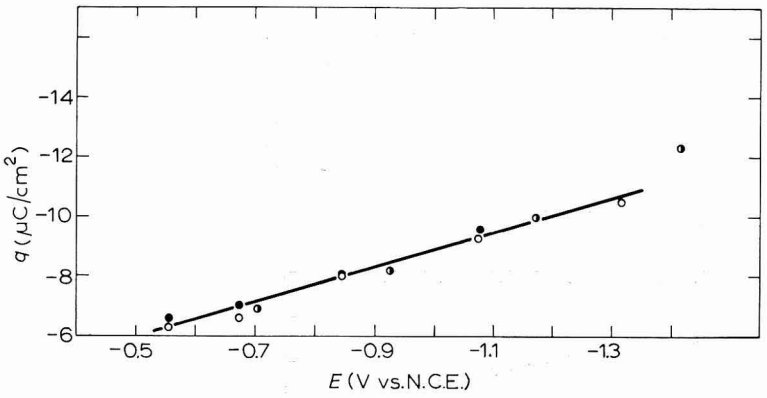

Fig. 7. Dependence of q^1 on electrode potential *vs.* NCE. (◑), 0.02 *M* KCl, 10^{-4} *M* $(C_4H_9)_4NCl$; (●), 1 *M* KCl, $6 \cdot 10^{-5}$ *M* $(C_4H_9)_4NCl$; (○), 1 *M* KCl, $2 \cdot 10^{-4}$ *M* $(C_4H_9)_4NCl$.

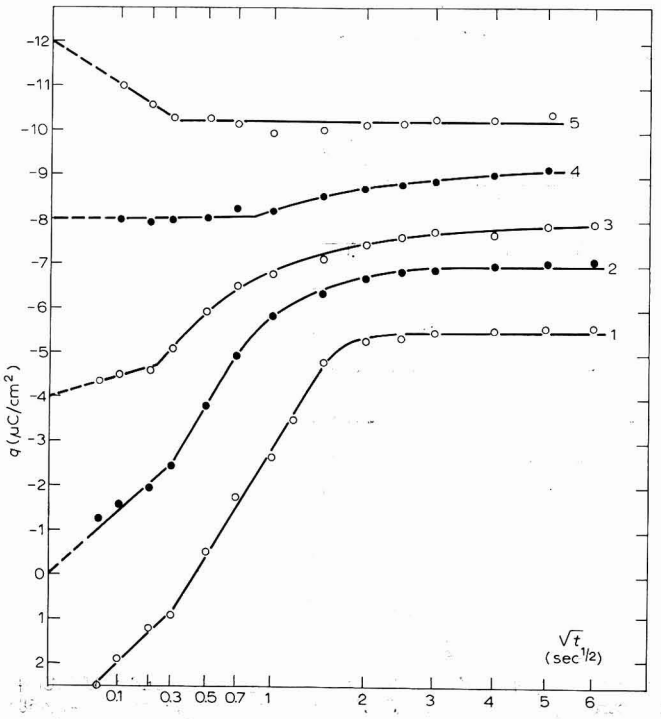

Fig. 8. q–t dependencies for 0.1 *M* KCl, $2 \cdot 10^{-4}$ *M* tribenzylammonium chloride. Electrode potentials: (1), −0.358; (2), −0.506; (3), −0.670; (4), −0.895; (5), −1.128 V *vs.* NCE.

The solution of tetrabutylammonium chloride was prepared by shaking a solution of tetrabutylammonium iodide (Fluka A.G.) with freshly precipitated silver chloride[10]. Tribenzylammonium chloride was kindly supplied by the Institute of Pharmacy and Biochemistry, Prague (Dr. M. KAKÁČ). The solutions of this substance contained 0.5% ethanol.

Results and discussion

If the electrode were covered by the limiting diffusion flux of the surface active substance, then eqn. (1) would be valid up to the time ϑ corresponding to a practically full coverage. The electrode would then attain a constant charge, q^1. Figure 2 shows the experimental q–t curves (in view of eqn. (1), $t^{\frac{1}{2}}$ instead of t was plotted on the abscissae axis since $\theta \sim t^{\frac{1}{2}}$). The break on the curves should correspond to the time ϑ which should be inversely proportional to $c_A{}^2$. This has been proved experimentally (see Fig. 3). If the value of the diffusion coefficient of tetrabutylammonium[11], $D_A = 5.2 \cdot 10^{-6}$ cm^2 sec^{-1}, is assumed, the maximum coverage, $\Gamma_m = 2.1 \cdot 10^{-10}$ mole cm^{-2}, is obtained.

Figures 4, 5 and 6 show q–t dependencies for various concentrations of KCl and tetrabutylammonium ion. These results prove the validity of eqn. (3). Figure 7 shows the dependence of the charge at full coverage, q^1, on electrode potential, E. This quantity is independent of the concentrations of both KCl and the surfactant.

The adsorption of tribenzylammonium ion is considerably more complicated as shown in Fig. 8. This may be connected with reorientations or phase changes in the absorbate[12].

J. Heyrovský Institute of Polarography,
Czechoslovak Academy of Sciences,
Prague (Czechoslovakia)

J. KORYTA
L. NĚMEC
J. PIVOŇKA
L. POSPÍŠIL

1 R. PARSONS, private communication.
2 J. KŮTA, J. WEBER AND J. KOUTECKÝ, *Collection Czech. Chem. Commun.*, 25 (1960) 2375.
3 R. W. SCHMID AND C. N. REILLEY, *J. Am. Chem. Soc.*, 80 (1958) 2087.
4 J. WEBER, J. KOUTECKÝ AND J. KORYTA, *Z. Elektrochem.*, 63 (1959) 583.
5 J. KORYTA, *Collection Czech. Chem. Commun.*, 18 (1953) 206.
6 A. FRUMKIN, *Z. Physik.*, 35 (1926) 792.
7 F. C. ANSON, *Anal. Chem.*, 38 (1966) 1924.
8 R. DE LEVIE, *J. Electroanal. Chem.*, 9 (1965) 117.
9 W. D. COOKE, M. T. KELLEY AND D. J. FISCHER, *Anal. Chem.*, 33 (1961) 1209.
10 J. KORYTA AND S. VAVŘIČKA, *J. Electroanal. Chem.*, 10 (1965) 451.
11 B. B. DAMASKIN, S. VAVŘIČKA AND N. B. GRIGORIEV, *Zh. Fiz. Khim.*, 36 (1962) 2530.
12 J. KORYTA, J. PIVOŇKA, N. YAKOVLEVA AND S. VAVŘIČKA, *17th Meeting of CITCE, Tokyo*, 1966.

Received August 6th, 1968

Elsevier Sequoia S.A., Lausanne – Printed in The Netherlands

Double layer thermodynamics for slow electrode reactions under steady-state conditions

The thermodynamics of the interface between metal and electrolyte solution, in the absence of electrochemical charge transfer, has been developed since the early work of LIPPMANN[1] and GOUY[2], and has been the subject of many recent reviews[3]. KRÜGER[4], and especially FRUMKIN[5], extended the treatment to the presence of species that can undergo electrode reactions. Their treatments are confined to Nernstian equilibrium between the applied potential and the activities of the reacting species at the electrode interface. The same applies to subsequent derivations[6].

Recently, TIMMER *et al.*[7] have indicated how these results can be applied to experimental conditions like those found in polarography. In the present communication we extend this approach to include slow electrode reactions, in which case equilibrium between applied potential and interfacial concentration is not necessarily established during the measurements. The discussion is restricted to steady-state techniques. The much more complicated case of slow electrode reactions under transient conditions has been studied extensively by DELAHAY *et al.*[8].

We restrict the discussion to a single redox system of the type:

$$R \rightleftharpoons O + ne \tag{1}$$

at the metal–electrolyte interface, in the presence of a large excess of inert electrolyte. Concentrations of O and R are assumed to be sufficiently small so that the difference between absolute and relative surface excesses may be ignored. Activity coefficients may be considered constant in view of the excess of inert electrolyte. Neglecting also any small concentration gradients of ions $i \neq O,R$, which are related, *via* local electroneutrality conditions, to the mass transport of O and R, the Gibbs adsorption equation at constant temperature and pressure yields:

$$-\left(\frac{\partial\sigma}{\partial E}\right)_{\mu^*} = Q + RT\left\{\Gamma_O \frac{d\ln c_O}{dE} + \Gamma_R \frac{d\ln c_R}{dE}\right\} \tag{2}$$

(σ: surface tension, E: potential, Q: surface charge density on metal, R: gas constant, T: absolute temperature, Γ: surface excess, c: interfacial concentration, just outside electrical double layer; μ^* indicates constant bulk composition.)

Under steady-state conditions, one often has

$$J = K_R(c_R^* - c_R) = -K_O(c_O^* - c_O) \tag{3}$$

where J is the mass flux at the electrode interface (*i.e.*, the faradaic current density divided by nF) and K_R and K_O are independent of concentration or potential (F: Faraday, c^*: bulk concentration, J is taken positive for oxidation).

The corresponding limiting oxidation (anodic) and reduction (cathodic) fluxes and the interfacial concentrations follow from eqn. (3) as:

$$\overrightarrow{J} = K_R c_R^* \qquad \overleftarrow{J} = -K_O c_O^* \tag{4}$$

$$c_R = (\overrightarrow{J} - J)/K_R \qquad c_O = (J - \overleftarrow{J})/K_O \tag{5}$$

and substitution into eqn. (2) yields:

$$-\left(\frac{\partial\sigma}{\partial E}\right)_{\mu^*} = Q + RT\left\{\frac{\Gamma_O}{J-\overleftarrow{J}} + \frac{\Gamma_R}{J-\overrightarrow{J}}\right\}\frac{dJ}{dE} \tag{6}$$

The simplest conditions for which eqn. (3) applies are those of a Nernst diffusion layer[9] of constant thickness, d, so that

$$K_R = D_R/d \qquad K_O = D_O/d \tag{7}$$

(D: diffusion coefficient)

At a rotating disk electrode one also has a diffusion layer, the thickness of which is independent of the rates of the electrode reactions[10]. Likewise, eqns. (3)–(6) apply, with[11]

$$K_R = aD_R^{\frac{2}{3}}\omega^{\frac{1}{2}}\nu^{-\frac{1}{6}}\{1-0.354(D_R/\nu)^{0.36}\} \tag{8}$$
$$K_O = aD_O^{\frac{2}{3}}\omega^{\frac{1}{2}}\nu^{-\frac{1}{6}}\{1-0.354(D_O/\nu)^{0.36}\}$$

(a: numerical constant, ω: angular velocity, ν: kinematic viscosity)

Note that, for the steady-state conditions discussed here, no assumptions need be made about the dependence of rate constants on potential. Equation (6) can be written only as a linear combination of $Q+nF\Gamma_O$ and $Q-nF\Gamma_R$ when

$$(J-\overleftarrow{J})/(J-\overrightarrow{J}) = \exp[nF(E-E')/RT] \tag{9}$$

(E': arbitrary integration constant) which implies Nernstian equilibrium since J in eqn. (9) depends on the applied potential but not on any kinetic parameters.

Provided that surface excesses are independent of time, eqn. (6) applies also to the case of Nernstian electrode reactions on a dropping mercury electrode, within the approximation of the Ilkovič differential equation[12]. Indeed, eqn. (6) is then just another form of eqn. (9) in ref. 7 for that case, with[13]

$$K_R = \sqrt{7D_R/3\pi t} \qquad K_O = \sqrt{7D_O/3\pi t} \tag{10}$$

(t: time). Extension to slow electrode processes on a dropping mercury electrode along the lines of the above simple approach is not feasible, since in this case the interfacial concentrations, and hence the corresponding surface excesses, are time-dependent. The resulting complication is more than merely mathematical, since an unambiguous separation of faradaic and charging currents is then no longer feasible[14], and consequently the mass flux, J, is no longer an experimentally accessible quantity. When such time-dependence is ignored by considering time-averaged values of concentrations and mass fluxes only[15], eqn. (6) is obtained again in close approximation. When Γ_O and Γ_R are independent of time as a result of, for example, formation of a complete monolayer, then eqn. (6) applies to d.c. polarography with or without superimposed a.c. signals, and regardless of the speed of the electrode reactions.

Equation 6 shows that deviations from the simple Lippmann equation[1]

$$-\left(\frac{\partial\sigma}{\partial E}\right)_{\mu} = Q \tag{11}$$

only occur for steady-state systems when $dJ/dE \neq 0$, and that there is no condition like $J=0$. Thus, in the regions of the limiting currents, eqn. (11) applies.

Whenever $dJ/dE \neq 0$, the surface charge density Q loses its thermodynamic meaning, as do related quantities like integral capacitance and rational potential.

However, electrochemical equations can usually be written so that the integral capacitance is multiplied by the rational potential, and this product, eqn. (6), remains well-defined. On the other hand, serious difficulties arise when one attempts to calculate the potential of the plane of closest approach, which is important in the Frumkin correction of electrochemical rate constants[16], unless Γ_O and Γ_R are both negligibly small.

Equation (6) is written in terms of directly measurable quantities but the origin of the terms $(J-\overleftarrow{J})^{-1}$ and $(J-\overrightarrow{J})^{-1}$ becomes more obvious when we reintroduce eqn. (5) and write

$$-\left(\frac{\partial\sigma}{\partial E}\right)_{\mu^*}=Q+RT\left\{\frac{\Gamma_O}{c_O K_O}-\frac{\Gamma_R}{c_R K_R}\right\}\frac{dJ}{dE} \tag{12}$$

If it is assumed that, in dilute solutions and to a first approximation, surface excesses are directly proportional to interfacial concentrations

$$\Gamma_O=b_O c_O \qquad \Gamma_R=b_R c_R \tag{13}$$

where b_O and b_R are independent of interfacial concentrations but may be arbitrary functions of potential, then an extremely simple expression is obtained, *viz.*

$$-\left(\frac{\partial\sigma}{\partial E}\right)_{\mu^*}=Q+B\frac{dJ}{dE} \tag{14}$$

$$B\equiv RT(b_O/K_O-b_R/K_R) \tag{15}$$

$$C=-\left(\frac{\partial^2\sigma}{\partial E^2}\right)_{\mu^*}=\frac{dQ}{dE}+\frac{dB}{dE}\frac{dJ}{dE}+B\frac{d^2J}{dE^2} \tag{16}$$

(C: thermodynamic double layer capacitance). Indeed, eqns. (10) and (14) appear to apply to the measurements of SLUYTERS-REHBACH *et al.*[17] on $Tl^+/Tl(Hg)$. Integration of C yields eqn. (14), from which B can be obtained on the assumption that Q is not noticeably affected by the presence of Tl^+ and Tl(Hg). Strictly speaking, this assumption, and those embodied in eqn. (13), are outside the realm of thermodynamics, since Q, Γ_O and Γ_R are not separately measurable quantities in this case.

Acknowledgement

This work was supported by the National Science Foundation.

Department of Chemistry,
Georgetown University,
Washington D.C. 20007
(U.S.A.)

ROBERT DE LEVIE

1 G. LIPPMANN, *Compt. Rend.*, 76 (1873) 1407; *Pogg. Ann.*, 149 (1873) 561; *J. Phys.*, (1) 3 (1874) 41.
2 G. GOUY, *Ann. Phys.*, (9) 7 (1917) 129.
3 *e.g.*, D. C. GRAHAME, *Chem. Rev.*, 41 (1947) 441; R. PARSONS, *Mod. Aspects Electrochem.*, 1 (1954) 103; P. DELAHAY, *Double Layer and Electrode Kinetics*, Interscience, New York, 1965; D. M. MOHILNER, *Electroanal. Chem.*, 1 (1966) 241.
4 F. KRÜGER, *Z. Elektrochem.*, 19 (1913) 681.
5 A. N. FRUMKIN, *Z. Physik. Chem.*, 103 (1922) 55.

6 *e.g.*, D. C. GRAHAME AND R. B. WHITNEY, *J. Am. Chem. Soc.*, 64 (1942) 1548; D. M. MOHILNER, *J. Phys. Chem.*, 66 (1962) 724.
7 B. TIMMER, M. SLUYTERS-REHBACH AND J. H. SLUYTERS, *J. Electroanal. Chem.*, 15 (1967) 343.
8 P. DELAHAY, K. HOLUB, G. G. SUSBIELLES AND G. TESSARI, *J. Phys. Chem.*, 71 (1967) 779; K. HOLUB, G. TESSARI AND P. DELAHAY, *J. Phys. Chem.*, 71 (1967) 2612; K. HOLUB, *J. Electroanal. Chem.*, 17 (1968) 277; G. G. SUSBIELLES AND P. DELAHAY, *J. Electroanal. Chem.*, 17 (1968) 289.
9 W. NERNST, *Z. Physik. Chem.*, 47 (1904) 52.
10 V. G. LEVICH, *Physicochemical Hydrodynamics*, Prentice Hall, Englewood Cliffs, N. J., 1962, p. 73.
11 D. P. GREGORY AND A. C. RIDDIFORD, *J. Chem. Soc.*, (1956) 3756.
12 D. ILKOVIČ, *J. Chim. Phys.*, 35 (1938) 129.
13 D. ILKOVIČ, *Collection Czech. Chem. Commun.*, 6 (1934) 498; J. HEYROVSKÝ AND D. ILKOVIČ, *Collection Czech. Chem. Commun.*, 7 (1935) 198.
14 P. DELAHAY, *J. Phys. Chem.*, 70 (1966) 2069, 2373.
15 J. HEYROVSKÝ AND J. KŮTA, *Principles of Polarography*, Academic Press, New York, 1966, pp. 208–212, and references given therein.
16 A. N. FRUMKIN, *Z. Physik. Chem.*, 164A (1933) 121.
17 M. SLUYTERS-REHBACH, B. TIMMER AND J. H. SLUYTERS, *Rec. Trav. Chim.*, 82 (1963) 553.

Received July 16th, 1968

The differential capacitance of zinc in aqueous solution—a further note

Introduction

The differential capacitance of zinc in aqueous electrolyte has been studied by KRASIKOV AND SYSOEVA[1] (KCl, pH 7), TSA AND IOFA[2] (Na_2SO_4, pH 3) and BROWN *et al.*[3] ($NaClO_4$, KCl, KNO_3 and Na_2SO_4, pH 6.6–7). The results differ from each other in the values of the p.z.c. (point of zero charge) obtained by capacitance minima, the shapes of the curves, and the extent of the regions of polarisability observed. The values of the electrode resistance reported by BROWN *et al.*[3] changed abruptly at a potential of 1.0 V (NHE) which was ascribed by the authors to OH^- adsorption on the electrode.

This paper reports on measurements of the differential capacitance of zinc in aqueous $NaClO_4$ electrolytes at a range of pH-values with suppression of OH^- adsorption so that measurements would be characteristic of the zinc–aqueous electrolyte interphase.

Experimental

The electrical circuit (by which the electrode impedance is matched as a series combination of resistive, R_E, and capacitive, C_L, components), electrolytic cell, pretreatment of electrodes and electrolyte, and experimental techniques have been described previously[3–4]. Experiments were made at pH-values in the range, 7–3.4. The lower limit of pH was fixed by the extent of the hydrogen evolution reaction in the experimentally polarisable region; visible hydrogen evolution, due to interaction of the electrolyte and an isolated electrode, occurred at pH 3.1. The frequency used for all impedance measurements was 1 kHz.

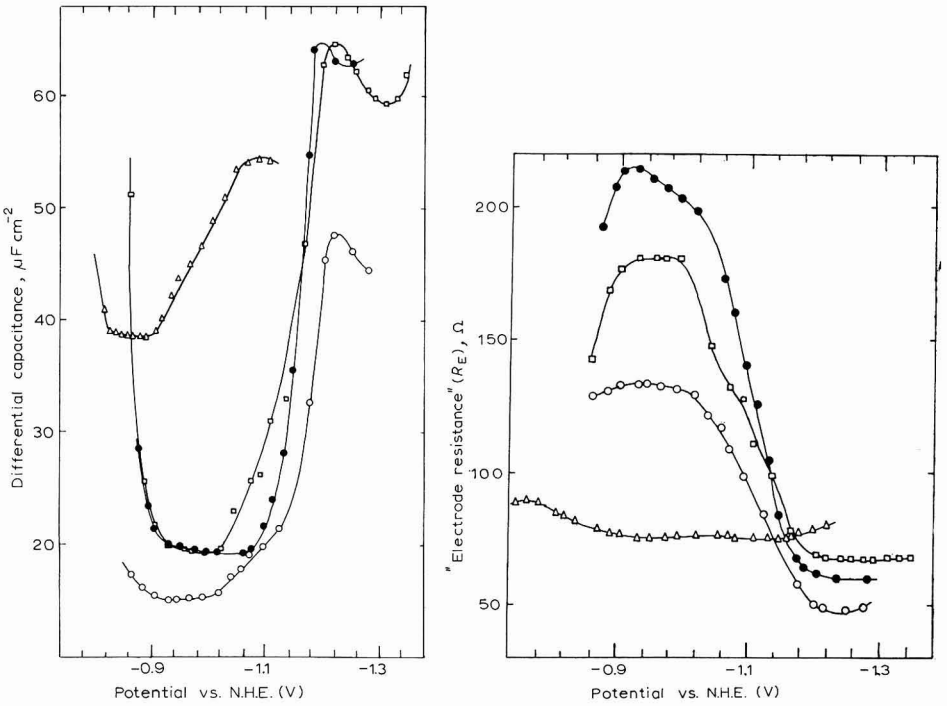

Fig. 1. Differential capacitance curves for polycrystalline zinc. 1 *M* $NaClO_4$; 23°; electrode area, $9.07 \cdot 10^{-2}$ cm^2. pH: (●), 6.62; (○), 5.56; (□), 4.6; (△), 3.48.

Fig. 2. Electrode resistance curves for polycrystalline zinc. 1 *M* $NaClO_4$; 23°. pH: (●), 6.62; (○), 5.56; (□), 4.6; (△), 3.48.

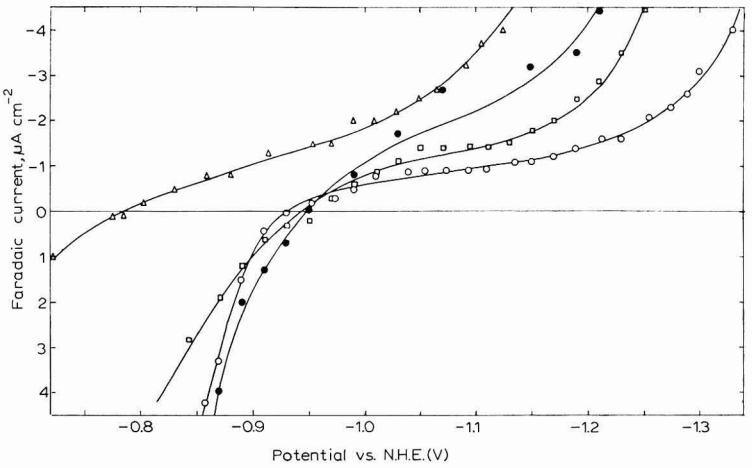

Fig. 3. Faradaic current–potential curves for polycrystalline zinc. 1 *M* $NaClO_4$; 23°. pH: (●), 6.62; (○), 5.56; (□), 4.46; (△), 3.48.

Results

Polycrystalline electrodes. Figure 1 shows differential capacitance data for polycrystalline zinc in 1 *M* $NaClO_4$ over a range of pH. The curve at pH 3.48 is significantly different from those at higher pH. Figure 2 shows the variation of R_E with potential over the same pH range. Generally, the curves show a marked change in R_E at about -1.1 V(NHE); this is absent at pH 3.48. Figure 3 records characteristic faradaic current *versus* potential curves. The experimentally polarisable region extends further into the anodic region for pH 3.48 electrolyte.

The effect of reducing the total ionic concentration at pH 3.48 on the differential capacitance curves is shown in Fig. 4. A minimum in capacitance is developed at -0.92 V in the most dilute electrolyte.

Single crystal (0001) electrodes. The results of electrometric and impedance measurements at single crystal electrodes followed a similar pattern to those obtained with polycrystalline electrodes. At pH 3.48, a somewhat different polarisable region, considerably greater values of C_L and absence of pronounced changes in R_E throughout the polarisable region than at higher pH, were observed.

The family of differential capacitance curves corresponding to dilutions at pH 3.48 is shown in Fig. 5. A shallow minimum is observed to develop at -0.9 V.

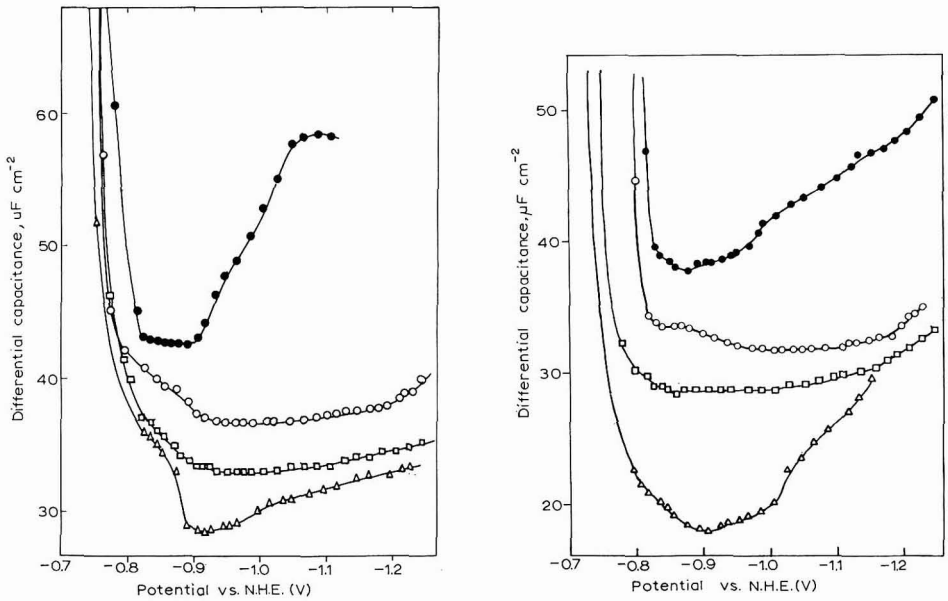

Figs. 4–5. Differential capacitance curves for: (4) polycrystalline zinc; (5) single crystal zinc. pH, 3.48; 23°; $NaClO_4$. (●), 0.98; (○), 0.13; (□), 0.03; (△), 0.005 *M*.

Discussion

There is little variation in the differential capacitance curves (Fig. 1) until pH 4, the results in the pH range, 4.6–7, being very close to those of BROWN *et al.*[3]. For these electrolytes, changes in the electrode resistance (Fig. 2) indicate anionic interaction at pH > 4.5 with the electrode which occur at -1.1 V and correspond with the steep capacitance rise to a peak at -1.22 V.

At pH 3.48, the transposition of the capacitance curve to more anodic potentials, the significant increase in differential capacitance and the relative constancy of the electrode resistance, R_E, at a low value throughout the experimentally polarisable region, indicates that interaction of OH^- with the electrode surface has been effectively suppressed.

The electrometric measurements (Fig. 3) indicate that the system, $Zn/NaClO_4 \cdot aq.$ is nowhere ideally polarisable. This is to be expected from the position of zinc in relation to other more polarisable elements (*e.g.*, Ag or Sn); *viz.*, zinc is rather electropositive in character and has a relatively high exchange current for the hydrogen evolution reaction.

The capacitance curves obtained by progressive dilution form a family (Fig. 4). The curve corresponding to the most dilute electrolyte shows a fairly well defined minimum at -0.92 V. In the absence of ionic adsorption this minimum can be taken as indicating the p.z.c.[5]. It is clear, however, that the limits of potential at which OH^- adsorption is completely suppressed and H^+ discharge occurs are fairly close so that some uncertainty must necessarily be attached to any value of the p.z.c. It is interesting to note, however, that -0.92 V is reasonably close to the value of the p.z.c. reported by TZA AND IOFA[2] (Na_2SO_4, pH 3) although the use of 2:1 electrolytes for the detection of the p.z.c. by capacitance minima is not quite exact[5]. It is also noteworthy that from work function–p.z.c. data for metals[5], the p.z.c. for zinc is to be expected in the region of -0.9 V; this correlation is approximate, however, and can be taken only as a rough guide.

Single crystal (0001) electrodes behave, in general, similarly to polycrystalline electrodes. The minimum in the differential capacitance curve, however, is broader than that observed with polycrystalline electrodes (Figs. 4 and 5). This is rather unexpected and as yet no satisfactory explanation has been formulated.

The value of the potential corresponding to the capacitance minimum for the (0001) face is -0.9 V in the most dilute electrolyte.

Acknowledgement

One of us (D.L.) acknowledges a grant from the Science Research Council.

Department of Chemistry, P. CASWELL
Loughborough University of Technology, N. A. HAMPSON
Leicestershire (England) D. LARKIN

1 B. S. KRASIKOV AND V. V. SYSOEVA, *Dokl. Akad. Nauk SSSR*, 114 (1957) 826.
2 C.-S. TZA AND Z. A. IOFA, *Dokl. Akad. Nauk SSSR*, 131 (1960) 1937.
3 D. S. BROWN, J. P. G. FARR, N. A. HAMPSON, D. LARKIN AND C. LEWIS, *J. Electroanal. Chem.*, 17 (1968) 421.
4 J. P. G. FARR AND N. A. HAMPSON, *Trans. Faraday Soc.*, 62 (1966) 3493.
5 P. DELAHAY, *Double Layer and Electrode Kinetics*, Interscience, New York, 1965, chapt. 6.

Received August 14th, 1968

Elsevier Sequoia S.A., Lausanne – Printed in The Netherlands

BOOK REVIEWS

Mass Spectrometry in Inorganic Chemistry, edited by J. L. MARGRAVE, *Advances in Chemistry Series*, No 72, American Chemical Society, Washington, 1968, viii + 329 pages; $12.00.

This volume, in the well-known and rapidly expanding ACS *Advances in Chemistry Series*, is the record of a symposium held in New York in September, 1966, under the chairmanship of J. L. MARGRAVE, and consists of 21 papers on various aspects of mass spectrometry in inorganic chemistry.

Among papers describing the mass spectra of inorganic molecules, studies on boranes are well represented, encompassing ion–molecule reactions with pentaborane (HERTEL AND KOSKI), intermediates in the photochemical oxidation of diborane (PORTER AND GRIMM), and a useful account of the analysis of boranes and carboranes (DITTER, GERHART AND WILLIAMS). Problems encountered in applications to labile systems, *e.g.*, B_4H_8CO, $Ni(CO)_4$, are discussed (STAFFORD, PRESSLEY AND BAYLIS). Several new ionic species were detected in the conversion of metathioboric acid to B_2S_3 at temperatures between 50 and 665° (EDWARDS AND GILLES). Studies with phosphorus hydrides (FEHLNER AND CALLEN) and interatomic compounds of Group V (CARLSON, KOHL AND UY) are also reported. Some emphasis on metal oxide (NORMAN, STALEY AND BELL) and halide systems (KISER, DILLARD AND DUGGER; ZMBOV AND MARGRAVE) is apparent. The paper by KISER *et al.* also includes an excellent review, with over 200 references, and his appeal for wider studies, so necessary two years ago, has been well answered in the period between this symposium and this review.

However, most use for this book will be found in the sections dealing with techniques and applications, as exemplified by the papers on chemical ionisation (FRANKLIN), high pressure systems (MILNE AND GREENE), automation in data collection (LOYD AND STAFFORD), electron multipliers in high temperature mass spectrometers (GINGERICH), and time-resolved mass spectrometry (MEYER AND AMES). Appearance and ionisation potential data, and heats of formation for perfluorosilanes and perfluoroborosilanes (MCDONALD, WILLIAMS, THOMPSON AND MARGRAVE) are reported. A comparison of theoretically predicted and experimental values for electron impact ionisation cross sections (STAFFORD) indicates some of the limitations of current theory, and attention is drawn to the necessity for caution in the interpretation of results from Knudsen effusion cell work (WESTMORE, FUJISAKI AND TICKNER), resulting from studies on the vaporisation of molecules such as Cd_3As_2. The use of mass spectrometry as a source of otherwise unobtainable data is shown in the cases of ion–solvent molecule interactions in the gas phase (KEBARLE), a shock-tube study of D_2–Ne mixtures (GAY AND KERN), and in the many other studies of unstable molecules already mentioned. Finally, mention must be made of an account of the mass spectrometer as a radiolytic and catalytic laboratory in the investigation of decomposition reactions in a high-pressure spectrometer (MELTON).

It is unfortunate that in this symposium no paper concerned with organometallic compounds or transition metal chelates was included, resulting in an impression that inorganic mass spectrometry is of use only in systems similar to those described.

The long delay in appearance of this volume, which contributes to this impression, was apparently caused by late receipt of only one paper (by eight months), and perhaps its omission would have resulted in a more timely publication. The production and appearance of this book are of high quality, with the exception of the index, which seems rather arbitrarily selective. The relative cheapness may make this book an attractive purchase for mass spectrometrists and others interested in the areas it covers.

M. I. BRUCE, University of Bristol

J. Electroanal. Chem., 20 (1969) 339–340

Polarography: Plenary Lectures from the International Congress of Polarography, Kyoto, Japan, September, 1966, Butterworths (for IUPAC), London, 1968, 124 pages, 50 s.

This slim volume collects the seven plenary lectures which have already appeared in *Pure and Applied Chemistry*, 15 (1967). The names of the distinguished authors lead one to expect a valuable collection and this expectation is indeed fully justified. Every electrochemist will find material here to stimulate his interest at a variety of levels.

KORYTA provides a compact and lucid summary of the theory of polarographic currents with a useful historical perspective. He emphasizes particularly the effect of adsorption both of reacting species and of other species from the solution. LAITINEN discusses the techniques of polarography and its relations in molten salts, giving helpful comments about each. He also reviews recent work on the equation for the polarographic wave. BARKER's article on the *Theory of the current in a.c. polarography* describes his method of treating the impedance of an electrode interface by equivalent circuits using transmission lines, voltage generators and current generators as well as the more usual resistors and capacitors. In my opinion this is a clearer account than he has given previously and should be the starting point for those planning the annual reading of BARKER's papers recommended by REINMUTH (*Anal. Chem.*, 40 (1968) 185). It also forms an excellent commentary on DELAHAY's recent work on the nature of the separation of faradaic and non-faradaic currents. The article by FRUMKIN AND DAMASKIN contains the distilled wisdom of many years' work from the first series of papers culminating in the classic review (FRUMKIN, *Ergeb. Exakt. Naturw.*, 7 (1928) 235) to the present day. The adsorption of a variety of types of organic compounds at the free water surface and the mercury–water interface is compared and contrasted. KEMULA discusses the sensitive method of deposition and stripping for trace analysis of metals. Practical details are described and the advantages of the method persuasively argued. ELVING summarizes recent work in organic polarography. He has in many cases provided a "review of reviews" which will be useful in finding one's way through this vast field. Finally, BREYER gives a sort of condensed supplement to *A.C. Polarography and Tensammetry* (BREYER AND BAUER, Wiley, 1963). The multiplicity of applications of these techniques is truly remarkable. If anyone is short of material for a research project, there is plenty here.

The book is well produced and well worth reading.

ROGER PARSONS, University of Bristol

Vol. 20 No. 2 JOURNAL OF ELECTROANALYTICAL CHEMISTRY FEBRUARY 1969
AND INTERFACIAL ELECTROCHEMISTRY

CONTENTS

The thermodynamic treatment of monolayer phase formation
R. D. ARMSTRONG AND E. BARR (Newcastle upon Tyne, Great Britain) 173

Instrument for the automatic measurement of the electrode admittance
R. DE LEVIE AND A. A. HUSOVSKY (Washington, D.C., U.S.A.) 181

Glass reference electrodes in molten (Li,K)NO_3
G. G. BOMBI, G.-A. MAZZOCCHIN AND M. FIORANI (Padova, Italy) 195

Behaviour of tin as metal–metal phosphate electrode and mechanism of promotion and inhibition of its corrosion by phosphate ions
S. A. AWAD AND A. KASSAB (Cairo, Egypt) 203

Polarography of carbon suspensions
I. F. JONES AND R. C. KAYE (Leeds, Great Britain) 213

A study of the fluoride complexes of cadmium by a.c. and d.c. polarography
A. M. BOND (Melbourne, Vic., Australia) 223

Supporting electrolyte effect on the $[Ni(CN)_4]^{2-}$ electrochemical reduction
G. TORSI AND P. PAPOFF (Bari, Italy) 231

Potentiometric estimation of potassium hydroxotetracyanotungstate(IV) and determination of standard potential
KABIR-UD-DIN, A. A. KHAN AND M. AIJAZ BEG (Aligarh, U.P., India) 239

Phosphororganische Verbindungen. 61. Polarographische Untersuchung quartärer Phosphonium- und Arsoniumsalze
L. HORNER UND J. HAUFE (Mainz, Deutschland). 245

Electrochemistry of aquodiethyllead(IV) ion
M. D. MORRIS (University Park, Pa., U.S.A.) 263

Polarographic investigation of metal acetylacetonates. VI. Cobalt(II) acetylacetonates
B. ĆOSOVIĆ AND M. BRANICA (Zagreb, Yugoslavia) 269

The use of complex-forming reagents in the polarographic analysis of inorganic substances. XIV. Polarographic behaviour of ethylenedisulphurdiacetic acid in the presence of a mercury salt
D. SUŽNJEVIĆ, J. DOLEŽAL AND M. KOPANICA (Belgrade, Yugoslavia and Prague, Czechoslovakia) 279

Die polarographische Reduktion von Solochromviolett RS und der Mechanismus der Komplexbildung mit Aluminium in methanolischer Lösung
L. HOLLECK, J. M. ABD EL KADER UND A. M. SHAMS EL DIN (Bamberg, Deutschland) 287

Adsorption behaviour of quinoline, 2- and 4-methylquinoline at mercury–solution and at air–solution interfaces. I. Electrocapillary curves, surface tension and surface potential
S. BORDI AND G. PAPESCHI (Firenze, Italy) 297

Polarographic, conductometric and potentiometric studies on polyethyleneimine
T. M. H. SABER AND A. M. SHAMS EL DIN (Cairo, Egypt) 311

Polarographic maximum suppressing ability of malathion in non-aqueous and aqueous systems
E. LADÁNYI AND D. N. RĂDULESCU (Cluj, Rumania) 319

Short communications

A chronocoulometric method with dropping electrode for adsorption study
J. KORYTA, L. NĚMEC, J. PIVOŇKA AND L. POSPÍŠIL (Prague, Czechoslovakia) . . . 327

Double layer thermodynamics for slow electrode reactions under steady-state conditions
R. DE LEVIE (Washington, D.C., U.S.A.) 332

The differential capacitance of zinc in aqueous solution. A further note
P. CASWELL, N. A. HAMPSON AND D. LARKIN (Loughborough, Great Britain) 335

Book reviews 339

ADVANCES IN COLLOID AND INTERFACE SCIENCE

An international journal devoted to experimental and theoretical developments in interfacial and colloidal phenomena and their implications in chemistry, physics, technology and biology

Contents of Volume 1

THE PHYSICAL ADSORPTION OF GASES ON SOLIDS (W. A. Steele, University Park, Pa., U.S.A.)

LA STRUCTURE DES SOLUTIONS AQUEUSES CONCENTREES DE SAVON (A. Skoulios, Strasbourg, France)

PARTICLE ADHESION. THEORY AND EXPERIMENT (H. Krupp, Frankfurt-M, Germany)

THE NATURE OF THE ASSOCIATION EQUILIBRIA AND HYDROPHOBIC BONDING IN AQUEOUS SOLUTIONS OF ASSOCIATION COLLOIDS (Pasupati Mukerjee, Los Angeles, Calif., U.S.A.)

SEMICONDUCTOR SURFACES AND THE ELECTRICAL DOUBLE LAYER (M. J. Sparnaay, Eindhoven, The Netherlands)

HETEROGENEOUS NUCLEATION FROM THE VAPOR (R. A. Sigsbee and G. M. Pound, Schenectady, N. Y., and Stanford, Calif., U.S.A.)

THIN LIQUID FILMS (A. Sheludko, Sofia, Bulgaria)

Contents of the first two issues of Volume 2

APPLICATION OF SLOW NEUTRON SCATTERING TO STUDIES IN COLLOID AND SURFACE CHEMISTRY (H. Boutin, H. Prask and R. D. Iyengar, Dover, N. J. and Bethlehem, Pa., U.S.A.)

LIGHT SCATTERING FROM LIQUID INTERFACES (A. Vrij, Utrecht, The Netherlands)

PRINCIPLES OF THE STABILITY OF LYOPHOBIC COLLOIDAL DISPERSIONS IN NON-AQUEOUS MEDIA (J. Lyklema, Wageningen, The Netherlands)

SURFACE CHEMICAL AND MICELLAR PROPERTIES OF DRUGS IN SOLUTION (A. T. Florence, Glasgow, Great Britain)

PARTIAL MISCIBILITY OF MULTICOMPONENT POLYMER SOLUTIONS (R. Koningsveld, Geleen, The Netherlands)

POROUS STRUCTURE OF ADSORBENTS AND CATALYSTS (M. M. Dubinin, Moscow, USSR)

Subscription price:
Dfl. 75.00, £ 8.14.6 or $ 21.00 per volume of four quarterly issues plus postage Dfl. 3.50, 8s. 3d., or $1.00.

Orders for single issues or full subscriptions may be sent to your regular bookseller or to Elsevier Publishing Company, P.O. Box 211, Amsterdam, The Netherlands.

Elsevier Publishing Company Amsterdam London New York

210 E